A Comparison of the Performance of High-Voltage Insulator Materials in a Severely Polluted Coastal Environment

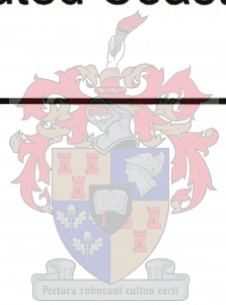

Wallace Lockwood Vosloo

Dissertation submitted for the Degree of Doctor of Philosophy
in Engineering Science at the University of Stellenbosch

Promoter:

Dr JP Holtzhausen, Department of Electrical and Electronic Engineering
University of Stellenbosch

March 2002

Stellenbosch University http://scholar.sun.ac.za

Declaration:

I, the undersigned, hereby declare that the work contained in this dissertation is my own original work and has not been previously, in its entirety, submitted at any university for a degree. The sources that I have used or quoted have been indicated and acknowledged by means of references.

Stellenbosch University http://scholar.sun.ac.za

Abstract

The main aim of this research programme was to compare the relative performance of different insulator materials used in South Africa when subjected to a severe marine pollution environment. A test programme and procedure, test facility and instrumentation were established. Some novel instrumentation and monitoring equipment were developed and built specifically for this research programme, supported by data analysing software programs. In order to compare material performance only, all non-material design variables between the test insulators had to be removed (e.g. creepage distance, connecting length, inter-shed spacing, profile, etc.). To achieve this some of the test insulators had to be specially manufactured. Leakage current, electrical discharge activity, climatic and environmental data was collected successfully over a one-year test period, starting with new test insulators.

The peak and energy values of the leakage current were identified as the two main parameters needed to describe the leakage current activity on the test insulators. A correlation was found between the climatic and environmental data and the leakage current data, and it was found that the leakage current can be determined successfully from some of the climatic and environmental parameters monitored by using multiple regression techniques. Surface conductivity and energy were found to be the best parameters to show the maximum and continuous interaction of the insulator material surface with the electrolytic pollution layer. A natural ageing and pollution test procedure was developed, which has become a South African standard and is gaining international acceptance.

A model and hypothesis are proposed to describe the electrical discharge activity that takes place on the test insulators and explain the difference in leakage current performance of the various materials.

Keywords: Insulator, Pollution, High Voltage, Leakage current, Material performance.

Stellenbosch University http://scholar.sun.ac.za

Samevatting

Die hoofdoel van hierdie navorsingsprogram was om die relatiewe prestasie van verskillende isolatormateriale wat in Suid-Afrika gebruik word te vergelyk in 'n swaar besoedelde marine omgewing. 'n Toetsprogram en prosedure, toets fasiliteit en instrumentasie is gevestig. 'n Paar nuwe instrumente en moniteer toerusting is ontwikkel en gebou spesifiek vir hierdie navorsingsprogram, gesteun deur data analise sagteware programme. Ten einde slegs materiaalprestasie te vergelyk, moes alle nie-materiaal ontwerpsveranderlikes tussen die toetsisolators verwyder word (bv. kruipafstand, konnekteer lengte, tussen-skerm spasiëring, profiel, ens.). Om dit reg te kry moes sommige van die toetsisolators spesiaal vervaardig word. Lekstroom, elektriese ontladingsaktiwiteit, klimaat en omgewingsdata is suksesvol versamel oor 'n een-jaar toetsperiode, beginnende met nuwe toets isolators.

Die piek en energie waardes van die lekstroom is identifiseer as die twee hoof parameters wat nodig is om die lekstroomaktiwiteit op die toetsisolators te beskryf. 'n Korrelasie is gevind tussen die klimaat- en omgewingsdata en die lekstroom data, en dit is gevind dat die lekstroom data suksesvol bepaal kan word van sekere van die klimaat- en omgewingsparameters wat gemoniteer is deur veelvoudige regressie tegnieke te gebruik. Oppervlakskonduktiwiteit en energie is gevind die beste parameters te wees om die maksimum en kontinûe interaksie van die isolatormateriaaloppervlak met die elektrolitiese besoedelingslaag aan te toon. 'n Natuurlike veroudering en besoedeling toetsprosedure is ontwikkel, wat 'n Suid-Afrikaanse standaard geword het en besig is om internastionale aanvaarding te wen.

'n Model en hipotese word voorgestel om die elektriese ontladingsaktiwiteit wat op die toetsisolators plaasvind te beskryf en om die verskil in lekstroomprestasie van die verskeie materiale te verduidelik.

Sleutelwoorde: Isolator, Besoedeling, Hoog Spanning, Leck stroom, Materiaal prestasie.

Stellenbosch University http://scholar.sun.ac.za

Acknowledgements:

I wish to record my sincere thanks and appreciation, in no specific order, to:

- My supervisor, Dr J P Holtzhausen, for his persistent encouragement and guidance.
- Eskom for supporting and sponsoring the research project.
- CT-Lab for their support with the OLCA, especially the programming.
- CSIR for their support with the CoroCAM.
- NETELEK for their support with the IH48 and IPMA.
- Cape Weather Wise for their information on the climatic conditions at Koeberg.
- Students and colleagues for their help with the observations and data capture.
- Dr Margie Hurndall for the technical editing.
- Hendrik Burger for his technical computer support.
- Dr Igor Gutman, Dr Andy Roediger, Dr Thomas Johansson, Dr Claude de Tourreil, Dr Ravi Gorur, Prof Stanislaw Gubanski, Martin Kuhl, Clive Lumb and others for the interest shown and the long discussions which led to many of the ideas and philosophies contained in this dissertation.
- My wife Karen, for all the emotional support and love, that only someone as special as she can give.

Stellenbosch University http://scholar.sun.ac.za

List of Contents

Stellenbosch University http://scholar.sun.ac.za

Stellenbosch University http://scholar.sun.ac.za

Stellenbosch University http://scholar.sun.ac.za

LIST OF ABBREVIATIONS

ATH	Aluminiumtrihydrate
AVG	Average
BTM	Bottom
CNTR	Control
CSIR	Council for Scientific and Industrial Research
DBC	Dry-band corona
DBD	Dry-band discharges
DDG	Directional dust deposit gauge
EDAX	Elemental analysis
EPDM	Ethylene propylene diene monomer
EPM	Ethylene propylene monomer
ERI	Energy Research Institute
ESCOM, Eskom	Electricity Supply Commission, later changed to Eskom
ESDD	Equivalent salt deposit density
ESP	Enhanced silicone polymer
FFT	Fast Fourier Transform
HFO	Heavy fuel oil
HTV	High-temperature vulcanised
IPMA	Insulator pollution monitoring apparatus
IPMR	Insulator pollution monitoring relay
KIPTS	Koeberg Insulator Pollution Test Site
LESDD	Local equivalent salt deposit density
NSDD	Non-soluble deposit density
OLCA	On-line leakage current analyser
PME	Pollution monitoring equipment

Stellenbosch University http://scholar.sun.ac.za

PTFE	Polytetrafluorethylene
RG	Resistive/semiconductive glazed
rms	Root mean square value of an alternating voltage or current
RTV	Room temperature vulcanised
SAIEE	South African Institue of Electrical Engineers
SAWB	South African Weather Bureau
SCD	Spot corona/discharges
SR	Silicone rubber
STRI	Research company in Sweden
TRFR	Transformer
VT	Voltage transformer
WDC	Water drop corona

Stellenbosch University http://scholar.sun.ac.za

1 INTRODUCTION

"If I have seen further it is by standing on the shoulders of giants" – ***Isaac Newton***

1.1 BACKGROUND

The main dielectric used in high-voltage networks is air at atmospheric pressure. Air is a good insulating material, provided that the electric stress is kept below the ionisation threshold. However, as air has no mechanical properties capable of supporting high-voltage conductors, various types of insulators were developed during the past century to perform the dual task of mechanically supporting and electrically insulating the lines and equipment. Such a task is particularly complex, bearing in mind the multiple extreme stresses present: mechanical, electrical and environmental.

The first insulator products used were made from glass and porcelain (ceramic materials) and these materials dominated the insulator market for many years. The performance of ceramic insulator materials has been the subject of many research projects, and application principles are well established [1].

Supported by developments in material science technology, efforts to improve the performance of insulators in polluted environments, to reduce manufacturing and operating costs, and to reduce susceptibility to vandalism, have resulted in new, lower weight insulator designs, made from non-ceramic materials. These include cycloaliphatic epoxy resin insulators and composite polymeric insulators (silicone rubber, ethylene propylene rubber and alloy rubber). These composite insulators usually consist of a polymeric-covered, glass-fibre core and polymeric sheds. The polymeric materials are often hydrophobic (repelling water), as opposed to hydrophilic (attracting water) ceramic insulators. As a result of their low wettability, some polymeric insulators perform exceptionally well in extremely polluted environments [2]. However, during prolonged exposure to pollution their hydrophobicity may decrease, resulting in higher leakage currents and/or material degradation [3].

High-temperature vulcanised (HTV) silicone rubber (SR) is the main type of non-ceramic insulating material used on the Eskom transmission power network (220 kV and above). However, on the Eskom sub-transmission power network (66 kV – 132 kV) the main types

Stellenbosch University http://scholar.sun.ac.za

of non-ceramic materials used are HTV SR, ethylene propylene diene monomer (EPDM) and alloy rubber. On Eskom's 11 and 22 kV reticulation networks cycloaliphatic epoxy resin insulators, SR, EPDM and alloy rubber insulators are used. Aluminiumtrihydrate (ATH) and/or silica quartz are the bulk fillers used. The alloy used is an EPDM, with a small amount of silicone oil present in the formulation. Research has shown that the alloy performs similarly to the EPDM [4].

In areas with pollution problems, silicone grease is often applied to ceramic insulators to enhance their hydrophobic properties and hence the overall electrical performance. This is very labour intensive and costly. As an alternative to regular greasing, room-temperature vulcanised (RTV) silicone rubber (SR) coatings have been developed and are applied to ceramic insulators for the same purpose. Such coatings have been used with success, also in South Africa, and are becoming increasingly popular [5]. The use of resistive/semi-conducting, glazed porcelain insulators, that inhibit the formation of a wet layer and dry-band discharge activity, are also being considered for use to improve insulator performance in heavily polluted areas. Surge arresters, line equipment, and station posts with non-ceramic insulation have also entered the electrical market. These are now used by Eskom, the main supplier and distributor of electricity in South Africa.

Due to continued research and development, and the aim of manufacturers to reduce costs, new materials and insulator designs regularly become available. Most of these materials and designs are as yet unproven; no long-term tests have yet been carried out and no long-term field experience exists.

Insulator failures are serious. Mechanical failures of insulators can lead to partial dropping of the conductor, which is a major safety risk. Furthermore, from utility experience, the incorrect choice of insulator products has, in the past, proven to be very costly and must be avoided in the future.

International research on insulator testing and ageing has led to the drawing up of basic guidelines on the assessment and application of non-ceramic insulators. These guidelines are, however, not necessarily applicable in South Africa, as they do not reflect local environmental and climatic conditions. Prediction of the performance of ceramic insulator products (glass and porcelain) under various environmental conditions can be made with a fair amount of confidence, but predicting the long-term performance of non-

Stellenbosch University http://scholar.sun.ac.za

ceramic insulator products (over several decades), especially under African conditions, poses a problem.

Eskom, as a large user of insulator products, cannot afford to use unknown products. It therefore initiated an extensive research and fault investigation programme to study the performance of insulator products under local conditions. It was to encompass evaluating insulator products at insulator test stations, monitoring the performance of in-service insulators and testing under controlled laboratory conditions. The overall goal of the research and investigation programme was to position Eskom as an informed buyer of insulator products and to enable the company to address operational problems. Electrical and mechanical failures of insulator products in operation also contributed to the need for this research.

As part of this programme, the author was tasked to compare the relative performance of the main types of insulating materials (the best of each type used for high-voltage insulators in South Africa) over a one-year period, starting with brand new clean insulators while observing the leakage current, climatic, environmental and surface conditions, and electrical discharge activity when subjected to a severely polluted coastal environment, as encountered along the West Coast.

In order to meet the above research objective a test programme and procedures, test facilities and new monitoring instrumentation had to be developed. The collected data and observations made over a focused one-year period had to be analysed. Emphasis was to be placed on trends, correlations and the relative performance ranking of insulators. It was envisaged that the knowledge gained could be used in the selection of suitable high-voltage insulator materials for use in severe coastal environments, both nationally and internationally.

1.2 LITERATURE SURVEY

The literature survey focuses on research carried out prior to 2000 on the performance of non-ceramic insulators in severe coastal environments in South Africa, in particular along the Cape West Coast. Insulator research on ceramic insulators and insulators in other (non-marine) environments have not been included. Although studied, international

Stellenbosch University http://scholar.sun.ac.za

research on the performance of non-ceramic insulators subjected to severe coastal conditions has also not been included in this discussion.

The first study of the performance of energised, non-ceramic insulators in a severe coastal environment in South Africa was performed by Macey from the then ESCOM (Electricity Supply Commission - changed to the company Eskom in 1985). In 1975 an 88 kV insulator pollution test station was built by Macey along the Cape West Coast, next to the Koeberg Nuclear Power Station, at 'Ou-Skip' rocks, 10 meters from the high-water mark. The test station was ready for operation in 1977. The test site was chosen because of the severe climatic and environmental conditions that prevail there. One of the main reasons for using this test station was to be able to study the effect of heavy marine contamination on the performance and life expectancy of various organic and inorganic insulating materials.

Silicone rubber (SR), cycloaliphatic epoxy resin, ethylene propylene monomer rubber (EPM), polytetrafluoroethylene (PTFE) and various ceramic (glass and porcelain) insulators were tested. The specific creepage distances on the non-ceramic insulators tested ranged from 58.3 to 100 mm/kV (which is very high) and the connecting length of the various insulators was chosen to be similar (2 300 mm). The leakage currents on the test insulators were monitored by means of a non-inductive shunt resistance, using mechanical surge counters (>75, 150 and 300 mA). The time to flashover was recorded as the time elapsed until the mercury switch made contact in the explosive Mace fuse (which disconnected from the insulator when a peak leakage current of 800 mA was reached). The wind speed and direction, temperature, atmospheric pressure, relative humidity, rainfall and severity of pollution (using directional dust-deposit gauges) were monitored. Visual observations of the surface conditions of the non-ceramic insulators were also made during the test programme.

Macey published the findings of this research programme carried out at the Koeberg insulator pollution test station in his MSc thesis "The Performance of High-Voltage, Outdoor Insulation in Polluted Environments" [6] and in a publication with the same title [7]. Macey's research showed that the test station was situated in a severe coastal environment. The pollution index recorded at Koeberg by the directional dust-deposit gauges was in the order of 2000 μS/cm, which is extremely heavy (>350 μS/cm is rated as very heavy). No severe material degradation was observed on the non-ceramic insulators tested. However, severe glass erosion was present on the glass cap-and-pin

Stellenbosch University http://scholar.sun.ac.za

disk insulators tested. The silicone rubber and PTFE insulators showed better leakage current performance than the other non-ceramic materials tested. The cycloaliphatic insulator showed poor electrical performance, even with longer creepage distance (100 mm/kV) than the other insulators.

Macey's research on non-ceramic insulators at Koeberg stopped during 1978. The duration of that test programme on non-ceramic insulators at Koeberg was therefore too short to allow conclusive recommendations to be made. The variation in insulator profile and specific creepage distances meant that Macey's results could not be used to compare the relative performance of the different materials. The University of Stellenbosch continued to carry out research only on ceramic insulators at Koeberg until the test station was finally closed and demolished in 1986.

During the late 1970's, ESCOM started experimenting with replacing glass insulators on existing lines with non-ceramic insulator materials. Amongst others, silicone rubber and ethylene propylene monomer rubber test insulators were installed on a 400 kV line running close to the West Coast, near the Koeberg Nuclear Power Station. Weihe, Macey and Reynders published the results in the publication "Field experience and testing of new insulator types in South Africa" [8]. The results showed that the silicone rubber insulators outperformed the ethylene propylene monomer rubber units. The latter had heavy discharges, audible up to 200 meters, and were removed after one year due to radial cracks on the bottom sheds. The available information is incomplete (e.g. no information on creepage distance, profile, etc.): there is too little detail to compare material performance.

During the early 1980's a test station was built at Alexanderbaai, which is situated north of Koeberg along the West Coast. Unfortunately the results were not published and the internal ESCOM reports mentioned by Macey were not available for study. However, on visiting the substation close by, a few of the original tested insulators were found in a store and inspected. The silicone rubber insulators were in good condition, while the ethylene propylene monomer rubber units showed chalking and signs of cracking (it must be noted that the latter units had a totally different profile and creepage distance to the silicone rubber units). Unfortunately no further information was available.

In 1989 Holtzhausen established the Elandsbaai insulator pollution test station. It was directly energised from the 50 kV Sishen-Saldanha railway line (transporting iron ore),

Stellenbosch University http://scholar.sun.ac.za

north of Koeberg, on the West Coast. The performance of the Sishen-Saldanha railway line was severely affected by numerous outages due to poorly performing line insulators. The first-generation polymeric insulators, made of EPM, were installed on this line and were failing due to severe material erosion and flashovers. This was one of the main reasons for starting the test station, which was financially supported by the South African National Energy Council, Eskom, and Spoornet. The test station included a leakage current (peak value for a set interval) and climate-monitoring logger. The publications "The on-site leakage current performance of insulators of various designs and materials as a function of weather data" by Holtzhausen, Smith and Potgieter [9] and "Leakage current monitoring on synthetic insulators at a severe coastal site" by Holtzhausen [10] summarises the research work done at Elandsbaai. The results showed that silicone rubber insulators, when compared to ethylene propylene diene monomer (EPDM) units at various creepage distances, had better leakage current performance. Cycloaliphatic insulators showed irreversible material degradation and poor leakage current performance. The modes of material degradation observed were discoloration, chalking, cracking, tracking, erosion and puncturing. A correlation between climate (rain and relative humidity) and leakage current was established. The knowledge gained from the Elandsbaai insulator pollution test station (before it was closed in 1994) resulted in the following recommendations for marine environments in South Africa: silicone rubber insulators with specific creepage distances larger than 25 mm/kV (preferably 31) should be used and EPDM insulators with specific creepage distances larger than 31 mm/kV should be used (preferably not recommended for marine conditions) [11]. The results from Elandsbaai showed that leakage current could be used to compare the relative performance of materials. It also showed the importance of measuring the climatic and environmental (pollution) conditions. Electrical surface discharge activity observations and recordings, using an ultraviolet image-intensified camera (CoroCAM), were made on the insulators by the author. The results clearly showed the different types of activity, such as corona, sparking and dry bands. The need for further research was identified. The problems associated with running a test station such a distance away from home prompted the idea of re-establishing the Koeberg insulator pollution test station and developing reliable logger equipment.

The publication "Service experience with polymeric insulators in Eskom, South Africa" by Ravera, Britten and Swift [12] summarises the research carried out and in-service experiences with non ceramic (polymeric) insulators in South Africa up to 1994. From the

Stellenbosch University http://scholar.sun.ac.za

publication it is evident that Eskom intended to continue using non-ceramic (polymeric) insulators, especially in areas of severe pollution, and for new line designs.

In 1994 the author, under the guidance of Holtzhausen, was tasked by Eskom to establish a new insulator pollution test station at Koeberg. Details of the new 22 and 66 kV Koeberg test station are contained in the publication "Insulator pollution performance test station: design and operation" [13]. The test station was designed to evaluate the relative performance of insulator products when subjected to a severe marine environment. Various insulators from different manufactures, made of different materials and having different profiles, specific creepage and arcing distances, were compared. In addition, the performance of various silicone greases and coatings were compared to the performance of untreated porcelain. The modes of material degradation observed were discoloration, chalking, cracking, tracking, erosion and punctures. Leakage currents in the order of 100 mA and above were recorded on non-ceramic insulators. The electrical surface discharges observed ranged from corona to arcing. The results published on the research at Koeberg [14] confirm the findings made at Elandsbaai and form the basis of the work for this dissertation.

During 1995 the author established the Brandsebaai insulator pollution test station along the West Coast, north of Koeberg. Details of the test station are contained in the publication "The design principles of on-line insulator test stations to be used on power distribution and transmission networks" [15]. Insulators of various materials and creepage distances were evaluated at the test station to find a possible alternative for the existing line insulation. The results showed once more that all the silicone rubber insulators tested outperformed the EPDM, enhanced silicone polymer (ESP) and ceramic units, and also confirmed the results found at Elandsbaai and Koeberg.

During 1996 the author, together with Hartings and Gutman in a collaboration research project with STRI in Sweden, established the Kelso on-line insulator test station and the Clansthal insulator test tower complete with leakage current, climate and environmental monitoring systems on the East Coast of Natal. Details of the test station and tower, and early results, are presented in the publication "Field testing of composite insulators at Natal test stations in South Africa" [16]. This on-going research programme focuses on testing insulators of different profiles, specific creepage and arcing distances, material types (porcelain, glass, SR and EPDM), and from different manufacturers. Maintenance methods such as silicone greasing and silicone coating are also investigated. Another

Stellenbosch University http://scholar.sun.ac.za

objective is to compare (to one another and internationally) the performances of the insulators installed on the East and West coast of South Africa. To date, the ageing modes observed in Natal (east coast) were found to be similar (though less severe) to those found at Koeberg (west coast).

During 1997 the author established an insulator test tower in Alexanderbaai. This was on a 220 kV line close to the substation, complete with climate and leakage current loggers. The performances of two different types of silicone rubber insulators were compared to that of glass. The silicone rubber insulators totally outperformed the glass, and there was also a difference in the performance of the two silicone rubber units relative to one another.

During the same year (1997) the author also installed leakage current monitoring equipment on new in-service silicone rubber insulators close to the Koeberg Nuclear Power Station on a 400 kV line. The leakage currents recorded were in the order of and below 10 mA. Electrical surface discharges were observed with an ultraviolet image-intensified camera (CoroCAM) and found to be present far from the live end along the insulator.

The publication "High-Voltage insulators: The backbone of transmission and distribution networks" [17] summarises the research and in-service experiences with non ceramic (polymeric) insulators in South Africa up to 1999. The publication shows that much ground has been covered towards a better understanding of the performance of non-ceramic insulators in South Africa. From the research to date it can be concluded that there is a difference in the performance of various non-ceramic (polymeric) insulator materials when subjected to a severe marine environment as encountered along the West Coast of South Africa. Silicone rubber insulators generally showed excellent performance when compared to porcelain, glass, EPDM, and cycloaliphatic units. The latter showed poor material and leakage current performance in West Coast marine environment. The silicone grease and coatings showed good performance when compared to bare porcelain. The resistive glazed porcelain yielded good results. However, in all the above tests there were too many other (non-material) variables that could have played a role in the performance. These include profile, inter-shed spacing, diameter, form factor, and connecting and creepage lengths. Thus, the effect of the material alone on the relative performance of various types of non-ceramic (polymeric) insulators is unknown. This prompted the research study described in this dissertation.

Stellenbosch University http://scholar.sun.ac.za

1.3 INSULATOR POLLUTION FLASHOVER - THE BASIC THEORY

Insulator pollution problems were experienced as early as the eighteenth century, as can be seen in this extract from the Encyclopaedia Britannica, Volume 'the second', by a Society of Gentlemen in Scotland, 1771, when electricity was thought to be *"a very subtile fluid matter, different in its properties from every other fluid we are acquainted with"* although it was not yet recognised as such*: "An iron wire, 12000 feet in length, was suspended about five feet from the ground by silk cords; one end of it was connected to the globe of an electrical machine, and at the other a lead ball was hung in order to perceive when the matter reached it. After five or six turns of the wheel, the matter had passed along the whole wire and communicated its virtue to the ball, which instantly attracted and repelled light bodies. The same effects are produced, though with more difficulty, when hair or woollen ropes were substituted in place of the silk ones: but they were entirely stopped by hemp ropes or when the silk ones were wetted".*

More than two centuries later, electrical insulation breakdown problems still exist due to pollution and wetting. However, there is a far better understanding of the processes leading to insulator pollution problems and how to mitigate them. The basic theories behind the insulator pollution flashover process are given below. They are partially based on the information obtained from a draft copy of the document "Polluted insulators: A review of current knowledge" compiled by CIGRE task force 33-04-01 [18]. Emphasis is placed on background information needed for a better understanding of the methodology followed in this research study.

The insulator pollution flashover process

In the CIGRE document [18] a description of the insulator pollution flashover process is given as follows:

" The pollution flashover process of insulators is greatly affected by the insulator's surface properties. Two surface conditions are recognised: either hydrophilic or hydrophobic. A hydrophilic surface is generally associated with ceramic insulators whereas a hydrophobic surface is generally associated with polymeric insulators, especially silicone rubber. Under wetting conditions - such as rain, mist etc. - hydrophilic surfaces will wet out

Stellenbosch University http://scholar.sun.ac.za

completely so that an electrolyte film covers the insulator. In contrast, water beads into distinct droplets on a hydrophobic surface under such wetting conditions.

In the Electra No. 64 publication [19], the pollution flashover process for ceramic insulators - that is, insulators with a hydrophilic surface - is described essentially as follows:

(a) The insulator becomes coated with a layer of pollution containing soluble salts or dilute acids or alkalis. If the pollution is deposited as a layer of liquid electrolyte - e.g. salt spray, stages (c) to (f) may proceed immediately. If the pollution is non-conducting when dry, some wetting process (stage (b)) is necessary.

(b) The surface of the polluted insulator is wetted either completely or partially by fog, mist, light rain, sleet or melting snow or ice and the pollution layer becomes conductive. Heavy rain is a complicating factor: it may wash away the electrolytic components off part or all of the pollution layer without initiating the other stages in the breakdown process, or it may - by bridging the gaps between sheds - promote flashover.

(c) Once an energised insulator is covered with a conducting pollution layer, a surface leakage current flows and its heating effect starts to dry out parts of the pollution layer.

(d) The drying of the pollution layer is always non-uniform and, in places, the conducting pollution layer becomes broken by dry bands that interrupt the flow of leakage current.

(e) The line-to-earth voltage is then applied across these dry bands, which may only be a few centimetres wide. It causes air breakdown to occur and the dry bands are bridged by arcs, which are electrically in series with the resistance of the undried portion of the pollution layer. A surge of leakage current occurs each time the dry bands on an insulator spark over.

(f) If the resistance of the undried part of the pollution layer is low enough, the arcs bridging the dry bands are able to burn continuously and so may extend along the insulator; thereby spanning more and more of its surface. This in turn decreases the resistance in series with the arcs, increases the current and permits the arcs to bridge even more of the insulator surface. Ultimately the insulator is completely spanned and a line-to-earth fault is established. "

Stellenbosch University http://scholar.sun.ac.za

One can summarise the whole process as an interaction between the insulator, pollutants, wetting conditions, and applied voltage. Thus, for a better understanding of the insulator pollution, wetting and the flashover process, the following should be studied:

- The local climate and environmental (pollution) conditions surrounding the insulator, with emphasis on wetting, pollution sources and types of pollution.
- The insulator pollution deposit process, wetting and the final surface pollution level.
- Visual observations of the insulator surface condition, looking for material degradation.
- The electrical surface discharge activity on the insulator.
- Leakage current flowing over the surface of the insulator.

The leakage current and surface resistance of a polluted insulator

It has been estimated that the power-frequency flashover voltage of an insulator can be reduced by a factor of as much as eight when moderately polluted [20]. It is therefore important to monitor the presence of a conducting electrolytic pollution layer on an insulator surface. Leakage current is recognised worldwide [21] as one of the main parameters for performance measurement of insulators. Small currents (in the order of several mA) can cause severe damage to non-ceramic insulating materials (due to sparking). This current degrades the insulation and can finally lead to electrical and/or mechanical breakdown of the insulator. It has also been shown that the flashover probability becomes very high if the insulator leakage current approaches a certain threshold value. This value has been defined, based on experimental work by Verma [22], as the peak leakage current one cycle before flashover (I_{max}):

$$I_{\max} = \left(\frac{S_{CD}}{15.32} \right)^2 \tag{1.1}$$

with S_{CD} the specific creepage distance, given by

$$S_{CD} = \frac{L}{U_{\max}} \tag{1.2}$$

where

L : total insulator creepage distance in mm

U_{max} : maximum rms system voltage phase to phase in kV

Stellenbosch University http://scholar.sun.ac.za

Thus the measured values of the peak leakage current over the insulator can be compared to the calculated I_{max} value and the risk of potential flashover determined. Holtzhausen [23] proposed a permissible value of the peak leakage current (I_{perm}) as:

$$I_{perm} = 0.25 \cdot I_{\max} \tag{1.3}$$

where

I_{perm} : highest permissible peak value of the leakage current in ampere

The surface layer resistance is the main factor determining the magnitude of the insulator leakage current and also whether an insulator will flash over or not.

To determine the surface layer resistance of a uniform electrolytic pollution layer on an insulator as described in steps (a) and (b) above, the following basic formula for the resistance R (MΩ) of a resistive element of length L (mm), cross sectional area A (mm^2) and volume resistivity ρ (MΩ.mm) is used: $R = \dfrac{\rho \cdot L}{A}$

Consider Figure1. 1, which shows the visual representation of the electrolytic pollution layer on an arbitrary insulator surface.

The following variables are defined in this figure:

R_{pol} : surface layer resistance of the insulator electrolytic pollution layer without an arc in MΩ,

ρ_{pol} : volume resistivity of the electrolytic pollution layer, in MΩ.mm

L : total insulator creepage distance, in mm

A_{pol} : cross sectional area of the electrolytic pollution layer at position l, in mm^2, as calculated by $A_{pol} = \pi \cdot D(l) \cdot h_{pol}$, where:

$D(l)$: diameter of insulator at position l along the insulator creepage path in mm

h_{pol} : thickness of the uniform electrolytic pollution layer in mm

Stellenbosch University http://scholar.sun.ac.za

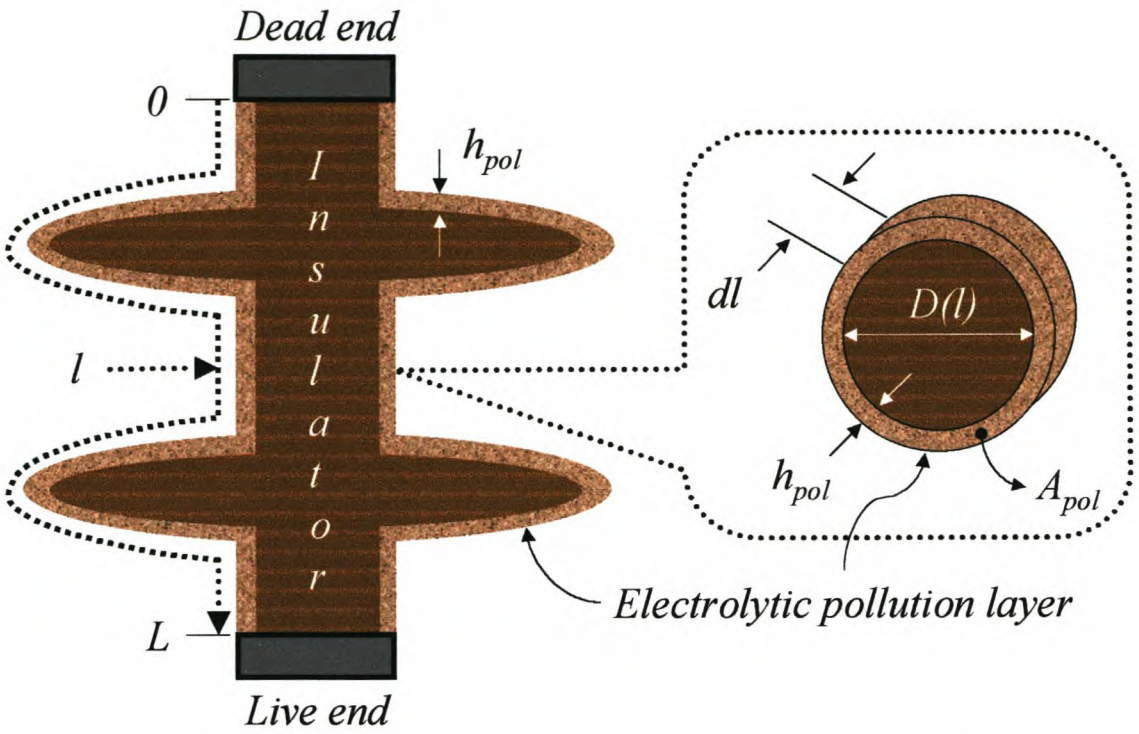

Figure1. 1 Visual representation of the electrolytic pollution layer on an insulator.

Dividing the surface electrolytic pollution layer into small incremental sections dl along the insulator creepage path L and using the basic formula $R = \frac{\rho \cdot L}{A}$, the resistance dR_{pol} of the incremental section is given by:

$$dR_{pol} = \frac{\rho_{pol} \cdot dl}{A_{pol}}$$

Substituting A_{pol} and integrating on both sides leads to $R_{pol} = \frac{\rho_{pol}}{h_{pol}} \int_0^L \frac{dl}{\pi \cdot D(l)}$ (1.4)

Also $\sigma = \frac{1}{\rho_{pol}}$ (1.5)

and $\sigma_s = \sigma \cdot h_{pol}$ (1.6)

where

σ : volume conductivity of insulator electrolytic pollution layer in μS/mm

σ_s : surface conductivity of insulator electrolytic pollution layer in μS

Stellenbosch University http://scholar.sun.ac.za

Substitution of (1.5) and (1.6) into (1.4) leads to

$$R_{pol} = \frac{F}{\sigma_s} \tag{1.7}$$

wherein $F = \int_0^L \frac{dl}{\pi \cdot D(l)}$ is defined as the form factor of the insulator (1.8)

The surface conductivity (σ_s) of the electrolytic pollution layer is dependent on the temperature. Wilkins [24] showed that, when heated from 20 to 100 °C, the surface conductivity of a salt solution layer may increase by a factor of 2.76 to 3.00. Thus, the surface conductivity of a "cold" non-energised insulator is lower than that of a "hot" energised insulator.

Equivalent circuit for the insulator leakage current, conductance and surface conductivity

Figure1.2 is a schematic electrical diagram representing the dry-band as described in steps (c) and (d) above, including the electrolytic pollution layer on an insulator.

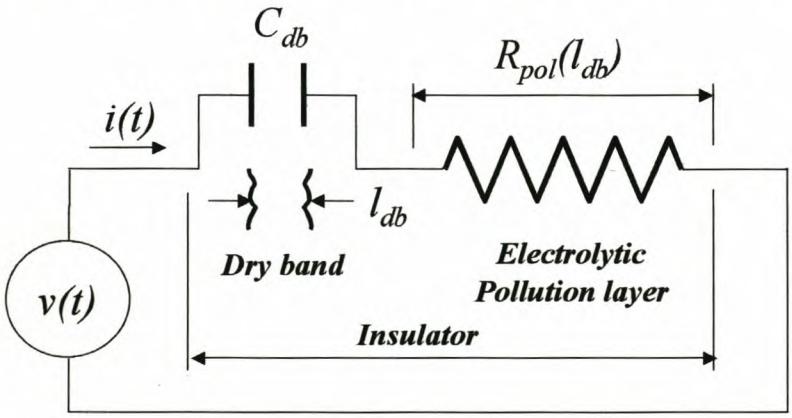

Figure1.2 Schematic electrical diagram representing the dry-band and electrolytic pollution layer on an insulator.

In the above figure:

C_{db} : capacitance of the dry-band in pF

$i(t)$: leakage current in mA

$v(t)$: supply voltage in kV

Stellenbosch University http://scholar.sun.ac.za

Taking the shortening of the uniform electrolytic pollution layer by the dry-band into consideration the surface resistance is calculated as:

$$R_{pol}(l_{db}) = R_{pol} \cdot \left(1 - \frac{l_{db}}{L}\right) \tag{1.9}$$

where

$R_{pol}(l_{db})$: resistance of the insulator electrolytic pollution layer with a dry-band in MΩ

l_{db} : length of the dry-band in mm

It should be noted that when $\frac{l_{db}}{L} << 1$ then $R_{pol}(l_{db}) \approx R_{pol}$

Figure1.3 is a schematic electrical diagram representing the dry-band discharge (spark/arc) as described in steps (e) and (f) above, including the electrolytic pollution layer on the insulator.

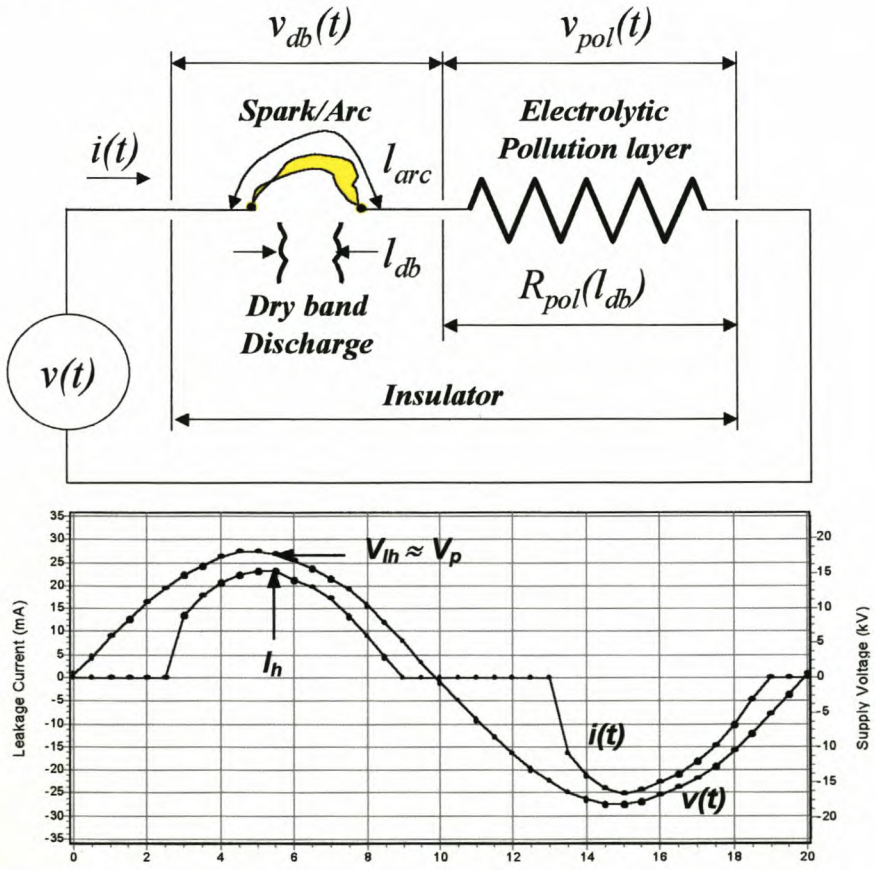

Figure1.3 Schematic electrical diagram representing the dry-band discharge (spark/arc) and electrolytic pollution layer on an insulator. An example of a typical leakage current and supply voltage waveform is included.

Stellenbosch University http://scholar.sun.ac.za

In the following section, the following definitions of the variables apply:

R_{ins} : resistance of the insulator in MΩ

G_{ins} : conductance of the insulator in μS

$G_{ins}(t)$: conductance of the insulator at time t in μS

$G_{pol}(l_{db})$: conductance of the electrolytic pollution layer considering the dry-band in μS

$v_{pol}(t)$: voltage across the electrolytic pollution layer in kV

I_h : peak value of the leakage current in mA

V_{Ih} : peak value of the supply voltage in kV when the leakage current is at a peak

V_p : peak value of the supply voltage in kV

$v_{db}(t)$: voltage across the dry-band in kV

The voltage equation for the complete circuit in Figure1.3 is given as:

$$v(t) = v_{db}(t) + v_{pol}(t)$$

Dividing both sides by $i(t)$: $\frac{v(t)}{i(t)} = \frac{v_{db}(t)}{i(t)} + \frac{v_{pol}(t)}{i(t)}$ (valid when $i(t) \neq 0$)

but since $R_{pol}(l_{db}) = \frac{v_{pol}(t)}{i(t)}$ it follows that

$$i(t) = \frac{v(t) - v_{db}(t)}{R_{pol}(l_{db})}$$

and that $\frac{i(t)}{v(t)} = \frac{1}{R_{pol}(l_{db})} \cdot \left(\frac{v(t)}{v(t)} - \frac{v_{db}(t)}{v(t)} \right)$

Also: $G_{ins}(t) = \frac{i(t)}{v(t)}$ (1.10)

and $G_{pol}(l_{db}) = \frac{1}{R_{pol}(l_{db})}$

$$\therefore G_{ins}(t) = G_{pol}(l_{db}) \cdot \left(1 - \frac{v_{db}(t)}{v(t)} \right)$$

The voltage drop across the dry-band is often small compared to the applied voltage, i.e.

$\frac{v_{db}(t)}{v(t)} << 1$, therefore: $G_{ins}(t) \approx G_{pol}(l_{db})$ (1.11)

Stellenbosch University http://scholar.sun.ac.za

The last equation implies that the surface conductance is constant, independent of t, and thus also applies at the instant when the current is at its peak, i.e.

$$G_{ins}(t) \approx G_{ins} = \frac{I_h}{V_{Ih}} \text{ or } G_{ins} = \frac{I_h}{V_p} \text{ (when } V_{Ih} \approx V_p) \tag{1.12}$$

Also: $$R_{ins} = \frac{1}{G_{ins}} = \frac{V_p}{I_h} \tag{1.13}$$

From (1.7) and (1.13) when $R_{ins} = R_{pol}$: $$\sigma_s = F \cdot G_{ins} \tag{1.14}$$

The surface conductivity of the insulator can therefore be estimated, using (1.12) and (1.14), by measuring the peak voltage and peak leakage current.

The voltage across the dry-band, $v_{db}(t)$, is a non-linear function of the current. At low values of current, near the zero crossing, conduction is ionic and the voltage is roughly proportional to the current. However, once a stable arc is established at higher current levels, the relationship is non-linear and displays a negative resistance, typically as given by the formula by Ayrton [25] as:

$$v_{db}(t) = A \cdot l_{arc} \cdot 10^{-3} \cdot \left(i(t) \cdot 10^{-3}\right)^{-a} \tag{1.15}$$

where

l_{arc} : length of the arc in mm (typically 10 mm)

A = 10 (arc constant)

a = 0.53 (constant)

This validates the assumption (1.11), i.e. $\frac{v_{db}(t)}{v(t)} << 1$, as the arc voltage decreases with increasing current and is therefore usually small in comparison to the supply voltage.

Experimental results obtained in the laboratory for low levels of arc currents indicate that at a peak arc current of 10 mA, the arc voltage across a 10 mm air gap is less than 1 kV peak. In practice the voltage across a dry band (v_{db}) should be further reduced due to the parallel conducting path in the dry band. This validates the assumption in Equation 1.11 above for low levels of current.

Stellenbosch University http://scholar.sun.ac.za

Insulator critical flashover voltage

When the insulator surface resistance (R_{ins}) reaches a critical low value the critical flashover voltage in kV of the insulator is given by the formula proposed by Rizk and modified by Holtzhausen [20] as:

$$V_c = k_1 \cdot 10^{-3} \cdot \left(\frac{R_c \cdot 10^6}{L} \right)^{k_2} \cdot L \qquad (1.16)$$

where

V_c : critical insulator flashover voltage in kV

R_c : critical insulator resistance in MΩ which is the critical value R_{ins}

k_1 = 7.6

k_2 = 0.35

1.4 RESEARCH OBJECTIVE AND SCOPE OF WORK

The main objective of this research programme is to compare the relative performance of various insulators over a one-year period, starting with brand new clean insulators, while observing the climatic, environmental, surface conditions, electrical discharge activity and leakage current of the main types of insulating materials used for high-voltage insulators in South Africa, when subjected to a severely polluted coastal environment as encountered along the local Cape West Coast.

Scope of work:

- Establish test programme and procedure
- Establish test facility
- Establish instrumentation
- Collect data and make observations over a one-year period
- Analyse data, investigation of trends, correlations and relative ranking of insulators.

It is envisaged that the knowledge gained could be used in the selection of suitable high-voltage insulator materials for use in severe coastal environments, both nationally and internationally.

Stellenbosch University http://scholar.sun.ac.za

1.5 STRUCTURE OF DISSERTATION

The dissertation comprises eight chapters.

In **Chapter 1** the background, literature survey, and basic theory of insulator pollution flashover is described, and the research objective and scope of work is stated.

In **Chapter 2** the philosophy behind the test programme, the methodology used to achieve the research objectives, and a description of the non-standard equipment developed to implement the test procedure are discussed.

In **Chapter 3** the influence of environmental and climatic conditions on high-voltage insulators is discussed. An environmental and climatic survey of the area surrounding the Koeberg Insulator Pollution Test Site (KIPTS) is discussed, with emphasis on the expected conditions to which the test insulators will are subjected during the test programme. Results of the monitoring of environmental and climatic conditions during the test programme are given and discussed.

In **Chapter 4** the insulator pollution and wetting processes encountered on the test insulators at KIPTS during the test programme are described. The modes of pollution deposit and wetting are emphasised. Insulator pollution present on the test insulators during the test programme was monitored and the results given and discussed.

In **Chapter 5** the results of the insulator surface condition inspections and of the electrical discharge activity monitored are described and discussed.

In **Chapter 6** the philosophy of why leakage current monitoring is important in the test programme and the reason why the various leakage current parameters are monitored are discussed. The results of the leakage currents monitored during the test programme are presented and discussed. The data where also tested for correlation. The leakage current data is compared with data obtained during the test programme from the environmental and climatic conditions, insulator pollution, and visual and electrical discharge activity for a focused period of one week, showing pollution and washing events.

Stellenbosch University http://scholar.sun.ac.za

In **Chapter 7** specific aspects emanating from the research program are discussed. For example, a new regression idea is proposed.

Chapter 8 contains a final summary of the findings, conclusions derived from the test programme, and recommendations.

These chapters are followed by the references and a list of publications that have emanated from this research, and Appendices A to F. Appendix A gives a list of the variables used, Appendix B includes the time line for the test programme, Appendix C describes the basic statistical methods used in this dissertation. In Appendix D the insulator surface condition inspections are given, Appendix E contains the electrical discharge activity observations and Appendix F indicates the leakage current measurements done.

Stellenbosch University http://scholar.sun.ac.za

2 TEST METHODOLOGY AND EQUIPMENT DEVELOPED TO ACHIEVE THE RESEARCH OBJECTIVE

"Genius is one per cent inspiration and ninety nine per cent perspiration" – ***Thomas Edison***

In this chapter the test programme devised and followed to achieve the research objective, as outlined in the previous chapter, is discussed. This includes descriptions of:

- the philosophy behind the test programme,
- test methodology used to achieve the research objective, and
- the special (non-standard) equipment developed for the test programme.

Due to the nature of the test programme an action research methodology [26] was followed. This methodology caters for the development of new ideas and methods required to achieve the goals.

2.1 PHILOSOPHY BEHIND THE TEST PROGRAMME

To achieve the overall research objective, namely "A Comparison of the Performance of High-Voltage Insulator Materials in a Severely Polluted Coastal Environment", the following philosophy was adopted:

- Identify the insulator materials to be evaluated.
- Eliminate the non-material design variables (e.g. creepage distance, connecting length, inter-shed spacing, profile, etc.).
- Compare the insulator performance results of the test insulators with those obtained from a stable insulator material within the same environment.
- Study insulator performance in both energised and non-energised modes in order to distinguish between the ageing effects from environmental and climatic conditions as opposed to the ageing effects from electrical energisation.
- Choose the test environment and test period such as to represent a severe coastal condition.

Stellenbosch University http://scholar.sun.ac.za

- Establish a suitable test procedure to monitor the performance variables using suitable and known test methods, and where no known methods and equipment exist, develop new methods and equipment.
- Be able to handle the large volume of data expected over the test period, and be able to analyse it to the depth required. Computer programs were to be developed for this purpose.
- It was envisaged that special care and dedication would be required for the duration of the project to ensure continuity and minimal loss of data.

2.2 METHODOLOGY USED TO ACHIEVE THE RESEARCH OBJECTIVE

From the above philosophy, a test methodology as described below was developed to achieve the research objective.

2.2.1 Choice of insulator materials

The two main insulator materials of interest (as described in section 1.1) were identified as

- High-temperature vulcanised (HTV) silicone rubber (SR), with fumed aluminiumtrihydrate (ATH) filler and
- Ethylene propylene diene monomer (EPDM) rubber, with fumed aluminiumtrihydrate (ATH) filler.

The following materials were also evaluated:

- Pre-primed (glazed, quartz-filled) porcelain surface coated with sprayable, two-part, (catalyst added to cure) room-temperature vulcanised (RTV), fumed ATH-filled silicone rubber (SR)
- Cycloaliphatic epoxy resin with silane-treated silica filler (quartz)
- Resistive/semiconductive (antimony-doped tin oxide), glazed (RG), aluminium-filled porcelain.

Stellenbosch University http://scholar.sun.ac.za

The performance of the five materials tested was compared to the glazed, quartz-filled porcelain. Porcelain is a stable insulating material when correctly manufactured and is inert to ageing. The glazed surface can nonetheless be damaged when electrically overstressed. It may melt, crack, puncture, flake, or become chipped or slightly roughened with time. These modes of ageing are, however, well understood and are not expected if the material is correctly applied.

2.2.2 Choice of test insulators

Many variables affect the performance of insulators, such as physical dimensions (creepage distance, arcing distance, shank diameter, shed diameter and profile etc), type of material, climatic and environmental conditions, and power system conditions (power-frequency and impulse over voltages).

As mentioned in section 2.1, part of the philosophy adopted was to eliminate the non-material design variables. The main variable that had to be eliminated was the physical dimensions of the insulator. Thus, the only difference between the insulators used in the programme was their material compositions. The insulator profile had to comply with IEC 60815 specification [1] and have a specific creepage distance of not less than 25 mm/kV.

HTV SR and EPDM insulators with identical dimensions (as they were from the same mould), which fully comply with the above criteria, were commercially available. However, there were no porcelain, cycloaliphatic epoxy resin nor RG porcelain insulators available with similar dimensions and shape. As the poor mechanical properties of porcelain and cycloaliphatic insulators with such dimensions would make it impractical to commercially manufacture such insulators (due to the small shank diameter required), special insulators had to be manufactured to meet the dimension requirements for the present test programme. After consultation with the manufacturers, a tolerance of ±5% in creepage distance was agreed upon. Due to the cost involved in manufacturing the insulators, a supply phase voltage of 12.7 kV rms (corresponding to a line or phase-to-phase voltage of 22 kV) was chosen. The different insulators used in the programme are shown in Figure 2. 1. The physical and electrical characteristics of the test insulators are given in Table 2. 1. For the purpose of simplification, the following abbreviations are introduced to identify the test insulators:

Stellenbosch University http://scholar.sun.ac.za

S - High-temperature vulcanised (HTV) silicone rubber (SR), fumed aluminiumtrihydrate (ATH)-filled

E - Ethylene propylene diene monomer (EPDM), fumed aluminiumtrihydrate (ATH)-filled

P - Glazed, quartz-filled porcelain

C - Pre-primed (glazed, quartz-filled) porcelain surface, coated with a sprayable, two-part (catalyst added to cure), room-temperature vulcanised (RTV), fumed ATH-filled silicone rubber (SR)

A - Cycloaliphatic epoxy resin with silane-treated silica filler (quartz)

R - Resistive/semiconductive (antimony-doped tin oxide) glazed (RG), aluminium-filled porcelain

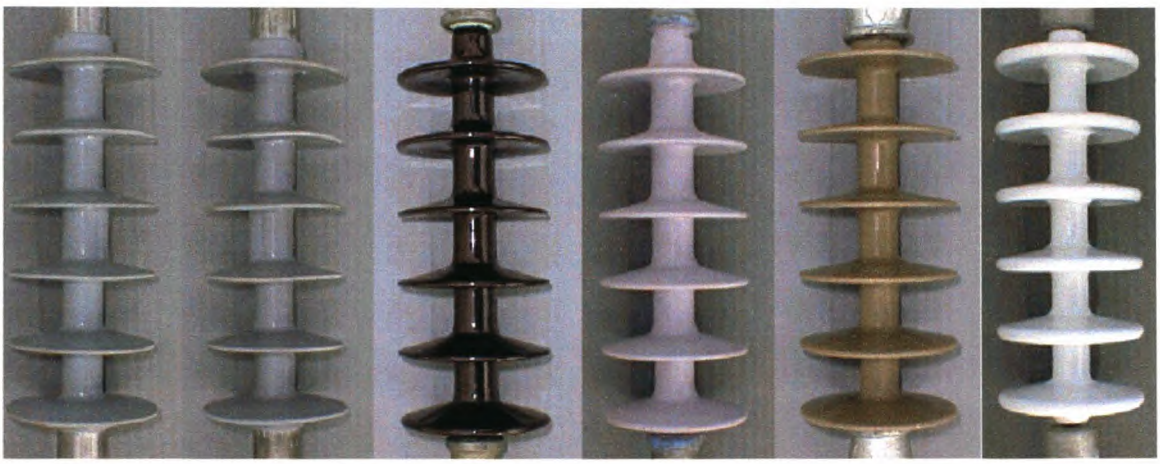

S **E** **P** **C** **A** **R**

Figure 2. 1 Photograph showing the different test insulators to be evaluated in the programme

Table 2. 1 Tabulation of the average dimensions of the test insulators (shown in Figure 2.2) and the IEC 60815 recommended requirements

Insulator physical and electrical characteristics		IEC 60815
Creepage distance (mm)	612	
Supply voltage (Umax, kV-rms, line voltage)	24	
Specific creepage distance (mm/kV)	25.3	
Arcing distance (mm)	304	
Shed diameter (mm)	95	
Shed spacing (mm)	44	
Shed clearance (mm)	40	> 20
Shed projection (mm)	35	
Shed spacing/clearance	1.26	> 0.65
Shed top inclination (deg)	13	> 5
Shed bottom inclination (deg)	3	> 2
Core diameter (mm)	25	
Surface area (cm^2)	1000	
Form factor	4.83	
Creepage factor	2	< 4
Profile factor	1.2	> 0.7

Stellenbosch University http://scholar.sun.ac.za

2.2.3 Choice of test location and test period

Previous studies by Macey, Vosloo, and Van Wyk [6, 13, 27] confirmed that the Koeberg insulator pollution test site (KIPTS) is characterised by dry summers, with rain occurring predominantly during winter. In addition, high winds and mist banks contribute to heavy marine and industrial pollution on the insulator surfaces. The pollution index at KIPTS is of the order of 2000 (μS/cm), which is extremely high (>350 μS/cm is rated by Macey [6] as very heavy). Results of preliminary studies showed that the material degradation and ageing modes at KIPTS after one year were more severe than those experienced in the IEC 5000-hour accelerated ageing test [28]. Field experience of flashovers on power lines also proved the area to be severe [8, 12]. KIPTS was therefore considered as the ideal severe coastal environment in which to evaluate insulator materials.

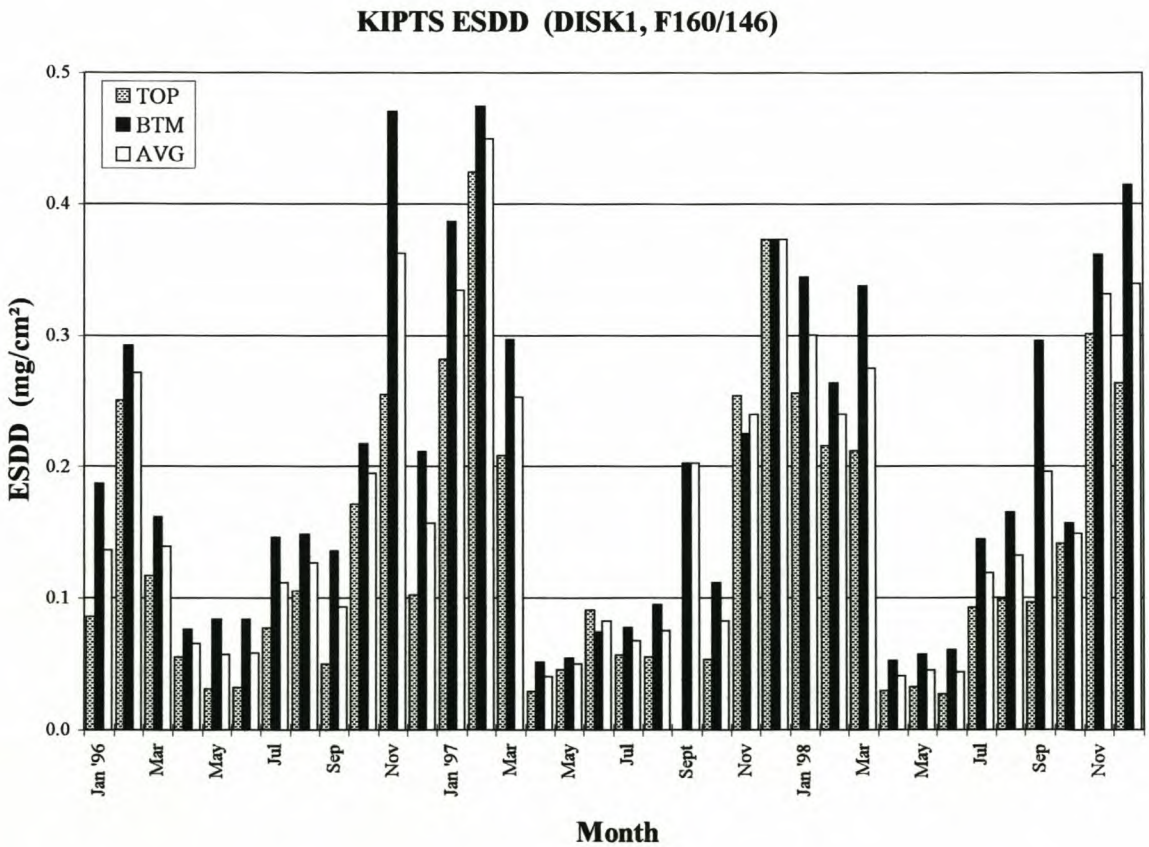

Figure 2. 2 Monthly equivalent salt-deposit density (ESDD) measurements at KIPTS on F160/146 glass disks (1996 - 1998)

Stellenbosch University http://scholar.sun.ac.za

The monthly values of equivalent salt-deposit density (ESDD) at KIPTS, for the years 1996 to 1998, are shown in Figure 2. 2. The lowest pollution levels recorded during this period were found to occur during the month of April each year. The pollution starts to increase during September and reaches maximum levels during the months of November to March (the summer months). The period from late April to early September is classified as the lower pollution winter-cycle, while the period from late September to early April is associated with the higher pollution summer-cycle.

Commencing in April 1999, the insulators to be used in the test programme were all to be energised simultaneously, and exposed to the severe coastal environment at KIPTS for a period of one full year. The test insulators were to be subjected to the lower pollution winter-cycle first, followed by the higher pollution summer-cycle.

2.2.4 Installation of test insulators

Both energised and non-energised insulators were tested in the programme. The non-energised insulators were used to determine how the materials aged due to the climatic and environmental conditions only, excluding electrical effects. Three insulators of each of the two main types S and E were installed for testing so that their results could be compared for consistency. In order to compare the performances of the S, E, C, A and R insulators to the reference insulator P, an insulator test grid as shown in Figure 2.3 was formulated. Ten energised (at phase voltage of 12.7 kV rms) and ten non-energised test positions were required. The numbers 1 to 10 indicate the test positions and the symbols S, E, P, C, A and R represent the materials. The visual appearance of the samples due to ageing was compared, as indicated by the dotted lines. The test insulators used (energised and non-energised), and their positions, can be summarised as follows:

1S, 6S, and 9S - High-temperature vulcanised (HTV) silicone rubber (SR), fumed aluminiumtrihydrate (ATH)-filled

2E, 7E, and 10E - Ethylene propylene diene monomer (EPDM), fumed aluminiumtrihydrate (ATH)-filled

3P - Glazed, quartz-filled porcelain

4C - Pre-primed (glazed, quartz-filled) porcelain surface, coated with sprayable, two-part (catalyst added to cure), room-temperature Vulcanised (RTV), fumed ATH-filled silicone rubber (SR)

Stellenbosch University http://scholar.sun.ac.za

5A - Cycloaliphatic epoxy resin with silane-treated silica filler (quartz)

8R - Resistive/semiconductive (antimony-doped tin oxide) glazed (RG), aluminium-filled porcelain.

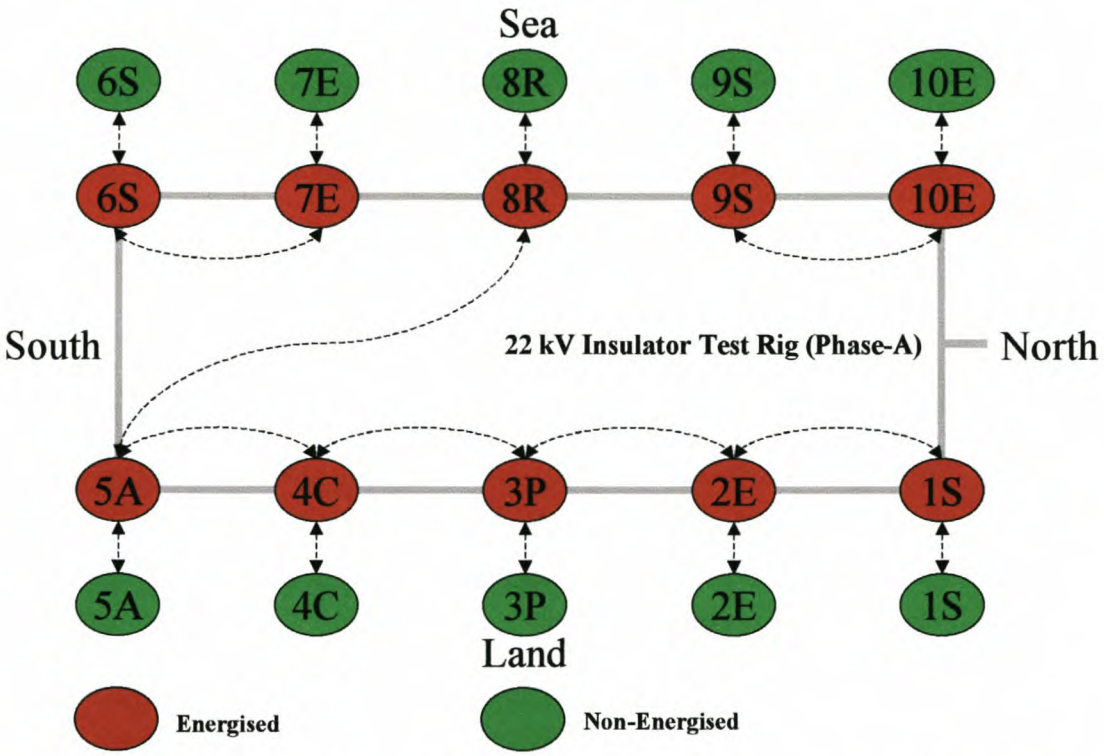

Figure 2. 3 Schematic layout of the test positions of the insulators (shown in Figure 2.1). (The dotted lines indicate the comparisons made)

The test insulators were installed on the Phase A arm of the 22 kV Insulator test rig (see section 2.3 for more information on the test rig). The test insulators 1S, 2E, 3P, 4C, 5A and 8R (energised and non-energised) were to be monitored and observed with minimum disturbance, to minimise any test-method induced impact on the ageing. The test insulators 6S and 7E (energised and non-energised) were used for the local ESDD (LESDD) and IPMA tests (as described in the test procedure, section 2.2.5). Material samples for the material studies were taken from test insulators 9S and 10E (energised and non-energised). The results are not included in this dissertation; they are reported separately as part of the larger Eskom research programme. During the first six weeks of the test programme the 8R insulators were not available. The test position was temporally filled by 8P, a glazed and quartz-filled porcelain longrod. The 8R test insulators were installed in test position eight during week seven.

Stellenbosch University http://scholar.sun.ac.za

2.2.5 Test procedure

During previous studies carried out at KIPTS, hydrophobicity loss within one month was found on both HTV SR and EPDM insulators [3]. It was also found that within this period the electrical discharge activity reached the stage of dry-band formation and leakage current levels of the order of tens of milli-amps [3]. For the duration of the present test procedure it was therefore decided that focussed detailed observations would be made during the first six weeks, followed by week-long observations every sixth week thereafter.

Climatic and leakage current parameters (as discussed in section 2.3) were to be continuously monitored using the IH48 and OLCA logger systems. Channel nine of the OLCA (complete with leakage current sensor) was left floating within the 22 kV insulator test rig to check for any possible background electronic noise. The environmental and climatic studies for the test programme were performed in accordance with the "Round Robin Pollution Monitoring Study Test Protocol", of CIGRE task force 33.04.03 [29] and Appendix A of IEC 60815 ("Guide for the selection of insulators in respect of polluted conditions") [1]. All test equipment was installed and calibrated, and trial runs carried out to check the operation thereof prior to commencing with the test programme.

Test procedure carried out in the first six weeks

The detailed test procedure carried out in the first six weeks was as follows:

a) Electrical surface activity observations were made every night between 22h00 and 24h00 on test insulators 1S, 2E, 3P, 4C and 5A using image-intensified, ultraviolet-sensitive, CoroCAM Mark I and Mark II video cameras (see section 2.3 for details of the CoroCAM systems). One-minute observations from both the land and sea sides (covering all angles of observation) were made using the CoroCAM Mark I, and stored on videotape. Using the CoroCAM Mark II the electrical surface activity on the selected test insulators was also monitored from the land side and one-minute recordings stored on videotape. In addition, the visual electrical surface activity, in synchronism with the leakage current present (for 16 voltage cycles, for a pre-selected leakage current trigger level), was captured and stored on hard drive using the CoroCAM Mark II.

Stellenbosch University http://scholar.sun.ac.za

b) Daily IPMA (see section 2.3 for detail of the IPMA) surface conductivity recordings were made on both glass disk (U120BS, cap and pin) and porcelain (identical to the P type) longrod insulators (and stored on hard drive). The installation of the two IPMA test insulators can be seen in Figure 2. 11.

c) Daily visual weather observations were made and tabulated. Climatic data (wind direction and speed, precipitation, and ambient temperature) recorded by the Koeberg weather station was obtained for correlation with the data recorded at KIPTS.

d) Equivalent salt-deposit density (ESDD) and non-soluble deposit density (NSDD) readings were taken (tabulated) on Fridays on both glass disk (U120BS, cap and pin) and porcelain (identical to P type) longrod insulators. The two ESDD and NSDD test insulators were installed on the IPMA structure (see Figure 2. 11).

e) Directional dust deposit gauge (DDG) readings were recorded on Fridays. The DDG was installed at a 3-meter level, the same level as the test insulators.

f) Localised ESDD (LESDD) readings were made (tabulated) on Fridays on insulators 6S and 7E on the energised and non-energised units. Four readings corresponding to the cardinal points (North, East, South, and West) were taken on the top of the sheds. The LESDD test commenced at the first shed on the live side for week one, ending with the sixth shed on the earth side for week six. By not performing tests on the same shed every week, the disturbance of the pollution layer was minimised.

g) IPMA surface conductivity (indicating the surface condition) recordings were made (and stored on hard drive) on Fridays on insulators 6S, 7E and 8P energised and non-energised.

h) Visual observations (tabulated) including hydrophobicity and digital photos (stored on hard drive) were made on Fridays on test insulators 1S, 2E, 3P, 4C and 5A energised and non-energised.

i) Material samples were taken on Fridays from the second shed on the live side from insulators 9S and 10E, energised and non-energised. This was done with a special sampling tool and associated test procedure [30]. The samples were taken to the University of Stellenbosch for analysis as part of the larger Eskom research programme.

j) Daily backups of all the recorded data were made.

Stellenbosch University http://scholar.sun.ac.za

Six-weekly, week-long test procedure

The detailed, week-long observation test procedure, performed every sixth week, was identical to that of the first six weeks, with the exception that the IPMA and the daily weather observations were omitted.

During the first week after completion of the test programme, IPMA surface conductivity (indicating the surface condition) recordings were made (and stored on hard drive) on test insulators 1S, 2E, 3P, 4C and 5A, energised and non-energised. These gave an indication of the conditions of the surfaces.

The results obtained during the test programme are presented and discussed in Chapters 3 to 6. The relevance of the parameters monitored in the test programme is discussed.

2.3 SPECIAL EQUIPMENT DEVELOPED FOR THE TEST PROGRAMME

Special non-standard equipment and procedures were required to be able to carry out the research required in order to achieve the research objectives. Suitable test procedures were formulated. The required test equipment was designed, and then built under the guidance of the author. The resulting equipment and related products are now commercially available on the international market. The development of these innovative systems led to the author being awarded the SAIEE (South African Institute of Electrical Engineers) President's Award in 1997. The equipment designed and/or developed and used is discussed below.

2.3.1 22 kV Insulator Test Rig

A 22 kV insulator test rig (see Figure 2. 4) was designed and built, under the guidance of the author, to house the ten energised and ten non-energised test insulators. Only one of the three available phases (phase-A) was used for the test programme, to ensure that all specimens were tested under the same voltage conditions.

The ten energised insulators to be tested were energised from a 400 V/22 kV, 50 kVA three-phase delta/star transformer (TRFR). An explosive Mace fuse was used to isolate

Stellenbosch University http://scholar.sun.ac.za

the test insulator from the 22 kV busbar for currents above 0.75 Ampere peak. The system was suitably protected and controlled from a control box (CNTR) attached to the unit. The star point of the transformer was directly earthed to the station earth. The test insulators were energised at a phase voltage of 12.7 kV (rms), 17.96 kV (peak). A single-phase voltage transformer (VT) monitored the voltage.

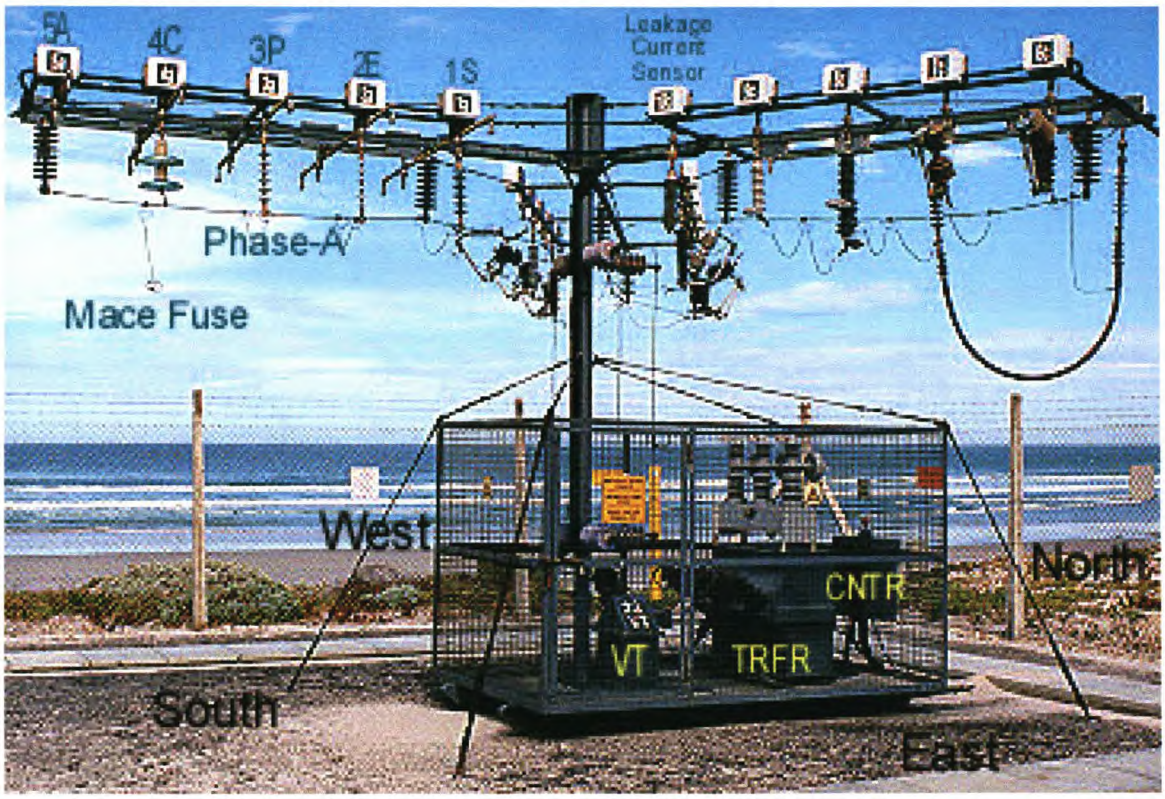

Figure 2. 4 22 kV insulator test rig, showing the orientation and main components

The short circuit current, I_{sc} phase to earth, was 86 A (rms) at the 22 kV busbar. The R/X ratio was 0.48 and the I_{sc}/I_H ratio 11.5, well within the IEC 60507 recommendations [31] (I_H being the highest peak leakage current expected).

A schematic electrical diagram representing the supply transformer impedance in circuit with the insulator is shown in Figure 2. 5. The voltage drop across the transformer impedance is calculated using the formula:

$$v_{Trfr}(t) = L_{Trfr} \cdot \frac{i(t+\Delta t) - i(t)}{\Delta t} + R_{Trfr} \cdot i(t) \qquad (2.1)$$

Stellenbosch University http://scholar.sun.ac.za

where

L_{Trfr} = 422.7 mH (Winding inductance)

R_{Trfr} = 63.02 ohm (Winding resistance)

Δt = 1 μs

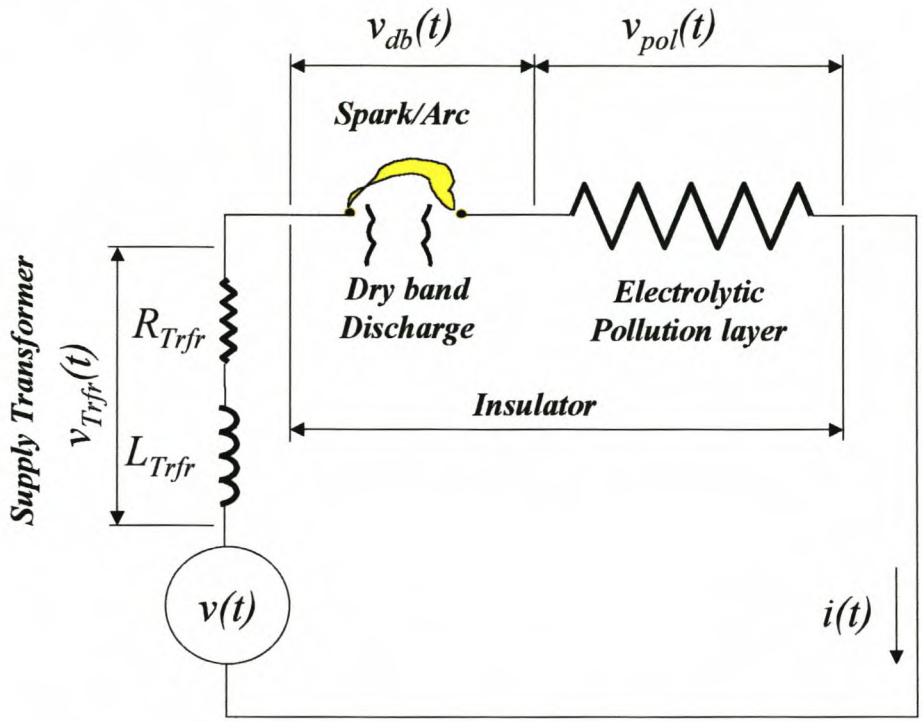

Figure 2. 5 Schematic electrical diagram representing the supply transformer impedance and insulator.

Using Eq. 2.1 and captured insulator leakage current and supply voltage waveform (as shown in Figure 2. 6 (a)) the expected voltage drop across the supply transformer impedance was calculated and plotted in relation to time (see Figure 2. 6 (b)).

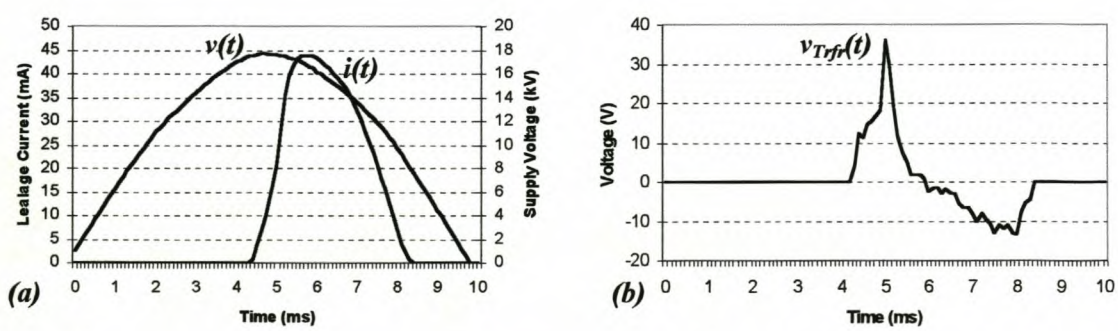

Figure 2. 6 Leakage current and supply voltage waveforms measured (a) and associated calculated test transformer voltage drop (v_{Trfr}) (b).

Stellenbosch University http://scholar.sun.ac.za

The expected voltage drop across the supply transformer impedance is in the order of tens of volts, and when related to the supply voltage of approximately 18 kV it can be neglected.

The 22 kV insulator test rig complete with leakage current logging systems (as discussed in section 2.3.2) was checked for possible phase shifts in the measuring circuits by using a resistive glazed insulator as test sample. The results obtained are shown in Figure 2. 7.

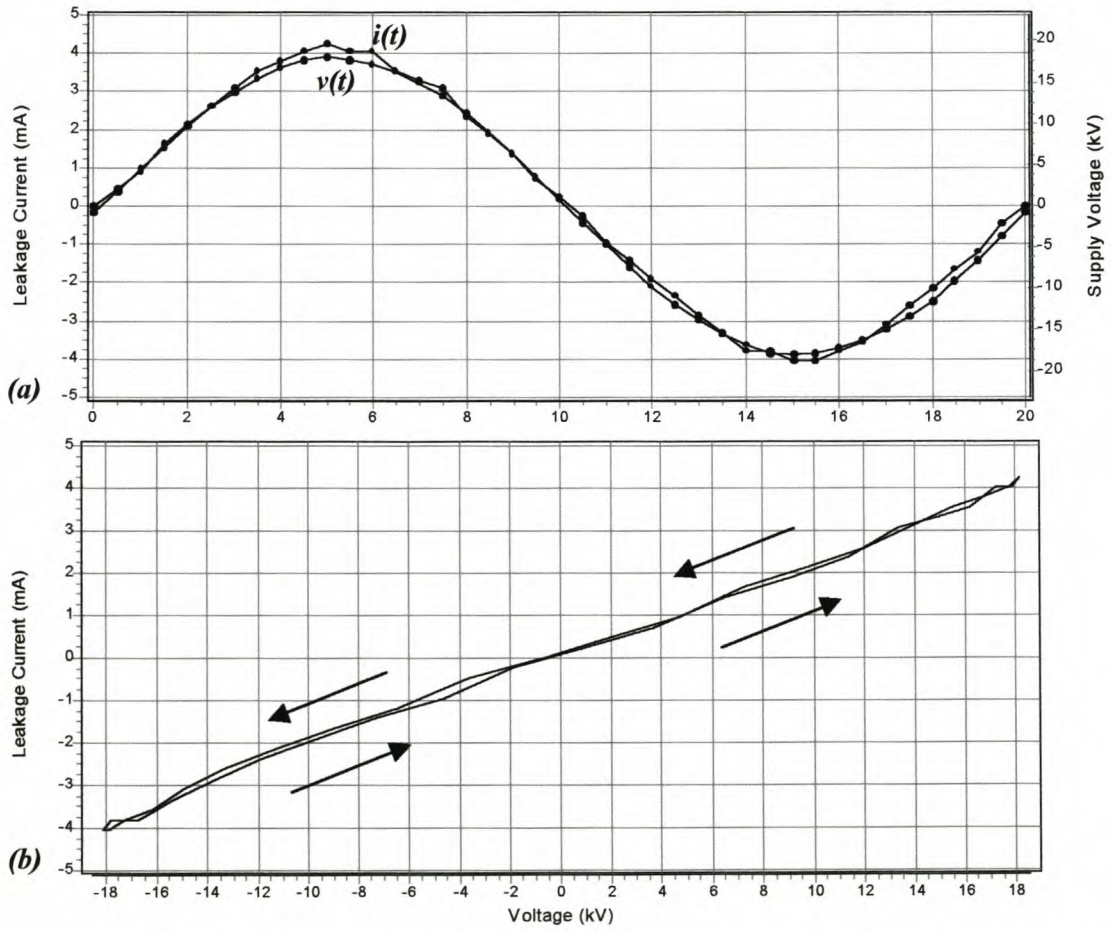

Figure 2. 7 Leakage current and supply voltage waveforms (a) measured on a resistive glazed insulator and associated impedance plot (b).

The supply voltage and resistive leakage current plot seen in Figure 2. 7 (a) shows that the two waveforms are in phase. This is confirmed by the resistive nature of the impedance plot shown in Figure 2. 7 (b).

Stellenbosch University http://scholar.sun.ac.za

2.3.2 Leakage current and climatic monitoring (IH48 and OLCA)

Commercially available leakage current and climatic data loggers were investigated. They were found to be unsuitable for the test programme. The author therefore investigated the various leakage current parameters monitored internationally and then, jointly with the local company NETELEK, developed a leakage current data-logger system (the IH48). The logger was successfully installed at KIPTS and details of the system were published [32]. A new smaller data-logger system, which monitors both leakage current and climatic conditions, was needed in the field and for the test programme. The author, together with another local company CT-Lab, developed the On-line Leakage current Analyser (OLCA) (see Figure 2. 8) to accommodate these needs. The OLCA is now commercially available and sold internationally. Both the IH48 and the OLCA were used in the test programme to monitor and record (on computer) the leakage currents. The IH48 was used as back up to the OLCA in event of failure and, in addition, to monitor the leakage current levels above the chosen OLCA sensor range of 500 mA. The leakage current sensor used is galvanically isolated (up to 6 kV) and has a bandwidth of 10 kHz.

Figure 2. 8 Main components of the on-line leakage current analyser (OLCA)

Stellenbosch University http://scholar.sun.ac.za

The following leakage current parameters were measured or calculated from the measured values (0.5 % accuracy), sampled at 2 kHz (40 samples/cycle in 50 Hz system) continuously, ignoring values below 0.5 mA, and stored every 10 minutes:

- Highest positive and negative leakage current peaks (-500 to 500 mA)
- Positive and negative leakage current pulse counters
- Positive and negative average leakage current (mA)
- RMS leakage current (mA)
- Positive and negative integrated charge (Coulomb)
- Integrated leakage current squared (Coulomb-Ampere)
- True power dissipation (Watt)
- Energy (Joule)
- Maximum leakage current waveform and associated voltage waveform (16 cycles) of the day is captured and stored

The following climatic parameters were monitored or calculated (1 % accuracy), sampled at 1 Hz continuously, and stored every 10 minutes:

- Wind speed (0 to 60 m/s) and direction (-0.5 ° to 357.5 °)
- Relative humidity (0 to 100%)
- Temperature (-50 °C to 50 °C)
- Dew point temperature (°C)
- Vapour pressure (hPa)
- Precipitation (in steps of 0.1 mm)
- UVB (280 to 315 nm) solar radiation (0 to 400 $\mu W/cm^2$)

Suitable computer software was developed to simplify the visual display, analysis and interpretation of the recorded leakage current and climatic data. Details of this program (now commercially available) are not included in this dissertation.

Stellenbosch University http://scholar.sun.ac.za

2.3.3 Image-Intensified, Ultraviolet-Sensitive, Video Camera System (CoroCAM)

During the preliminary work carried out at Elandsbaai, the need arose to examine discharges associated with dry-band activity. It was realised that UV radiation associated with these discharges plays an important role in the ageing of polymeric materials. The availability of image intensifiers for UV radiation was therefore investigated.

Image-intensified, ultraviolet-sensitive, video cameras available on the market were found to be either unsuitable or too expensive for the test program. The author therefore, in collaboration with the South African Council for Scientific Industrial Research (CSIR), developed the CoroCAM Mark I and CoroCAM Mark II to meet the requirements of the test programme. Both these products are now commercially available and sold internationally.

The CoroCAM Mark I (see Figure 2.9) is a night-time corona observation camera. The camera was first developed for use at the salt/clean fog chamber at the University of Stellenbosch and the Elandsbaai Insulator Test Site [10]. The lens is made of quartz, ensuring minimal optical losses. The camera is fitted with filters to partially eliminate the background light and to enhance the corona observed. A controllable image intensifier (10 000 x), sensitive in the ultraviolet spectrum, is used to amplify the light signal. The image is displayed on the viewfinder and can be recorded on videotape if required.

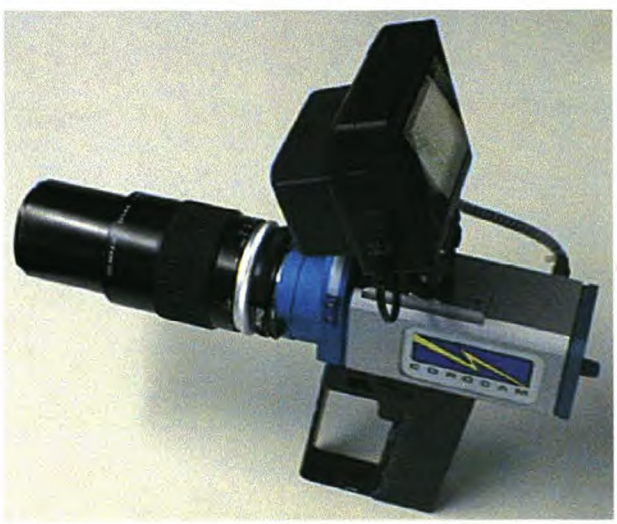

Figure 2. 9 CoroCAM Mark I, image-intensified, ultraviolet-sensitive, night-time video camera.

Stellenbosch University http://scholar.sun.ac.za

Later, the need to monitor the leakage current in synchronism with the visual observation was identified. Hence, the idea of using a second standard video camera, looking at both the CoroCAM and digital oscilloscope simultaneously, was investigated. It gave useful results, but the system was difficult to operate. The author then conceived the idea of converting the analogue leakage current signal into a frequency-modulated signal and recording it (in synchronism with the visual observation) onto the videotape audio channel. The recording could then be viewed by converting the stored signal back to analogue and displaying it on an oscilloscope. Such a system was built and operated successfully. However, the bandwidth of the videotapes available at the time was a limiting factor. The next idea was to synchronise the CoroCAM Mark I with a digital storage oscilloscope and a video frame-grabber card. The systems were designed, built, and operated with some success, but the apparatus was not user-friendly.

The CoroCAM Mark II (see Figure 2. 10) was designed to overcome these problems. The amplification of the photon multiplication tube was increased ten fold, to 100 000 x, and the image intensifier was made gate controlled. The camera is fully weatherproof and controllable from a distance of up to 40 m. The filters are enhanced, to aid outdoor observations. The leakage current, supply voltage (sampled at 10 kHz) and visual observation are recorded in synchronism and stored on a disk. The system is fully integrated and the user defines the leakage current trigger level, the exposure time and where on the 50 Hz cycle the image-intensifier gate opens.

Figure 2. 10 CoroCAM Mark II, image-intensified, ultraviolet-sensitive, video camera and leakage current frame-grabber system

Stellenbosch University http://scholar.sun.ac.za

The CoroCAM Mark II is designed as an insulator research tool. However, the camera has daytime corona observation capabilities, as described in an award-winning paper: Vosloo, Stolper, Baker, "Daylight Corona Discharge Observation and Recording System", 10th ISH, Montreal, 1997 [33].

2.3.4 Insulator Pollution Monitoring Apparatus (IPMA)

The IPMA is a device used to measure the surface conductance of an installed non-energised, naturally polluted insulator when artificially wetted. The surface conductivity and associated ESDD values can then be calculated. The first IPMA built in South Africa was at the University of Stellenbosch as part of an MSc study by Potgieter [24]. The device was based on the ideas used by two organisations, both in Italy: ENEL's surface conductance measurements on naturally wetted polluted insulators, and the pollution monitoring equipment (PME) of CESI (the naturally polluted insulator was enclosed and wetted artificially) [35]. The first IPMA was installed at Koeberg (after laboratory calibration) along with a mobile insulator test rig. The main emphasis of the work done by Potgieter was to determine a relationship between the leakage currents (30 minute highest peak) on naturally energised insulators compared to the surface conductance measured on insulators installed in the IPMA. A correlation was found with the level of humidity [34].

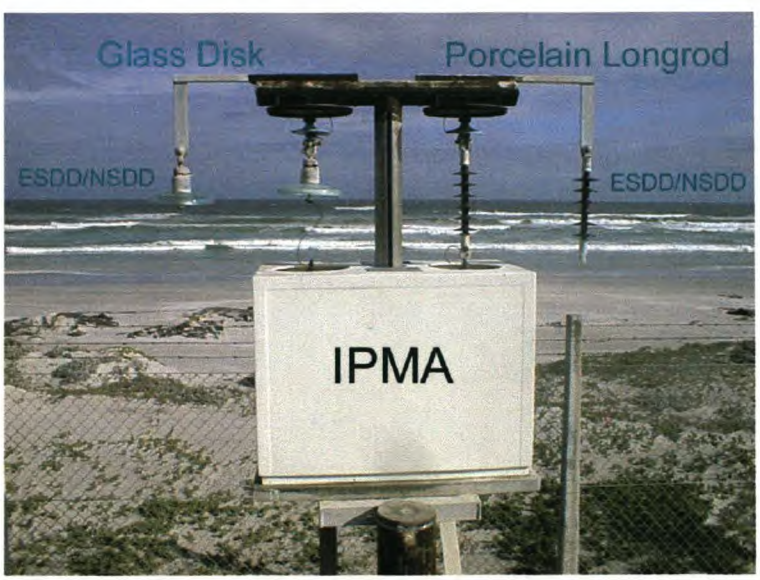

Figure 2. 11 Insulator pollution monitoring apparatus (IPMA) showing the IPMA and ESDD/NSDD monitored glass disk and porcelain longrod insulators

Stellenbosch University http://scholar.sun.ac.za

However, the first IPMA had mechanical constraints, and hence, under the guidance of the author and Dr Holtzhausen, a new and more suitable IPMA was designed and built, and used in the present project. Emphasis was placed on reducing the size, implementing a controllable steam generator, and improving the control and measuring circuits. The new IPMA was first laboratory calibrated, and then field calibrated, as part of two MSc studies by Davel and van Wyk [36, 37], under the mentorship of the the author and Dr Holtzhausen. The IPMA was installed at KIPTS (see Figure 2.11) for field calibration. Various papers resulted from these studies, including two award-winning papers [38, 39].

Initially the IPMA was used with ceramic insulators only. However, using it with insulators naturally aged at KIPTS, it was found that the IPMA could also be used to determine the surface conductivity of non-ceramic insulators with acceptable accuracy and repeatability [40].

The IPMA is presently in use at KIPTS to determine the pollution severity levels on ceramic insulators, as ESDD values, twice daily (12h00 and 24h00). The surface conductivity and condition can also be determined on both ceramic and non-ceramic 22 kV insulators.

A new commercial device combining the surface conductivity measurements of the IPMA (naturally and artificially wetted) with leakage current measurements on insulators in the power network is currently under construction [41] (patent number: 2000/0496). After calibration, the Insulator Pollution Monitoring Relay (IPMR) will be installed within Eskom substations, giving daily pollution profiles and warnings.

Stellenbosch University http://scholar.sun.ac.za

3 A STUDY OF THE ENVIRONMENTAL AND CLIMATIC CONDITIONS

"We are better at predicting events at the edge of the galaxy or inside the nucleus of an atom than whether it will rain on Aunty's garden party three Sundays from now ... " – ***Jules Henri Poincare***

Environmental and climatic conditions interact and directly affect the performance of high-voltage insulators in various ways.

- The direction and speed of the wind (which is dependant on solar radiation), precipitation (rain, mist, dew), relative humidity and the position of pollution sources all determine the final pollution deposit on an insulator surface. Particles become wind-borne and can be carried for great distances before fall-out occurs. Salt storms can also result in the deposition of a highly conductive electrolytic layer on an insulator surface.
- Climatic parameters such as ultraviolet solar radiation can have detrimental effects (chalking, crazing, and cracking) on the ageing of non-ceramic materials.
- Solar radiation can also heat the insulator surface during the day, helping to prevent wetting, or heat the atmosphere at sunrise, resulting in the formation of dew.

Therefore, an understanding of the environmental and climatic conditions at KIPTS, in general and during the test programme, is needed to help explain the insulator pollution and ageing process.

3.1 ENVIRONMENTAL CONDITIONS

Information and techniques described in the "Round Robin Pollution Monitoring Study Test Protocol", of the CIGRE task force 33.04.03 [29], and appendix A of IEC 60815, "Guide for the selection of insulators in respect of polluted conditions" [1], was used to study the environment at KIPTS.

Stellenbosch University http://scholar.sun.ac.za

3.1.1 Survey of Environmental pollution sources

An environmental survey was performed on the area around Koeberg. Firstly, a topographical map of the area surrounding KIPTS was obtained and 5 km radius circles were drawn, outwards up to 20 km. The cardinal points North, East, South and West were indicated – see Figure 3. 1.

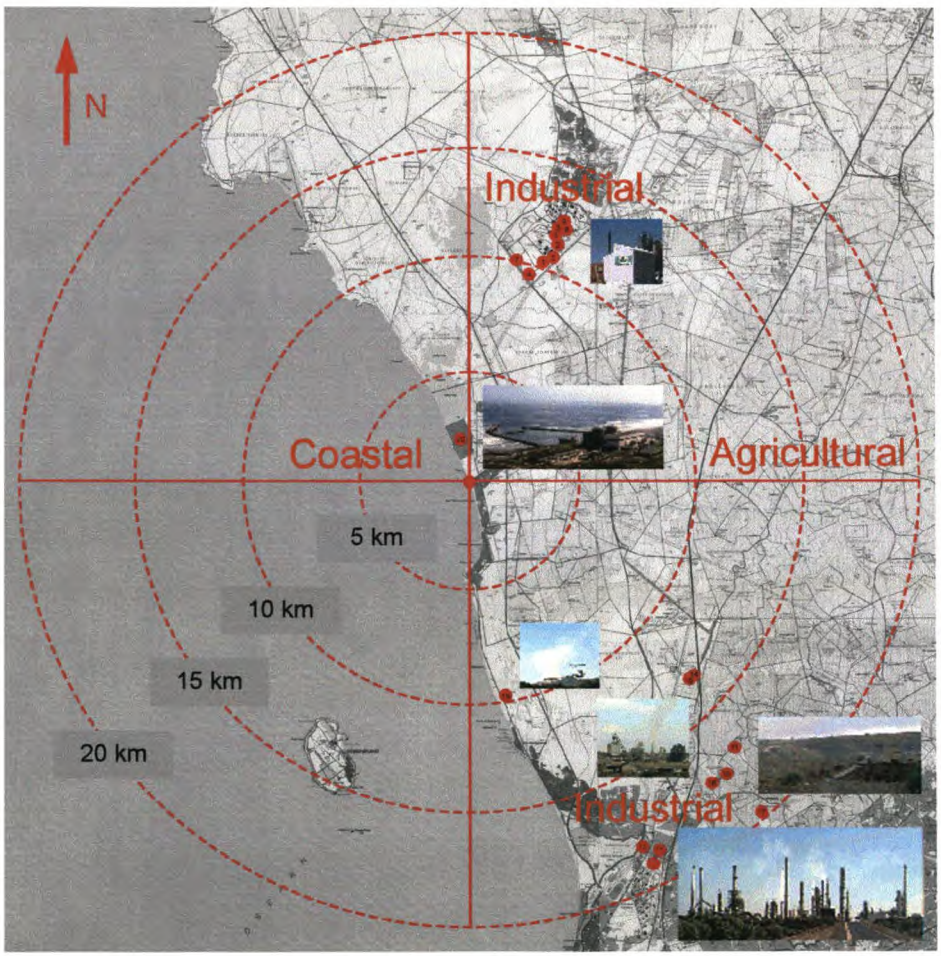

Figure 3. 1 Map of pollution sources (coastal, industrial and agricultural), shown by dots and photos, within a radius of 20 km from KIPTS.

Possible pollution sources were identified by investigating the map in detail, driving around and inspecting the area, flying over the area in both summer and winter periods, and discussions with personnel of the Koeberg Nuclear Power Station weather office. Photographs (digital) and the positions of the various pollution sources (using a Global Positioning System) were recorded. The main sources of pollution were identified as

Stellenbosch University http://scholar.sun.ac.za

marine, industrial and agricultural, and are shown by dots in Figure 3. 1. Photographs of the main industrial pollution sources are also indicated in Figure 3. 1.

The main pollution sources (detailed in Table 3. 1) surrounding KIPTS (indicated at the centre of the map Figure 3. 1) are summarised as follows:

- The Atlantic Ocean lies to the west of the test station. Wave action, sea breezes/winds and periodic mist banks are the cause of an influx of moisture and salt particles in the vicinity of the test station. Organic matter such as plankton is also present in the air.
- The breakwater wall at the Koeberg Nuclear plant north of KIPTS causes local salt mist banks to occur.
- To the east a predominantly agricultural area (wheat, vineyards) is found with occasional veld fires, ploughing, harvesting and crop spraying.
- North-east of KIPTS (10 - 13 km) an industrial area (Atlantis) emits burnt diesel, coal and heavy fuel oil (HFO) particles into the atmosphere.
- 10 km south of the station a lime plant (Kilson) is operational.
- To the south-south-east heavy industries such as Kynoch Fertiliser Plant and Caltex Oil Refineries are the main causes of severe particle emissions.

Table 3. 1 Summary of pollution sources and types of pollution surrounding KIPTS, their orientation and distances with respect to KIPTS

Area	Pollution Source	Direction from KIPTS	Distance from KIPTS	Type of pollution
Atlantis	Atlantis Diesel Engines (ADE)	NNE	10 km	Burn diesel and coal
	Aries Packing	NNE	12 km	Burn diesel
	Baja Industries	NNE	12 km	Burn HFO
	Barbican Investments	NNE	10 km	Burn coal
	Biopolymers	NNE	11 km	Burn HFO
	Unita	NNE	12.5 km	Burn scrapwood
	Promeal	NNE	10 km	Burn diesel and coal
	Rotex	NNE	12.5 km	Burn coal and HFO
	SA Fine Worsteds	NNE	13 km	Burn coal and HFO
Duinefontein	Koeberg Nuclear Power Plant	N	2 km	Burn diesel
Bloubergrand	Kilson Lime Works	SSE	10 km	Lime
Milnerton	Caltex Refinery	SSE	18 km	SOx, NOx, burn gas and oil
	Kynoch Fertiliser	SSE	18 km	NOx, CO_2, and Particulate
	Fertiliser Producers	SSE	18 km	NOx, CO_2, and Particulate
	Alpha Stone and Ready Mix	SE	17 km	Particulate
	FFS Refiners	SE	13 km	SO_2,NO_2 and burn HFO
	Wastetech	SE	13 km	Burn diesel
	CBS Ciolli Brothers	SE	17 km	Particulate
	Tygerberg Quarries and Concrete	SE	20 km	Particulate
	More Asphalt	SE	17 km	Burn HFO

Stellenbosch University http://scholar.sun.ac.za

The Energy Research Institute (ERI) of the University of Cape Town (UCT) performed a brown-haze study for the Cape Peninsula in 1977. The results of this study were investigated and a summary of the primary atmospheric emissions found by the ERI shown in Table 3. 2.

Table 3. 2 Summary of primary atmospheric emissions in the Cape Town area as determined by the Energy Research Institute at UCT. Both the emission rates in tons/year and the percentages are shown.

	EMISSION RATES (tons/year)					EMISSION %				
	SO_2	NOx	VOCs	PM10	PM2.5	SO_2	NOx	VOCs	PM10	PM2.5
Residential										
Coal	185	15	49	40	16	0.6	0.1	0.1	0.3	0.3
Paraffin	344	61	4	8	8	1.1	0.2	0	0.1	0.1
LPG	0	31	11	2	2	0	0.1	0	0	0
Wood	1	542	2387	1877	1314	0	1.9	4.3	16.3	21.8
Transport										
Petrol vehicles	1591	16848	33696	562	472	4.9	59.4	60.9	4.9	7.8
Diesel vehicles	2716	1781	460	1927	1773	8.4	6.3	8.3	16.8	29.4
Brake and tyre wear				86	0	0	0	0	0.7	0
Paved roads				2129	213	0	0	0	18.5	3.5
Unpaved roads				1391	139	0	0	0	12.1	2.3
Aviation fuel	46	576	470	33	30	0.1	2	0.8	0.3	0.5
Ship diesel	69	739	31	52	47	0.2	2.6	0.1	0.4	0.8
Ship bunker oil	1145	582	109	67	60	3.6	2.1	0.2	0.6	1
Industry and commerce										
Coal	4750	1875	6	975	390	14.7	6.6	0	8.5	6.5
HFO (Heavy Fuel Oils)	7686	695	4	451	406	23.9	2.5	0	4	6.7
FFS fuels (Fuel Firing Systems)	146	154	1	100	90	0.5	0.5	0	0.9	1.5
Diesel	84	900	38	64	59	0.3	3.2	0.1	0.5	1
Power paraffin	39	7	0	1	1	0.1	0	0	0	0
Caltex	10880	1643	1700	432	302	33.8	5.8	3	3.8	5
Kynoch		888		28	25	0	3.1	0	0.2	0.4
Athlone power station	2261	893	3	464	186	7	3.2	0	4	3.1
Other										
Tyre burning	241	13	107	335	168	0.7	0.1	0.2	2.9	2.8
Medical incineration	1	2	0	3	3	0	0	0	0	0
Wildfires	40	107	647	460	322	0.1	0.4	1.2	4	5.3
Other VOC (Volatile Organic Compounds)			15618			0	0	28.2	0	0
Total	32225	28352	55341	11487	6026	100	100	100	100	100

It was found that the main sources of man-made pollution in the Western Cape are emissions from petrol and diesel vehicles; the burning of wood, coal and HFO; and the Caltex oil refinery. The above survey further showed that the main pollution sources surrounding the KIPTS are marine, industrial and agricultural.

Stellenbosch University http://scholar.sun.ac.za

3.1.2 Environmental measurements

Environmental measurements such as equivalent salt deposit density (ESDD), non-soluble deposit density (NSDD) and directional deposit gauges (DDG) were performed using the techniques described in the "Round Robin Pollution Monitoring Study Test Protocol", of the CIGRE task force 33.04.03 [29] and in accordance with the test procedure and time interval described in Chapter 2, section 2.2.5.

A summary of the various pollution classification levels in accordance to CIGRE [42], IEEE [43], IEC [1], Riquel [44] and Macey [6] are given in Table 3. 3. The cold (20°C) layer conductivity of the pollution on the insulator surface is included, although it is not used in this chapter (it will be referred to later in the dissertation, in Chapter 7).

Table 3. 3 Summary of the various pollution classification levels.

	ESDD (mg/cm²)			NSDD (mg/cm²)	DDG(µS/cm)	Layer Conductivity (µS)	
Severity	**CIGRE**	**IEEE**	**IEC 60815**	**Riquel**	**Macey**	**CIGRE**	**IEC 60815**
None	0.0075 - 0.015					0.75 - 1.5	
Very Light	0.015 - 0.03	0 - 0.03				1.5 - 3	
Light	0.03 - 0.06	0.03 - 0.06	0.03 - 0.06	0.15 - 0.44	0 - 75	3 - 6	15 - 20
Medium	0.06 - 0.12	0.06 - 0.10	0.10 - 0.20	0.45 -0.85	76 - 200	6 - 12	24 - 35
Heavy	0.12 - 0.24	> 0.10	0.30 - 0.40	0.90 - 1.95	201 - 350	12 - 24	> 36
Very Heavy	0.24 - 0.48		> 0.80	> 1.95	> 350	24 - 48	
Exceptional	> 0.48					> 48	

3.1.2.1 Equivalent salt deposit density (ESDD)

The ESDD technique constitutes the washing off of a large polluted section on an insulator surface with distilled water. Typical areas to be tested would be a whole porcelain long rod, or top and bottom surface of a glass cap and pin insulator, etc.

The ESDD value is defined as the equivalent amount of NaCl deposit in mg/cm^2 on the surface area of an insulator which will have an electrical conductivity equal to that of the actual deposit dissolved in the same amount of water [19]. Even though other salts ($CaSO_4$, KCl, SiO_2, etc.) may be found in the deposit layer, only the amount of NaCl that will deliver the equivalent conductivity is considered.

The ESDD value is obtained from the measurements of the volume conductivity, solution temperature, and volume of the wash water. The conductivity probe measures the

Stellenbosch University http://scholar.sun.ac.za

volume conductivity, σ_t, at ambient solution temperature t_s . The measurement is then corrected to a standard 20°C by using the equation:

$$\sigma_{20} = (\sigma_t - \sigma_d) \cdot [1 - k_t (t_s - 20)] \tag{3.1}$$

where

σ_t : measured volume conductivity in μS/cm

σ_d : measured volume conductivity of distilled water in μS/cm

t_s : solution temperature in °C

σ_{20} : volume conductivity corrected to 20°C

k_t : temperature constant (0.0228 @ 20 °C)

The temperature constant is calculated using the equation:

$$k_t = -3.200 \cdot 10^{-8} \cdot t_s^{\,3} + 1.032 \cdot 10^{-5} \cdot t_s^{\,2} - 8.272 \cdot 10^{-4} \cdot t_s + 3.544 \cdot 10^{-2} \tag{3.2}$$

The salinity, S_a (kg/m^3), of the suspension at 20°C is given as:

$$S_a = (5.7 \cdot 10^{-4} \cdot \sigma_{20})^{1.03} \tag{3.3}$$

The equivalent salt deposit density (*ESDD*) in mg/cm^2 is given as:

$$ESDD = \frac{S_a \cdot V_d}{A_{ins}} \tag{3.4}$$

where

V_d : volume of distilled water used (cm^3)

A_{ins} : area of washed/sampled insulator (cm^2)

The calculated ESDD value is then related to a specific pollution severity level by using the values given in Table 3. 3. In this study the values prescribed by CIGRE [42] are used.

Stellenbosch University http://scholar.sun.ac.za

Note: an ESDD of 0.1 mg/cm^2 is roughly equivalent to a surface conductivity (σ_s) of 10 μS [31].

ESDD measurements were performed on the porcelain longrod and glass disk insulators. The values for both winter and summer test programme cycles are shown in Figure 3. 2.

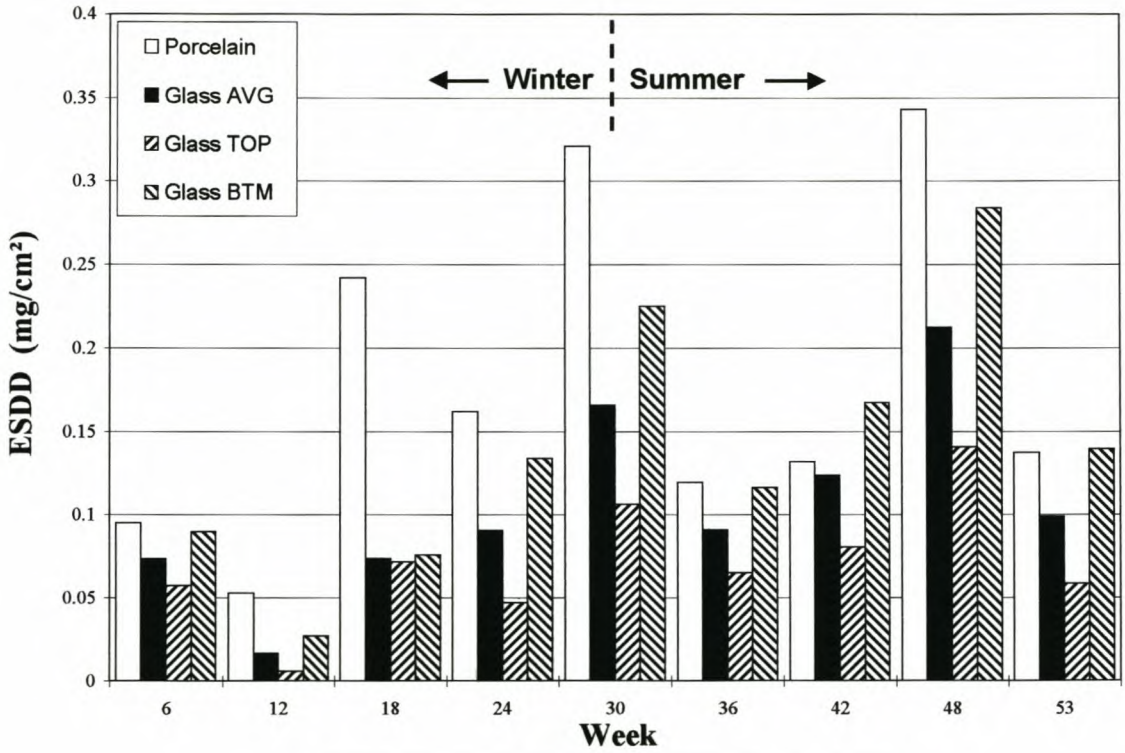

	ESDD (mg/cm²)			
	GLASS DISK		PORCELAIN LONGROD	
	Winter	Summer	Winter	Summer
Max	0.166	0.212	0.321	0.343
	Heavy	Heavy	Very-Heavy	Very-Heavy
Min	0.016	0.091	0.053	0.119
	Very-Light	Medium	Light	Medium
Ave	0.084	0.138	0.174	0.210
	Medium	Heavy	Medium	Heavy

Figure 3. 2 Six-weekly ESDD measurements on the porcelain longrod insulator. Values for the average (AVG), shed top (TOP) and bottom (BTM) of the glass disk insulator are shown for both the winter and summer test programme cycles

The average ESDD pollution levels measured can be classified as medium during winter, and heavy in summer.

Note: The porcelain longrod has a higher pollution level when compared to that measured on the glass disk.

Stellenbosch University http://scholar.sun.ac.za

3.1.2.2 Non-soluble deposit density (NSDD)

The NSDD defines the amount of non-soluble, inert deposits per square centimetre of the insulator surface. The non-soluble elements have little or no direct contribution to the conductance of the pollutant but rather act as binding material for the conducting particles such as salts. An internationally accepted pollution severity classification for NSDD values has not been established, however the values proposed by Riquel [44] are used in this dissertation.

The NSDD measurement is normally performed using the liquid pollution solution obtained from the ESDD measurements. The liquid is filtered through a pre-dried, clean and weighed filter paper. The soluble pollution drains through and the non-soluble contaminated filter paper is then dried and weighed. The NSDD value is calculated using:

$$NSDD = \frac{M_2 - M_1}{A_{ins}} \tag{3.5}$$

where

NSDD : non-soluble deposit density in mg/cm^2

M_1 : weight of dry clean filter paper in mg

M_2 : weight of dry contaminated filter paper in mg

The calculated NSDD value is then related to a severity level by using the values given in Table 3. 3.

NSDD measurements were performed on the porcelain longrod and glass disk insulators and the values are shown in Figure 3. 3 for both winter and summer test programme cycles.

The average NSDD pollution levels measured can be classified as light during both winter, and summer. However, in summer the levels are higher than in winter.

Stellenbosch University http://scholar.sun.ac.za

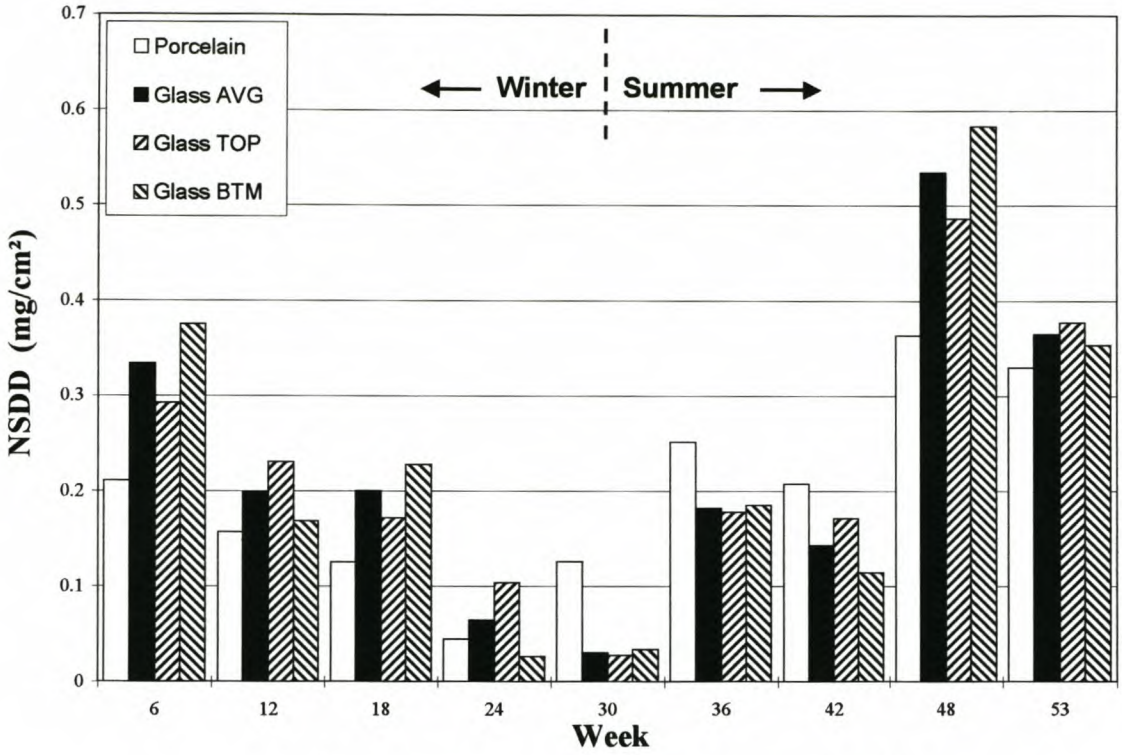

	NSDD (mg/cm²)			
	GLASS DISK		PORCELAIN LONGROD	
	Winter	Summer	Winter	Summer
Max	0.334	0.535	0.211	0.364
	Light	Medium	Light	Light
Min	0.031	0.031	0.044	0.126
	Very-Light	Very-Light	Very-Light	Very-Light
Ave	0.166	0.251	0.133	0.256
	Light	Light	Light	Light

Figure 3. 3 Six-weekly NSDD measurements on the porcelain longrod insulator. Values for the average (AVG), shed top (TOP) and bottom (BTM) of the glass disk insulator are shown for both the winter and summer test programme cycles

3.1.2.3 Directional deposit gauge (DDG)

Four dust gauges (as shown in Figure 3. 4) were used to collect the pollution particles in the atmosphere. They were installed 3 metres above ground level and each gauge set to one of the four cardinal points of the compass. The pollution was collected in the four plastic containers attached to the bottom of the gauges. These containers were removed at set intervals and their contents mixed with 500 ml of distilled water. The conductivities of the solutions were measured and the pollution index defined as the average of the conductivities of the four gauges, expressed in μS/cm and normalised to a 30-day interval. Normally these containers are removed at monthly intervals. However, for this study the

Stellenbosch University http://scholar.sun.ac.za

DDG measurements were made weekly for the first six weeks and then every sixth week thereafter.

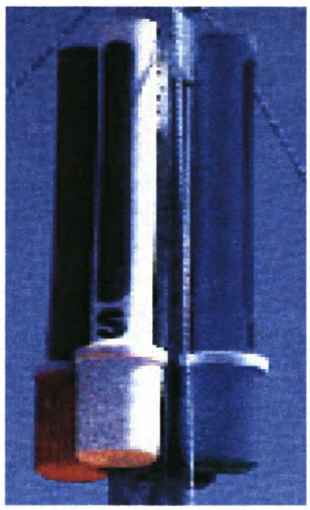

Figure 3. 4 Directional Dust Deposit Gauges.

The normalised DDG value is calculated using the equation:

$$DDG = \sigma_{20} \cdot \frac{V_d}{500} \cdot \frac{30}{D} \qquad (3.6)$$

where

DDG : directional deposit gauge conductivity in μS/cm

D : days DDG installed

DDG measurements were performed and the values are shown in Figure 3. 5 for both the winter and summer test programme cycles.

The average DDG pollution levels measured can be classified as exceptional during both winter (905 μS) and summer (1565 μS). In summer the levels are higher than in the winter. The directional ranking showing from which direction the highest pollution emanates was found to be West, North, South, East during winter and South, West, North, East in summer.

Stellenbosch University http://scholar.sun.ac.za

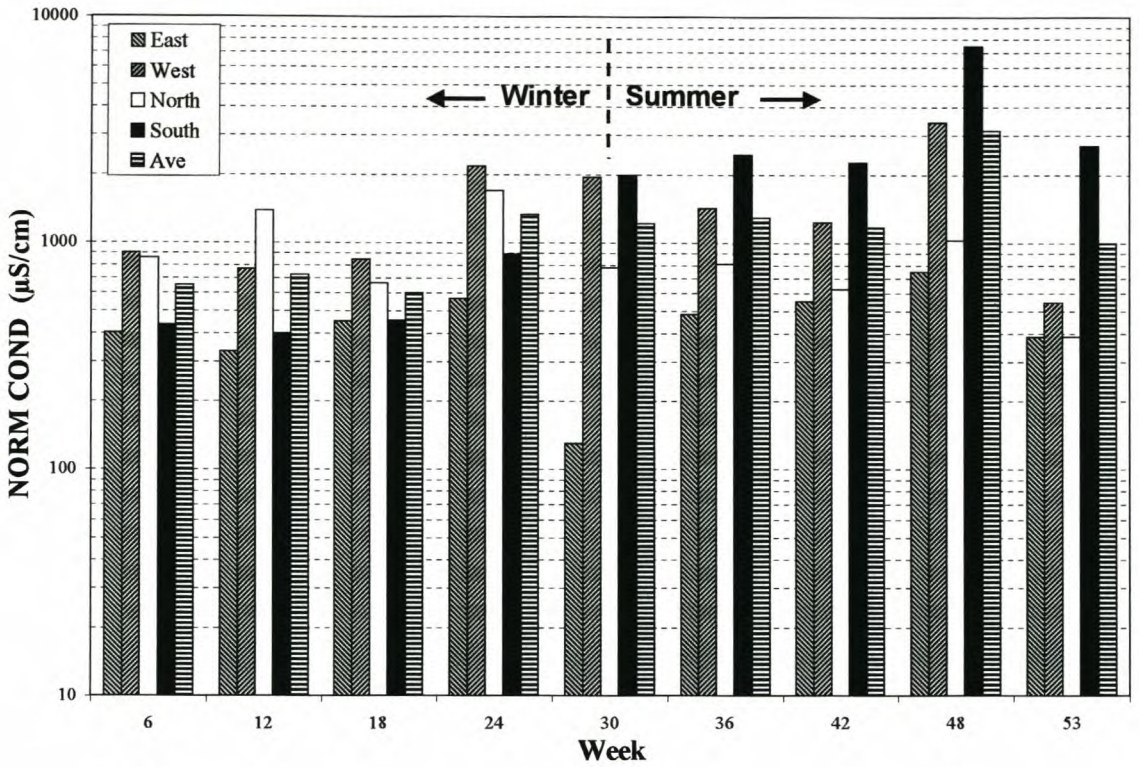

	DDG(µS/cm)							
	Winter				Summer			
	N	E	S	W	N	E	S	W
Max	1707	567	1986	2179	1025	746	7429	3414
	Exceptional	Very Heavy	Exceptional	Exceptional	Exceptional	Very Heavy	Exceptional	Exceptional
Min	661	131	399	767	385	131	1986	546
	Very Heavy	Medium	Very Heavy	Very Heavy	Very Heavy	Medium	Exceptional	Very Heavy
Ave	1078	377	833	1330	724	461	3360	1716
	Exceptional	Very Heavy	Very Heavy	Exceptional	Very Heavy	Very Heavy	Exceptional	Exceptional

Figure 3. 5 Six-weekly DDG measurements of environmental pollution at a 3-meter level for the cardinal points North, East, South and West, in both winter and summer

A chemical analysis was performed on the liquid pollution contents of the DDG. The results obtained from the elemental analysis (EDAX) done for the cardinal points North, East, South and West, for both the winter and summer periods of the test programme, are shown in Table 3. 4. The various elements detected and their percentages are also shown.

Stellenbosch University http://scholar.sun.ac.za

Table 3. 4 Results obtained from the elemental analysis (EDAX) done on the contents of the DDG. The various elements detected and their percentages are shown.

	Elemental Analysis (EDAX) of DDG									
	Na	Mg	Al	Si	S	Cl	K	Ca	Ti	Fe
North	0.55	0.16	0.04	0.50	0.80	7.76	0.25	0.53	0.00	0.00
East	0.61	0.07	0.00	0.31	0.80	7.30	0.16	0.43	0.00	0.00
South	0.48	0.23	0.06	2.46	0.50	7.03	0.15	1.20	0.00	0.26
West	0.38	0.19	0.00	1.68	3.48	3.50	0.10	0.38	0.00	0.00
Winter (%)	2.01	0.64	0.10	4.95	5.58	25.59	0.66	2.55	0.00	0.26
North	0.12	0.06	0.70	3.28	2.93	5.83	0.46	0.40	0.17	0.10
East	0.34	0.19	0.13	3.15	0.56	9.67	0.25	0.33	0.00	0.10
South	0.11	0.08	0.27	9.46	0.44	1.96	0.13	1.72	0.00	0.13
West	0.27	0.18	0.00	8.90	0.26	3.36	0.13	1.23	0.26	0.00
Summer (%)	0.84	0.51	1.10	24.80	4.19	20.81	0.97	3.68	0.43	0.33

Possible chemical compositions of the environmental pollution and the most likely sources thereof were derived [45] from the elemental analysis (EDAX) results in Table 3. 4. These are summarised in Table 3. 5.

Table 3. 5 Possible chemical compositions of the environmental pollution and the most likely sources thereof, as derived from the elemental analysis (EDAX) results in Table 3. 4

	Possible Chemical Compositions										
	Na	Mg	Al	Si	S	Cl	K	Ca	Ti	Fe	
Air					S	$Cl_{(-)}$		$Ca_{(2+)}$	Ti	$Fe_{(2+)}$	N_2 O_2 H_2O
Sea Sand				Si		$Cl_{(-)}$		$Ca_{(2+)}$			
Sea Salt	$Na_{(+)}$	$Mg_{(2+)}$	$Al_{(3+)}$		$SO_{4(2-)}$	$Cl_{(-)}$	$K_{(+)}$	$Ca_{(2+)}$			$CO_{3(2-)}$
Marine	NaCl Na_2SO_4	$MgCl_2$ $MgSO_4$	$AlCl_3$	SiO_2			K_2SO_4 KCl	$CaCl_2$			
Industrial					H_2SO_4 SOx	HCl		$CaSO_4$		$FeCl_2$ Fe_2O_3 $FeSO_4$	COx NOx HNO_3

The results in Table 3. 5 show that marine and industrial pollution is present. The most dominant pollutant found was $Cl^{(-)}$, although high levels of S and resulting $SO_4^{(2-)}$ were also found. Sand deposits were more dominant in the summer, emanating from the south-west.

Stellenbosch University http://scholar.sun.ac.za

3.2 CLIMATIC CONDITIONS

The "Round Robin Pollution Monitoring Study Test Protocol" of the CIGRE task force 33.04.03 [29] and Appendix A of IEC 60815 [1] "Guide for the selection of insulators in respect of polluted conditions" were used to study the climate at KIPTS.

3.2.1 Climatic survey

The climate of the south-western Cape is well documented in the publication "The weather and climate of the extreme south-western Cape" issued by the South African Weather Bureau (SAWB) [46]. However, climate can vary within climatic regions, thus the weather station (Cape Weather Wise) situated close to KIPTS (within 1km) was asked for a climatic description. Cape Weather Wise had the following to say about the climate to be expected at Koeberg:

- **General description:** *"Koeberg is situated 20 km north of Cape Town, on the south-western tip of Africa, in the region generally known as the Western Cape, which is in the climate region of Southern Africa that is classified as Mediterranean Climate. The main feature of this climatic region is that the bulk of the rainfall occurs in winter. During the rainy months, April to September, approximately 320 millimetres of rain can be expected with as much as 15 rainy days per month. During the dry summer months however, only 3 to 5 rainy days occur, with the summer average rainfall of just more than 80 mm. Strong gusts of wind occur during the summer southerly associated with the ridging of a high-pressure system from the Atlantic to the Indian Ocean. In winter, frontal weather causes strong winds, hence the well-known name Cape of Storms. Gusts in excess of 35 metres per second have been recorded on numerous occasions. With the cloudy winters and sunny summers a total reversal of the so-called radiation climate is observed versus the summer rainfall regions."*

- **Rainfall:** *"The rainfall of the Mediterranea-type climate district, in which Koeberg is situated, has a very low seasonal variability of below 20%. The pronounced maximum occurs in winter. The long-term average yearly rainfall equals 400 mm, with the highest monthly rainfall recorded in July (79 mm) and the lowest in November (8 mm). It must be stressed that although the long-term average can be termed 'normal', in no single year is the rainfall distributed 'normally'. The winter rains occur mostly out of*

Stellenbosch University http://scholar.sun.ac.za

Cumulus and Nimbostratus cloud formations during the winter months as pre- and post frontal precipitation. During summer, unstable and hot conditions can result in thunder activity (rare, less that 5 times per year) causing thundershowers out of Cumulonimbus. Coastal lows hugging the Cape in their movement from the West Coast to the East Coast, sometimes cause drizzle and light rain out of low Stratus and Stratocumulus. The statistical expectancy of precipitation intensity show that the maximum rainfall in a 60-minute period will not exceed 30 mm for a 20-year return period and 40mm for a 100-year return period."

- **Fog:** *"The West Coast is liable to have a considerable amount of fog due to the cooling of moist air over the Benguela current. Sometimes the fog forms at sea then drifts inland on a light north-westerly breeze. If the ground is cold the fog persists, it lifts after sunrise and disperses an hour or two later. The approach of a depression causes a pressure gradient from the interior plateau to the coast. The air blowing over the coast is warm, and steep inversions form, which encourage the formation of fog. Inversion fogs or frontal fogs form when precipitation, especially drizzle, is evaporated into stable air cooled by contact with the surface of the ground beneath. Generally, the month with the most fog is April and the one with the least is July. The foggy season usually starts in late summer to early winter, but there is no month free from fog."*

- **Ambient temperature:** *"Situated on the Atlantic Coast, temperature variations are moderated especially when the wind is onshore. Microclimatological effects however, influence the temperature variations to such a degree that daily fluctuations exceeding 20 degrees Celsius are commonly observed. During subsistence conditions with a high pressure system being centralised over the area, clear skies and terrestrial radiation can cause the temperature to drop to close to freezing point. Daytime radiation results in a rapid rise in temperature that exceeds 20 degrees Celsius. The more intense the inversion before its disappearance, the more spectacular will be the rise in temperature. The average minimum temperature for July is 13 degrees Celsius and the average maximum for February is 19.3 degrees Celsius."*

- **Wind:** *"Airflow is a direct result of pressure differences. As the Cape area is influenced by the strong pressure gradients of the mid-latitudes, the wind energy exceeds most other areas in Southern Africa. The ridging anticyclone situated over the south Atlantic in summer, with strong pressure gradients, results in strong*

Stellenbosch University http://scholar.sun.ac.za

southerly flow over the Cape Peninsula during the summer months. Contrasting with this, the winter northerly flow is caused by pre-frontal conditions that are also associated with cloudy weather and low temperatures. The southerly flow experienced after the passage of the frontal system has less strength than the summer southerly. On the Atlantic coast, where Koeberg is situated, a south-westerly sea breeze results when significant solar heating of the interior occurs. This condition starts during mid-morning and lasts until late afternoon. The influx of marine air from the Atlantic Ocean heats rapidly over the warm land and air at distances greater than 6 km from the sea can no longer be classified as being marine. Drainage conditions are evident during night-time cooling of the higher interior or when a high-pressure system over the interior causes easterly berg winds."

- **Dispersion:** *"To understand the dispersion potential, knowledge of the mid-latitude and major weather systems such as South Atlantic anticyclones and frontal systems are required. In winter, when frequent frontal systems pass over the Cape Peninsula, strong northerly to westerly winds occur 34% of the time. When upper air high-pressure systems occur inland, drainage conditions exist along the coast, which results in poor ventilation with a subsequent decline in dispersion potential. The depth of the nocturnal inversion layer, limiting dispersion, was found to be in the region of 300m. The terrestrial radiation at night, occurring frequently with relative calm wind conditions and clear skies at night in early winter, causes strong inversion conditions, resulting in a virtual impermeable layer restricting dispersion below 300m. In summer however, strong pressure gradients with the advent of the ridging South Atlantic anticyclone, cause strong southerly winds, which have excellent dispersion potential. These winds occur 39% of the time."*

- **Variability of the Cape weather:** *"Due to topographical influences, enhanced by the two oceans bordering the Cape Peninsula, the spatial variability of the weather is indicated by rainfall differences. These statistical differences exceed a factor of four within a 400 square kilometre area. Yearly rainfall totals vary from just over 300 mm on the West Coast to long-term averages exceeding 1200 mm in mountainous terrain within 40 km between stations. This same variability is evident when comparisons are made from one year to another. Over a 20-year period, the maximum rainfall in one year exceeded 640 mm and the lowest rainfall recorded was less than 245 mm. Short-term variability is also evident in the weather that can be experienced over a very short period. A typical example of this variability is when a high-pressure system*

Stellenbosch University http://scholar.sun.ac.za

over the interior causes land breezes commonly known as 'bergwinds' - the winds originate in the east and heats up as it descends down the escarpment at a speed of approximately 20 km/h. This is a condition when even in the winter months the surface temperature will exceed 30 degrees Centigrade. This typical pre-frontal condition normally lasts one day and then a cold front, with gale force north-westerly conditions and a dramatic temperature drop down to below 15 degrees, occurs."

3.2.2 Climatic measurements

The climatic parameters (precipitation, relative humidity, ambient temperature, wind speed and direction, and UV-B solar radiation) were measured in 10-minute intervals for the duration of the test period, as discussed in the test procedure (chapter 2, section 2.2.5). The test period was sub-divided into winter (12/04/199 to 10/10/1999) and summer (11/10/1999 to 16/04/2000) (see time-line table in Appendix B). If no data was recorded or calculated a blank space is plotted. The results are given below.

3.2.2.1 Precipitation

Precipitation wets the pollution on the insulator surface, which can then dissolve into a conducting electrolytic layer, and thus result in the flow of leakage currents. Precipitation can also lead to the washing off of pollution from the insulator surface. It is estimated [18] that rain in excess of 10 mm could wash 90% or more of the pollution from a ceramic insulator surface. It has also been shown [18] that light rain may, by dissolving and associated seepage, remove active pollution from the insulator surface. A combination of rain and wind is the best natural insulator cleaner [18]. Rain is rated as light when <0.5 mm/hour, moderate between 0.5 to 4 mm/hour and heavy when >4 mm/hour. A correlation between electrical activity and precipitation is expected. Thus, measuring the precipitation is important for this study.

The precipitation (rain) measured during the test period is shown in Figure 3. 6. A total of 290.3 mm of rain was measured during the 182 winter days and 24.3 mm during the 188 days of summer. Thus, a total of 314.6 mm of precipitation was measured for the test period, which is a typical average value expected at KIPTS. The pH levels of the precipitation measured averaged 5.6, which is slightly acidic.

Stellenbosch University http://scholar.sun.ac.za

The precipitation data indicates that the area is a winter-rainfall area with dry summers. However, there were precipitation events even in the summer, when relatively high levels were recorded for the 10-minute interval.

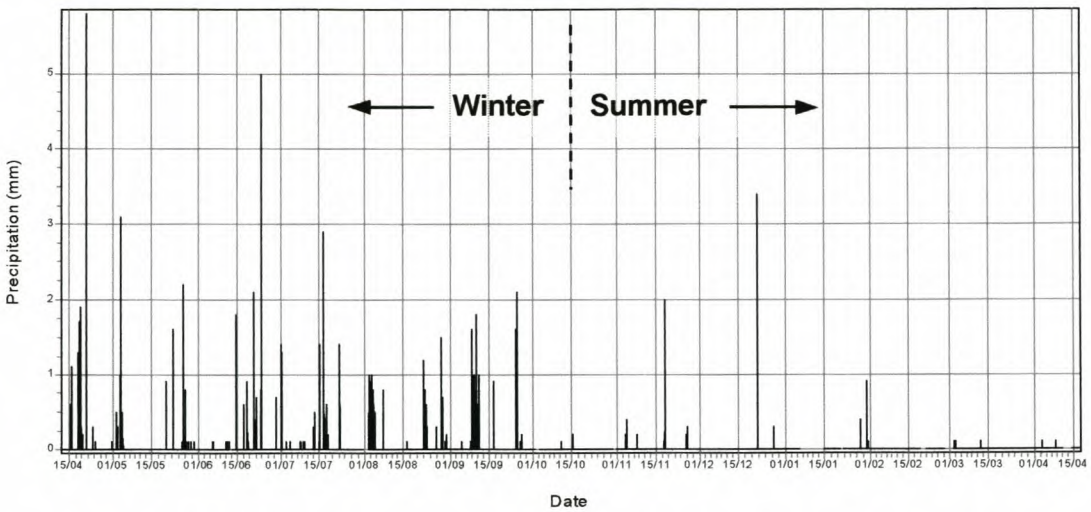

Figure 3. 6 Precipitation (rain) measurements during the winter and summer periods.

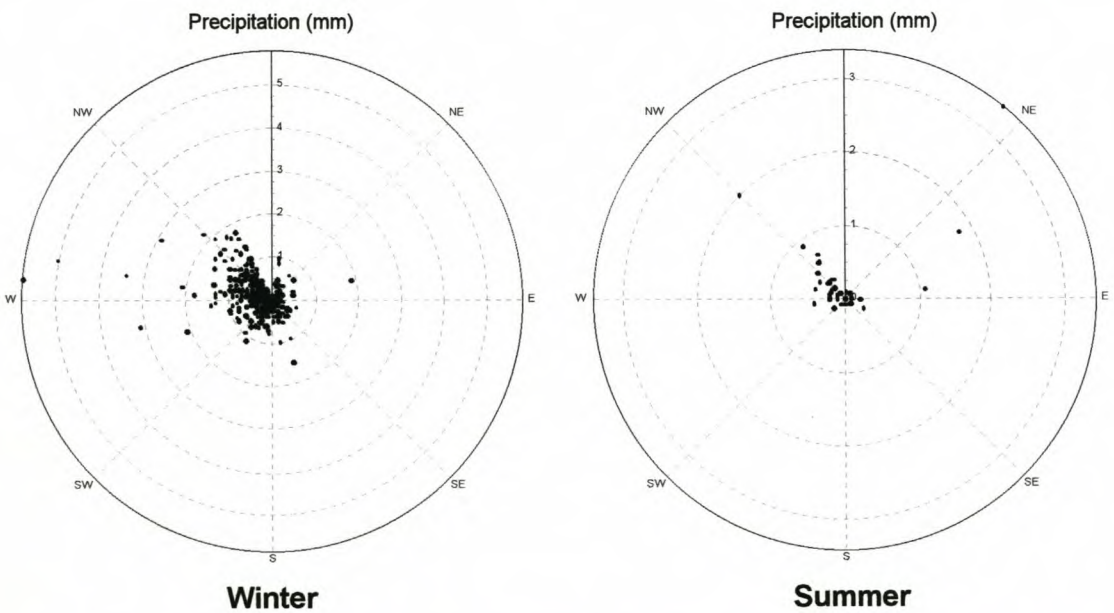

Figure 3. 7 Polar plots of wind direction in relation to winter and summer precipitation (rain) measurements, showing the dominant direction from which the precipitation emanates.

The precipitation was plotted in relation to the wind direction prevailing at the time of measurement (as per statistical method described in Appendix C 5) (see Figure 3. 7).

Stellenbosch University http://scholar.sun.ac.za

The winter and summer polar plots both show that the prevailing wind at the time of precipitation was dominantly north-westerly. It is expected that there should be a correlation between the precipitation, wind direction and leakage current.

3.2.2.2 Relative humidity

Relative humidity is an indicator of the moisture level in the atmosphere. When the relative humidity percentage is high (larger that 75%) there is a good chance that the pollution on the insulator surface could be wetted, which could then dissolve into a conducting electrolytic layer, and thus result in the flow of leakage currents. High levels of relative humidity for long periods of time can also lead to the washing off of pollution from the insulator surface. A correlation between electrical activity and relative humidity is expected. Thus, measuring the relative humidity is important for this study.

The relative humidity measured is shown in Figure 3. 8. The lowest 10-minute average humidity level measured was 20% and the highest 100%.

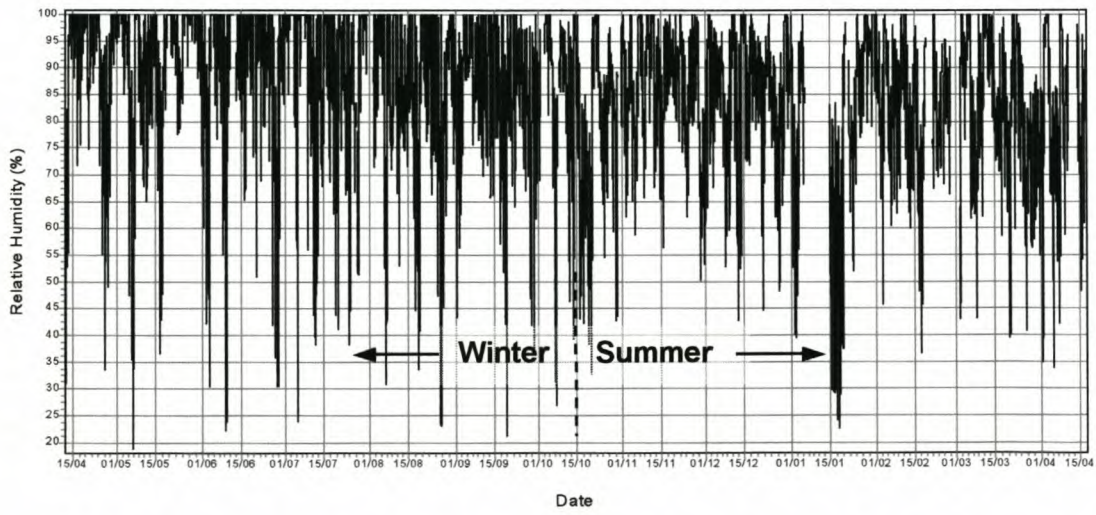

Figure 3. 8 Relative humidity measurements during the winter and summer periods.

The 'probability of exceeding abscissa' plots (as per statistical method described in Appendix C 4) of the relative humidity for both the winter and summer periods are shown in Figure 3. 9.

Stellenbosch University http://scholar.sun.ac.za

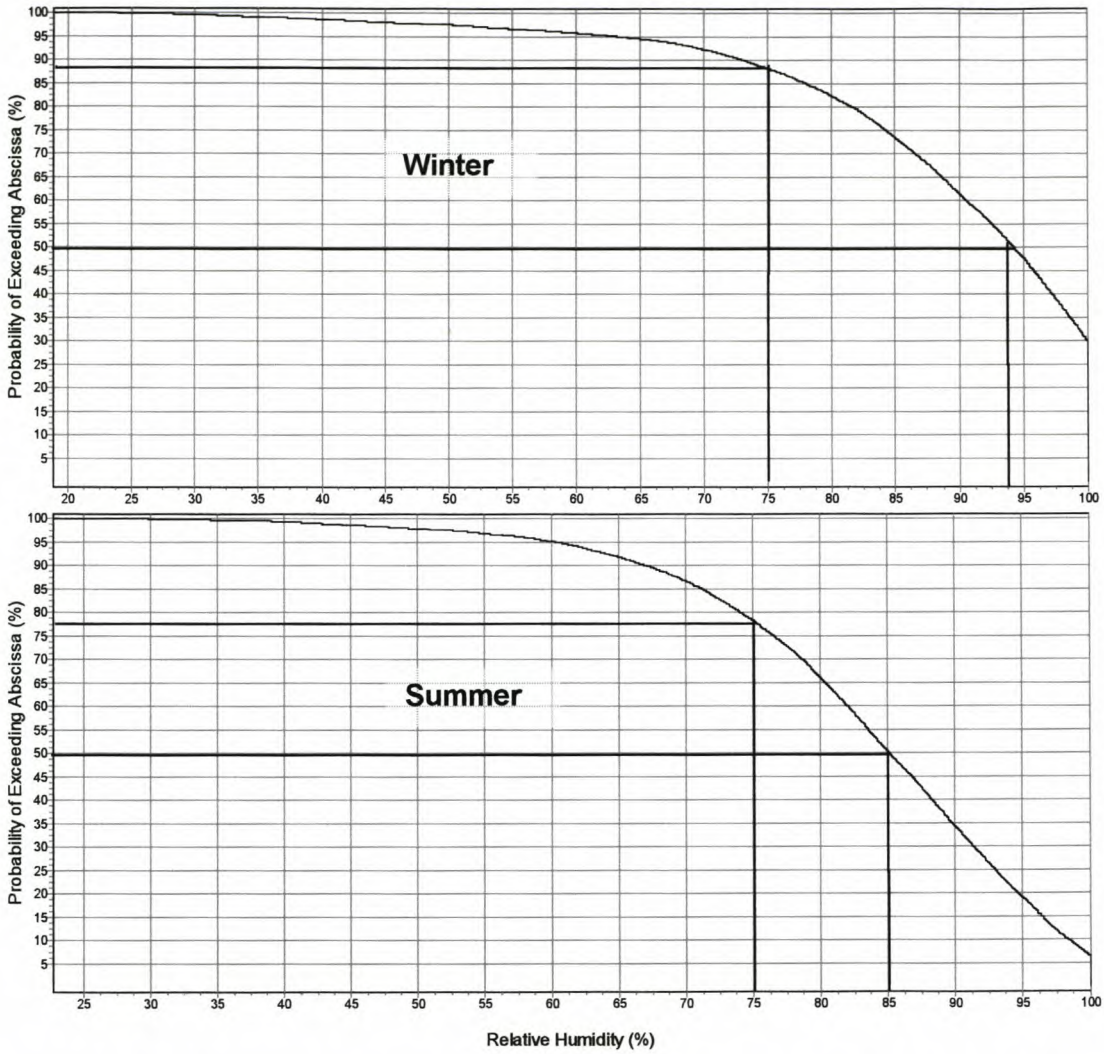

Figure 3. 9 Probability of the relative humidity measurements exceeding a certain value during the winter and summer periods.

From the probability plots in Figure 3. 9 there is a 50% probability that the relative humidity will be higher than 94% in winter and 85% in summer. The probability of the relative humidity levels exceeding 75% is approximately 88% in winter and 78% in summer. Thus, the relative humidity levels measured at KIPTS were above the critical 75% level for most of the time.

It is important to note that the humidity sensor becomes polluted with the same pollutant as the insulators being tested, which was found to be predominantly NaCl. The relative humidity just above a solution of aqueous NaCl is given as 76% at an ambient temperature of 20 °C [47] (salt within a salt shaker is normally moist). It is thus assumed that the actual ambient relative humidity further away from the sensor is lower than

Stellenbosch University http://scholar.sun.ac.za

measured. However, the relative humidity measured is deemed more representative of the levels at the insulator surface by leaving the sensor in a natural polluted state.

The time-of-day trends (as per statistical method described in Appendix C 3) of the 10-minute minimum, average and maximum (100%) relative humidity values for the winter and summer periods are shown in Figure 3. 10.

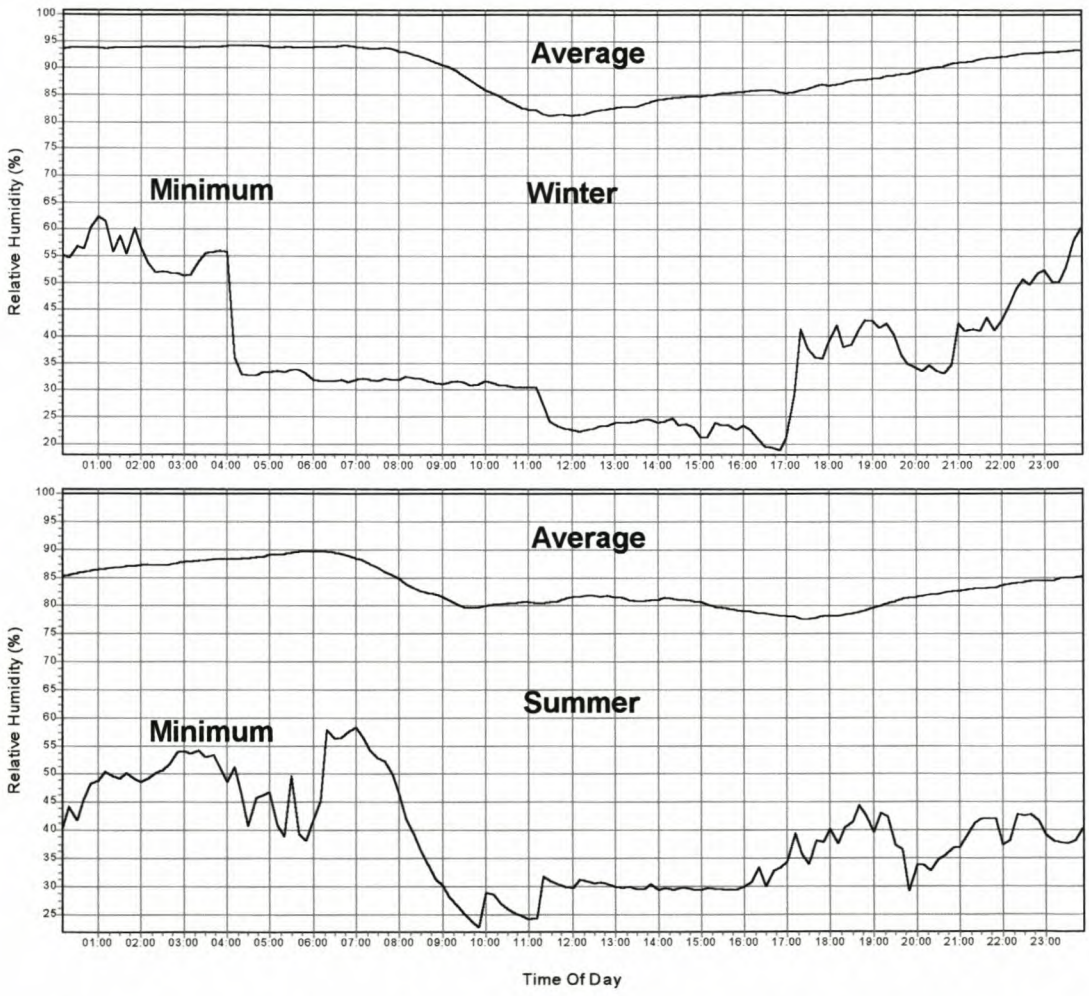

Figure 3. 10 Time-of-day trends of the minimum, average and maximum (100%) relative humidity measurements during the winter and summer periods.

The time-of-day trends show that the average relative humidity levels are above 75% throughout the day. The average relative humidity levels at night are above 90% during winter and above 85% in summer. Thus, the probability of critical wetting of the insulator surface is high in both the winter and summer periods.

Stellenbosch University http://scholar.sun.ac.za

3.2.2.3 Ambient temperature

The ambient temperature plays a role in the wetting of the insulator. An inverse relationship between the relative humidity and temperature is suspected. The temperature and relative humidity determine the dew point temperature according to the following relationship [48]:

$$T_{Dew} = \left(\frac{2720 \cdot (T_a + 273.16)}{((T_a + 273.16) \cdot \log(100/Rh))/2 + 2720} \right) - 273.16 \qquad (3.7)$$

where

T_{Dew} : dew point temperature in °C

T_a : atmospheric temperature in °C

Rh : relative humidity

When the insulator surface temperature falls below the atmospheric dew point temperature, dew (moisture condensation) will form on the insulator surface. This phenomenon often occurs in the early morning hours when the insulator is at a lower temperature than that of the ambient air, when the ambient temperature of the moist air is heated by the first rays of the sun. The ambient temperature results recorded during the winter and summer test periods can be seen in Figure 3. 11.

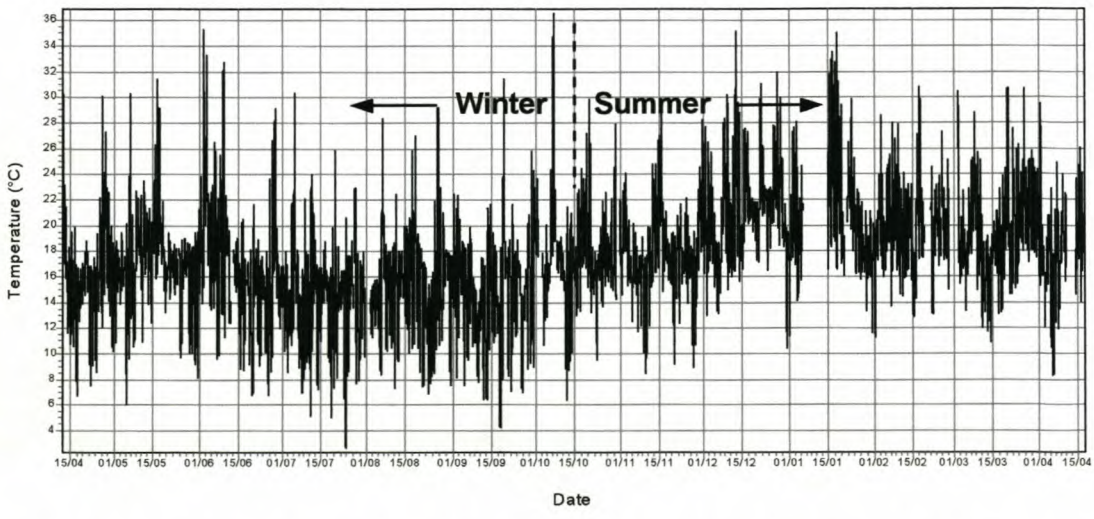

Figure 3. 11 Ambient temperature measurements during the winter and summer periods.

Stellenbosch University http://scholar.sun.ac.za

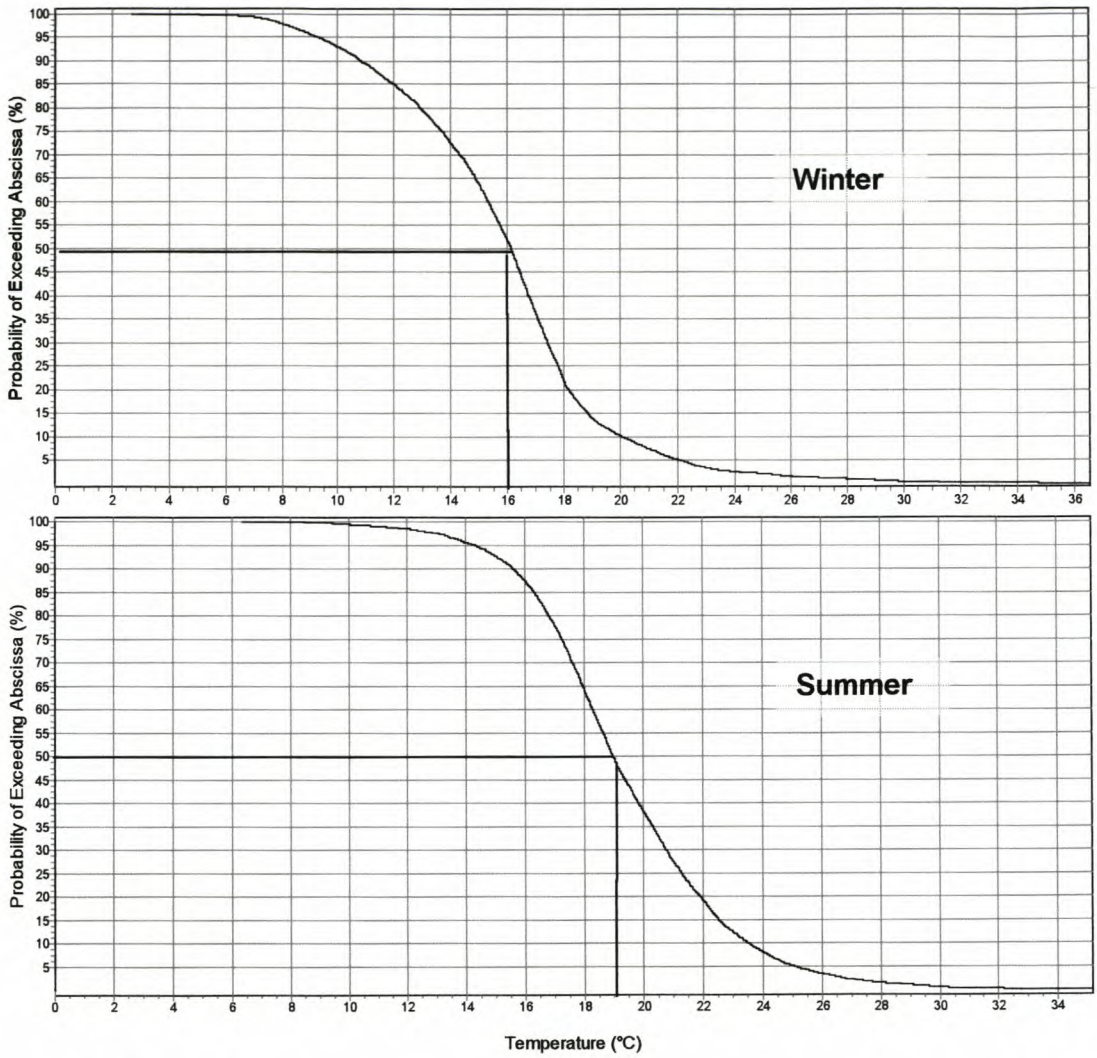

Figure 3. 12 Probability of the ambient temperature measurements exceeding a certain value during the winter and summer periods.

Figure 3. 12 shows the ambient temperature probability plots (as per statistical method described in Appendix C 4) for winter and summer. There is a 50% probability that the temperature will be above 16 °C in winter, and above 19 °C in summer.

The time-of-day trends (as per statistical method described in Appendix C 3) in Figure 3. 13 show the average night-time winter temperature of 14 °C and 18 °C during the daytime. The average night-time temperature during the summer is 19 °C and 20 °C in the day-time. The maximum temperature was generally found to be at 16h00 in the afternoon and the minimum temperature just before or at sunrise in the morning.

Stellenbosch University http://scholar.sun.ac.za

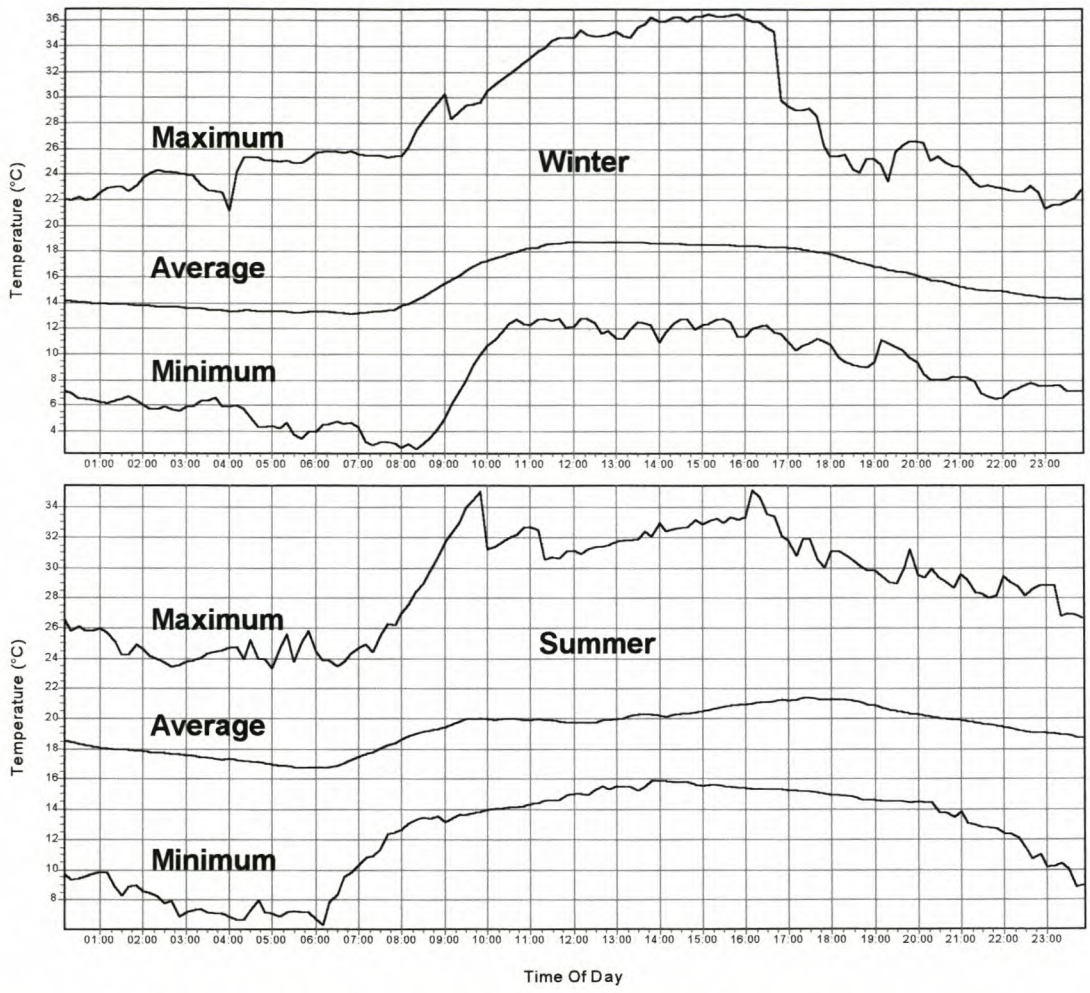

Figure 3. 13 Time-of-day trends of the minimum, average and maximum ambient temperature measurements during the winter and summer periods.

3.2.2.4 Wind speed and direction

Wind plays a major role in the transportation and depositing of pollution and moisture on an insulator surface. A relationship between ESDD and wind was found [49]; it showed that an increase in wind speed results in an increase in the pollution deposit to the power three (cubic relationship). Wind becomes the dominating pollution deposit factor when the wind speeds exceed 2 m/s [18]. Pollution deposit on the insulator is expected on the wind side [18]. Strong winds carrying sand particles or rain may remove pollution from the insulator surface [18].

The wind speeds measured during the winter and summer test periods can be seen in Figure 3. 14.

Stellenbosch University http://scholar.sun.ac.za

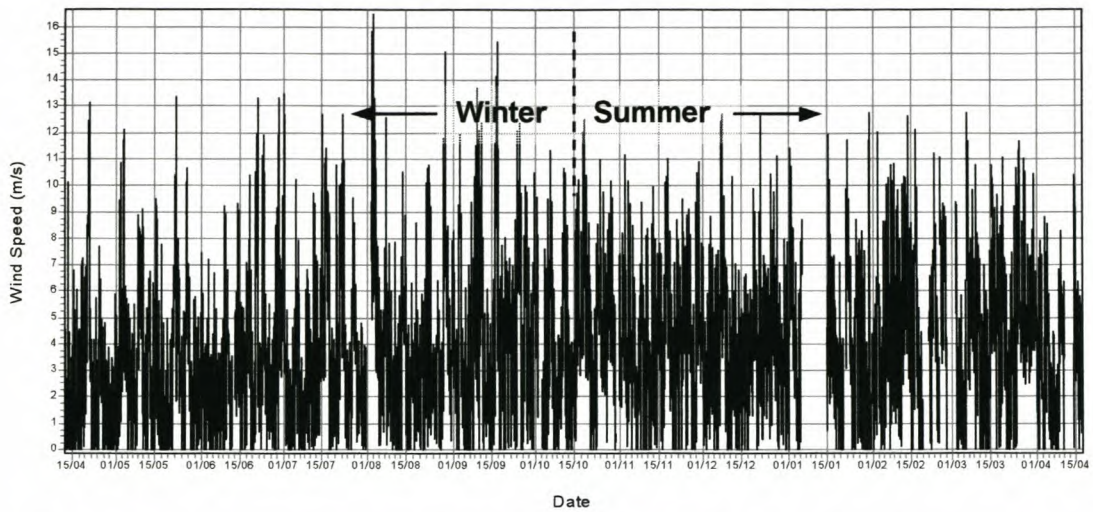

Figure 3. 14 Wind speed measurements during the winter and summer periods.

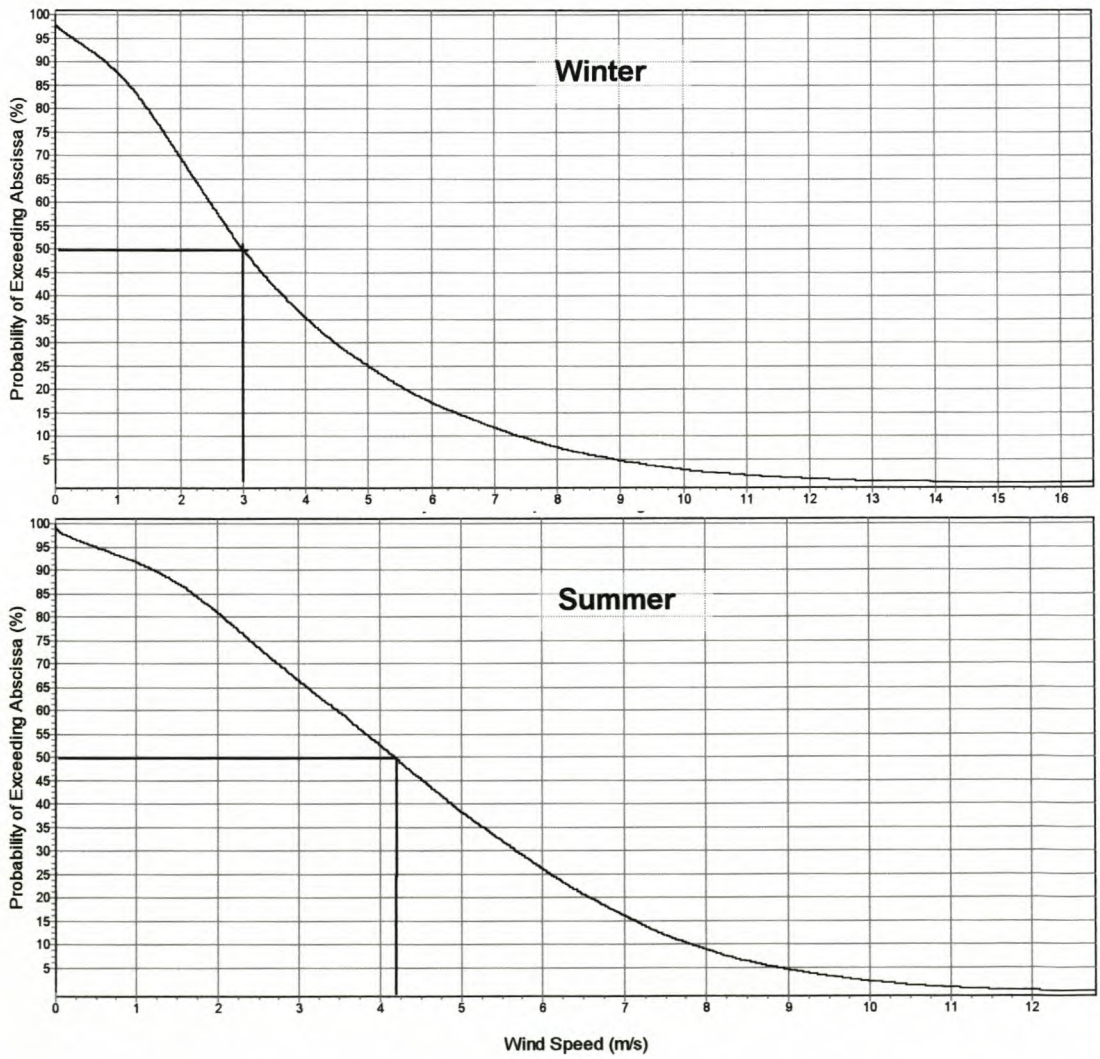

Figure 3. 15 Probability of the wind speed measurements exceeding a certain value during the winter and summer periods.

Stellenbosch University http://scholar.sun.ac.za

Figure 3. 15 shows the probability plots (as per statistical method described in Appendix C 4) for the wind speed. There is a 50% probability that the wind speed during the winter will be higher than 3 m/s (light breeze) and 4.2 m/s (gentle breeze) during the summer.

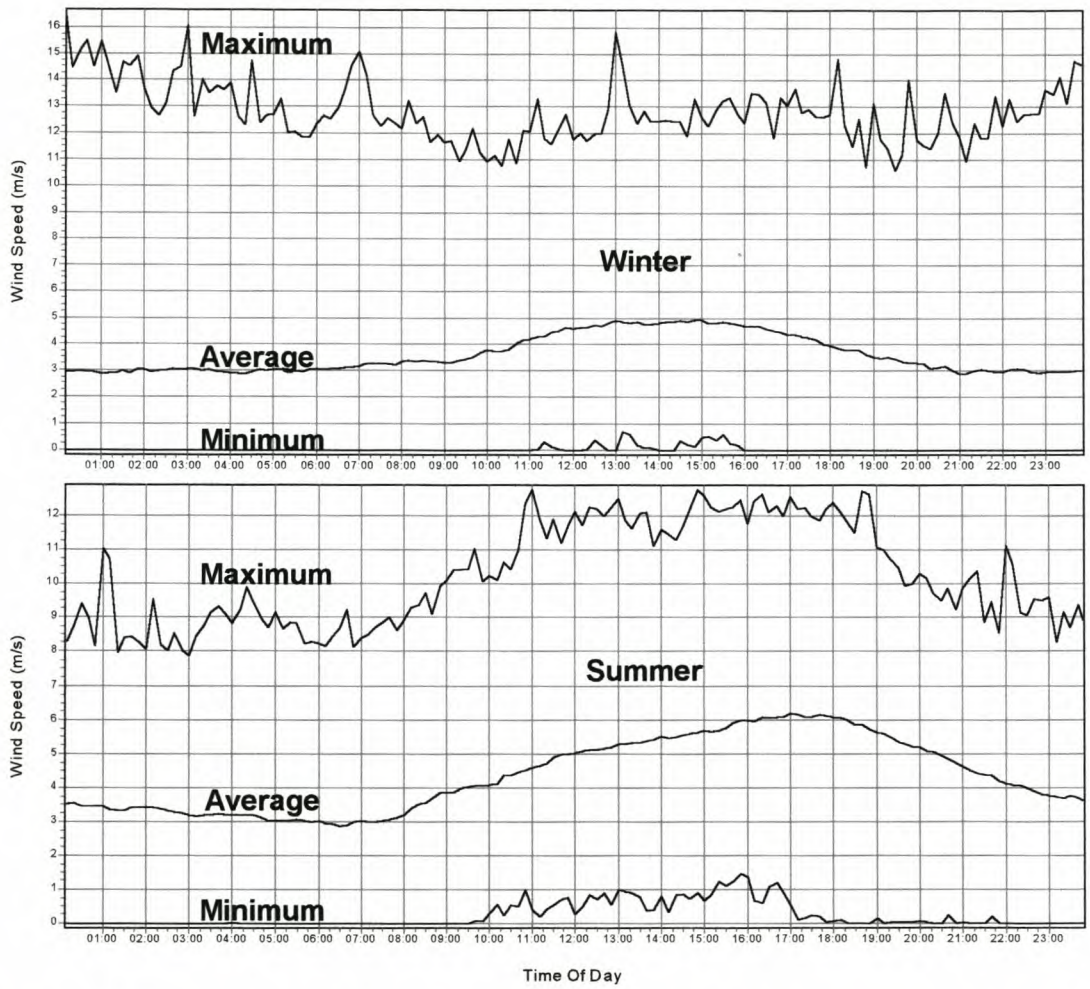

Figure 3. 16 Time-of-day trends of the minimum, average and maximum wind speed measurements for the winter and summer periods.

The time-of-day plots (as per statistical method described in Appendix C 3) of the wind speed for the winter and summer periods are shown in Figure 3. 16. The average wind speed is lower at night and starts to increase as the sun rises. The average wind speed reaches a maximum during the afternoon (more pronounced in summer - 17h00).

The wind speed measurements in the various wind directions were grouped in preset wind speed 'bins'. Figure 3. 17 and Table 3. 6 show the wind rose plots and data of wind speed (percentage of occurrence in preset value 'bins') in relation to wind direction.

Stellenbosch University http://scholar.sun.ac.za

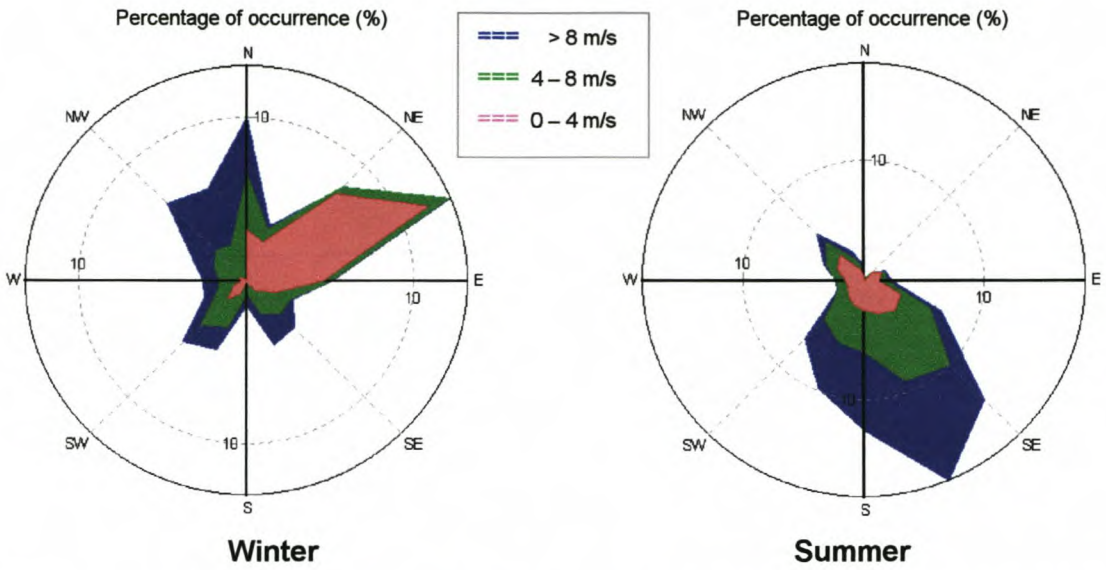

Figure 3. 17 Wind rose plots of wind direction in relation to percentage of occurrence of wind speed for preset values. The winter and summer plots show the dominant wind speeds and directions.

Table 3. 6 Table of percentage of occurrences of wind speeds grouped in preset wind speed 'bins' in relation to wind direction for the winter and summer periods.

Direction	Winter				Summer			
	0-4 m/s	4-8 m/s	>8 m/s	Total	0-4 m/s	4-8 m/s	>8 m/s	Total
N	4.5	2.7	2.7	9.9	1.6	0.4	0.3	2.3
NNE	4.1	0.6	0.2	4.9	1.3	0.1	0.0	1.4
NE	8.0	0.4	0.1	8.5	2.1	0.0	0.0	2.1
ENE	11.5	1.0	0.1	12.6	2.7	0.1	0.1	2.9
E	5.7	0.4	0.1	6.2	2.4	0.5	0.4	3.3
ESE	3.6	0.7	0.1	4.4	4.1	2.3	0.9	7.3
SE	2.8	1.5	1.0	5.3	4.4	5.6	3.6	13.6
SSE	2.4	1.5	1.6	5.5	3.9	5.3	8.0	17.2
S	2.2	0.6	0.5	3.3	3.5	3.1	5.7	12.3
SSW	2.8	1.7	1.2	5.7	3.3	2.9	3.6	9.8
SW	3.4	1.7	1.2	6.3	2.9	2.5	1.9	7.3
WSW	2.8	0.8	0.7	4.3	2.6	0.6	0.1	3.3
W	2.4	0.9	0.8	4.1	2.7	0.6	0.1	3.4
WNW	2.5	1.2	1.1	4.8	3.4	0.8	0.2	4.4
NW	2.1	2.0	3.2	7.3	3.8	1.3	0.9	6.0
NNW	2.1	1.9	2.9	6.9	2.1	0.8	0.5	3.4
Total	62.9	19.6	17.5	100.0	46.8	26.9	26.3	100.0

Stellenbosch University http://scholar.sun.ac.za

From Figure 3. 17 and Table 3. 6 it is evident that the dominant wind during winter is east-north-easterly and south-south-easterly during summer. The strongest winds are north-westerly in winter and south-south-easterly in summer.

3.2.2.5 UV-B solar radiation

Solar radiation plays a significant role in the heating of the ambient air mass, which has an influence on wind speeds and direction, and relative humidity levels. Solar radiation also results in the heating of the insulator surface. As previously stated (in section 3.2.2.3) the insulator surface temperature in relation to ambient dew point temperature may result in the wetting of the insulator surface. When the sun rises in the early morning and heats the ambient air the insulator surface may be wetted at that specific point. During the day the solar radiation keeps the insulator surface at a temperature higher than ambient, thus resulting in a lower probability of surface wetting. The high-energy UV-B photons may also result in the ageing of non-ceramic or polymer surfaces, as shown by Gorur [50].

The UV-B solar radiation measurements during the summer and winter periods are shown in Figure 3. 18.

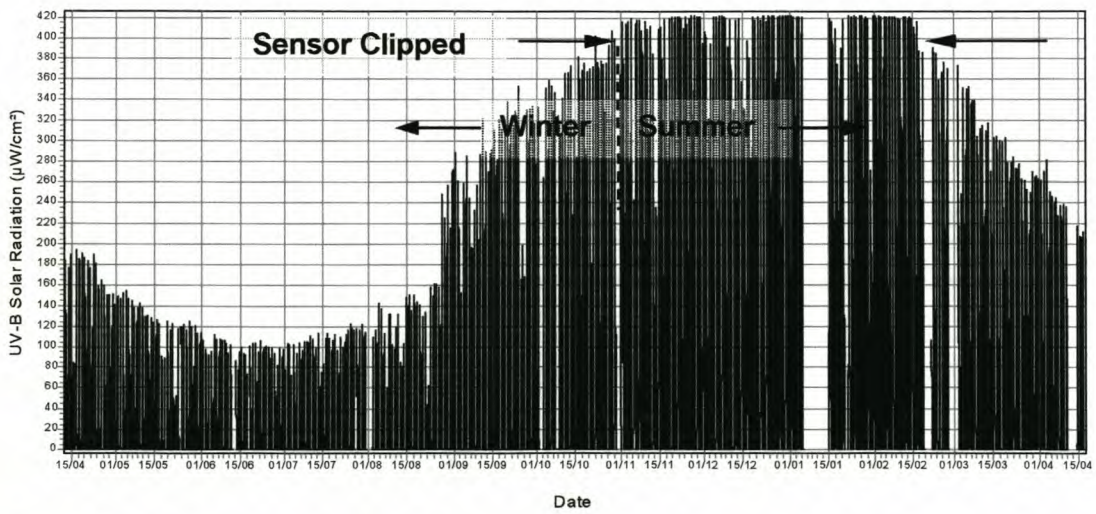

Figure 3. 18 UV-B solar radiation measurements during the winter and summer periods.

It is clear from Figure 3. 18 that there is a significant difference between UV-B solar radiation levels measured in summer and in winter. The summer levels are much higher than the winter levels. The sensor could not measure the maximum levels of UV-B in

Stellenbosch University http://scholar.sun.ac.za

summer. An extrapolated maximum value is estimated to be at least 450 μW/cm^2. The typical maximum UV-B (350 nm) value at the equator at noon is expected to be in the order of 250 μW/cm^2 [51]. Thus, the levels of UV-B solar radiation at KIPTS are extremely high, and high-energy photons, which can result in polymer breakdown, are expected.

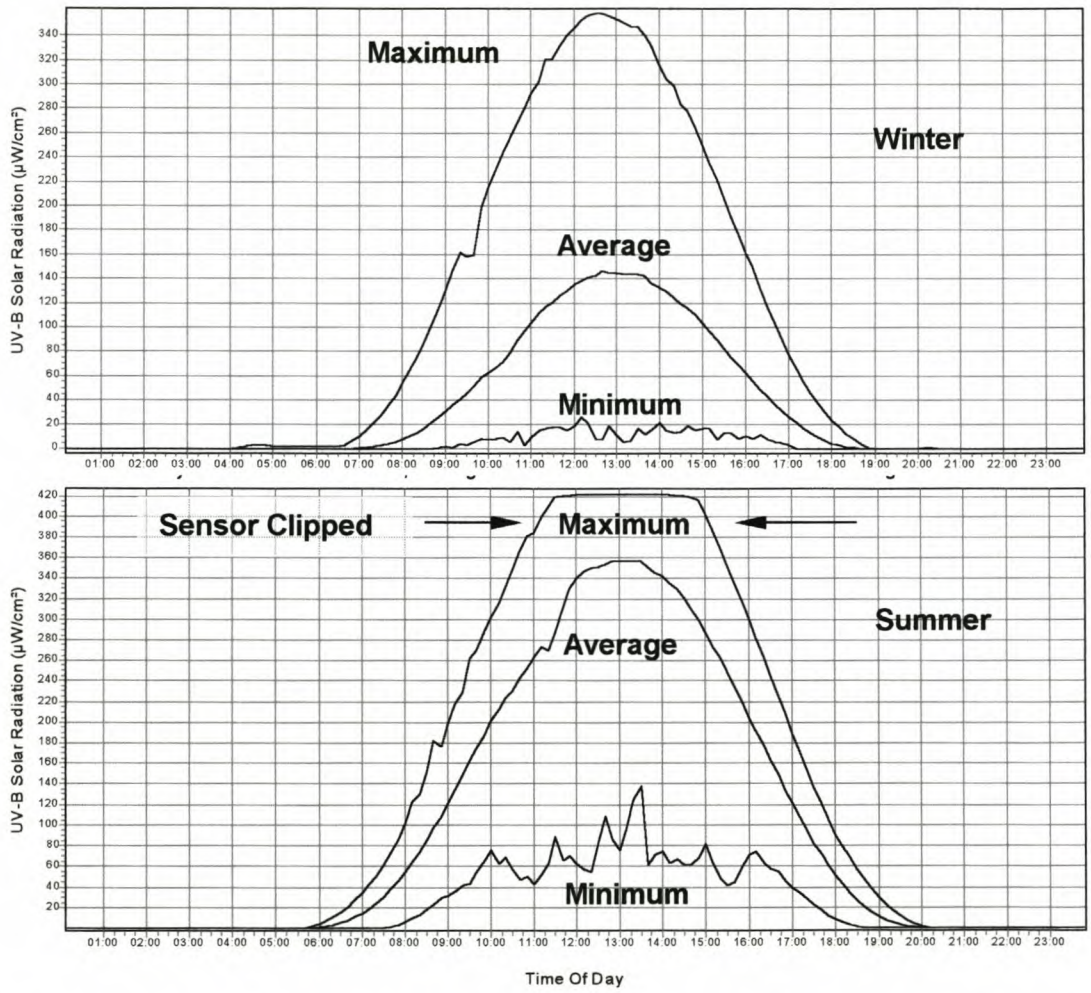

Figure 3. 19 Time-of-day trends of the minimum, average and maximum UV-B solar radiation measurements during the winter and summer periods.

Figure 3. 19 shows the time-of-day plots (as per statistical method described in Appendix C 3) showing the maximum, minimum and average values recorded during winter and summer. The sunrise and sunset, and day and night times can be clearly seen.

Stellenbosch University http://scholar.sun.ac.za

3.2.3 Correlation of climatic parameters monitored

Due to the volume of climatic data collected over the test period of one year it was difficult to relate the climatic parameters by visual comparison of the graphically displayed data (it could be done for smaller selections). Scatter plots of various climatic parameters in relation to one another was attempted (e.g. relative humidity versus temperature), however the scatter was found to be too large for easy interpretation. Work done by STRI in a confidential report "Multivariate Analysis Methods for Database" and a publication by Ahmad et al [52] triggered the idea of using correlation as a statistical method to compare and relate the interaction of the climatic parameters to one another.

Cross-correlation between the various climatic parameters was done using the Cross-correlation statistical method as described in Appendix C 7. The results are shown in Table 3. 7. The directional wind speed used was calculated by using the statistic method as described in Appendix C 6. Note, positive values indicate a direct relationship and negative an inverse. Absolute values close to 100 show a very good correlation whereas values close to 0 indicate virtually no correlation.

The following was observed from the correlation of results (Table 3. 7):

- The temperature is high when the relative humidity is low, and vice versa. There is an ambient temperature increase with solar radiation. The ambient temperature increases with wind speeds emanating from the south-west in winter and the south-east in summer.
- The relative humidity levels drop when the wind speed increases, especially that of the south-easterly winds. However, there is an increase in relative humidity with northerly winds, especially in summer. Solar radiation reduces the relative humidity levels.
- There is a correlation between the directional wind speed and solar radiation. During the day the solar radiation increases and so does the south-westerly wind speeds. As the solar radiation decreases, the easterly wind speed increases. This pertains to the coastal flow of air mass during the day and the land flow during the night.
- The rainfall correlates with wind speeds from the north and west.

These observations were discussed with Cape Weather Wise and corresponds to the typical climate expected at KIPTS.

Stellenbosch University http://scholar.sun.ac.za

Table 3. 7 Cross-correlation matrix of the climatic conditions at KIPTS in relation to one another.

			Cross correlation (x100) matrix for the climatic conditions monitored in relation to one another								
			Temperature	Humidity	UV-B	Rainfall	Wind Speed	Wind Speed			
								340 (North)	70 (East)	160 (South)	250 (West)
Winter	Temperature		100.0	-60.7	39.0	-3.5	25.0	3.9	4.8	18.4	15.5
	Humidity		-60.7	100.0	-31.1	6.8	-19.3	2.5	-19.2	-20.2	-1.7
	UV-B		39.0	-31.1	100.0	-4.2	20.1	0.4	-12.6	19.4	24.2
	Rainfall		-3.5	6.8	-4.2	100.0	15.2	13.3	-4.2	-1.7	13.3
	Wind Speed		25.0	-19.3	20.1	15.2	100.0	49.1	14.8	3.1	62.3
	Wind Speed	340 (North)	3.9	2.5	0.4	13.3	49.1	100.0	-13.1	-36.3	25.0
		70 (East)	4.8	-19.2	-12.6	-4.2	14.8	-13.1	100.0	8.9	-38.1
		160 (South)	18.4	-20.2	19.4	-1.7	3.1	-36.3	8.9	100.0	0.8
		250 (West)	15.5	-1.7	24.2	13.3	62.3	25.0	-38.1	0.8	100.0
Summer	Temperature		100.0	-66.5	22.3	-0.9	41.2	-11.3	23.8	33.3	8.2
	Humidity		-66.5	100.0	-15.1	3.1	-37.4	25.5	-30.5	-37.2	0.2
	UV-B		22.3	-15.1	100.0	-2.1	23.4	7.3	-27.6	12.5	41.2
	Rainfall		-0.9	3.1	-2.1	100.0	4.4	10.8	1.8	-2.6	1.9
	Wind Speed		41.2	-37.4	23.4	4.4	100.0	-0.5	31.1	67.3	45.0
	Wind Speed	340 (North)	-11.3	25.5	7.3	10.8	-0.5	100.0	-19.2	-37.9	6.0
		70 (East)	23.8	-30.5	-27.6	1.8	31.1	-19.2	100.0	9.5	-43.2
		160 (South)	33.3	-37.2	12.5	-2.6	67.3	-37.9	9.5	100.0	3.9
		250 (West)	8.2	0.2	41.2	1.9	45.0	6.0	-43.2	3.9	100.0
Full Year	Temperature		100.0	-65.4	34.7	-5.3	34.9	-10.3	15.4	34.3	13.6
	Humidity		-65.4	100.0	-24.4	6.8	-30.0	14.5	-25.3	-33.5	-2.4
	UV-B		34.7	-24.4	100.0	-4.1	23.8	-3.6	-20.1	22.0	34.1
	Rainfall		-5.3	6.8	-4.1	100.0	10.4	13.8	-2.9	-3.3	9.2
	Wind Speed		34.9	-30.0	23.8	10.4	100.0	26.3	23.6	52.4	53.4
	Wind Speed	340 (North)	-10.3	14.5	-3.6	13.8	26.3	100.0	-15.5	-38.0	16.0
		70 (East)	15.4	-25.3	-20.1	-2.9	23.6	-15.5	100.0	10.7	-40.1
		160 (South)	34.3	-33.5	22.0	-3.3	52.4	-38.0	10.7	100.0	3.9
		250 (West)	13.6	-2.4	34.1	9.2	53.4	16.0	-40.1	3.9	100.0

Stellenbosch University http://scholar.sun.ac.za

3.3 CONCLUDING REMARKS ON THE ENVIRONMENTAL AND CLIMATIC CONDITIONS

From the environmental and climatic study and data measured it can be concluded that KIPTS is situated in a dominantly marine-pollution environment. There are sources of industrial and agricultural pollution, but these are secondary. The pollution levels at KIPTS are heavy during the summer and medium during the winter months. There are pollution events that are exceptionally high. In a CIGRE study [53], of which the author is a working member, the pollution severity at KIPTS has been correlated to that of other test stations in the world. It was shown that KIPTS is the most severe insulator pollution test-site in the world.

Climatically, the rainfall at KIPTS occurs mainly in winter, with very little rainfall in summer. The humidity is above 75% most of the time, with levels higher than 90% at night. This indicates that there is a good probability of critical wetting of the insulator surface most of the time.

The dominant wind direction during winter is north-easterly, and south-westerly in summer. The wind speeds can be extremely high (gale force). Westerly winds bring marine pollution, south-easterly winds bring industrial pollution, north-easterly winds bring rain, and easterly winds tend to be hot.

The UV-B levels are extremely high, thus UV-induced material degradation is expected.

Stellenbosch University http://scholar.sun.ac.za

4 A STUDY OF THE INSULATOR POLLUTION AND WETTING PROCESS

"Natural Science does not simply describe and explain nature; it is part of the interplay between nature and ourselves; it describes nature as exposed to our method of questioning." - ***Werner Heisenberg***

In Chapter 3 the environmental (pollution) and climatic (weather) conditions at KIPTS are discussed, giving a good idea of the natural ambient conditions the test insulators were subjected to. In this chapter, the resulting pollution and interaction with the insulator surface, including wetting, are discussed.

4.1 THE INSULATOR POLLUTION PROCESS

The insulator pollution process is well documented and explained in a draft copy of the document "Polluted insulators: A review of current knowledge" compiled by CIGRE task force 33-04-01 [18]. The basic insulator pollution process at KIPTS was monitored based on the ideas presented in the CIGRE document and is reported below.

4.1.1 Insulator pollution deposit observations

Visual observations of insulator pollution deposit were made at the time intervals described in Chapter 2, section 2.2.5, and the following were found:

- Light pollution build-up and salt crystals were noted from week 1 on both the energised and non-energised insulators.
- The first signs of directional pollution dominant from the south were observed mainly on the shed tips and rod housing (sheath) from week 5 onwards. However, it was less in week 12 when it rained before the inspection.
- The directional pollution build-up was always less prominent on the energised insulators, and in week 36 it was noted that the pollution on the energised insulators showed signs of flaking and breaking up.
- There was no significant difference between the consistency of the pollution deposits on the various material types of test insulators.

Stellenbosch University http://scholar.sun.ac.za

Directional pollution build-up on the south-eastern side (right hand side on photos in Figure 4. 1) of the non-energised porcelain insulator at KIPTS can be seen in Figure 4. 1. This is normally found during the drier summer months, when winds blow predominantly from the south-east and collect particles from the main industrial pollution sources.

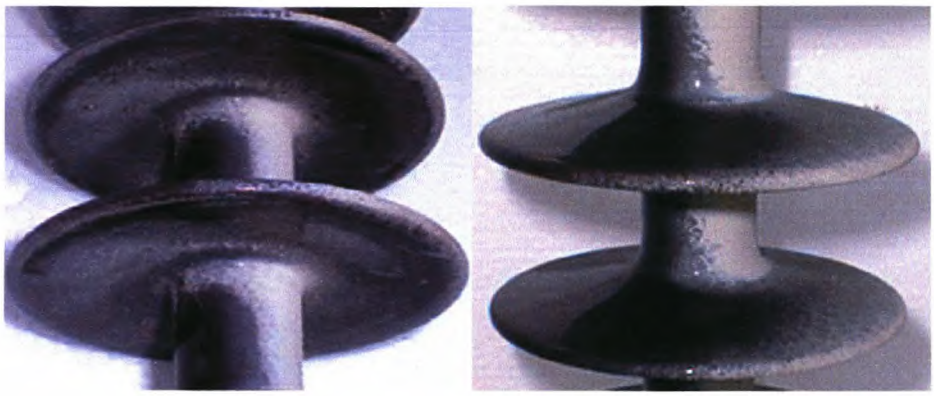

Bottom Top

Figure 4. 1 Photograph showing the directional pollution build-up on a non-energised porcelain test insulator.

The visual pollution build-up on the energised porcelain insulator was lower than that on the non-energised porcelain insulator, as shown in Figure 4. 2. The pollution build-up was also higher on the south-eastern rim of the bottom of the shed. This correlates well with the expected theories of wind-borne pollution processes. This was also true for all the other test insulators, as shown in Figure 4. 3.

New Non-Energised Energised

Figure 4. 2 Photograph showing the pollution build-up on the porcelain test insulators, with the non-energised insulator showing the highest pollution deposit.

Stellenbosch University http://scholar.sun.ac.za

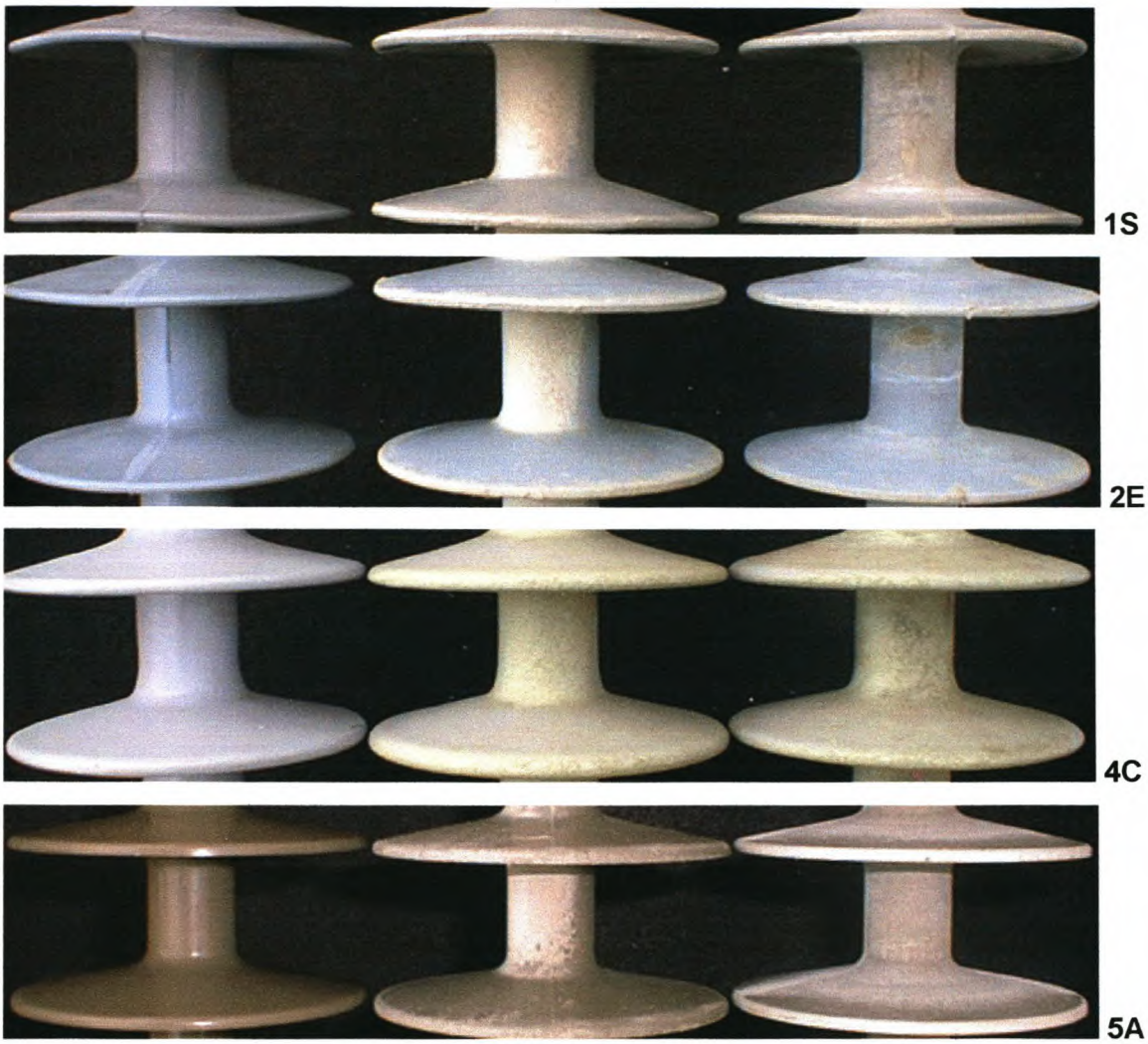

Figure 4. 3 Photograph showing the pollution build-up on the different test insulators.

It is hypothesised that the differences in pollution build-up and distribution could be due to the leakage current and discharge activity on the energised insulator breaking down the pollution deposit and rendering it more soluble, which then helps distribute the pollution over the surface.

It was found that wind is the main carrier of pollution at KIPTS. The other effects (gravity and electric field) mentioned in the CIGRE review [18] were found to be secondary.

The wind speed in relation to ESDD was measured for a glass cap-and-pin disc insulator at 2-hourly intervals for 1 day, to establish whether there is a relationship. Figure 4. 4 shows the wind speed and ESDD measurements made. It can be seen that there is a

Stellenbosch University http://scholar.sun.ac.za

close relationship. The measured ESDD results were compared to predicted SDD results (also shown in Figure 4. 4) using the measured wind speed and the following formula proposed by Mizuno et al [49]:

$$SDD = K \cdot \sum_i V_i^3 \cdot t_i \qquad (4.1)$$

where

SDD : salt deposit density in mg/cm^2

K : constant that depends on location and type of insulator (5.2 - 8.0 x 10^{-6})

V_i : average wind velocity in m/s for each time interval

t_i : length of time interval

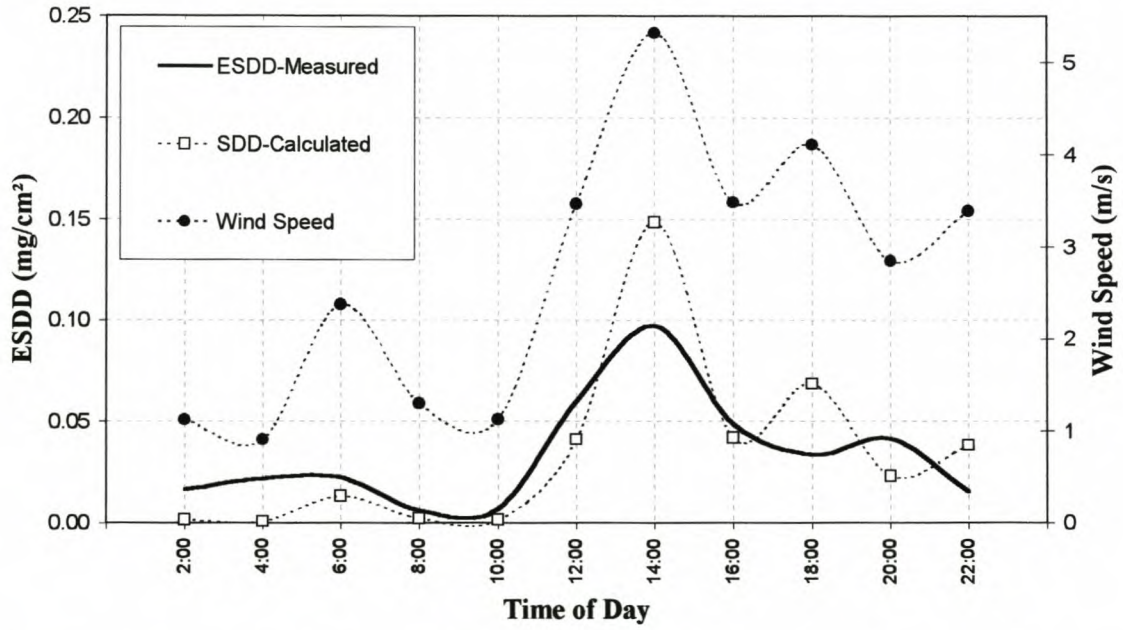

Figure 4. 4 Measured average ESDD and calculated SDD on glass (cap-and-pin, U120BS) disk insulator and wind speed, taken at two-hourly intervals over one day, at KIPTS.

In order to obtain the same total ESDD and SDD values for the day (0.388 mg/cm^2) the constant K was determined as 8.23 x 10^{-6}. It was found that the constant needed for predicting pollution deposit at KIPTS is higher than the range proposed by Mizuno et al [49]. The total ESDD was measured as 0.0323 mg/cm^2 on a disk left for the 24-hour period. The difference in these values shows that there is natural washing taking place, due to condensation seepage, even though it did not rain, indicating that the pollution retention factor is low.

Stellenbosch University http://scholar.sun.ac.za

4.1.2 Insulator pollution measurements

Insulator pollution measurements such as localised equivalent salt-deposit density (LESDD), and surface conductivity data obtained using the insulator pollution monitoring apparatus (IPMA) were recorded in accordance with the test procedure and time interval described in Chapter 2, section 2.2.5.

4.1.2.1 Monitoring localised equivalent salt-deposit density (LESDD)

Localised ESDD (LESDD) measurements were made on insulators 6S and 7E energised and non-energised using the method as discussed in the paper "A novel method to measure the contamination level of insulators – spot contamination measurement" [54]. Four readings corresponding to the cardinal points (north, east, south, and west) were taken on the top of the sheds. The LESDD test commenced at the first shed on the live side and was done subsequently on the next shed up towards the earth side, and then restarting at the live side. By not sampling on the same shed for every test, the disturbance of the pollution layer was minimised. The LESDD sampling tool and associated measuring equipment is shown in Figure 4. 5 below.

Figure 4. 5 LESDD sampling tool and associated toolbox with measuring equipment.

Stellenbosch University http://scholar.sun.ac.za

The LESDD was calculated using the same equations as for ESDD (see section 3.1.2.1). The only differences were the surface area tested (78.57 mm^2) and the volume of distilled water used (100 µl). The results are shown in Figure 4. 6 to Figure 4. 9 below.

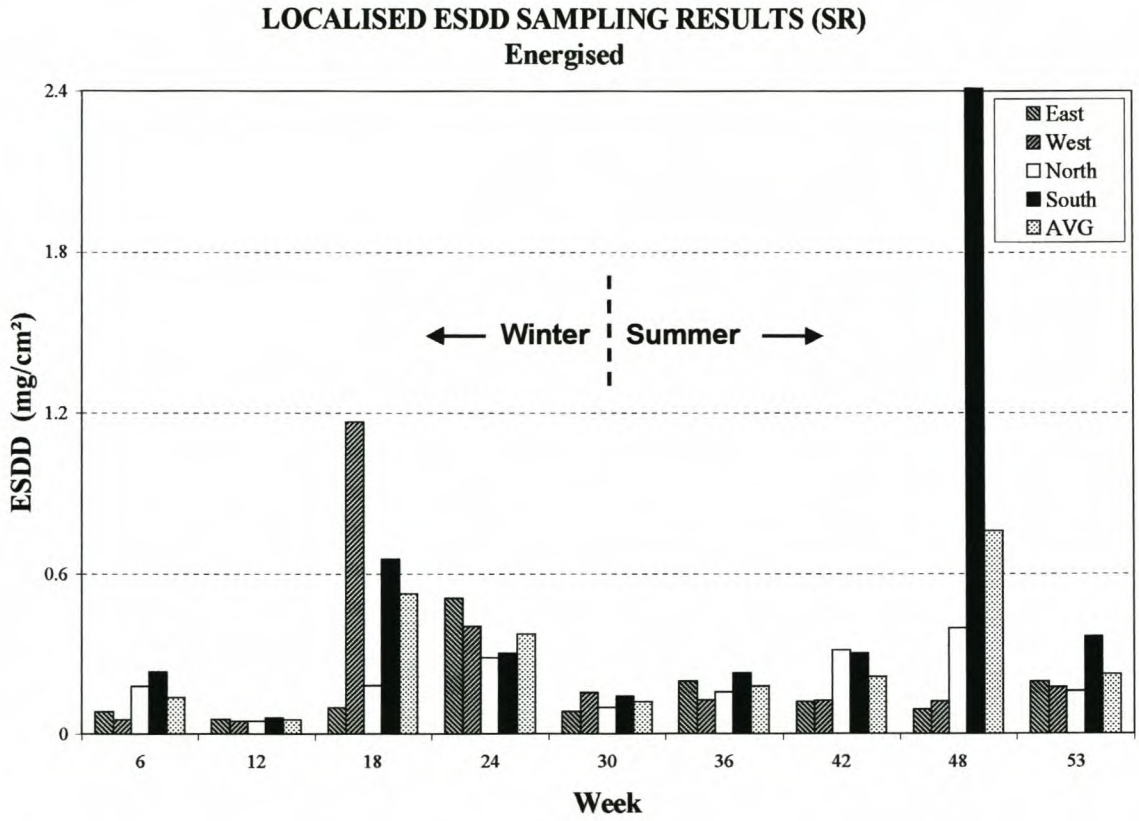

	SR, Energised, LESDD (mg/cm²)							
	Winter				Summer			
	N	E	S	W	N	E	S	W
Max	0.286	0.511	0.655	1.167	0.396	0.197	2.434	0.175
	Very-Heavy	Exceptional	Exceptional	Exceptional	Very-Heavy	Heavy	Exceptional	Heavy
Min	0.049	0.056	0.060	0.049	0.096	0.082	0.141	0.121
	Light	Light	Medium	Medium	Medium	Medium	Heavy	Heavy
Ave	0.158	0.166	0.279	0.365	0.225	0.137	0.695	0.141
	Heavy	Heavy	Very-Heavy	Very-Heavy	Very-Heavy	Heavy	Exceptional	Heavy

Figure 4. 6 Six-weekly LESDD measurements on the energised SR insulator 6S taken on the top of the shed at the cardinal points (north, east, south and west), for both the winter and summer test programme cycles.

The average LESDD levels measured on the top of the shed of the energised SR insulator 6S were found to be 0.242 mg/cm^2 (on the verge of very heavy) in winter and 0.300 mg/cm^2 (very heavy) in summer.

Stellenbosch University http://scholar.sun.ac.za

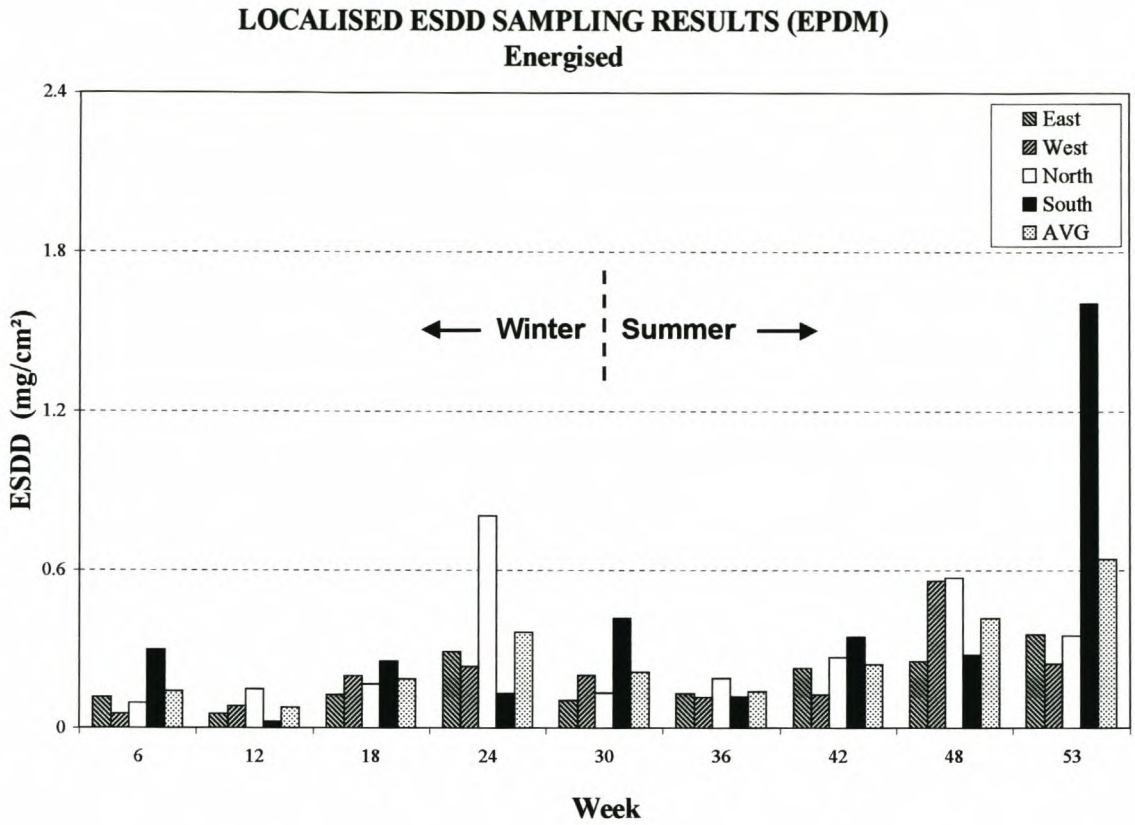

	EPDM, Energised, LESDD (mg/cm²)							
	Winter				Summer			
	N	E	S	W	N	E	S	W
Max	0.803	0.291	0.419	0.236	0.572	0.359	1.607	0.559
	Exceptional	Very-Heavy	Very-Heavy	Heavy	Exceptional	Very-Heavy	Exceptional	Exceptional
Min	0.097	0.055	0.024	0.055	0.133	0.105	0.120	0.117
	Medium	Light	Very-Light	Light	Heavy	Medium	Medium	Medium
Ave	0.270	0.139	0.226	0.155	0.303	0.216	0.555	0.250
	Very-Heavy	Heavy	Heavy	Heavy	Very-Heavy	Heavy	Exceptional	Very-Heavy

Figure 4. 7 Six-weekly LESDD measurements on the energised EPDM insulator 7E taken on the top of the shed at the cardinal points (north, east, south and west), for both the winter and summer test programme cycles.

The average LESDD levels measured on the top of the shed of the energised EPDM insulator 7E were found to be 0.198 mg/cm^2 (heavy) in winter and 0.331 mg/cm^2 (very heavy) in summer.

Stellenbosch University http://scholar.sun.ac.za

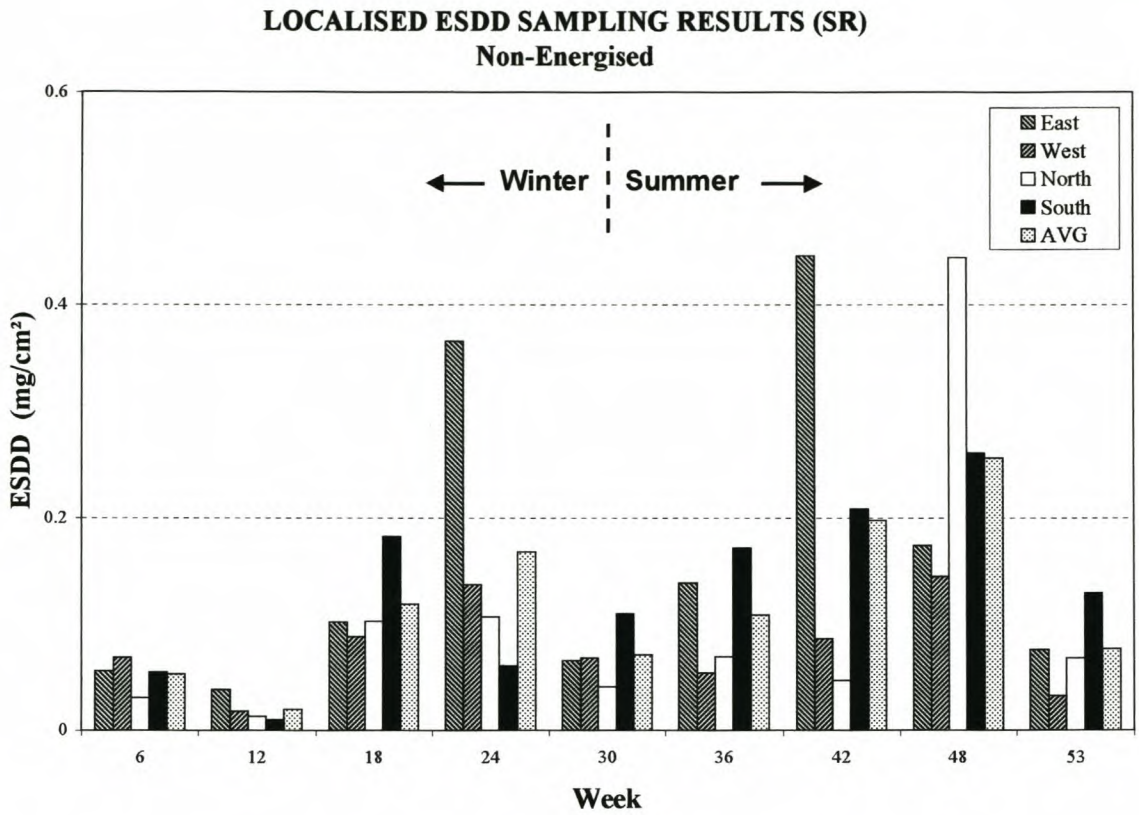

	SR, Non - Energised, LESDD (mg/cm²)							
	Winter				Summer			
	N	E	S	W	N	E	S	W
Max	0.107	0.366	0.182	0.137	0.444	0.446	0.260	0.145
	Medium	Very-Heavy	Heavy	Heavy	Very-Heavy	Very-Heavy	Very-Heavy	Heavy
Min	0.013	0.038	0.010	0.018	0.041	0.066	0.110	0.032
	Very-Light	Light	None	Very-Light	Light	Medium	Medium	Light
Ave	0.059	0.125	0.084	0.076	0.134	0.180	0.176	0.077
	Light	Heavy	Medium	Medium	Heavy	Heavy	Heavy	Medium

Figure 4. 8 Six-weekly LESDD measurements on the non-energised SR insulator 6S taken on the top of the shed at the cardinal points (north, east, south and west) is shown for both winter and summer test programme cycles.

The average LESDD levels measured on the top of the shed of the non-energised SR insulator 6S were found to be 0.086 mg/cm^2 (medium) in winter and 0.142 mg/cm^2 (heavy) in summer. This corresponds with the ESDD classification in Chapter 3, section 3.1.2.1.

Stellenbosch University http://scholar.sun.ac.za

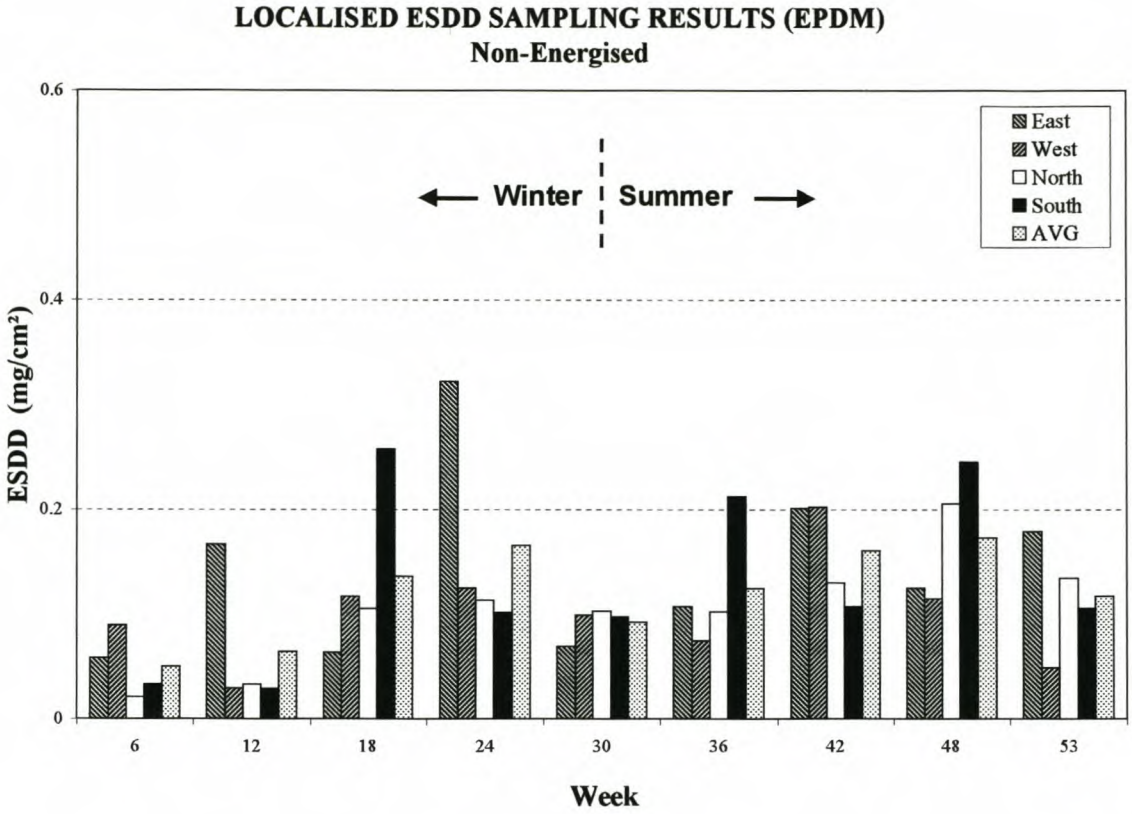

	EPDM, Non - Energised, LESDD (mg/cm²)							
	Winter				Summer			
	N	E	S	W	N	E	S	W
Max	0.113	0.322	0.258	0.125	0.205	0.201	0.246	0.203
	Medium	Very-Heavy	Very-Heavy	Heavy	Heavy	Heavy	Very-Heavy	Heavy
Min	0.021	0.058	0.029	0.030	0.103	0.069	0.098	0.049
	Very-Light	Light	Very-Light	Very-Light	Medium	Medium	Medium	Light
Ave	0.075	0.136	0.104	0.092	0.135	0.136	0.154	0.108
	Medium	Heavy	Medium	Medium	Heavy	Heavy	Heavy	Medium

Figure 4. 9 Six-weekly LESDD measurements on the non-energised EPDM insulator 7E taken on the top of the shed at the cardinal points (north, east, south and west) is shown for both winter and summer test programme cycles.

The average LESDD levels measured on the top of the shed of the non-energised EPDM insulator 7E were found to be 0.102 mg/cm^2 (medium) in winter and 0.133 mg/cm^2 (heavy) in summer. This corresponds with the ESDD classification in Chapter 3, section 3.1.2.1.

To interpret the data of the above graphs' data the 'probability of exceeding abscissa' plots (as per statistical method described in Appendix C 4) of the LESDD data for both winter and summer periods are shown in Figure 4. 10.

Stellenbosch University http://scholar.sun.ac.za

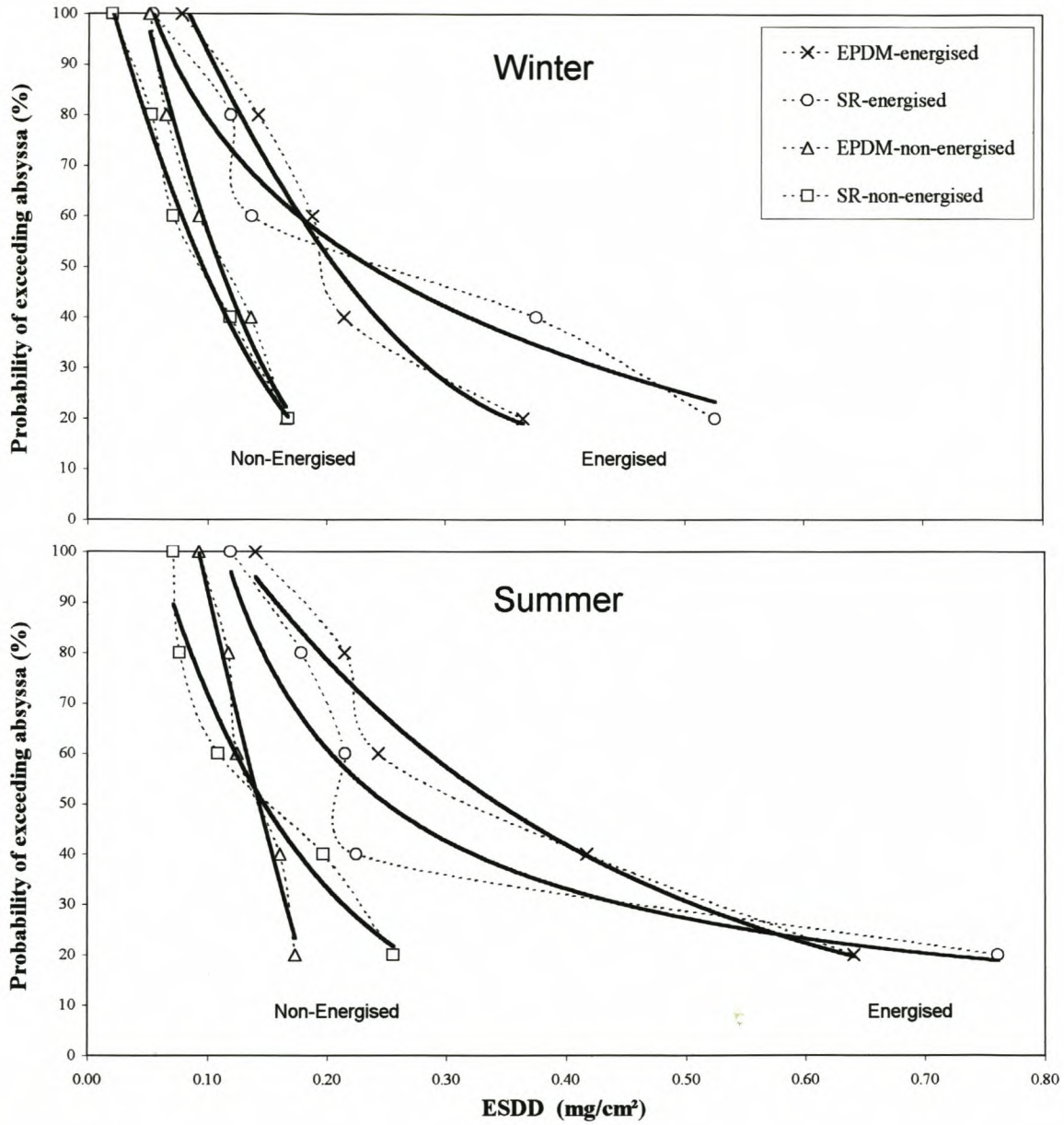

Figure 4. 10 Probability of the average (AVG) LESDD measurements on the energised and non-energised SR and EPDM insulators 6S and 7E is shown for both winter and summer test programme cycles.

From the above probability graphs it is clear that the energised SR and EPDM insulators had higher average values of LESDD than the non-energised units during both the winter and summer test periods.

Stellenbosch University http://scholar.sun.ac.za

This seems to be contradictory to the visual observations, which show more pollution on the non-energised units. The difference between LESDD values for energised and non-energised units is also not due to electrostatic catch as the pollution measurements were made from live to dead ends, and the visual pollution observations also show no significant difference in the pollution deposit between live and dead ends.

Why is there a difference? The author's hypothesis in section 4.1.1 that *"the difference in pollution build-up and distribution could be due to the leakage current and discharge activity on the energised insulator breaking down the pollution deposit and rendering it more soluble, which then helps distribute the pollution over the surface"* is further supported by the LESDD findings and can now be used to help explain the difference.

4.1.2.2 Measurements of surface conductivity using the insulator pollution monitoring apparatus (IPMA)

IPMA surface conductivity measurements were made on insulators 6S, 7E and 8P energised and non-energised. The weekly (Friday) results for the first six weeks and then for week 53 on test insulators 1S, 2E, 3P, 4C and 5A are shown in Figure 4. 11 and Figure 4. 12.

A short description of the IPMA test procedure is described as follows:

a) The test insulator is placed in a closed, controlled environment (chamber).
b) A heater and/or air blower is engaged to dry the test insulator.
c) The insulator is energized for five 3 kV AC voltage cycles and the voltage and leakage current over the test insulator is measured as a dry reference.
d) The wetting cycle is then begun; a short pulse of steam is injected into the chamber and the voltage and leakage current are recorded in the same manner as (c) above. The wetting cycle continues until a decline in leakage current is registered (the current decreases for more than three successive wetting cycles). The number of wetting cycles for the test is referred to as iterations.
e) The insulator is then dried as per (b) above and returned to its natural environment.
f) The surface conductance of the test insulator, when artificially wetted, can then be calculated from the voltage and leakage current results using Eq. 1.14.

Stellenbosch University http://scholar.sun.ac.za

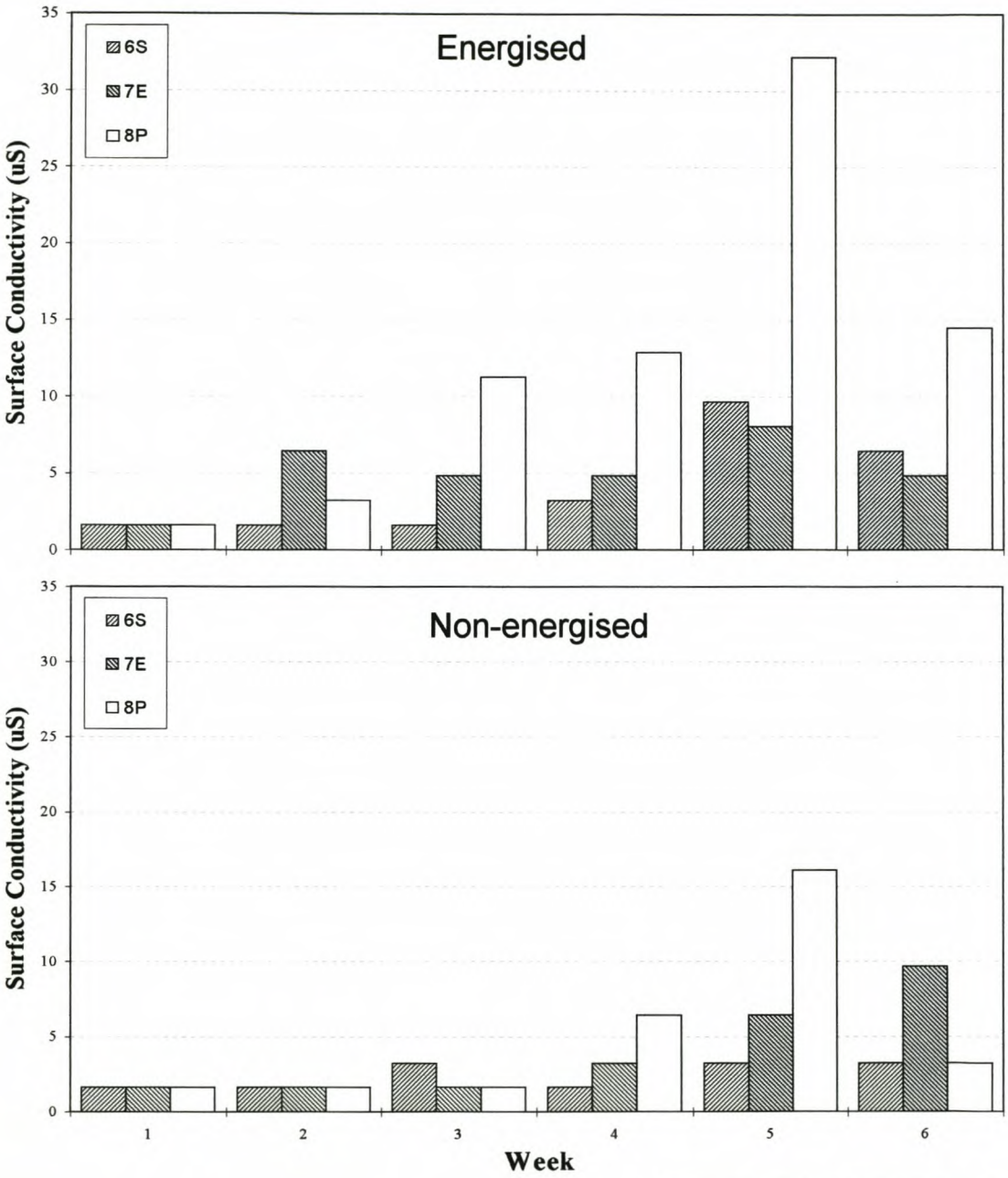

	Ratio of IPMA Energised/Non-Energised		
Week	6S	7E	8P
1	1.00	1.00	1.00
2	1.00	4.00	2.00
3	0.50	3.00	7.00
4	2.00	1.50	2.00
5	3.00	1.25	2.00
6	2.00	0.50	4.50
Average	1.58	1.88	3.08

	Ratio of IPMA (6S,7E)/8P			
	Energised		Non-Eergised	
Week	6S/8P	7E/8P	6S/8P	7E/8P
1	1.00	0.62	1.00	1.00
2	0.50	1.24	1.00	1.00
3	0.14	0.27	2.00	1.00
4	0.25	0.23	0.25	0.50
5	0.30	0.16	0.20	0.40
6	0.44	0.21	1.00	3.00
Average	0.44	0.45	0.91	1.15

Figure 4. 11 Weekly IPMA surface conductivity recordings (indicating the surface condition) for the first six weeks of the test period on the SR, EPDM and porcelain insulators 6S, 7E and 8P.

Stellenbosch University http://scholar.sun.ac.za

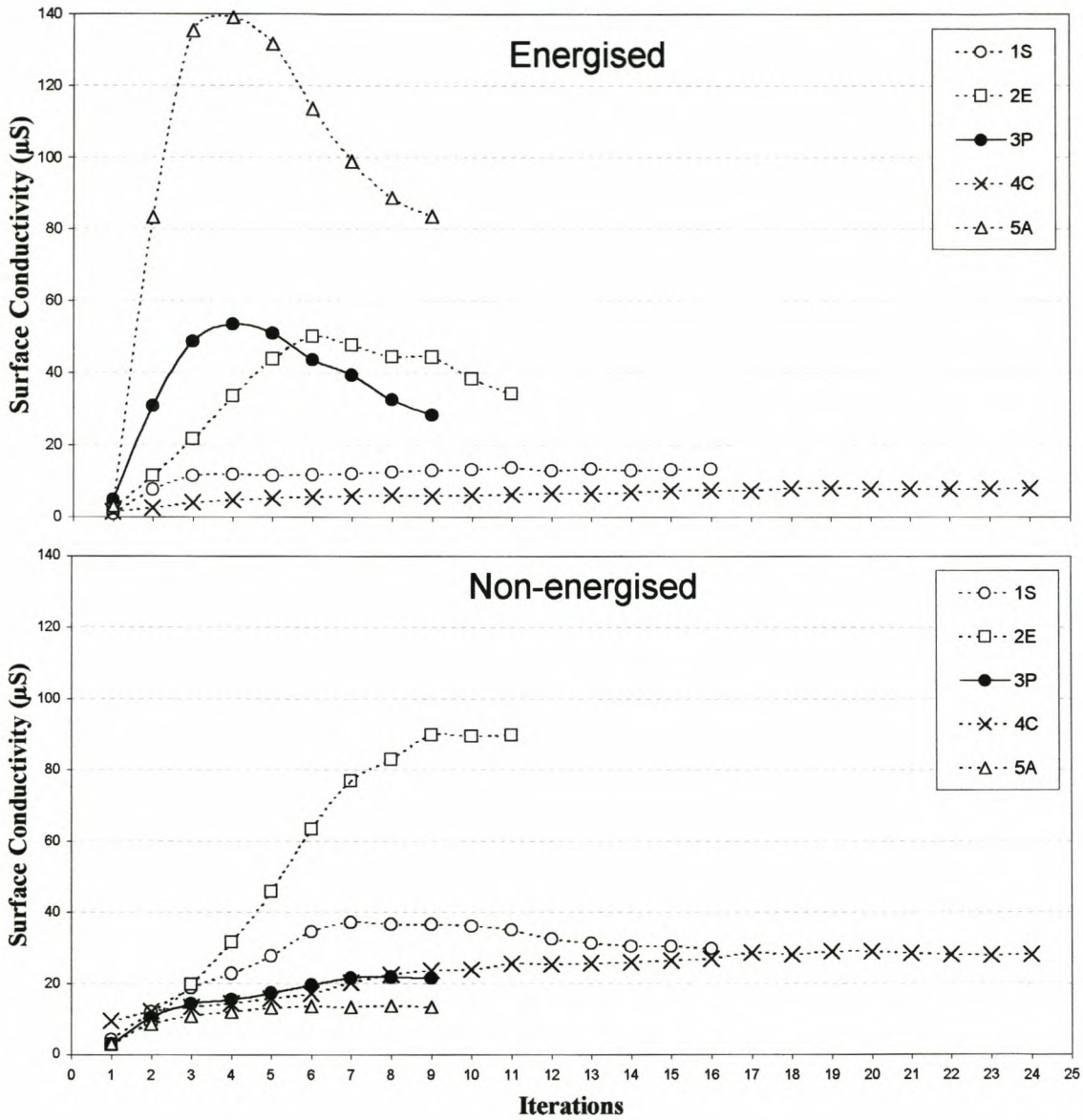

	Ratio of IPMA (1S,2E,4C,5A)/3P Week 53	
	Energised	Non-Energised
1S/3P	0.3	1.7
2E/3P	0.9	4.2
4C/3P	0.2	1.3
5A/3P	2.6	0.6

	Ratio of IPMA Energised/Non-Energised Week 53
1S	0.4
2E	0.6
3P	2.5
4C	0.3
5A	10.2

Figure 4. 12 IPMA surface conductivity recordings (indicating the surface condition) made after completion of the test period (week 53) on insulators 1S, 2E, 3P, 4C and 5A

Stellenbosch University http://scholar.sun.ac.za

The IPMA surface conductivity measurements in Figure 4. 11 show that the energised test insulators have, on average, higher surface conductivity readings than non-energised ones, which confirms the LESDD findings. The average ratio for the energised test insulators shows lower surface conductivity values for both SR and EPDM compared to that of the reference porcelain insulator. Why do the energised SR and EPDM insulators have lower values when compared to the porcelain insulator?

It is hypothesised that there is a change in the insulator material surface property, especially in the region of the dry band on the energised units. This region then has a different surface conductivity, shown by the overall IPMA surface conductivity measurements. It is further suggested that the material interacts with the pollution layer, also resulting in a change in surface conductivity. These phenomena are not expected on a stable porcelain material surface and that is why the porcelain test insulators are used as reference for determining the influence of the pollution layer on the surface conductivity only.

The IPMA surface conductivity measurements in Figure 4. 12 were made on the naturally aged test insulators, energised and non-energised, at the end of the test period (week 53). The energised and non-energised test insulators of the same material type were tested at the same time in the IPMA, thus the iterations (number of wetting cycles) were identical. The number of iterations is an indicator of the solubility of the pollution layer. The more iterations needed, the less soluble the pollution layer. The surface conductivity results, number of iterations and the pollution levels are shown in Table 4. 1.

Table 4. 1 Table of IPMA surface conductivity measurements and pollution-severity classifications (from Table 3.3, chapter 3) for week 53 on energised and non-energised insulators 1S, 2E, 3P, 4C and 5A. The numbers of test iterations are also shown.

	IPMA, SURFACE CONDUCTIVITY (µS)		
	Week 53		
	Energised	Iterations	Non-Enegised
1S	13.64	16	37.52
	Heavy		Very-Heavy
2E	50.60	11	90.61
	Exceptional		Exceptional
3P	53.77	9	21.83
	Exceptional		Heavy
4C	8.09	24	29.27
	Medium		Very-Heavy
5A	139.78	9	13.74
	Exceptional		Heavy

Stellenbosch University http://scholar.sun.ac.za

The surface conductivity results in Figure 4. 12 show that the pollution layers on the energised test insulators generally dissolved faster than the layers on the non-energised insulators. The number of iterations needed to reach a peak value of surface conductivity was less for the energised insulators. Thus, energisation influences the pollution by making it more soluble, which supports the hypothesis proposed originally in section 4.1.1 and expanded here in section 4.1.2.2 (namely that there is a change in the insulator material surface property).

The higher number of iterations for the SR test insulators (RTV coating and HTV) indicates that the pollution layer takes longer to dissolve than do the reference porcelain and other insulators tested. It is assumed that hydrophobicity transfer from the SR material to the pollution layer has taken place, as described by Kindersberger and Kuhl [55]. This also implies a change in the resistivity (ρ) of the pollution layer and a possible decrease in the area available for current flow.

The RTV SR-coated porcelain insulators had more iterations and lower surface conductivity values than the HTV SR test insulators. This implies that the RTV SR allowed more hydrophobicity transfer than the HTV SR, which correlates with the findings of Cherney and Gorur [56].

The IPMA surface conductivity values measured in week 53 on the energised SR (RTV coating and HTV) and EPDM test insulators were found to be lower than on the non-energised insulators. This contradicts the previous findings that the energised insulators have higher surface conductivity values than the non-energised ones. Why is this so? The hypothesis that the material changes in the dry-band regions is the most plausible. The idea that energisation activates and facilitates the hydrophobicity transfer cannot be used as this cannot occur on the EPDM test insulator. The aluminiumtrihydrate (ATH) filler is the only common material component. It is known [57] that when subjected to electrical discharge activity, the ATH filler changes, and the resultant surface has a high component of aluminium oxide (Al_2O_3). Aluminium oxide is hard, has a very low solubility and is non-conducting. Thus, a surface area with large concentrations of aluminium oxide in relation to the pollution will be difficult to dissolve, have a higher resistivity (ρ) and result in a lower surface conductivity than a normally polluted surface. This supports the hypothesis that the dry-band region has a different surface conductivity, which influences the overall IPMA surface conductivity measurements.

Stellenbosch University http://scholar.sun.ac.za

There was a big difference in surface conductivity values between energised and non-energised cycloaliphatic test insulators (5A). The non-energised unit's value was very close to that measured for the reference porcelain insulator, possibly indicating that the non-energised cycloaliphatic insulator material had minimal interaction with the pollution layer. However, the big difference in surface conductivity measurements on the energised cycloaliphatic insulator supports the hypothesis that there is an interaction between the insulator surface material and the pollution layer, possibly increasing the surface area available for current flow.

It should be noted here that the filler normally used in the cycloaliphatic insulators is silica (quartz) and there is no known interaction between electrical discharge activity and silica (quartz) filler. Thus, the interaction process previously described between the electrical discharge activity in the dry-band region and the aluminium oxide filler does not hold for silica (quartz) fillers.

The ranking of the energised insulators based on the measured surface conductivity values and ratios in Figure 4. 12 is given from low to high as:

(Low) 4C, 1S, 2E, 3P and 5A (High)

The SR insulators 4C and 1S was close to one another and had the lowest surface conductivity values. The EPDM (2E) and porcelain reference (3P) insulators were also close to one another. The cycloaliphatic (5A) insulator had the highest surface conductivity value.

4.2 INSULATOR WETTING PROCESS

The insulator wetting process is well documented and explained in the document "Polluted insulators: A review of current knowledge" compiled by CIGRE task force 33-04-01 [18]. The basic insulator wetting process at KIPTS was monitored based on the ideas presented in the CIGRE document and is reported below.

Stellenbosch University http://scholar.sun.ac.za

4.2.1 Insulator wetting observations

Hydrophobicity inspections were made using STRI Guide 1, 92/1 "Hydrophobicity Classification Guide" [58]. Typical photographs of the hydrophobicity classes (HC 1 to 6) are given in Figure 4. 13 below, as copied directly from the STRI guide. HC 7 classifies a continuous water film present over the entire area.

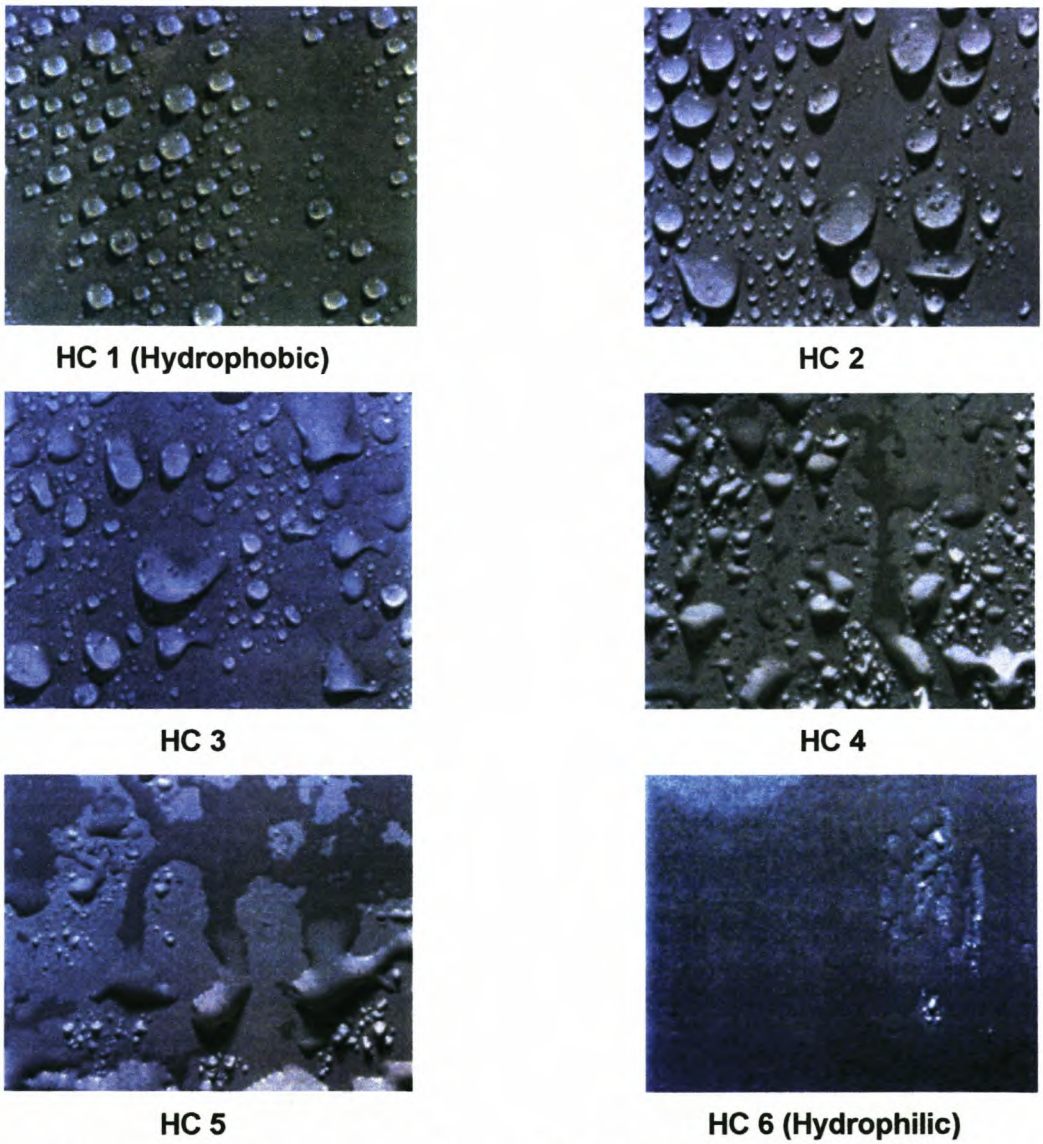

HC 1 (Hydrophobic) HC 2

HC 3 HC 4

HC 5 HC 6 (Hydrophilic)

Figure 4. 13 Typical photographs of surfaces with HC from 1 to 6 (natural size), as copied directly from the STRI guide [58].

The weekly hydrophobicity measurements (made on Fridays from 10h00 to 14h00) on insulators 1S, 2E, 3P, 4C and 5A are shown in Table 4. 2.

Stellenbosch University http://scholar.sun.ac.za

Table 4. 2 Weekly hydrophobicity measurements (made on Fridays) on insulators 1S, 2E, 3P, 4C and 5A.

	Energised					Non-energised				
Week	**1S**	**2E**	**3P**	**4C**	**5A**	**1S**	**2E**	**3P**	**4C**	**5A**
1	2	7	6	2	2	2	7	6	2	2
2	6	6	7	6	3	6	6	7	6	5
3	6	6	7	6	3	6	6	7	6	5
4	6	6	7	4	4	6	6	7	6	6
5	5	6	7	6	4	6	6	7	6	6
6	6	6	7	5	5	6	6	7	6	6
12	6	6	7	6	6	6	6	7	6	6
18	6	6	7	5	6	6	6	7	6	6
24	6	6	7	6	6	6	6	7	6	6
30	6	6	7	6	6	6	6	7	6	6
36	6	6	7	6	6	6	6	7	6	6
42	7	7	7	7	7	7	7	7	6	7
48	7	7	7	7	7	7	7	7	7	7
53	5	6	7	6	7	6	6	7	6	7

The measurements in Table 4. 2 show that surface hydrophobicity was lost on all the test insulators within the first six weeks, on both energised and non-energised. However, when observing the insulator surface under natural light wetting (especially in the early morning), small water drops were observed which then later form larger water drops, and in some cases under heavier wetting conditions formed patches of water, which finally filmed. The STRI hydrophobicity scale is based on 'heavy wetting' conditions to obtain a repeatable measuring method. When applying less water than specified, the wetting of the surface could render a better hydrophobicity class, as observed during light wetting conditions in service. The standard hydrophobicity measurements are therefore rather conservative.

4.2.2 Insulator heating and cooling measurements

Solar radiation thermally heats material surfaces. The heat capacity of a material determines the amount of energy that will be absorbed and the thermal conductivity determines the rate of heat transfer. The temperature of an insulator surface is thus determined by these material properties, which could have an influence on the wetting of the insulator surface. The heating effects of solar radiation and natural cooling on the various test insulators (1S, 2E, 3P, 4C, and 5A) were investigated in the laboratory and field. The results are reported and discussed below.

Stellenbosch University http://scholar.sun.ac.za

4.2.2.1 Laboratory measurements

New test insulators (1S, 2E, 3P, 4C and 5A) were suspended from a metal support frame, and bimetallic thermocouples were connected to the bottom of the sheds.

The test insulators were heated, in wind-free, indoor, laboratory conditions, by an artificial white light, from room temperature (24 °C) until the last insulator reached 36 °C. The insulator-surface temperature readings are shown for one-minute intervals in Figure 4. 14.

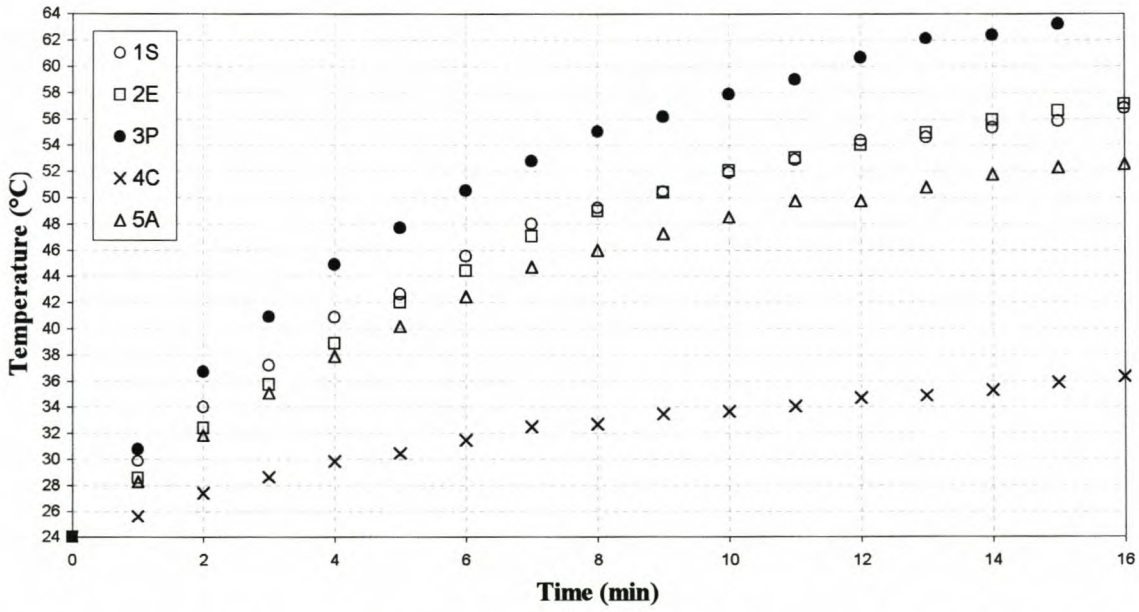

Figure 4. 14 Temperatures of insulators 1S, 2E, 3P, 4C and 5A heated by artificial white light from room temperature (24 °C) until the last insulator reached 36 °C.

The results in Figure 4. 14 show that the porcelain insulator (3P) heats faster than the others and also reaches the highest temperature. The HTV SR (1S) and EPDM (2E) insulators tend to heat at the same rate and to the same end value, closely followed by the cycloaliphatic insulator. The RTV SR-coated insulator takes the longest time to heat and has a far lower final value.

In another test, test insulators 1S, 2E, 3P, 4C and 5A were heated by an artificial white light source to 38 °C. The one-minute interval, insulator-surface temperature readings, taken while the insulators cooled down naturally (in wind-free, indoor, laboratory conditions) to room temperature (16 °C), are shown in Figure 4. 15.

Stellenbosch University http://scholar.sun.ac.za

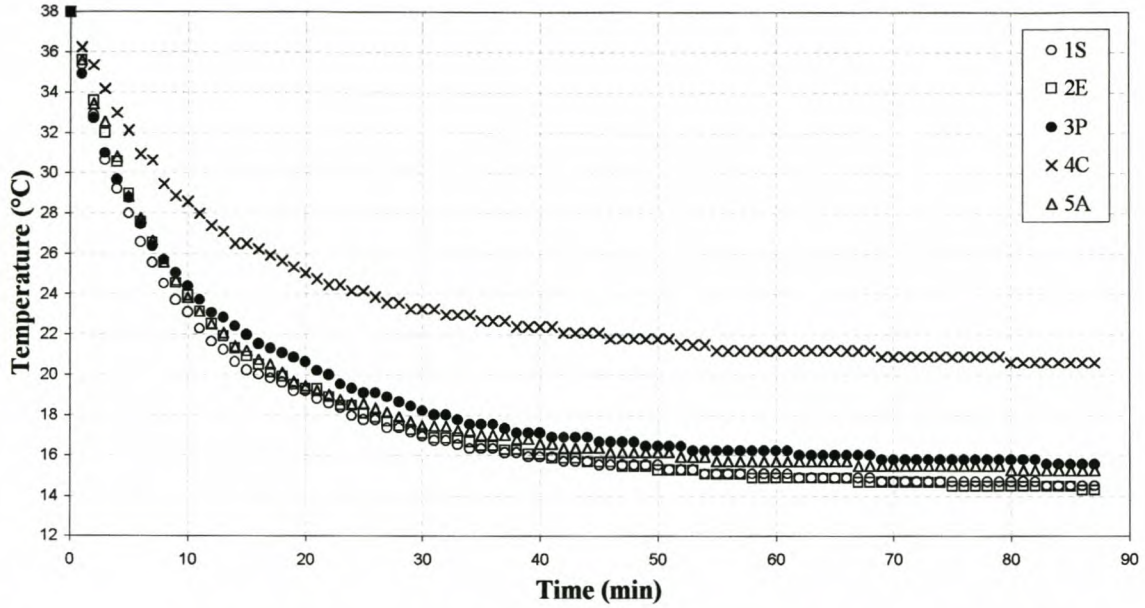

Figure 4. 15 Temperatures of insulator surfaces of insulators 1S, 2E, 3P, 4C and 5A, heated by an artificial white light source to 38 °C and then cooled down naturally to room temperature (16 °C).

The results in Figure 4. 15 show that the RTV SR-coated insulator takes the longest time to cool and has a far higher final value than the other test insulators.

From the above it can be concluded that the RTV SR-coated insulator (4C) takes longer to heat up and to cool down than the other test insulators.

4.2.2.2 Field measurements

The effects of solar radiation and the surrounding environment on the heating of the test insulators were investigated by monitoring the material temperature on the non-energised test insulators 1S, 2E, 3P, 4C and 5A installed at KIPTS. This was done using bimetallic thermocouples connected to the top sheds.

Figure 4. 16 shows the insulator surface temperature, ambient temperature and UV-B solar radiation readings at fifteen-minute intervals.

Stellenbosch University http://scholar.sun.ac.za

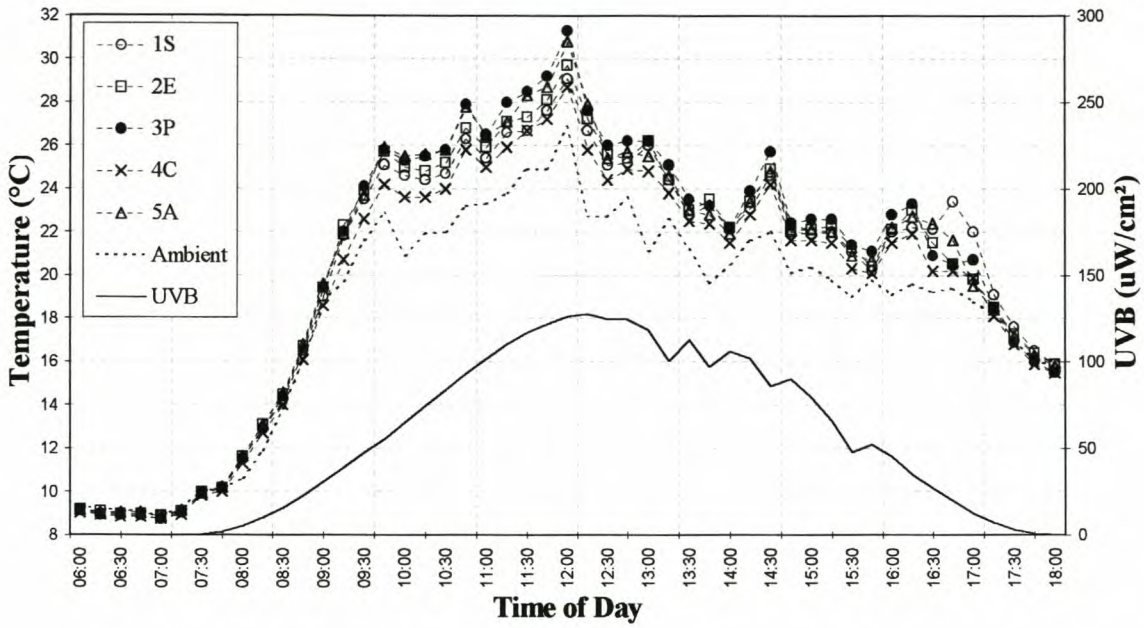

Figure 4. 16 The insulator-surface temperature and UV-B solar radiation readings on insulators 1S, 2E, 3P, 4C and 5A as heated and cooled by natural light, upon exposure to the surrounding environment.

The test insulator temperatures in Figure 4. 16 show good correlation with the solar radiation and a direct correlation with the ambient temperature, though the insulator-surface temperature readings were much higher than the ambient temperature readings. The difference in rate of heating of the test insulator materials corresponds to the laboratory measurements shown in Figure 4. 14. It can therefore be concluded that solar radiation heats the insulator surface to a temperature higher than ambient on all the test insulators under consideration. The porcelain test insulator (3P) is heated to the highest temperature and the RTV SR-coated porcelain insulator (4C) to the lowest, however still well above ambient.

The different heating and cooling profiles could possibly be due to the colour of the insulators.

The effect of solar radiation on the wetting of insulator 3P when heated and then cooled in a natural environment is illustrated in Figure 4. 17. The insulator surface temperature, ambient and dew point temperature (calculated using Eq. 3.7, in chapter 3), UV-B solar radiation, relative humidity, and leakage current readings are shown at fifteen-minute intervals.

Stellenbosch University http://scholar.sun.ac.za

The leakage current will only be present when succesful wetting of the insulator pollution layer has occurred, resulting in an electrolytic conducting layer. It is normally expected that when a relative humidity (RH) level of 75% and above is present, critical wetting should occur, resulting in a leakage current. However, from the results in Figure 4. 17 it is seen that even though the RH is above 75%, critical wetting does not occur during the day when UV-B solar radiation increases the insulator surface temperature above the dew point temperature.

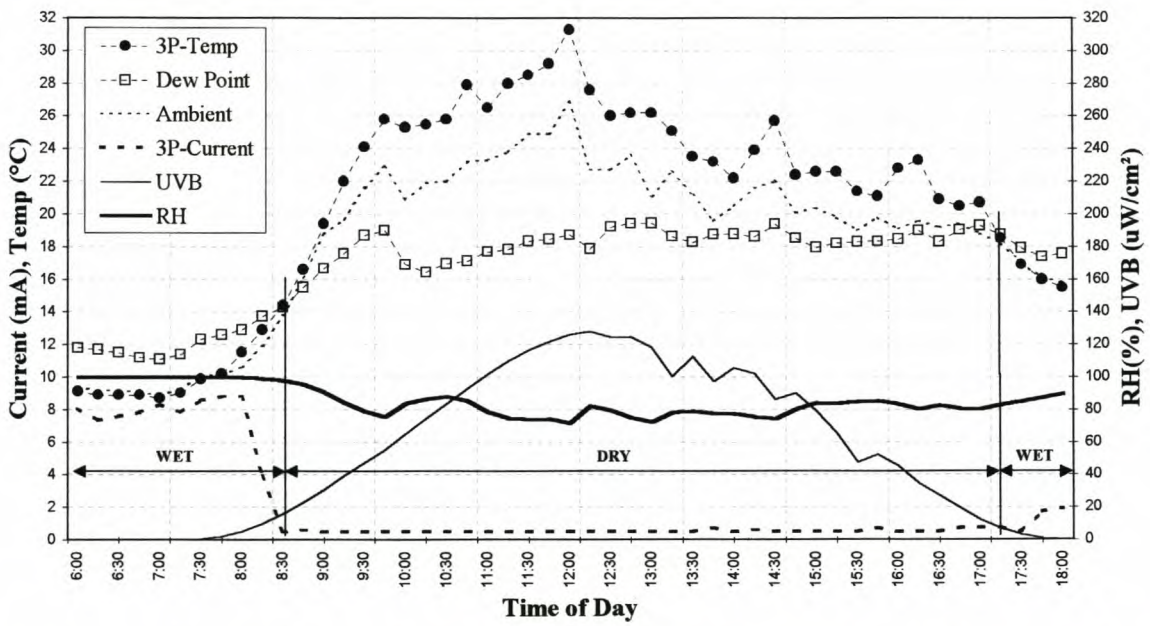

Figure 4. 17 Insulator 3P surface temperature (heated and cooled by natural light and the surrounding environment), ambient and dew point temperatures, UV-B solar radiation, relative humidity, and leakage current readings at fifteen-minute intervals.

These results (in Figure 4. 17) show that solar radiation has an effect on the wetting of the test insulators and the resulting leakage currents. It is therefore assumed that the leakage current levels during the daytime will normally be much lower than during the night, mainly due to solar radiation heating of the test insulator surface.

Note: This will not be true when it rains or when strong moisture-carrying winds or mist/fog prevail during the daytime.

Stellenbosch University http://scholar.sun.ac.za

4.3 CONCLUDING REMARKS ON THE INSULATOR POLLUTION AND WETTING PROCESS

The visually observed pollution deposits on the different test insulators were similar, although more dominant on the non-energised test insulators, especially on the shank and shed tips on the southern side. The southerly winds are the main carriers and depositors of visually observed pollution at KIPTS. A relationship between wind speed and pollution deposit was established.

From the insulator pollution and wetting observations on the test insulators at KIPTS, it is concluded that the insulator pollution and surface conductivity levels on the energised insulators are higher than those of the non-energised insulators (confirmed by LESDD and IPMA surface conductivity measurements). This is attributed to the pollution being dissolved on the energised insulators due to electrical leakage current and discharge activity.

The results suggest that there is an interaction between the insulator material surface and the pollution layer, which alters the resistivity (ρ) and the surface area (A_{pol}) available for leakage current flow. Hydrophobicity transfer was also confirmed on the SR test insulators. It was more prominent on the RTV SR coating. It is further suggested that the material in the dry-band area changes due to electrical leakage current and discharge activity.

A ranking of the energised test insulators is suggested, based on the IPMA surface conductivity values (week 53). The test performance decreased in the following order: 4C (best performer), 1S, 2E, 3P (reference) and 5A (worst performer).

Solar radiation has a great effect on the wetting of the insulator surface as it heats the insulator to a temperature above dew point.

Further research work is necessary to investigate the effect of the thermal properties of the various insulator materials on the leakage current performance of the insulators.

Stellenbosch University http://scholar.sun.ac.za

5 INSPECTIONS OF INSULATOR SURFACE CONDITION AND OBSERVATIONS OF ELECTRICAL DISCHARGE ACTIVITY

"In the field of observation, chance favours only the prepared mind" – ***Louis Pasteur***

Environmental and climatic conditions interact with insulator pollution, as described in Chapters 3 and 4. These could cause irreversible changes to insulator surface material.

Material ageing modes such as discolouration, chalking, crazing, dry bands, tracking and erosion can be seen with the naked eye on an insulator surface. Detailed visual inspections can therefore reveal much about the insulator surface condition.

The electrical discharge activity on the insulator, such as corona, streamers, sparking and arcing, may lead to material degradation. These discharges have associated leakage currents ranging from micro-amps to amps. Knowledge of the dominant discharge types and when they are observed for the first time on the test insulators may reveal information regarding their electrical and material performance.

The information gained from visual inspections and electrical discharge activity observations could facilitate the evaluation of the relative performance of the test insulators.

5.1 INSPECTIONS OF INSULATOR SURFACE CONDITION

Insulator surface condition inspections were performed in accordance with the test procedure and time intervals as described in section 2.2.5. The inspection methods and results are discussed below.

5.1.1 Insulator surface condition inspection methods

The visual inspections were done using STRI Guide 5, 98/1 "Guide for Visual Identification of Deterioration & Damages on Suspension Composite Insulators" [59].

Hydrophobicity inspections were done simultaneously, as described in section 4.2.1.

Stellenbosch University http://scholar.sun.ac.za

The visual inspections were carried out without touching the insulator surface nor disturbing the pollution layer. Thus, signs of deterioration observed could possibly be only in the pollution layer, i.e. not affecting the material itself. Definitions and photographs of the observed types of deterioration or damage are given below.

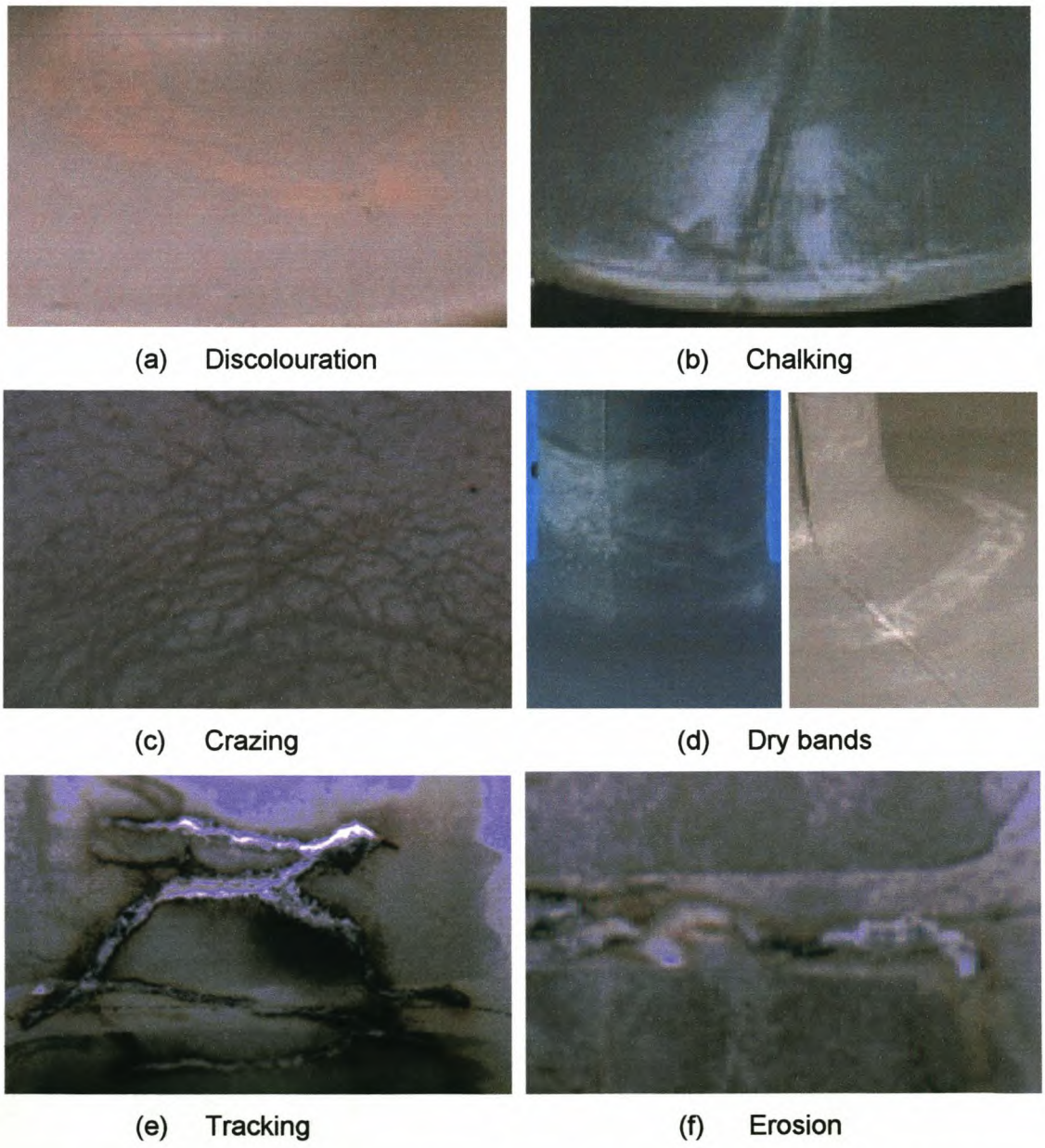

(a) Discolouration (b) Chalking

(c) Crazing (d) Dry bands

(e) Tracking (f) Erosion

Figure 5.1 Photographic examples of the types of degradation and damages observed on the test insulators.

Discolouration: Discolouration is a change in the base colour of the housing material of the composite insulator [60]. See Figure 5.1 (a).

Stellenbosch University http://scholar.sun.ac.za

Chalking: Chalking is the appearance of some filler particles of the housing material, forming a rough or powdery surface [60]. See Figure 5.1 (b).

Crazing: Crazing comprises of surface micro-fractures of depths approximately 0.01 to 0.1 mm [60]. When the surface fractures are deeper than 0.1 mm, they are then referred to as "alligatoring" or crocodile skin [60]. See Figure 5.1 (c).

Dry bands: Dry bands are the signs left on the insulator material surface after dry-band activity has taken place. See Figure 5.1 (d).

Tracking: Tracking is the irreversible degradation by the formation of conductive (often carbonaceous) paths starting and developing on the surface of an insulating material. These paths are conductive even under dry conditions [60]. For this dissertation, it was decided not to disturb the insulator surface, therefore conductivity tests were not carried out. Thus, in the context of this dissertation any visual signs of black tree shaped discoloration on the surface are referred to as tracking, even though not confirmed by measurement. See Figure 5.1 (e).

Erosion: Erosion is the irreversible and non-conducting degradation of the surface of an insulator that occurs by loss of material [60]. This can be uniform, localised or tree-shaped. See Figure 5.1 (f).

5.1.2 Insulator surface condition inspection

The result of visual surface condition inspection, made on Fridays (10h00 to 14h00) on test insulators 1S, 2E, 3P, 4C and 5A, energised and non-energised, are summarised in Table 5. 1. The level of surface degradation is graded as light (L), medium (M), heavy (H) or very heavy (VH).

Details of the weekly and six-weekly visual observations are given per insulator, energised and non-energised, in Appendix D.

Table 5.1 Table of insulator surface condition inspections on energised and non-energised test insulators 1S, 2E, 3P, 4C and 5A.

	Insulator surface condition inspections made on Fridays (10h00 to 14h00) on insulators 1S, 2E, 3P, 4C and 5A																																		
	Energised																														Non-energised				
	Discolouration					Chalking					Crazing					Dry Bands					Tracking					Erosion					Discolouration				
Week	1S	2E	3P	4C	5A	1S	2E	3P	4C	5A	1S	2E	3P	4C	5A	1S	2E	3P	4C	5A	1S	2E	3P	4C	5A	1S	2E	3P	4C	5A	1S	2E	3P	4C	5A
1		L																																	
2	L	L		L	L																														
3	L	L		L	L											X	X		X																
4	L	L		L	L											X	X		X																
5	L	L		M	L											X	X	X	X	X															
6	M	L		M	L											X	X	X	X	X															
12	M	L		M	L									L	L	X	X	X	X	X															
18	M	L		M	L									L	L	X	X	X	X	X				L											
24	M	M		H	M						L	L		M	L	X	X	X	X	X				L	L										L
30	M	M		H	H					L	L	L		M	L	X	X	X	X	X	L*			M	L										L
36	M	M		H	H					L	L	L		M	L	X	X	X	X	X	L*			M	M	L*			L	L					L
42	M	M		H	H					M	M	L		M	M	X	X	X	X	X	L*			H	M	L*			L	L					L
48	M	M		H	VH					M	M	L		H	M	X	X	X	X	X		L		H	M	L*			L	L					L
53	M	M		H	VH					M	M	L		H	H	X	X	X	X	X				H	H	L*	L		L	M		L			L

L - Light M - Medium H - Heavy VH - Very Heavy X - Present * - At end fitting interface

A summary of the insulator surface condition inspections per test insulator is given below. Figure 5.4 shows photographs of the test insulators 1S, 2E, 3P, 4C and 5A, new, non-energised and energised, after week 53. Figure 5.5 shows microscope (60 x magnification) photographs of the surface condition of the test insulators new, non-energised and energised after week 53.

Surface condition inspections on HTV SR insulator 1S

1S - Energised: The first signs of light discolouration (possibly due to dry-band activity) were observed in week 2. Clear signs of dry-band activity with light discolouration were observed in weeks 3 to 5. From week 6 onwards these became more prominent, with discolouration increasing to medium. On final inspection it was evident that the dry-band activity resulted in medium discolouration of the insulator material surface, although it did not lead to material degradation of concern. The medium white discolouration could possibly be light chalking, but this could not be confirmed.

Light corrosion run -from the dead end-fitting was noted on the shed top (also on the non-energised) from week 18 onwards, progressing to the shed tip. Signs of end-fitting corrosion affecting the polymeric material moulded over it were first observed on the dead end in week 4, and on the live end in week 12. The corrosion had protruded through the material moulded over the end fittings by week 18. On the live end-fitting material interface signs of tracking starting from a corrosion protrusion were observed in week 30. This developed into erosion in week 48. The localised corrosion protrusions, tracking and erosion on the end-fitting material interfaces are of concern. They will, however, have no effect on the performance of rest of the insulator.

Light signs of crazing in the pollution layer were observed for the first time in week 24. These gradually increased and from week 42 onwards it was classed as medium. On closer inspection with a microscope, the crazing seemed to be restricted to the pollution layer only and would thus not affect the material. Darker lines within the crazing pattern were initially thought to be the start of light tracking in the pollution layer, but these did not develop further.

1S - Non-energised: Signs of end-fitting corrosion affecting the polymeric material moulded over it were first observed on both the live and dead ends in week 18. The same

phenomenon was observed on the energised insulator, but at an earlier stage (week 4), suggesting that energisation accelerates the process but is not the main cause. No notable further signs of deterioration were found.

Surface condition inspections on EPDM insulator 2E

2E - Energised: Signs of light, patchy discolouration were found after week 1. These gradually increased until it was classed as medium from week 24 onwards. The colour, ranging from black, to brown, to white, or a combination thereof, sometimes gave the impression of the onset of light crazing or tracking. Some patchy discolouration could be due to dry-band activity, but in this case clear bands were not observed.

In week 3 the first signs of dry-band activity, showing light discolouration, were found. These gradually increased until it was classed as medium discolouration from week 48 onwards.

Light corrosion run-off from the dead end-fitting was noted on the shed top (also on the non-energised) after week 1, later progressing to the shed tip. Signs of end-fitting corrosion affecting the polymeric material moulded over it were first observed on the dead end in week 6, and on the live end in week 12. The corrosion had protruded through the material moulded over the end fittings by week 18. The localised corrosion protrusions on the end-fitting material interfaces are of concern. They will however have no effect on the performance of the rest of the insulator.

Light signs of crazing in the pollution layer were observed from week 24 onwards. On closer inspection with a microscope, light crazing seemed to be present in the material where the pollution had washed off.

Light tracking (could possibly have been only in the pollution layer) was observed in week 48 and had developed to very light material erosion by week 53.

2E - Non-energised: Signs of end-fitting corrosion affecting the polymeric material moulded over it were first observed on both the live and dead ends in week 18. The same phenomenon was observed on the energised insulator, but at an earlier stage (week 6), suggesting that energisation accelerates the process but is not the main cause. Signs of

light discolouration were observed on the shed tops, on the northern side, for the first time in week 53. This could possibly be the onset of light chalking or crazing due to solar radiation. No notable further signs of deterioration were found.

Surface condition inspections on Porcelain insulator 3P

3P - Energised: No signs of material deterioration were found. Signs of dry-band activity were noted, in the form of a white residue, from week 5 onwards. Signs of light crazing and tracking were noted in the pollution layer at times. Light corrosion run-off from the dead end-fitting was noted on the shed top (also on the non-energised) from week 1 onwards.

3P - Non-energised: No signs of material deterioration were found.

Surface condition inspections on RTV SR-coated porcelain insulator 4C

4C - Energised: Signs of light, patchy discolouration (pink in colour) on the bottom of all sheds were found from week 2. The first signs of possible dry-band activity were observed in week 3. Signs of light discolouration (pink in colour) gradually increased to medium discolouration from week 5 and heavy from week 24, with colour variations of white, pink and black. Final inspection showed that the pink discolouration was in the material, while the black and white discolouration seemed to be in the pollution layer only.

Light signs of crazing (possibly in the pollution layer) were observed for the first time in week 12 and gradually increased to medium from week 24 and to heavy from week 48 onwards. On closer inspection, with a microscope, the crazing seemed to be restricted to the pollution layer. Darker lines within the crazing were often thought to be the start of light tracking in the pollution layer, as with the SR insulator.

Light tracking (possibly in the pollution layer) was first observed in week 18. This gradually increased to medium in week 30 and heavy from week 42 onwards. The tracking was mainly present around the shank adjacent to the end fittings. On closer final inspection it was noted that the tracking had hardened the pollution layer. The material under the tracked pollution layer had also degraded and eroded down to the porcelain.

This was restricted to a small area however, mainly on the shank adjacent to the end fittings.

Light erosion was observed from week 36 onwards, where tracking was previously present. See comment in previous paragraph (on tracking).

Light corrosion run-off from the dead end-fitting was noted on the shed top (also on the non-energised) from week 1 onwards.

4C - Non-energised: No signs of material deterioration were found. However, the coating started to peel from the corroded end fittings (also on the energised) from week 18 onwards.

Surface condition inspections on Cycloaliphatic insulator 5A

5A - Energised: The first signs of blackening in the mould line were observed in week 2 and white discolouration adjacent to the mould line was observed from week 5 onwards. This continued until the white discolouration adjacent to the mould line started to widen towards the shed tips in week 24.

Dry-band activity was observed from week 5, showing light discolouration. This discolouration progressed until it was classed as medium from week 24, as heavy from week 30, and as very heavy from week 48 onwards.

Light crazing (black in colour) was first observed in week 12 and progressed to medium (white in colour) in week 42 and heavy in week 53 (see Figure 5.2). On closer inspection the crazing was found to be present in the material. The first light chalking was seen in week 30, progressing to medium from week 42 onwards. The chalking started and remained dominant in the mould-line areas (see Figure 5.2).

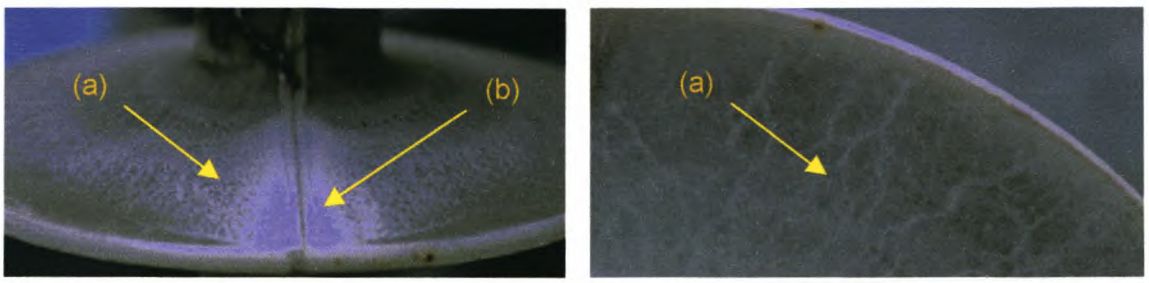

Figure 5.2 Photographs showing (a) crazing and (b) chalking on shed top and bottom of insulator 5A, as seen in week 53.

Light tracking was first observed on the shank at the mould line in week 24. It progressed to medium in week 36 and heavy in week 53 (see Figure 5.3). Tracking was present in the material and resulted in severe degradation. The tracking evolved into light erosion in certain areas by week 36, and medium by week 53 (see Figure 5.3).

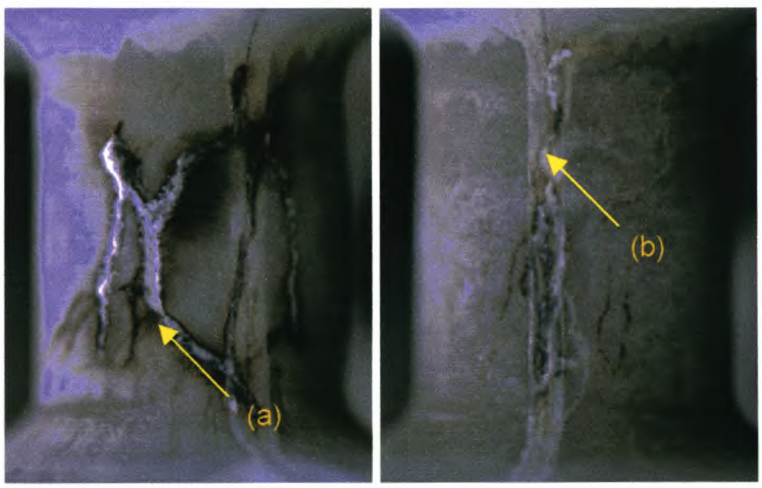

Figure 5.3 Photos showing (a) tracking and (b) erosion on insulator 5A seen in week 53.

The insulator had a characteristic bad smell from week 18 onwards. The smell was probably a result of the breakdown products of the epoxy resin, which will include the amine group from the catalyst [45].

Light corrosion was observed on the end fittings from week 24 and run-off onto the shed from week 30 onwards (also on the non-energised).

5A - Non-energised: Light whitening in the mould line was observed from week 24 onwards. No further signs of deterioration were found.

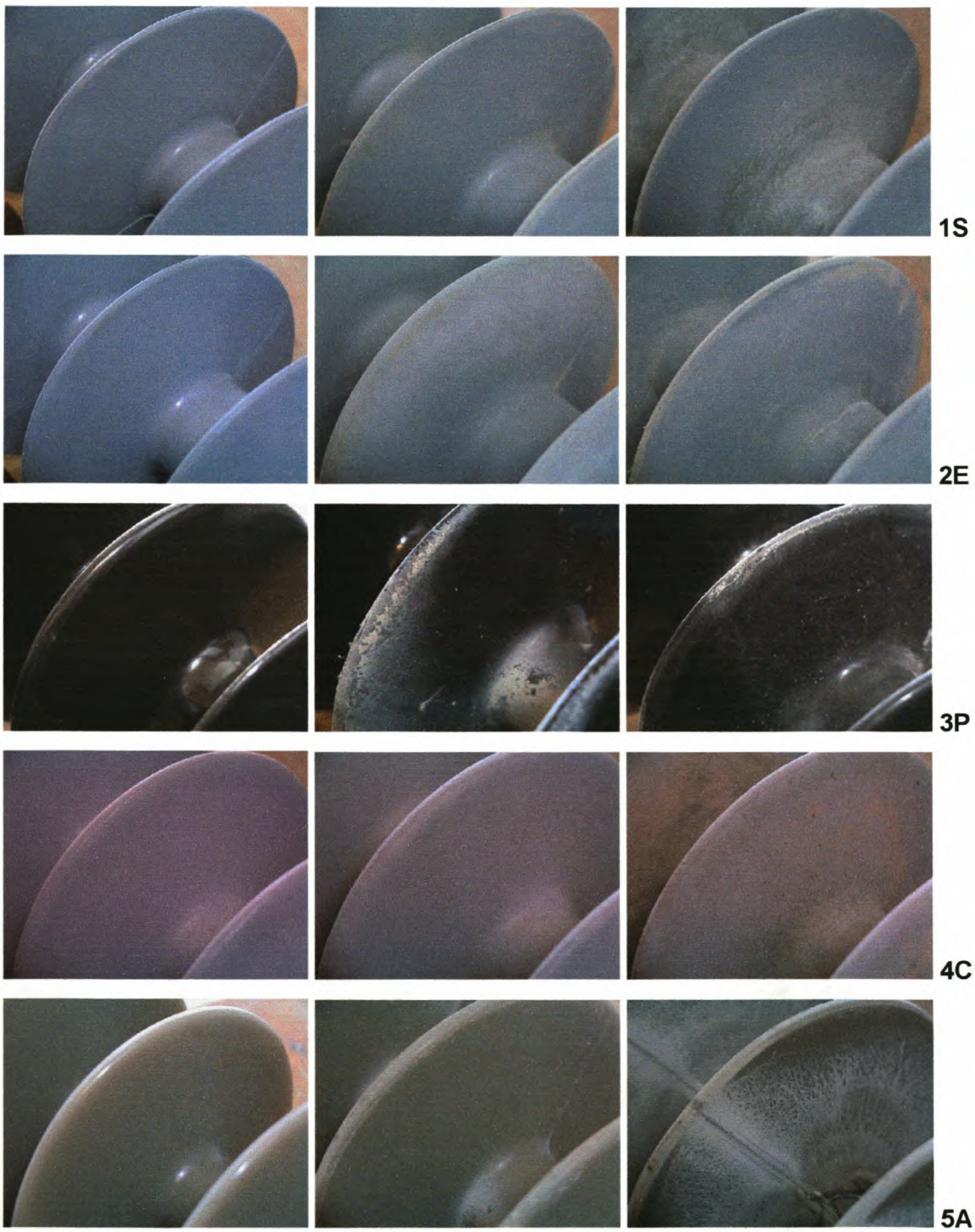

Figure 5.4 Photographs of the test insulators 1S, 2E, 3P, 4C and 5A, new, non-energised and energised, after week 53

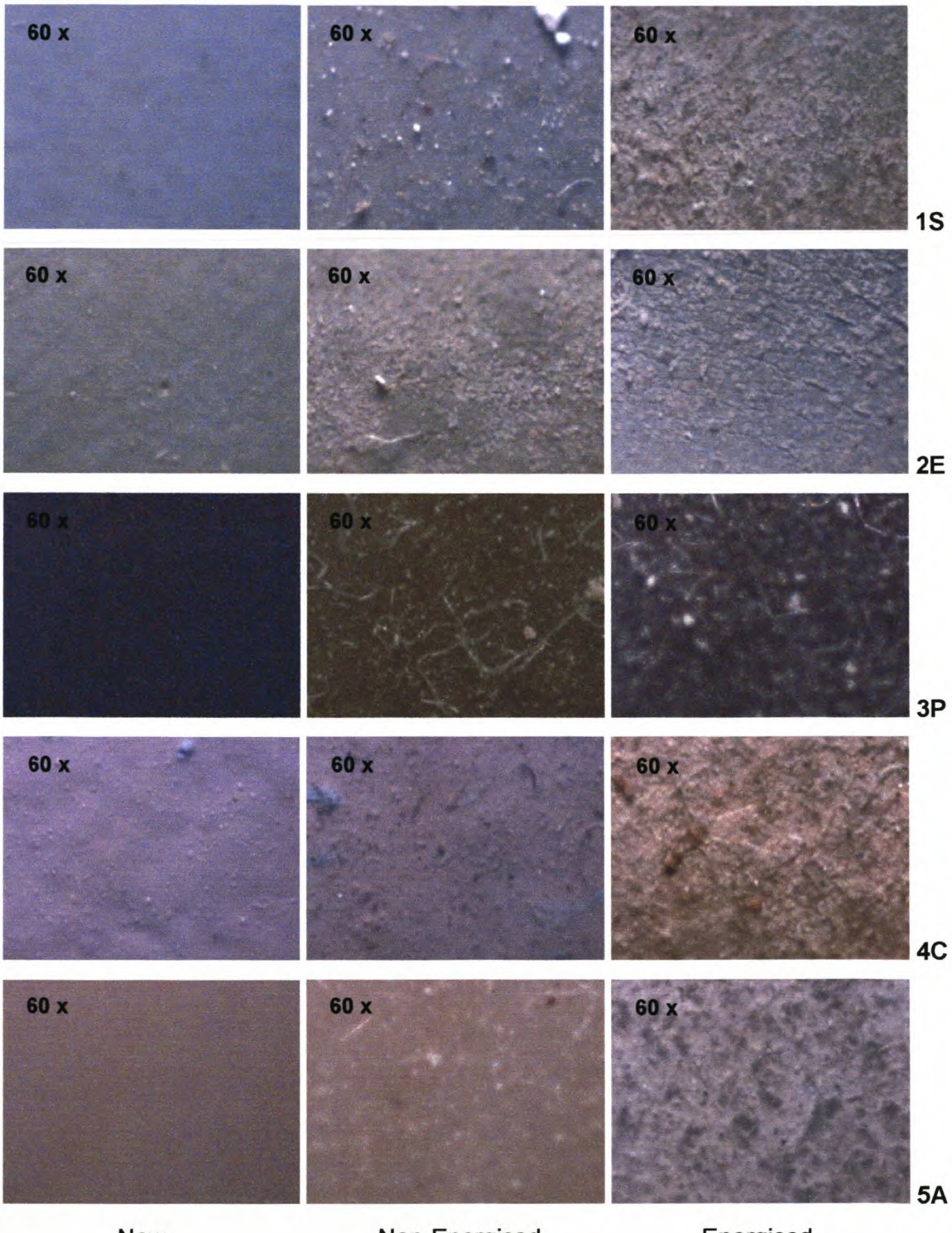

Figure 5.5 Microscope (60 x magnification) photographs of the surface conditions of the test insulators 1S, 2E, 3P, 4C and 5A, new, non-energised and energised, after week 53.

5.2 OBSERVATIONS OF ELECTRICAL DISCHARGE ACTIVITY

Electrical discharge activity observations were performed in accordance with the test procedure and time interval as described in section 2.2.5. The inspection methods and results are discussed in the sections that follow.

5.2.1 Electrical discharge activity observation methods

Electrical discharge activity observations were made using the CoroCAM Mark I and II UV-sensitive, image-intensified, corona observation cameras (see description of cameras in section 2.3.3).

5.2.1.1 Visual electrical discharge observations using the CoroCAM Mark I

The CoroCAM Mark I was used to make observations and 1-minute recordings from both land and sea sides, covering all angles of observation. The recordings were stored on videotape. All the results of the nightly observations were tabulated in relation to the daily weather parameters monitored, including weekly hydrophobicity observations.

Definitions and examples of the various types of discharge activities observed and identified are given below.

Water drop corona (WDC): Water droplets increase the electric field strength, which may produce corona around the water drop. See Figure 5.6 (a).

Spot corona / discharges (SCD): Corona around an electrolytic filament or discharges between water droplets or electrolytic filaments. See Figure 5.6 (b).

Dry-band corona (DBC): Corona within the dry-band zone. See Figure 5.6 (c).

Dry-band discharges (DBD): Streamer, spark and arc discharges over the dry-band zone. See Figure 5.6 (d).

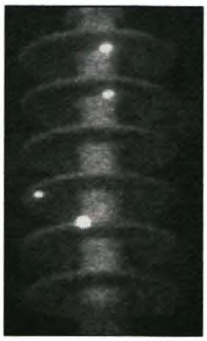

(a) Water drop corona (WDC)

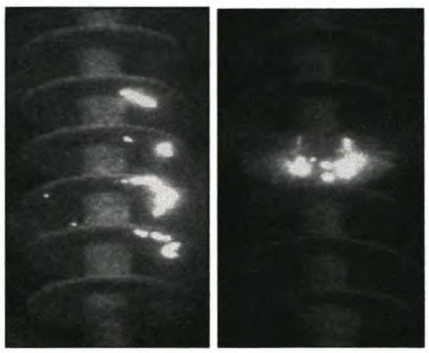

(b) Spot corona / discharge (SCD)

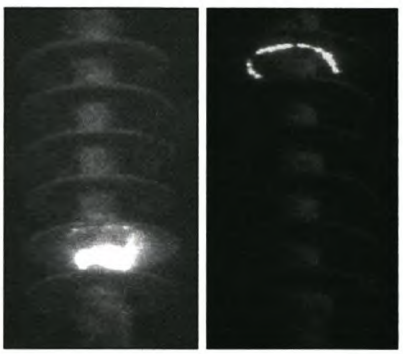

(c) Dry-band corona (DBC)

(d) Dry-band discharge (DBD)

Figure 5.6 Examples of electrical discharge activity observed.

5.2.1.2 Electrical discharge observations and leakage current recordings using the CoroCAM Mark II

Electrical surface activity on the test insulators was captured and stored on hard drive using the CoroCAM Mark II. The activity and the leakage current present at the time of the activity were captured in synchronism (for 16 voltage cycles, for a pre-selected leakage current trigger level). In addition, the visual electrical surface activity was also monitored from the land side and one-minute recordings stored on videotape.

Examples of a typical dry-band sparking discharge (Figure 5.7) and dry-band arcing discharge (Figure 5.8) are shown below.

The sparking is characterised by single pulses of low leakage current magnitude (order of mA) and the arcing by continuous large leakage current pulses (present for a few consecutive cycles).

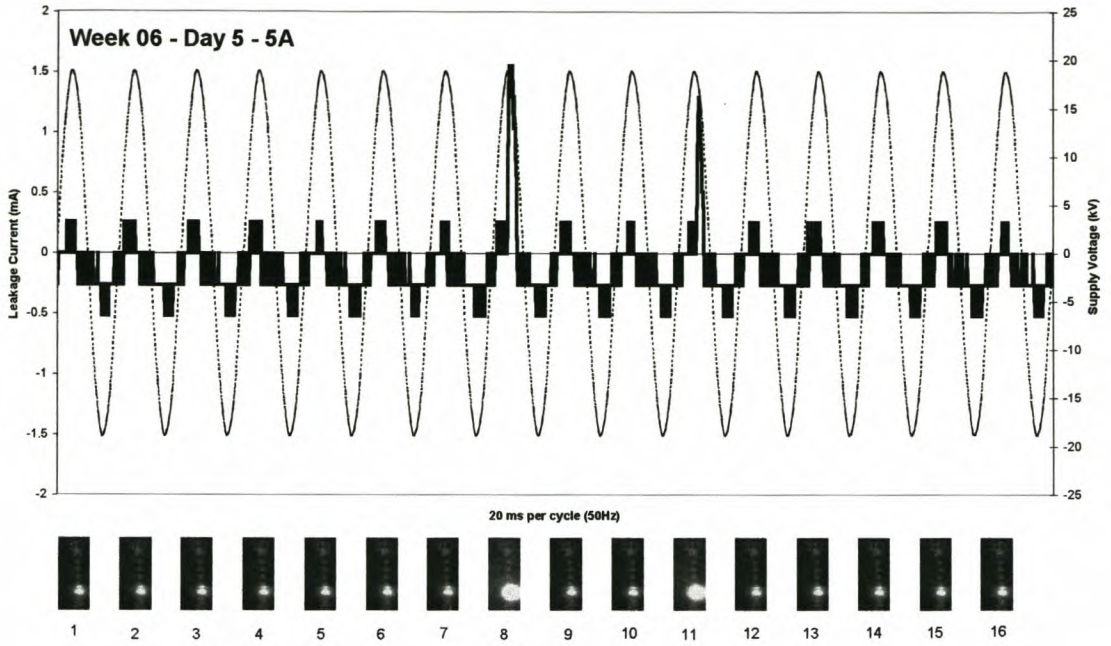

Figure 5.7 Example of dry-band sparking discharges (very low current amplitude) on test insulator 5A.

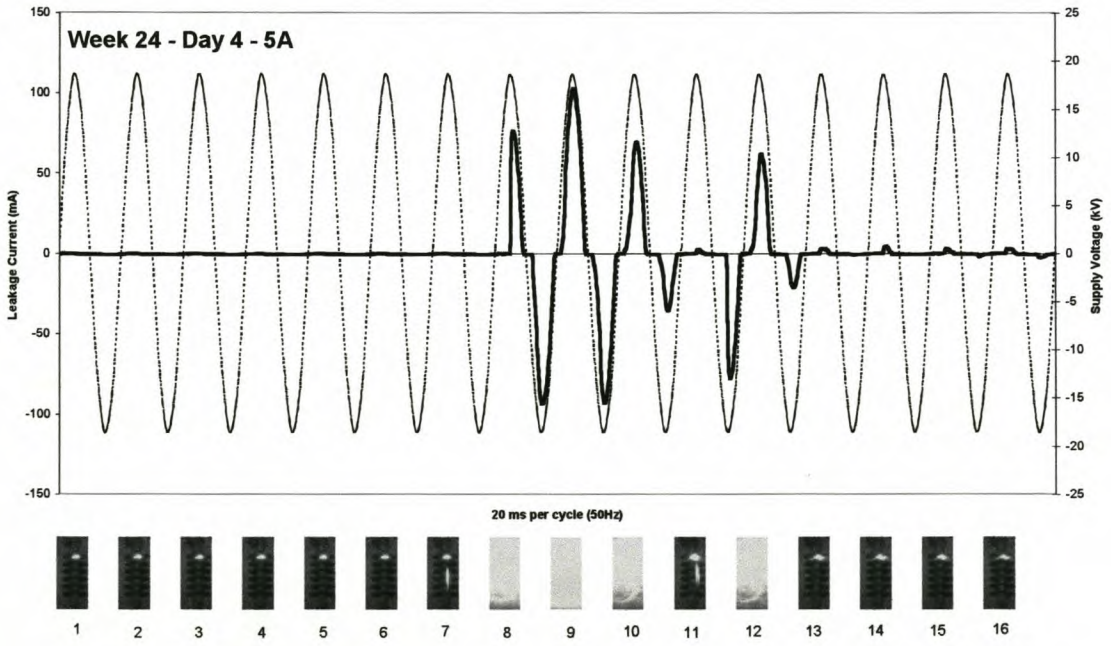

Figure 5.8 Example of dry-band arcing discharges on test insulator 5A.

Hundreds of these recordings were made during the research programme and the results summarised together with the CoroCAM Mark I results in Tables 5.2 and 5.3. The peak leakage current pulse measurements, associated with the discharge, are also reported.

During the CoroCAM Mark II recordings it was noted that a longitudinally-shaped discharge was present over the insulator sheds, one cycle prior to the commencement of the leakage current pulse (see Figure 5.8, photos 7 and 11) [further examples can be seen in Figure 5.9].

Thinking that this was a new phenomenon never seen before, it was debated with fellow researchers. Several plausible hypotheses were put forward.

(a) (b) (c) (d)

Figure 5.9 Examples of longitudinally-shaped discharges recorded.

Many hours were spent trying to explain this phenomenon. During later laboratory tests, carried out to investigate the plausibility of some of the hypotheses proposed, it was found that the 'discharge' took place over a metal electrode with the same potential from top to bottom, which is electrically impossible.

The camera was turned in relation to the electrode at different angles, checking for possible lens flare. The longitudinally-shaped 'discharge' remained in the same place, even though the camera was shifted. The camera was then flipped on the tripod through 90 degrees to the left. The 'discharge' was now perpendicular to the electrode, showing that the phenomenon must be related to some lens or camera process.

When the same experiment was carried out at KIPTS on the energised test insulators, exactly the same phenomenon was observed (see Figure 5.10). The phenomenon has, as yet, not been explained by the optical experts at the CSIR (manufacturers of the CoroCAM camera systems); it is currently under further investigation by them.

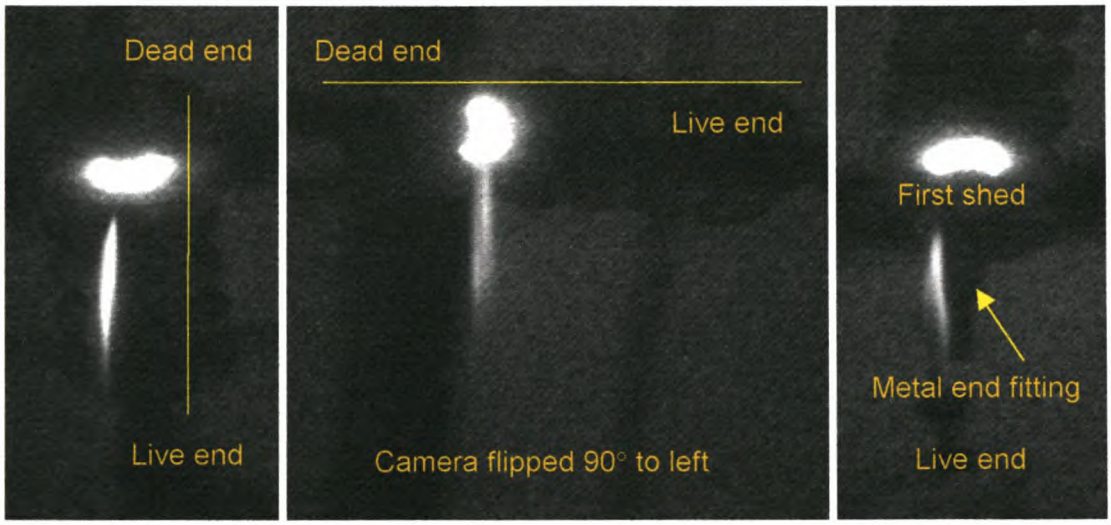

(a) (b) (c)

Figure 5.10 Examples of longitudinally-shaped discharges:
(a) over the insulator surface,
(b) with the camera flipped 90° to the left the discharge is perpendicular to the insulator, and
(c) the discharge over an equipotential end fitting.

One major question about this phenomenon still remains unanswered - why does this longitudinally-shaped 'discharge' always take place 1 cycle prior to a leakage current pulse or pulse train? Furthermore, why is it mainly coupled to dry-band arcing type of discharges? This is not further discussed in this dissertation.

5.2.2 Electrical discharge activity observations

The results of electrical discharge activity observation are summarised in Tables 5.2 and 5.3 (and the first time a particular activity was observed on each insulator is highlighted).

Details of the electrical discharge observations, along with the climatic and environmental conditions, and hydrophobicity, are given in Appendix E.

Table 5.2 Electrical discharge activity, leakage current and daily weather (week 1-12).

Week	Date	Electrical discharge activity observations made nightly (21h00 to 24h00+) on insulators 1S, 2E, 3P, 4C and 5A																									Daily weather parameters													
		Water Drop Corona					Spot Corona/Discharges					Dry Band Corona					Dry Band Discharges					Leakage Current (mA)					Rainfall	Relative Humidity (%)			Temperature (°C)			Wind speed (m/s) and Direction				UV-B (µW/cm²)	
		1S	2E	3P	4C	5A	1S	2E	3P	4C	5A	1S	2E	3P	4C	5A	1S	2E	3P	4C	5A	1S	2E	3P	4C	5A	(mm)	Ave	Max	Min	Ave	Max	Min	Ave	Max		Dominant	Ave	Max
1	1999/04/12																										0.0	61	82	31	21.4	30.3	17.0	1.4	4.6	NNW	ESE	44	184
	1999/04/13	X	X																								0.0	90	100	56	16.8	21.4	13.5	2.3	10.1	NW	NW	34	176
	1999/04/14	X						X																			0.0	99	100	92	15.0	18.3	11.7	1.9	3.9	NW	ENE	45	190
	1999/04/15		X																								10.7	99	100	88	14.7	19.5	10.8	2.2	6.8	WNW	ENE	17	85
	1999/04/16	X	X																								0.0	94	100	72	14.7	19.9	10.6	2.4	6.1	SSW	SSW	45	193
	1999/04/17	X	X																								0.0	95	100	76	13.2	16.7	6.7	2.2	4.6	W	W	43	185
	1999/04/18			X			X	X					X					X					1				21.0	98	100	92	14.8	16.6	12.5	3.2	7.3	NNW	NW	25	191
2	1999/04/19	X					X	X										X					2				4.4	100	100	97	15.7	17.0	13.9	4.0	6.9	WNW	NW	42	186
	1999/04/20		X		X	X	X	X	X			X	X				X	X				2	1				0.0	90	100	75	16.9	18.9	14.6	8.5	12.7	NW	N	39	183
	1999/04/21			X	X		X	X																			16.3	97	100	90	15.3	17.9	9.4	4.7	13.1	NW	WNW	35	176
	1999/04/22				X		X		X	X			X					X					7				0.0	97	100	87	13.2	16.8	7.6	1.7	4.2	SW	SW	37	189
	1999/04/23				X			X		X		X	X				X	X				8	3				0.3	99	100	93	14.2	17.5	9.2	1.7	5.8	WNW	ENE	36	181
	1999/04/24		X		X	X				X		X	X				X	X				8	12				0.1	94	100	72	14.3	19.4	8.6	3.3	7.7	SSE	SSE	37	158
	1999/04/25				X	X		X		X		X															0.0	81	94	55	17.4	22.2	13.3	3.4	5.6	SE	ESE	37	165
3	1999/04/26				X	X		X				X															0.0	74	94	34	18.9	30.1	12.1	1.6	4.8	S	ENE	34	160
	1999/04/27	X	X		X	X		X		X		X					X					2					0.0	81	96	49	19.4	27.3	14.7	1.9	3.4	ENE	ENE	31	150
	1999/04/28				X					X		X	X				X					6					0.0	89	100	66	18.8	22.6	14.8	1.1	3.9	ENE	ENE	33	150
	1999/04/29				X				X	X		X	X	X			X	X	X			4	12	3			0.0	99	100	91	16.9	19.9	13.0	1.5	3.5	ENE	ENE	35	151
	1999/04/30								X		X	X	X		X		X	X				12	20				0.1	99	100	95	15.6	18.6	10.3	1.9	5.9	SW	NE	31	141
	1999/05/01								X			X	X		X	X	X	X		X		4	8		1		0.0	99	100	96	15.8	18.8	10.9	1.6	3.9	SW	NE	35	149
	1999/05/02						X	X	X						X	X											2.4	100	100	98	16.4	18.2	13.9	3.8	10.9	SSW	N	28	147
4	1999/05/03				X	X	X				X		X					X					3				8.1	97	100	85	16.6	19.4	14.4	5.7	12.1	NW	N	23	152
	1999/05/04					X	X			X	X		X					X					3				1.4	95	100	86	16.3	17.6	12.6	3.5	6.2	NW	NNW	29	154
	1999/05/05					X		X		X																	0.0	82	100	48	14.4	20.1	6.1	2.6	5.5	SSE	ESE	33	146
	1999/05/06						X	X		X	X																0.0	53	89	19	19.3	30.3	9.6	2.3	4.4	ESE	ENE	29	145
	1999/05/07				X		X		X	X	X		X	X				X					2				0.0	86	100	58	15.7	20.9	12.2	2.5	5.5	WSW	ENE	29	138
	1999/05/08								X	X		X	X	X			X	X	X	X		2	20	1			0.0	98	100	84	17.1	22.7	10.7	4.3	8.9	SSE	SSE	27	138
	1999/05/09								X	X		X	X				X	X			X	4	11			1	0.0	87	100	76	19.2	22.2	17.1	6.3	8.4	SSE	SSE	32	142
5	1999/05/10							X	X			X	X		X	X	X	X		X		2	9		1		0.0	83	100	68	18.9	22.4	12.8	5.1	9.1	SE	SE	31	138
	1999/05/11							X				X	X	X	X	X	X	X		X	X	14	10		1	2	0.0	89	100	65	16.7	23.5	11.0	1.7	5.4	SSW	ENE	28	129
	1999/05/12							X				X	X		X	X	X	X		X	X	15	24		2	3	0.0	91	100	71	18.4	21.0	16.5	3.0	6.5	SSW	SSW	29	130
	1999/05/13							X				X	X		X	X	X			X	X	10			1	2	0.0	95	100	79	17.2	21.4	13.9	2.3	6.8	SE	SSW	27	128
	1999/05/14	X	X		X				X			X	X	X	X	X	X	X	X	X	X	36	24	12	4	4	0.0	98	100	90	16.8	20.3	12.4	2.1	6.3	SSW	ESE	27	124
	1999/05/15	X		X	X	X		X	X			X		X	X	X	X		X	X		1		5	2		0.0	88	100	67	20.9	26.3	17.1	5.3	9.5	SSE	SE	27	126
	1999/05/16			X	X		X	X	X	X	X																0.0	67	95	37	23.0	31.5	15.9	2.6	5.6	NE	E	27	122
6	1999/05/17			X	X	X	X		X			X	X		X	X	X			X		2			2		0.0	78	90	48	21.0	29.1	17.8	2.3	7.8	SSE	ENE	16	91
	1999/05/18			X			X		X				X	X	X	X	X	X	X	X	X		9	9	2	2	0.0	95	100	82	18.3	21.9	15.6	0.8	4.8	NW	ENE	19	89
	1999/05/19		X	X			X						X	X	X	X		X	X	X	X		25	8	4	2	0.0	100	100	100	15.6	17.2	13.3	1.5	5.0	NNW	SW	24	125
	1999/05/20	X		X				X				X	X	X	X	X	X	X		X		15	15		2		1.2	99	100	92	17.1	19.5	15.9	1.9	4.4	SE	WSW	22	116
	1999/05/21	X	X									X	X	X	X	X	X	X	X	X	X	13	28	12	4	2	0.0	99	100	95	16.7	18.2	14.3	2.8	6.9	NW	NW	23	123
	1999/05/22	X										X	X	X	X	X			X	X	X		7	2		2	8.0	98	100	89	16.8	18.6	15.1	6.7	13.4	NNW	N	9	52
	1999/05/23					X	X		X	X			X			X		X			X		14				0.0	87	97	78	16.9	18.2	14.7	5.1	8.0	WSW	NW	21	117
12	1999/06/28						X		X	X			X			X		X					9				0.0	63	98	30	21.2	29.2	15.8	5.1	9.1	SW	N	19	83
	1999/06/29	X		X			X		X	X	X		X					X	X		X		8	3		2	2.1	92	100	58	16.6	19.8	13.8	7.2	13.3	NW	NW	15	99
	1999/06/30							X	X	X		X	X			X	X	X	X		X	7	18	6		14	0.0	96	100	83	14.2	16.8	12.1	5.7	9.6	NW	N	21	98
	1999/07/01					X	X			X	X					X					X		9			3	9.4	99	100	95	15.0	16.9	10.5	6.7	13.5	NW	N	12	78
	1999/07/02								X	X		X	X			X	X	X	X		X	2	7	3		9	0.0	99	100	85	13.8	18.0	10.2	2.2	5.3	NNE	NNE	22	103
	1999/07/03							X				X	X	X	X	X	X	X				9	12				0.2	100	100	100	12.6	15.0	8.6	1.3	3.1	WSW	NE	15	73
	1999/07/04						X	X	X	X	X		X														0.1	97	100	79	15.1	21.8	10.7	2.1	4.7	SSW	ENE	21	101

Table 5.3 Electrical discharge activity, leakage current and daily weather (week 18-53).

Week	Date	Electrical discharge activity observations made nightly (21h00 to 24h00+) on insulators 1S, 2E, 3P, 4C and 5A																									Daily weather parameters													
		Water Drop Corona					Spot Corona/Discharges					Dry Band Corona					Dry Band Discharges					Leakage Current (mA)					Rainfall	Relative Humidity (%)			Temperature (°C)			Wind speed (m/s) and Direction				UV-B (µW/cm²)	
		1S	2E	3P	4C	5A	1S	2E	3P	4C	5A	1S	2E	3P	4C	5A	1S	2E	3P	4C	5A	1S	2E	3P	4C	5A	(mm)	Ave	Max	Min	Ave	Max	Min	Ave	Max		Dominant	Ave	Max
18	1999/08/09				X				X	X		X	X			X	X	X			X	13	5			9	0.0	92	100	81	14.9	18.0	11.7	2.9	6.0	WNW	NNE	17	102
	1999/08/10						X		X	X	X		X			X		X					8				0.0	89	100	67	14.9	18.7	10.6	3.3	7.9	SSE	SSE	19	123
	1999/08/11			X			X			X	X		X	X				X	X	X			3	12	1		0.0	86	100	53	14.8	22.5	7.4	1.4	3.9	SSW	ENE	30	132
	1999/08/12								X	X	X	X	X					X	X		X		14	16		12	0.0	90	100	78	14.8	18.0	9.5	3.0	5.9	NNE	N	17	84
	1999/08/13								X	X	X	X	X				X	X	X		X	4	9	8		7	0.0	84	98	75	16.0	18.0	14.5	5.7	10.5	NNW	N	19	103
	1999/08/14			X					X	X		X	X			X	X	X	X	X	X	50	48	20	4	20	0.0	89	97	72	15.9	20.0	13.0	5.3	8.9	NNW	N	30	148
	1999/08/15			X	X				X	X		X	X			X	X	X	X	X	X	30	14	21	10	24	0.0	96	100	82	15.4	20.0	10.6	2.6	4.7	WSW	N	28	150
24	1999/09/20				X		X	X	X		X				X			X	X		X		45	30		2	0.0	90	100	77	16.4	17.6	9.7	4.6	7.1	SW	SW	67	338
	1999/09/21								X	X		X	X			X	X	X	X		X	15	20	20		120	0.0	87	100	68	14.7	18.9	8.4	4.1	7.3	SW	SSE	76	317
	1999/09/22	X							X			X	X		X	X	X	X	X	X	X	40	68	6	12	30	0.0	89	100	64	14.9	21.6	7.1	3.5	6.4	SSW	SE	76	315
	1999/09/23								X			X	X		X	X		X	X	X	X		60	14	12	80	0.0	93	100	85	15.4	18.0	11.4	3.8	8.7	SSW	SW	79	329
	1999/09/24											X	X	X	X	X	X	X	X	X	X	100	140	55	20	30	2.0	90	100	79	16.5	18.9	13.0	6.8	12.1	NW	NW	63	353
	1999/09/25		X				X		X	X	X		X					X					7				5.7	87	100	71	14.2	17.0	7.4	6.8	12.4	W	SW	34	198
	1999/09/26									X	X	X	X	X	X	X	X	X	X	X	X	32	45	20	16	90	1.1	86	98	67	11.7	14.5	7.0	2.1	5.8	SSE	SSE	30	167
30	1999/11/01						X		X			X	X		X	X	X	X		X	X	30	32		16	42	0.0	92	100	74	18.3	22.7	14.5	5.0	8.2	SSE	SSE	132	416
	1999/11/02						X					X	X	X	X	X	X	X		X	X	35	20		15	64	0.0	81	93	62	20.5	24.2	18.0	6.4	11.2	S	SE	111	414
	1999/11/03	X					X		X			X	X		X	X	X	X	X	X	X	42	42	48	34	108	0.0	90	100	80	18.0	20.4	15.3	3.2	10.2	SSW	WNW	113	416
	1999/11/04	X					X	X	X	X	X								X					2			1.2	87	100	65	16.5	17.6	15.0	5.6	9.3	SSW	SSW	112	419
	1999/11/05						X		X	X	X		X					X					5				0.0	78	88	59	15.6	20.2	12.5	3.5	8.5	SSE	SSE	37	242
	1999/11/06						X		X		X	X			X		X	X	X	X	X	24	32	30	20	120	0.0	86	100	69	16.7	19.4	12.7	2.7	6.5	SSE	WNW	114	417
	1999/11/07								X			X	X		X	X	X	X	X	X	X	30	60	35	19	40	1.0	96	100	86	16.0	17.6	11.7	2.9	5.9	WNW	NW	76	417
36	1999/12/13				X		X	X	X	X	X																0.0	83	95	52	22.3	29.6	17.6	2.1	6.7	NW	SSW	120	419
	1999/12/14						X		X		X	X	X		X		X	X	X	X	X	64	66	25	5	90	0.0	99	100	95	18.5	20.1	15.7	2.4	6.8	NW	NW	98	357
	1999/12/15								X		X	X	X		X			X			X		28			60	0.0	94	100	73	20.3	27.5	16.6	3.1	5.3	NW	SW	101	331
	1999/12/16		X				X		X		X		X		X			X					9				0.0	83	94	72	23.7	27.6	20.4	2.4	6.7	SSW	E	117	398
	1999/12/17										X	X	X	X	X		X	X	X	X	X	30	50	42	24	20	0.0	92	100	80	21.7	23.9	20.2	2.6	5.9	NW	NW	100	381
	1999/12/18								X		X	X	X			X	X	X			X	18	30			160	0.0	91	98	80	21.3	22.1	20.6	3.7	6.1	WNW	WNW	123	421
	1999/12/19							X	X			X			X	X		X			X		32			24	0.0	90	97	78	21.0	21.8	19.6	5.7	9.9	NW	NW	117	417
42	2000/01/24								X		X	X	X	X	X	X	X	X	X	X	X	15	24	35	5	40	0.0	82	98	68	21.2	25.2	16.4	1.5	4.0	W	SSW	104	421
	2000/01/25								X			X	X		X	X	X	X	X	X	X	20	110	72	16	120	0.0	95	100	81	19.5	22.8	16.3	4.1	8.7	SSW	SW	118	420
	2000/01/26								X		X	X	X		X		X	X	X	X	X	40	78	62	36	296	0.0	87	93	77	19.5	22.6	16.4	5.4	8.0	S	SSE	124	421
	2000/01/27								X			X	X		X	X	X	X	X	X	X	16	100	36	30	108	0.0	91	99	81	18.8	21.8	15.8	4.1	8.3	SW	SW	123	421
	2000/01/28								X			X	X		X	X	X	X			X	63	70			40	0.7	94	100	80	18.3	21.1	16.4	4.0	7.5	SW	SW	120	421
	2000/01/29	X							X			X	X		X	X	X	X	X	X	X	75	82	20	10	128	0.0	96	100	90	17.1	19.2	13.4	1.7	4.1	W	WNW	114	419
	2000/01/30			X					X			X	X		X	X	X	X	X	X	X	46	50	60	65	20	2.8	91	100	79	19.0	21.2	15.0	6.7	12.8	NW	NNW	55	270
48	2000/03/06						X	X	X		X				X												0.0	83	100	62	19.5	22.9	16.2	7.3	12.8	SSE	SSE	89	352
	2000/03/07						X	X	X	X	X			X													0.0	76	88	63	21.0	25.3	17.8	5.2	8.0	S	SE	88	339
	2000/03/08						X	X	X	X	X	X	X		X	X	X	X	X	X	X	8	8	48	2	28	0.0	74	88	43	22.2	28.8	19.5	6.1	9.9	S	SE	87	338
	2000/03/09						X	X	X	X		X	X			X	X	X	X		X	9	30	30		16	0.0	89	100	73	19.4	25.7	15.0	4.8	10.8	SSE	SSE	80	303
	2000/03/10							X			X	X		X	X		X	X	X	X	X	24	16	80	6	80	0.0	85	97	62	19.7	25.1	14.6	5.5	8.2	SSE	SSE	79	312
	2000/03/11							X	X		X	X	X			X	X	X	X	X	X	30	50	60	8	96	0.0	99	100	96	15.0	18.6	12.0	2.0	5.1	SW	WNW	77	315
	2000/03/12		X				X	X	X	X		X	X		X	X	X	X	X	X	X	16	90	20	16	10	0.1	97	100	87	15.8	19.2	13.2	2.8	7.0	SW	SW	78	309
53	2000/04/10						X	X	X	X		X	X			X	X	X	X		X	14	24	50		36	0.0	88	96	71	18.2	22.5	15.6	4.0	6.2	SE	SE	53	236
	2000/04/11						X	X	X	X		X					X	X	X		X	24	24	48		24													
	2000/04/12						X		X			X	X		X	X	X	X	X	X	X	30	60	28	20	130													
	2000/04/13						X	X	X	X	X										X					36													
	2000/04/14						X	X	X	X	X			X													0.0	86	98	72	18.6	23.7	14.6	5.2	10.4	S	SSE	50	217
	2000/04/15																										0.0	71	85	48	20.4	26.0	17.4	4.4	6.5	SE	SE	48	208
	2000/04/16						X	X	X				X		X	X		X	X	X	X		14	30	6	40	0.0	85	96	61	18.6	24.2	14.1	3.0	5.8	SSW	E	46	211

A summary of the insulator surface electrical discharge activity observations per test insulator (as detailed in Tables 5.2 and 5.3) is given below in Table 5.4. Comments on the electrical surface discharge activity observations relevant to all the test insulators are also given.

Table 5.4 Summary of the insulator surface electrical discharge activity observations.

	1S		2E		3P		4C		5A	
	Week	Day	Week	Day	Week	Day	Week	Day	Week	Day
WDC first seen	1	2	1	2	1	7	2	2	2	2
WDC % of observation days	16		13		13		20		12	
SCD first seen	1	7	1	3	2	2	2	4	3	5
SCD % of observation days	44		39		65		43		34	
DBC first seen	2	2	1	7	3	4	3	5	3	6
DBC % of observation days	61		73		19		47		50	
DBD first seen	2	2	1	7	3	4	3	5	4	7
DBD % of observation days	54		73		44		39		52	
Leakage current (mA)	1 - 100		1 - 140		1 - 80		1 - 66		1 - 296	

The following comments are relevant to the electrical surface discharge observations on the test insulators 1S, 2E, 3P, 4C and 5A:

- WDC (Water drop corona) was mainly observed on the sheds (bottom or tips), from the dead to the live end and more dominant in the beginning (contrary to the currently accepted theories, which expect it on the live side only, close to the end fitting [61]). WDC was seen more often on insulators 1S (16% of observation days) and 4C (20%) than on insulators 2E (13%), 3P (13%) and 5A (12%).
- SCD (Spot corona/discharges) were present on the shank and sheds, from the live to the dead end. SCD were seen most often on insulator 3P (65%). On the other insulators SCD ranged from 34 to 44% of observation days.
- DBC (Dry-band corona) was present mainly on the shank, ranging from the live to the dead end. DBC was seen most often on insulators 2E (73%) and 1S (61%). On the other insulators DBC ranged from 19% (on 3P) to 50% (on 5A).
- DBD (Dry-band discharges) were mainly present in the areas of the DBC, and discharges were seen on the shank, shank-to-shed or shed-to-shed, from the live to the dead end. DBD were seen most often on insulator 2E (73%). On the other insulators DBD ranged from 39% to 54%.
- The electrical discharge activity seemed at times to be increased in the presence of wind and rain. As the wind speed increased the discharge activity seemed to increase

dramatically. As rain began to fall, the discharge activity was found to suddenly increase.

5.2.3 Electrical field calculations

Electric field simulations were done using the ELECTRO, 2-dimensional, electric field solver software (version 4.1), as developed by Integrated Engineering Software. The ELECTRO software uses the boundary element method as a means of calculating the electrical fields and potential plots.

It was decided to use the boundary element method as it had been proven in the paper by Rasolonjahary et al. "Computation of electric fields and potential on polluted insulators, using a boundary element method" [62] that it works well to simulate a pollution layer on an insulator. Private communication with Mr. Clive Lumb from the manufacturer Sediver confirmed that the ELECTRO package using the boundary element method could be used for the proposed electric field calculations.

The SR test insulator 1S was simulated to scale for three typical conditions, identified from the visual surface condition and electrical discharge activity observations. The resultant equipotential and equi-electric field line plots are shown for a clean insulator (Figure. 5.11), for an insulator with an electrolytic pollution layer (Figure. 5.12), and for an insulator with an electrolytic pollution layer with a dominant dry band (1 cm) in the middle (Figure. 5.13). Mr. Clive Lumb from Sediver checked the calculations and plots. Unfortunately no details of the constant values used in the program for the material may be disclosed in this dissertation due to manufacturer confidentiality.

The equipotential and equi-electric field line plots of the new, clean and dry insulator (see Figure 5.11) show that the electrical stresses are the highest in the regions adjacent to the live end-fitting. The stresses on the insulator material surface do not exceed 5.86 kV/cm.

The equipotential and equi-electric field line plots on an insulator with an electrolytic pollution layer (Figure. 5.12) show that the voltage is fairly evenly distributed over the insulator surface from live to dead end, as would be expected with a resistor. However, the equi-electric field line plots indicate that the highest electric field stresses are present on the shed rims (tips). The maximum field stress calculated was 8.51 kV/cm.

The equipotential and equi-electric field line plots of an insulator with an electrolytic pollution layer and dry band on the shank in the middle (Figure. 5.13) show that the voltage is transferred from the live end-fitting to the dry band and the earth potential is transferred down from the dead end-fitting to the dry band. Thus a large portion of the voltage is present over the dry band. This was confirmed by the results of practical field measurements at KIPTS on the test insulators, using an electrostatic voltmeter. The potential along the test insulators was measured and a close correlation to the ELECTRO simulation was found. From the equi-electric field line plots, it can be seen that the electric field stresses are the highest in the dry-band area. An electric field stress of 35.32 kV/cm was calculated, which is well beyond the stress needed for air breakdown, which could lead to discharge activity.

The electric field simulations above confirm the electric discharge activity results obtained, especially the water drop corona observations closer to the shed tips, and not in the expected [61] area close to the live end-fitting. This indicates that when an insulator surface becomes polluted, the voltage distribution and electric field stresses can occur anywhere along the axial length of the insulator.

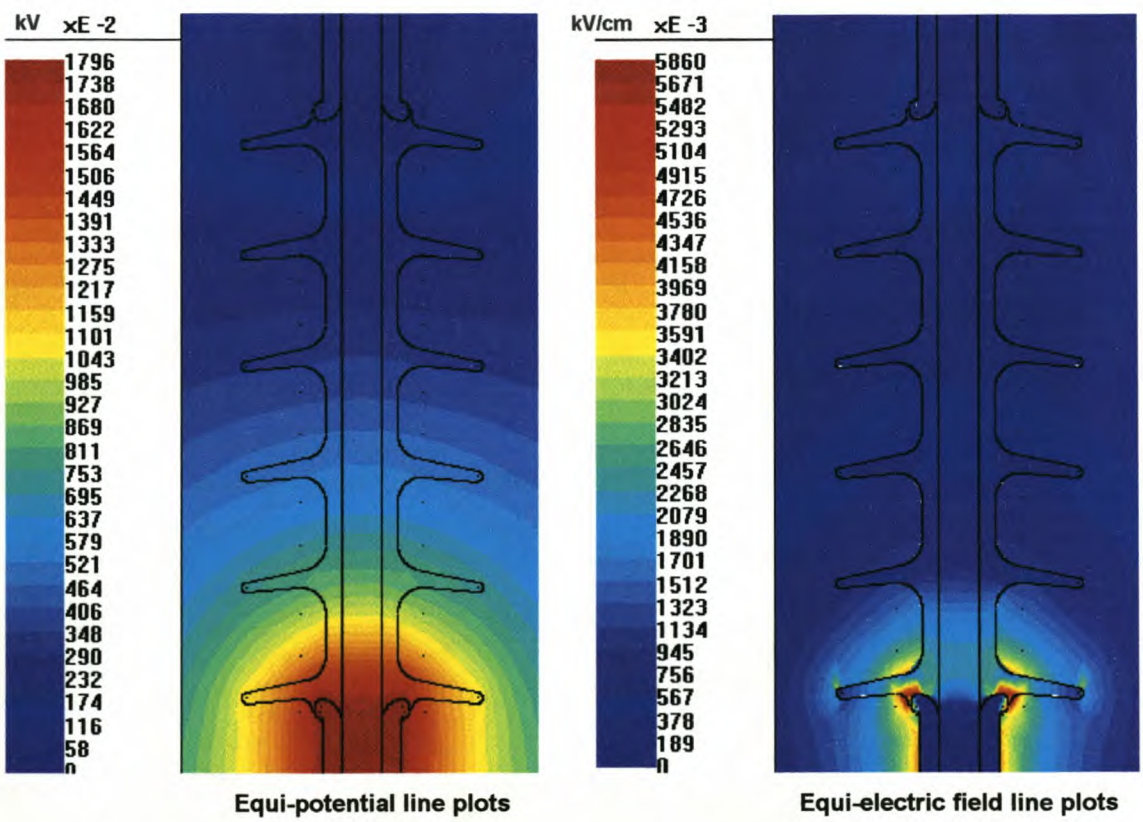

Figure 5.11 Simulation results for a new, clean and dry insulator (1S).

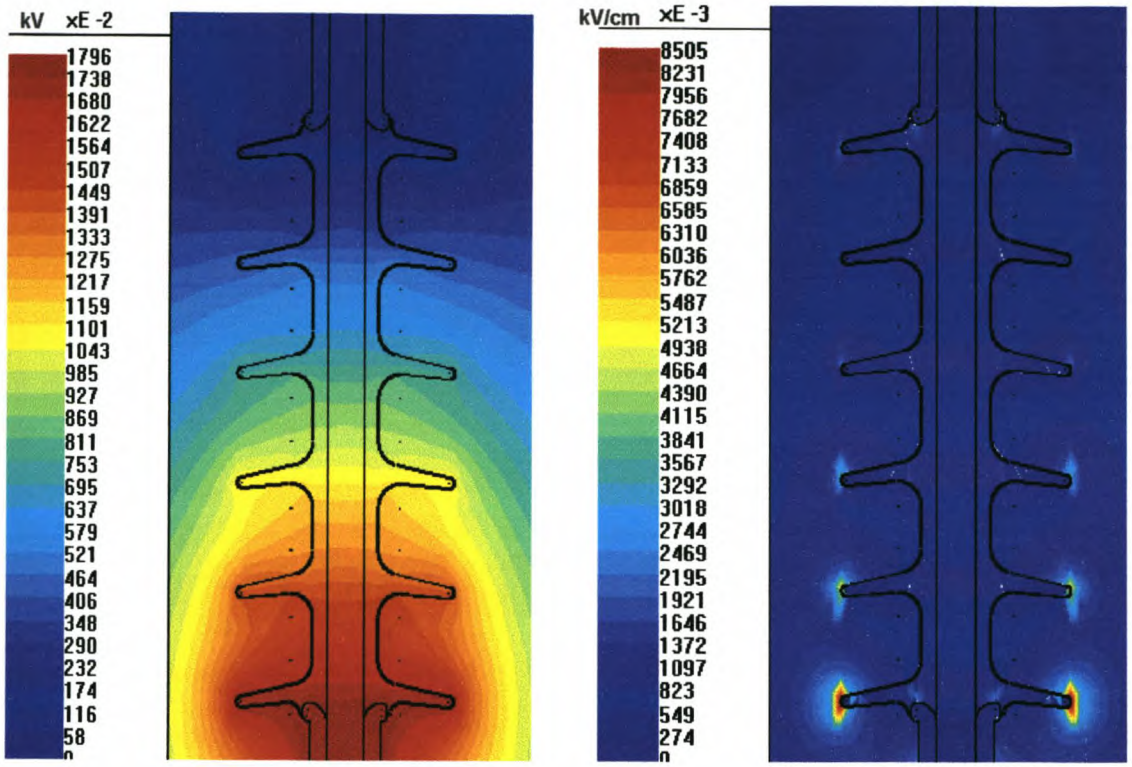

Figure 5.12 Simulation results for insulator 1S with uniform electrolytic pollution layer.

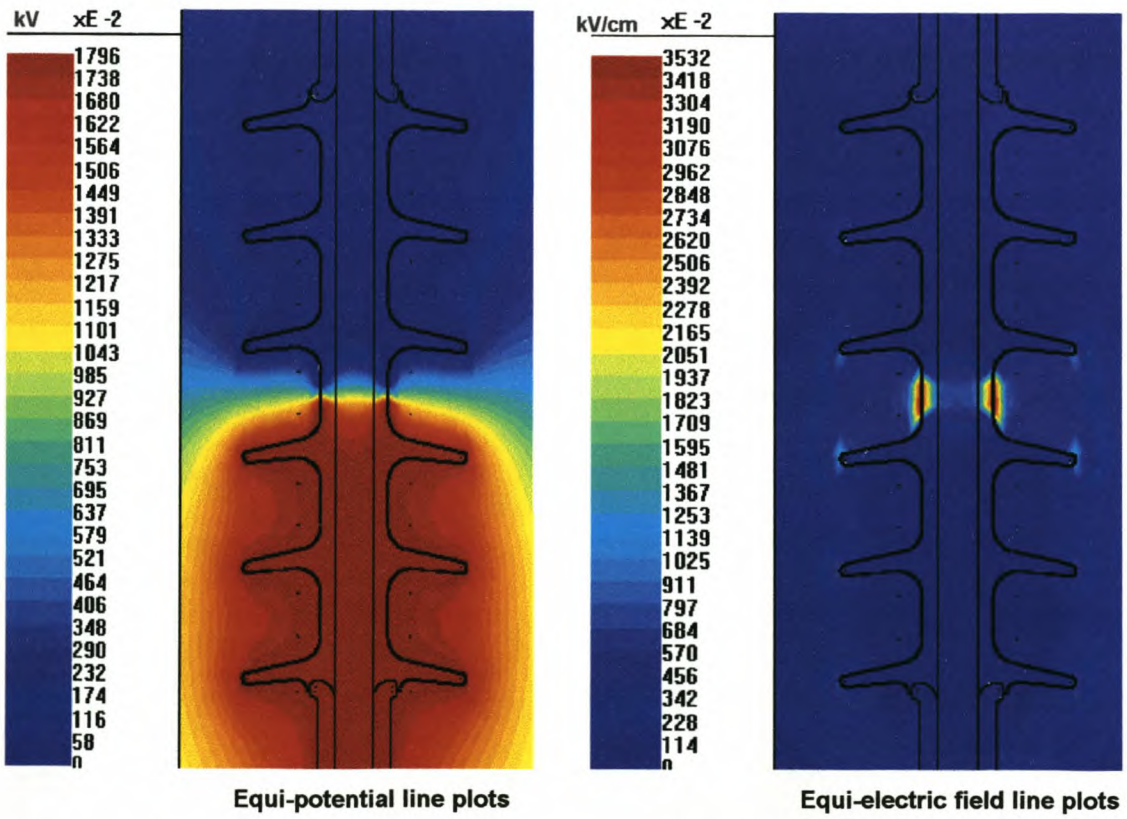

Figure 5.13 Simulation results for insulator 1S with uniform electrolytic pollution layer and a 1 cm dry band.

5.3 CONCLUDING REMARKS ON THE INSULATOR SURFACE CONDITION INSPECTIONS AND ELECTRICAL DISCHARGE ACTIVITY OBSERVATIONS

Water drop corona was found to be present on all the test insulators. Contrary to current belief that it will be present mainly at the live side, and close to the end-fitting, as suggested in the work of Phillips [61], it was found to be towards the shed tips and anywhere from the live to the dead end (see Figure 5.6 (a)). The water drop corona was mainly present at the beginning of the test period (observed more often in weeks 1 to 6 than after week 6).

Dry-band corona and discharges were found to be the most dominant form of electrical discharge activity on all the insulators. This occurred mainly on the shank, ranging from the live to the dead end. The electrical field calculations confirmed that the stresses in the dry-band regions were very high, and that a large percentage of the supply voltage was transferred to the dry band.

The electrical discharge activity was influenced by wind (flare up) and rain (sudden increase).

Comments on the visual observations of the material are given below:

- Degradation on the HTV SR insulator 1S was found to be minimal and restricted to the pollution layer.
- The EPDM insulator 2E showed signs of crazing (see Figure 5.5, 2E) on the sheds and light erosion in the shank area. Chalking was found on the non-energised EPDM insulator 2E.
- The porcelain, as expected, showed no degradation.
- Material erosion and tracking were present on the RTV SR-coated porcelain insulator, exposing the porcelain at the shank areas close to the end fittings. However, the larger part of the area at the end fittings was still coated and functional.
- The cycloaliphatic insulator 5A showed clear signs of severe material degradation, chalking, tracking and erosion. From a visual perspective, this insulator had failed due to severe material degradation. It should be noted that the non-energised

cycloaliphatic insulator 5A showed minimal signs of material degradation (only light discoloration in the mould line).

A higher visible pollution build-up was found on the SR insulators than on the other insulators.

From both the visual surface condition inspections and electrical discharge activity observations, the cycloaliphatic insulator 5A was by far the worst performer of all the test insulators.

6 CONTINUOUS MEASUREMENT OF INSULATOR LEAKAGE CURRENT

*"Measure what is measurable, and make measurable what is not so" - **Galileo Galilei***

As explained in section 1.3, leakage current is recognised worldwide as one of the main parameters for the measurement of insulator performance. Insulator impedance is the main factor determining the magnitude and shape of the insulator leakage current. It is influenced by the interaction of the insulator surface with the environmental and climatic conditions surrounding it (electrolytic pollution layer, dry-band with spark/arcs).

However, what parameters of the leakage current must be monitored and why? To answer this, a fundamental understanding of the leakage current and supply voltage waveforms, of which a typical example is shown in Figure 6. 1, is required.

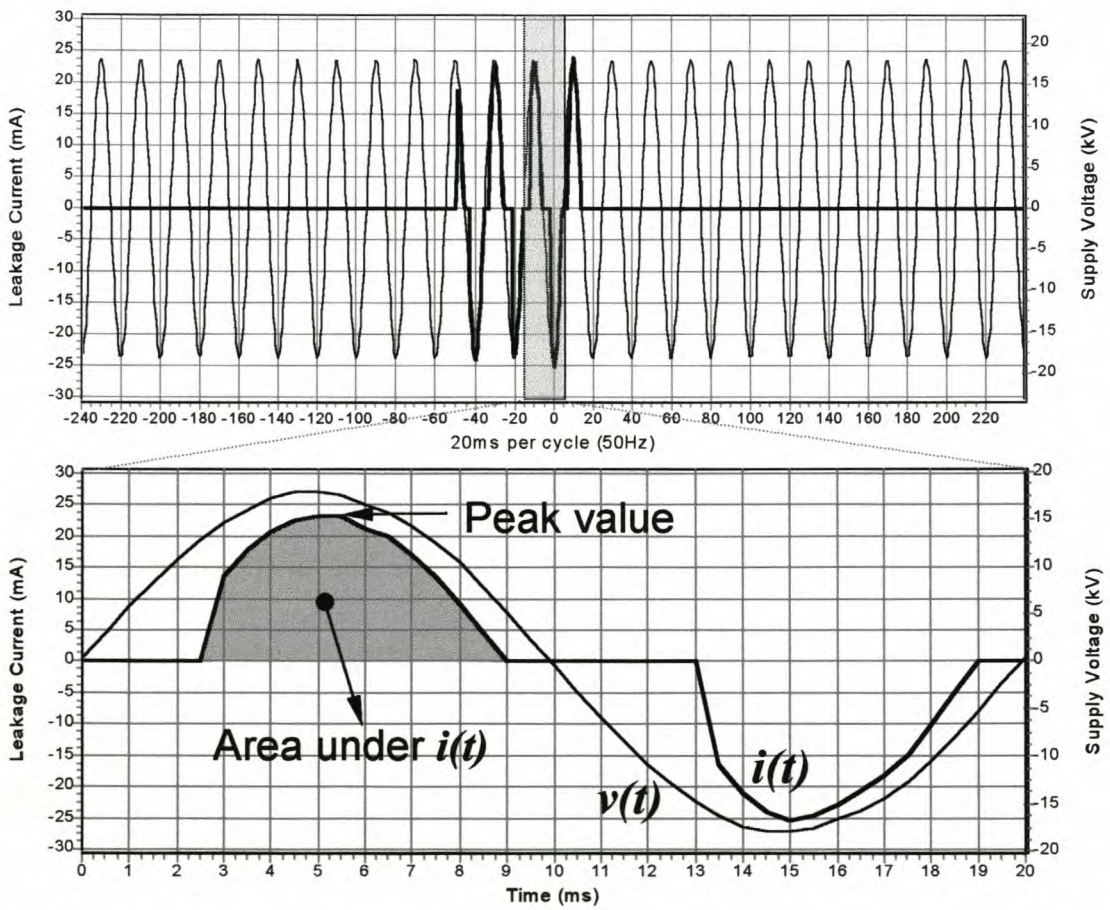

Figure 6. 1 Typical leakage current *i(t)* and supply voltage *v(t)* waveforms showing an expanded view of the shaded 20 ms cycle.

The peak of the leakage current, indicating the magnitude of the current pulse, can be related to the likelihood of flashover using the empirical formula of Verma [22], shown in Chapter 1, Eq. (1.1). Thus, peak leakage current values of the test insulators can be used to compare their relative performances in terms of the likelihood of flashover. The rate of occurrence of the peak leakage current pulses can be used to indicate the flashover risk.

The rate of occurrence of peak leakage current pulses can also be analysed for various current magnitude ranges, indicating the magnitude of current pulses that are dominant. As discussed in section 1.3, small currents (the lower magnitude leakage current pulses, in the order of several mA) can cause damage to non-ceramic insulator materials and possibly cause ageing. It is expected that there will be high counts of the lower magnitude leakage current pulses in the beginning (on new material), becoming less over time, while the opposite is expected for the higher magnitude leakage current pulses.

However, leakage current waveforms having exactly the same peak values could vary from pure sinusoidal to pulse-shaped, from capacitive to resistive, and the non-linear nature of the spark/arc over the dry-band could result in a large variation of wave shapes. Thus, the peak value of the leakage current cannot be used on its own to characterise the waveform.

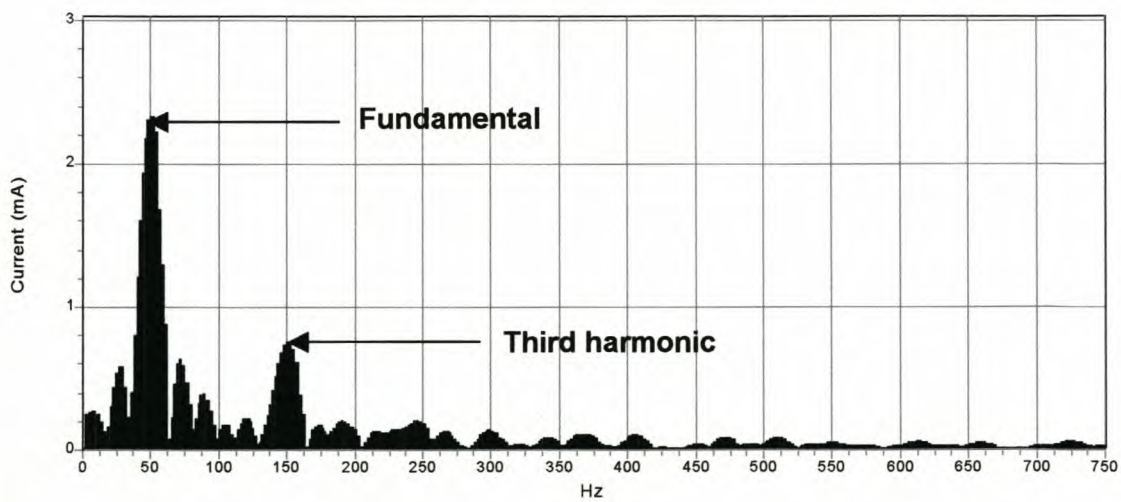

Figure 6. 2 Fast Fourier Transform (FFT) plot of the leakage current waveform that is shown in Figure 6. 1.

The leakage current waveform can be analysed for harmonic content by carrying out a Fast Fourier Transform (FFT) to obtain a frequency fingerprint. The FFT plot of the

leakage current waveform train of Figure 6. 1 is shown in Figure 6. 2. A strong 50 Hz fundamental and 150 Hz third harmonic was found, which correlate to the findings of Fernando [63]. However, the FFT method was developed to describe repetitive waveforms of the same shape and not waveforms of a non-repetitive nature, such as leakage current pulses. It cannot be assumed that the shape of a single 20 ms waveform, or a captured leakage current pulse train, is repetitive in time. Thus, the use of FFT is not recommended to characterise the leakage current waveform or for comparative studies.

The instantaneous v-i characteristic, plotted with time (one 20 ms cycle) in Figure 6. 3, could possibly be used to characterise the insulator leakage current waveform in relation to the supply voltage.

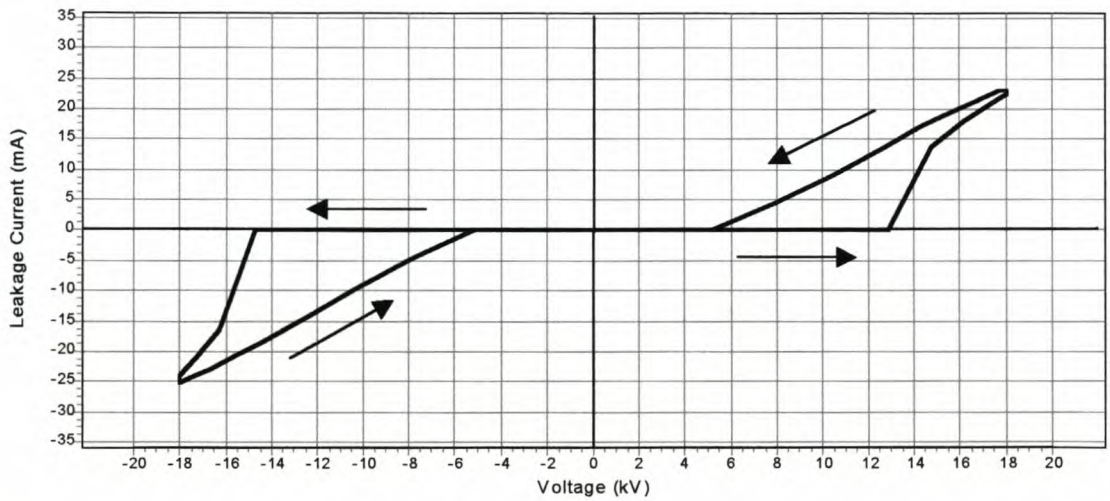

Figure 6. 3 Instantaneous v-i characteristic of the insulator leakage current and supply voltage waveform shown in Figure 6. 1.

When the insulator impedance is purely resistive, the instantaneous v-i characteristic plot will be a near straight line (see example in Figure 2.7 (b)). Figure 6. 3 shows a non-linear impedance insulator v-i characteristic plot. The shape of the insulator v-i characteristic plots varies widely between 20 ms voltage cycles, mainly due to the non-linear nature of the spark/arcs over the dry-bands. Thus to use these plots to graphically represent how insulator impedance varies over time is considered impractical for this study.

The insulator impedance can be plotted over time as the ratio of the supply voltage over the insulator leakage current. However, when the leakage current approaches zero the insulator impedance tends to infinity, making it difficult to represent graphically. To

overcome this difficulty the inverse ratio (the ratio of the insulator leakage current over the supply voltage in time) is used, which represents the insulator conductance $G_{ins}(t)$. The insulator conductance is then related to the insulator conductivity, according to Eq. (1.8) and Eq. (1.10), which takes the profile (form factor) of the insulator into consideration, and is represented as:

$$\sigma_{ins}(t) = F \cdot G_{ins}(t) \tag{6.1}$$

where

$\sigma_{ins}(t)$: conductivity of the insulator at time t in μS

The insulator conductivity (in time) for the leakage current and supply voltage waveforms is plotted in Figure 6. 4 below. The maximum insulator conductivity σ_{ins} for the 20 ms cycle is used to represent the nature and severity of the electrolytic pollution present on the insulator surface.

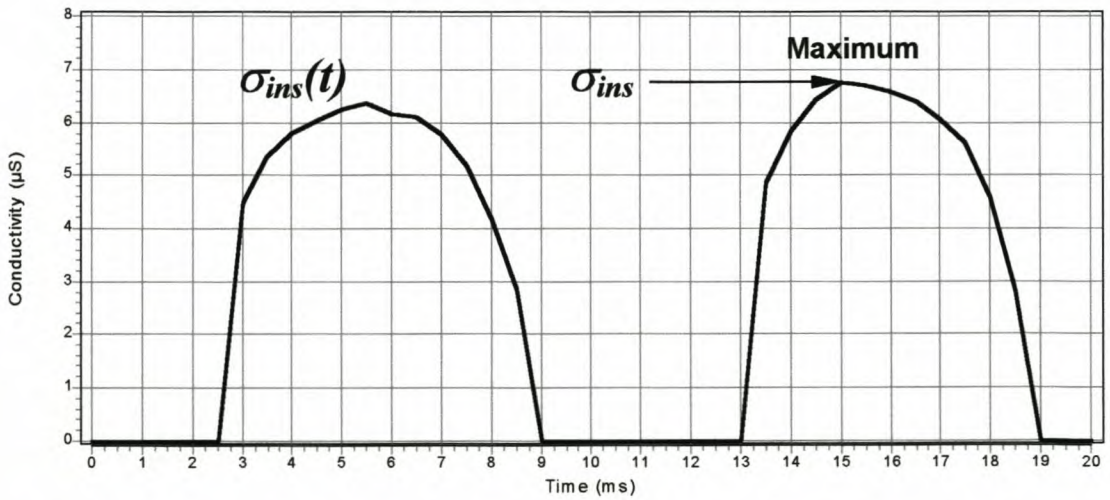

Figure 6. 4 Insulator conductivity $\sigma_{ins}(t)$ and the maximum value σ_{ins} for the 20 ms cycle shown in Figure 6. 1.

The minimum insulator resistance for the 20 ms cycle can be calculated from the maximum conductivity assuming $R_{pol} \approx R_{ins}$, using Eq. (1.7). The expected insulator flashover voltage can then be calculated from the minimum insulator resistance using Rizk's formula Eq. (1.16). This critical flashover voltage can be used to compare the performance of the test insulators, in terms of the likelihood of flashover.

The area under the leakage current curve (see Figure 6. 1) takes the shape and amplitude of the waveform into consideration. This area is calculated as the integral of the leakage current waveform in relation to time, and indicates the amount of electrical charge Q (coulomb) flowing over the insulator. The accumulative amount of charge flowing over the test insulators can be used to compare the test insulators to one another.

However, leakage current waveforms having exactly the same accumulative electrical charge values could vary in position in relation to the supply voltage waveform and hence have different energy and power dissipation values. The energy calculation not only takes the shape and amplitude of the leakage current waveform into consideration but also its position in relation to the supply voltage waveform. The sinusoidal 50 Hz supply voltage waveform as shown in Figure 6. 1 is common to all the insulators tested and is thus used as reference (even though it may alter slightly, in magnitude only, due to dips or surges on the supply network). Figure 6. 5 below show real time power and accumulated energy plots for the insulator leakage current shown in Figure 6. 1.

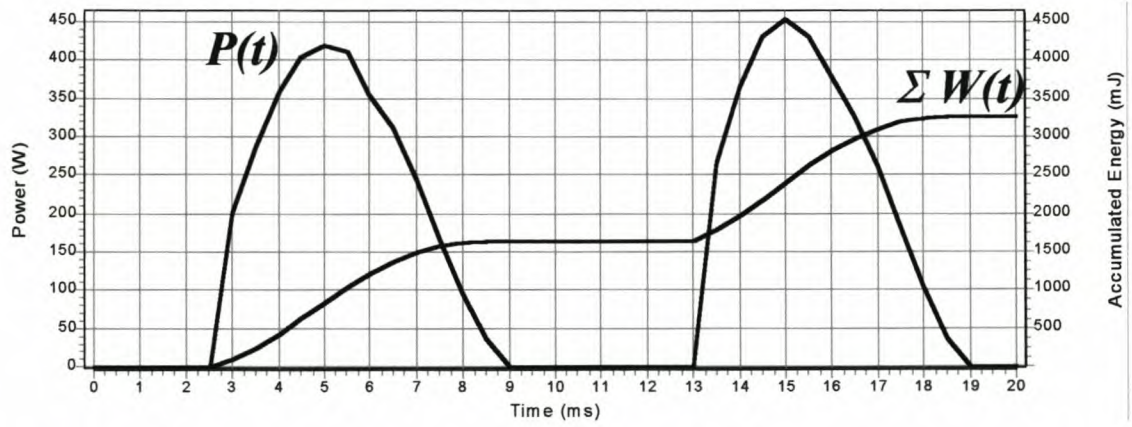

Figure 6. 5 Real-time true power $P(t) = v(t) \cdot i(t)$ and accumulated energy $\Sigma W(t)$ (where $W(t) = P(t) \cdot \Delta t$) plots for the insulator leakage current shown in Figure 6. 1.

True power is an instantaneous value. When averaged over time, singular high value events could possibly disappear into the average value. The accumulated energy is used in this dissertation to indicate the amount of power dissipated with time over the insulator.

It is envisaged that monitoring the peak value, rate of peak occurrence for different current levels (bin counts), conductivity, accumulative charge, and energy of the leakage current flowing over an insulator, will give the best possible indication of the performance of the

insulator as a whole and how it is coping with the environment and can thus be used to compare the performances of the test insulators.

6.1 MEASUREMENTS OF INSULATOR LEAKAGE CURRENT

The leakage current parameters (peak, daily bin counts, daily waveforms, conductivity, accumulative charge and energy) were measured (or calculated) at 10-minute intervals for the duration of the test period as discussed in the test procedure (Chapter 2, section 2.2.5). The test period was sub-divided into winter (12/04/199 to 10/10/1999) and summer (11/10/1999 to 16/04/2000) (see time table in Appendix B). If no data was recorded or calculated a blank space was plotted. Further details of the measured and derived (calculated) parameters are given below:

- **Peak leakage currents:** The OLCA instrument compares each leakage current sample measured with registers holding the previous positive and negative peak values. When a higher peak value is detected then the old stored register value is replaced with the new peak reading. At the end of each 10-minute interval both positive and negative register values are stored to memory. The peak leakage current registers are then zeroed and the process is repeated for the following 10-minute interval. The peak leakage current graphs in this dissertation are absolute value plots, plotted in relation to time (as described in Appendix C1).

- **Daily peak leakage current pulse bin counters:** Per selected period, the stored positive and negative peak leakage current measurements (per 10-minute intervals) are filtered into daily positive and negative leakage current pulse counter bins of pre-selected values, falling within (1 to 5 mA), (5 to 20 mA), (20 to 100 mA), (100 to 250 mA) and (250 to 500 mA). The daily peak leakage current bin count graphs in this dissertation are resulting value plots, plotted in relation to time (as described in Appendix C1). Note: The numbers of bin counts are based on only one peak value stored per 10-minute interval, and are thus much less than the actual number of pulses that may have occurred for that value or any lower value (totally ignored).

- **Daily peak leakage current and supply voltage waveforms and associated conductivity and accumulated energy:** The daily maximum peak leakage current and associated supply voltage waveforms captured and plotted, consist of 640

samples each (40 samples per 20 ms, 50 Hz cycle). The first half (8 cycles) shows pre-maximum information and the other half (8 cycles) post-maximum information.

The conductivity was calculated and plotted for a selected 20 ms cycle using Eq. (6.1).

The accumulated energy (as described in Appendix C2) for the same 20 ms cycle was calculated and plotted per sampling interval as the product of the leakage current and supply voltage values multiplied by the sampling time interval Δt.

- **Daily peak waveform conductivity:** The daily maximum conductivity plots reported, based on leakage current waveform, show daily values calculated using Eq. (1.8) and Eq. (1.12) as:

$$\sigma_{ins} = F \cdot G_{ins} \tag{6.2}$$

where

σ_{ins} : conductivity of insulator in μS

- **Accumulative charge:** The OLCA instrument accumulates the values of the positive and negative samples in two separate registers until the end of the 10-minute interval. The accumulated register readings are then multiplied with the sampling interval Δt. The resulting values are the positive and negative charges per 10-minute interval. The applied equation for the positive charge calculation is given as:

$$Q_{ins}(pos) = \sum_{n=0}^{N} pos(i(n)) \cdot \Delta t \tag{6.3}$$

where

$Q_{ins}(pos)$: positive electrical charge in Coulomb.

$pos(i(n))$: n^{th} positive value of the leakage current i at time t in ampere

T = 600 s

f = 2000 Hz

N = $f.T$ = 1 200 000

Δt = $\frac{1}{f}$ = 0.5 ms

The same formula (Eq. 6.3) holds for the negative electrical charge (*pos* replaced with *neg*). The accumulative (resulting) 10-minute interval charge is then plotted in relation to time (as described in Appendix C2).

- **Energy:** The OLCA instrument accumulates the product of each sampled leakage current value and its corresponding voltage over the 10-minute interval and stores the value to memory. The 10-minute accumulated energy is then calculated by multiplying this value with the sampling interval Δt. The applied equation for the energy calculation is given as:

$$W_{ins} = \sum_{n=0}^{N} i(n)v(n) \cdot \Delta t \qquad (6.4)$$

where

W_{ins} : energy loss over the insulator in joules.

$i(n)$: n^{th} value of the leakage current i at time t in ampere

$v(n)$: n^{th} value of the supply voltage v at time t in volts.

The 10-minute interval accumulated electrical energy is then plotted in relation to time and shows the rate of change in the energy.

Note: The 10-minute average power can be determined from the energy plots by dividing the 10-minute accumulated energy value by the time T.

The above leakage current parameters captured and/or calculated for the test insulators 1S, 2E, 3P, 4C, 5A and 8R during the winter and summer test periods are represented graphically in sections 6.1.1 to 6.1.6 below.

The peak leakage current plots are shown first, followed by the maximum peak leakage current and voltage waveforms (including conductivity and accumulated energy) measured during the test period. The daily peak waveform conductivity is shown next, followed by the electrical energy (indicating rate of change) and accumulative electrical charge plots. The daily peak leakage current bin count plots and associated first peak leakage current and waveform measured in each bin range are shown in Appendix F.

6.1.1 Leakage current measurements on HTV SR insulator 1S

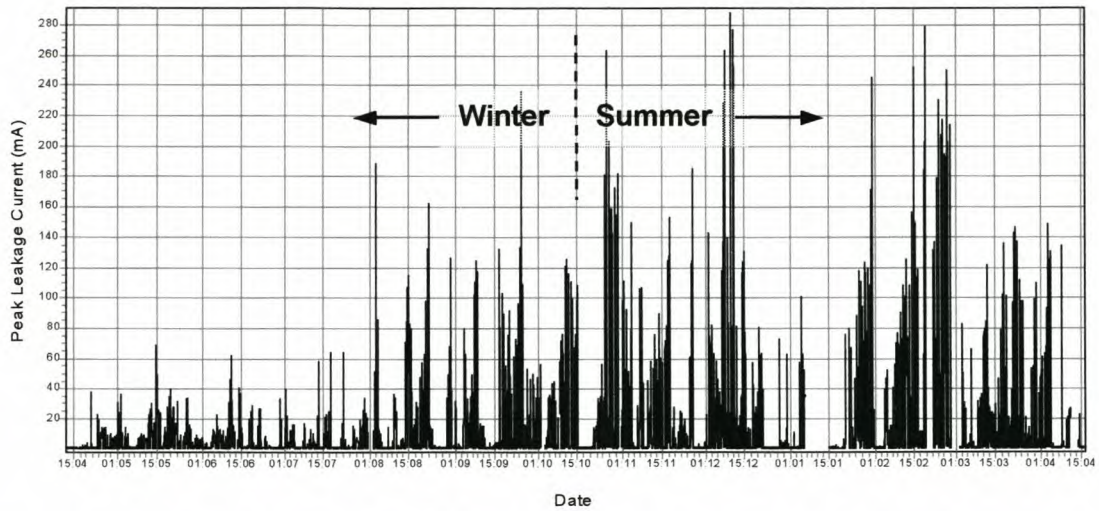

Figure 6. 6 Peak leakage current measurements on insulator 1S for both winter and summer test programme cycles.

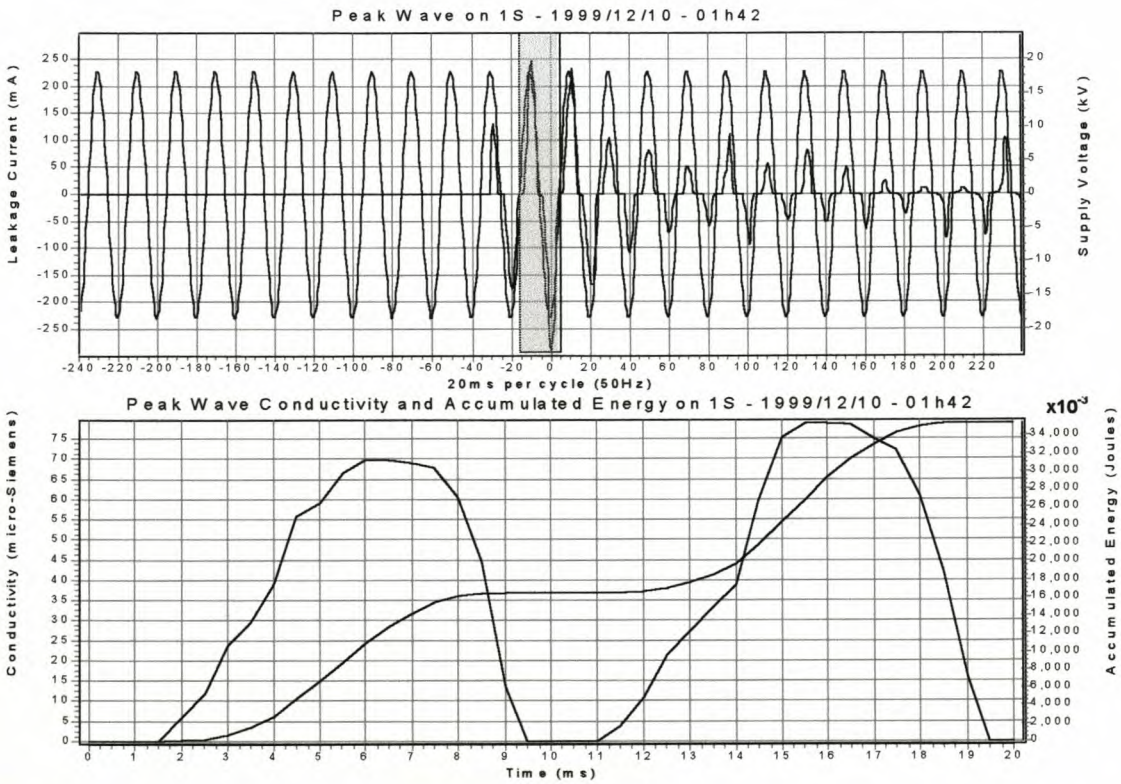

Figure 6. 7 Maximum daily peak leakage current and voltage waveform measured during the test period with associated conductivity and accumulated energy for the selected shaded area (20 ms cycle) for insulator 1S.

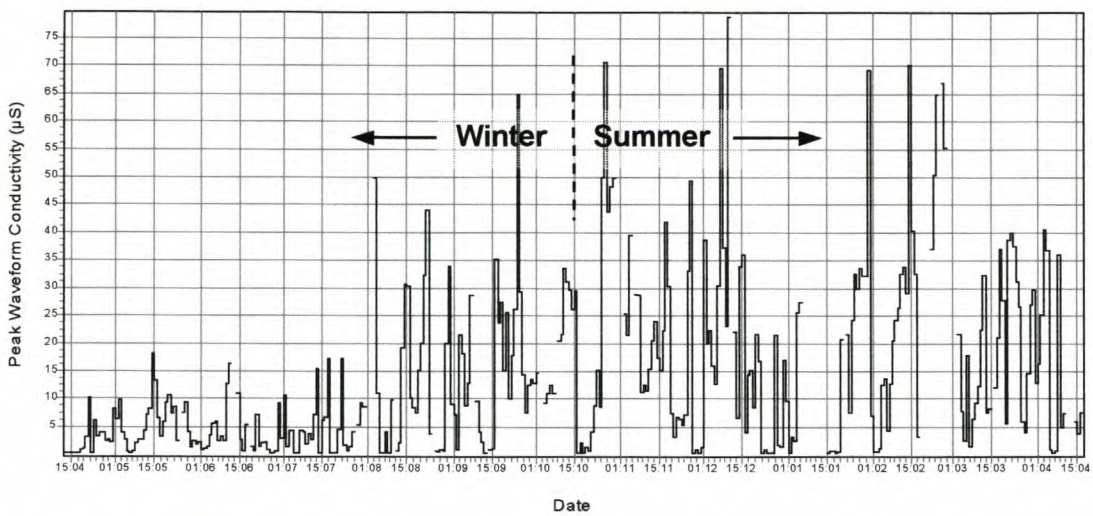

Figure 6. 8 Daily peak waveform conductivity measurements on insulator 1S for both winter and summer test programme cycles.

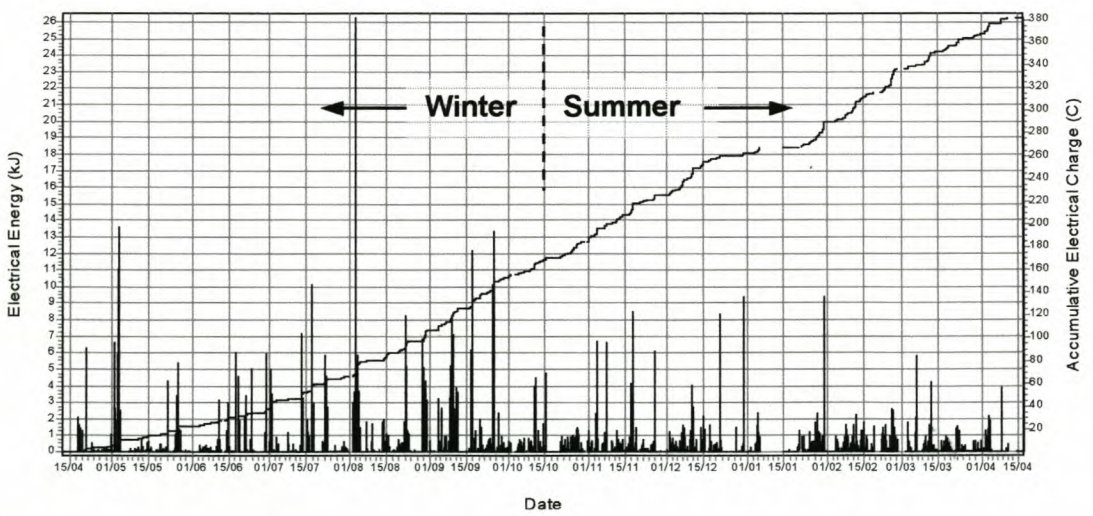

Figure 6. 9 Electrical energy and accumulative charge measurements on insulator 1S for both winter and summer test programme cycles.

6.1.2 Leakage current measurements on EPDM insulator 2E

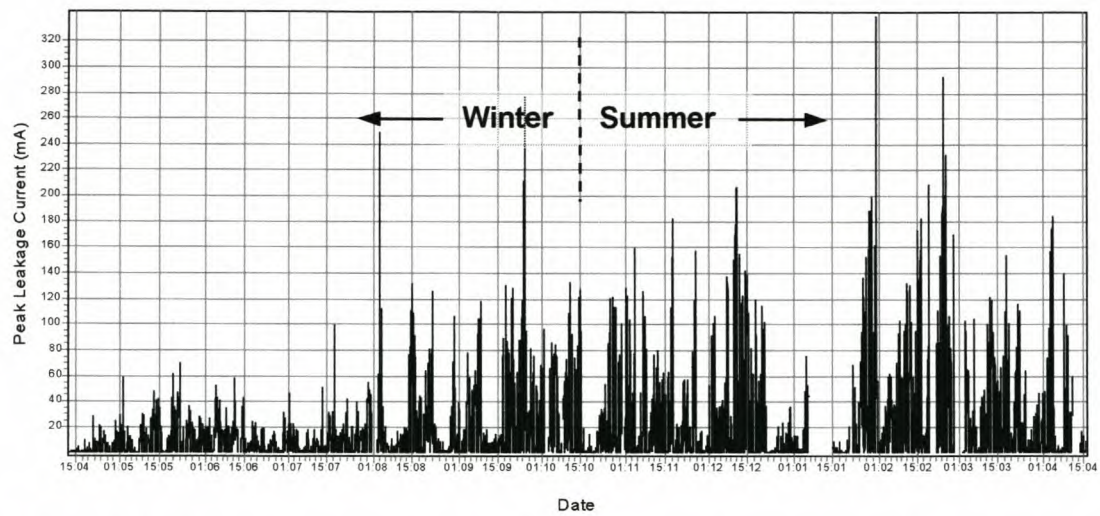

Figure 6. 10 Peak leakage current measurements on insulator 2E for both winter and summer test programme cycles.

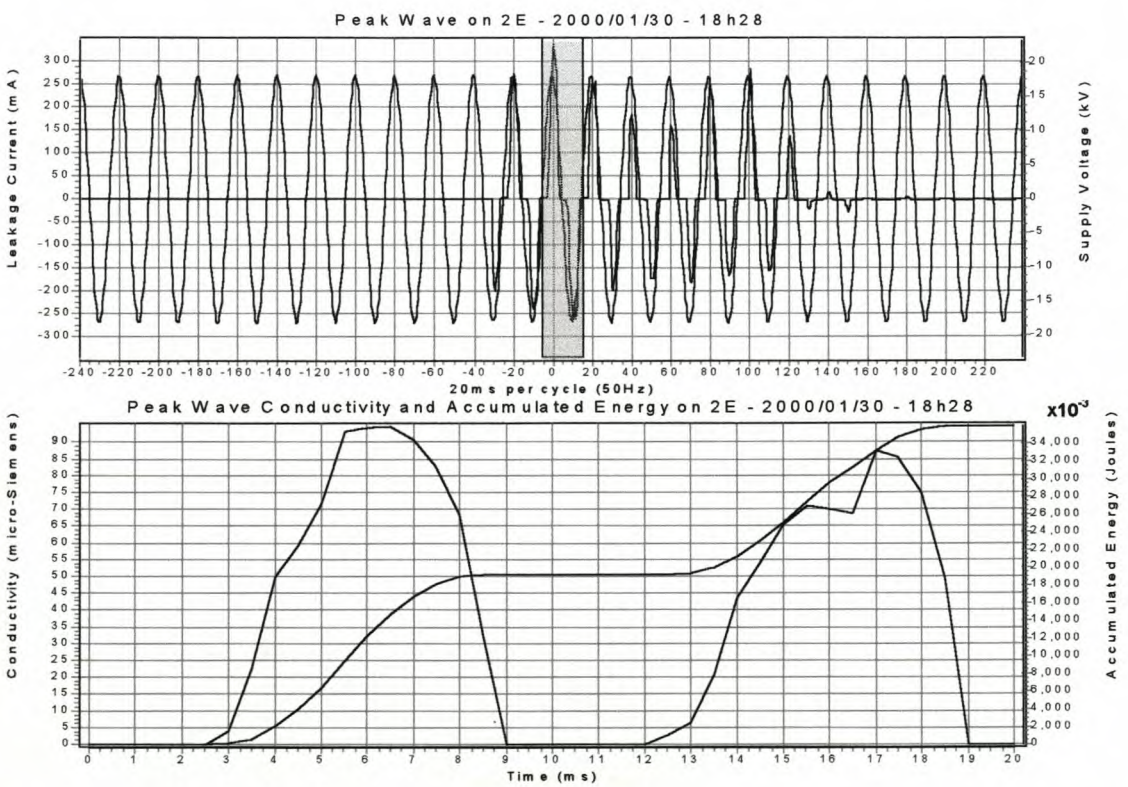

Figure 6. 11 Maximum daily peak leakage current and voltage waveform measured during the test period with associated conductivity and accumulated energy for the selected shaded area (20 ms cycle) for insulator 2E.

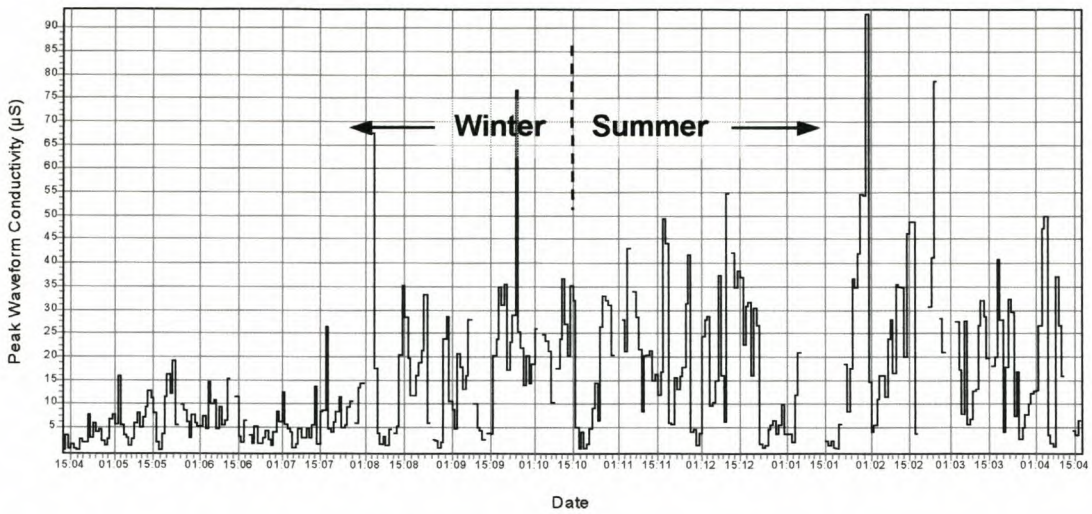

Figure 6. 12 Daily peak waveform conductivity measurements on insulator 2E for both winter and summer test programme cycles.

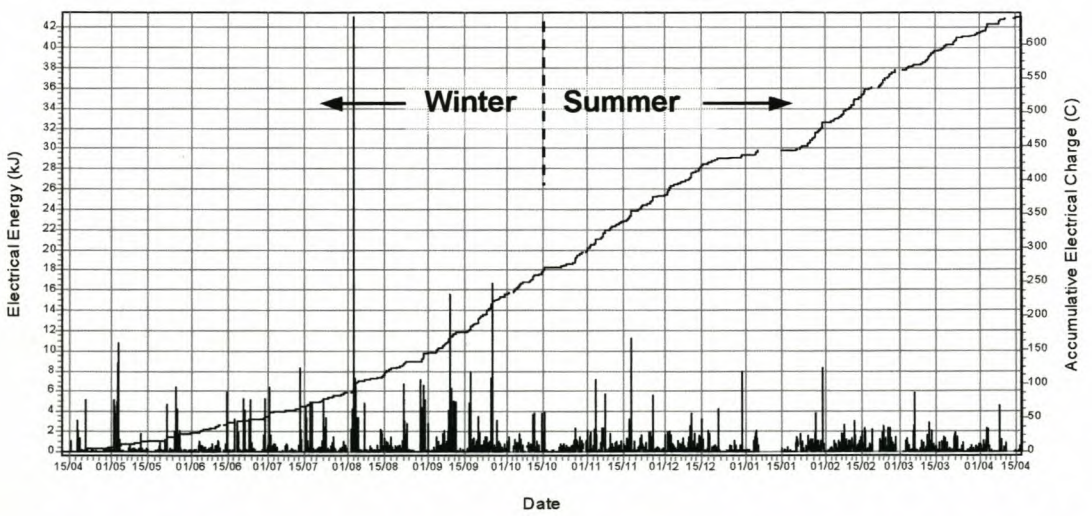

Figure 6. 13 Electrical energy and accumulative charge measurements on insulator 2E for both winter and summer test programme cycles.

6.1.3 Leakage current measurements on porcelain insulator 3P

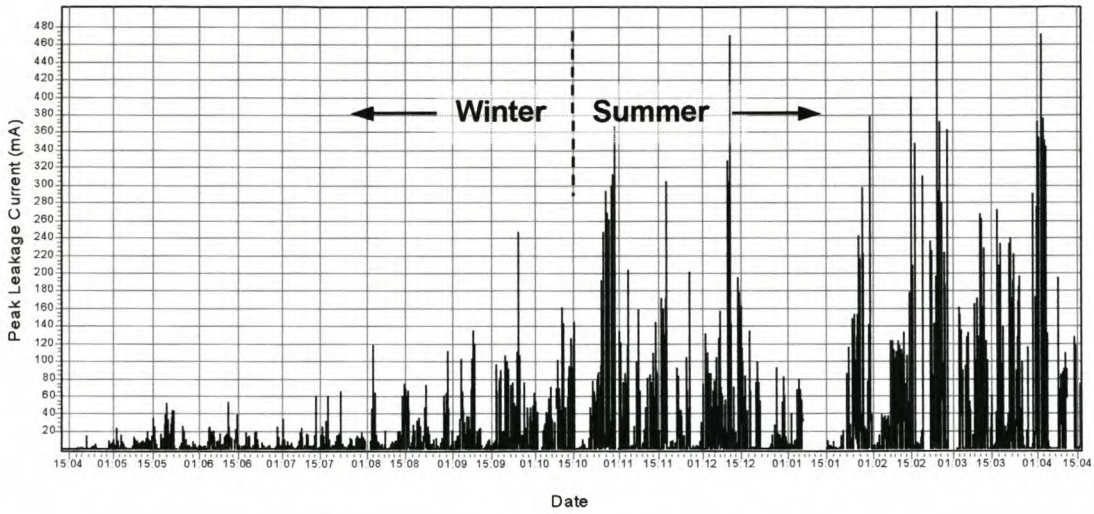

Figure 6. 14 Peak leakage current measurements on insulator 3P for both winter and summer test programme cycles.

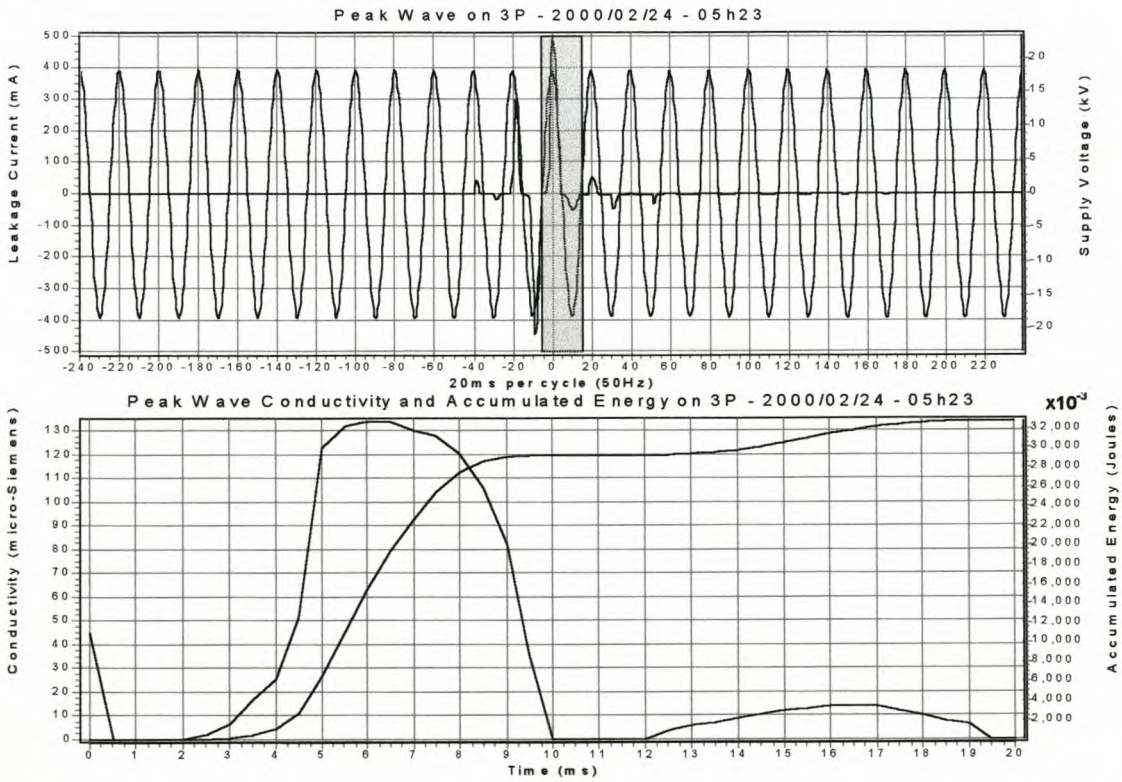

Figure 6. 15 Maximum daily peak leakage current and voltage waveform measured during the test period with associated conductivity and accumulated energy for the selected shaded area (20 ms cycle) for insulator 3P.

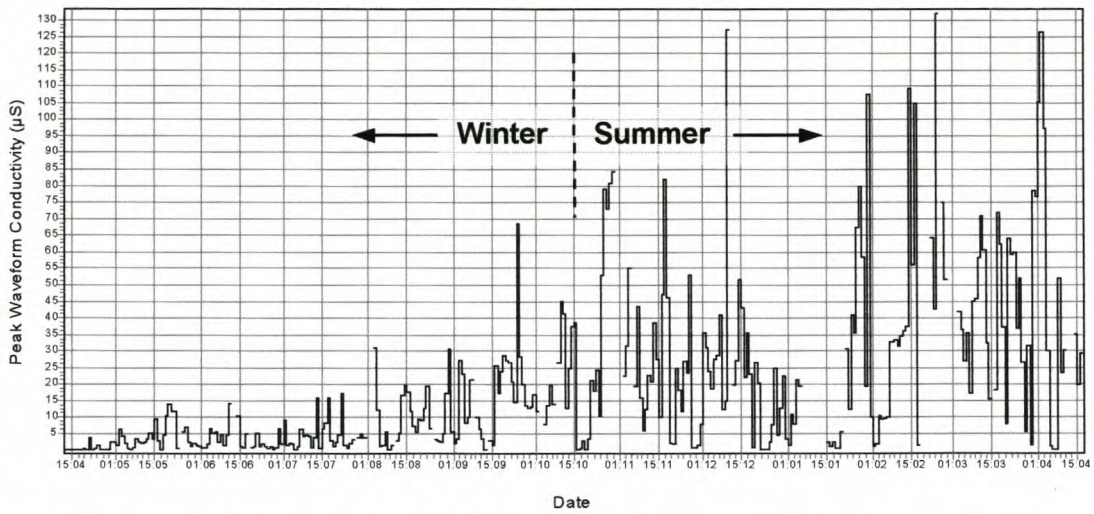

Figure 6. 16 Daily peak waveform conductivity measurements on insulator 3P for both winter and summer test programme cycles.

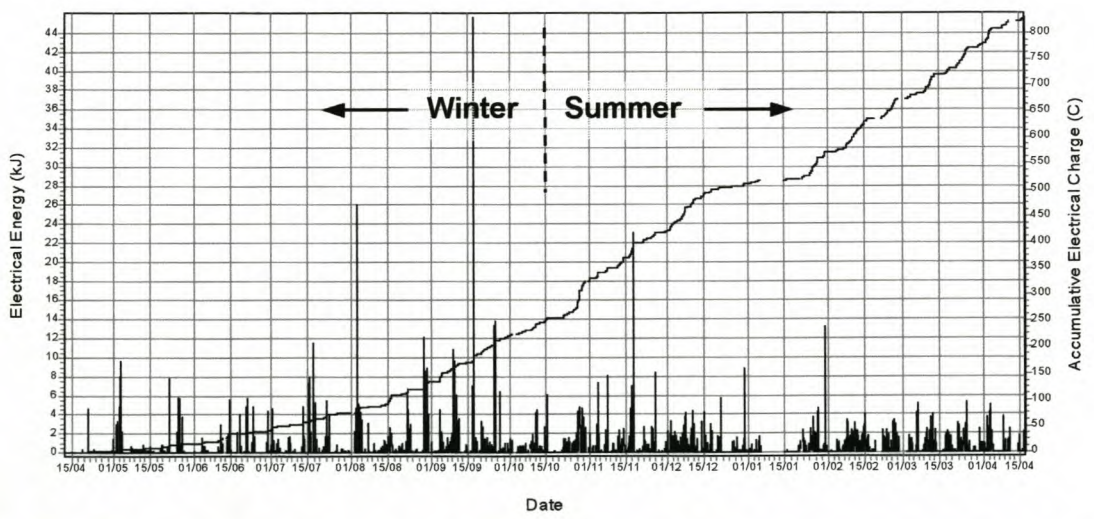

Figure 6. 17 Electrical energy and accumulative charge measurements on insulator 3P for both winter and summer test programme cycles.

6.1.4 Leakage current measurements on RTV SR coated porcelain insulator 4C

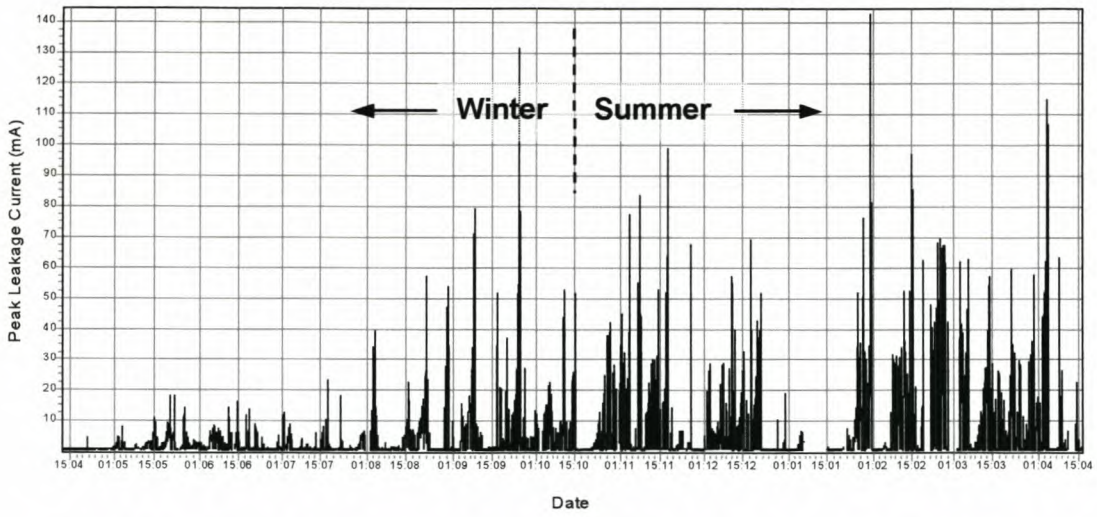

Figure 6. 18 Peak leakage current measurements on insulator 4C for both winter and summer test programme cycles.

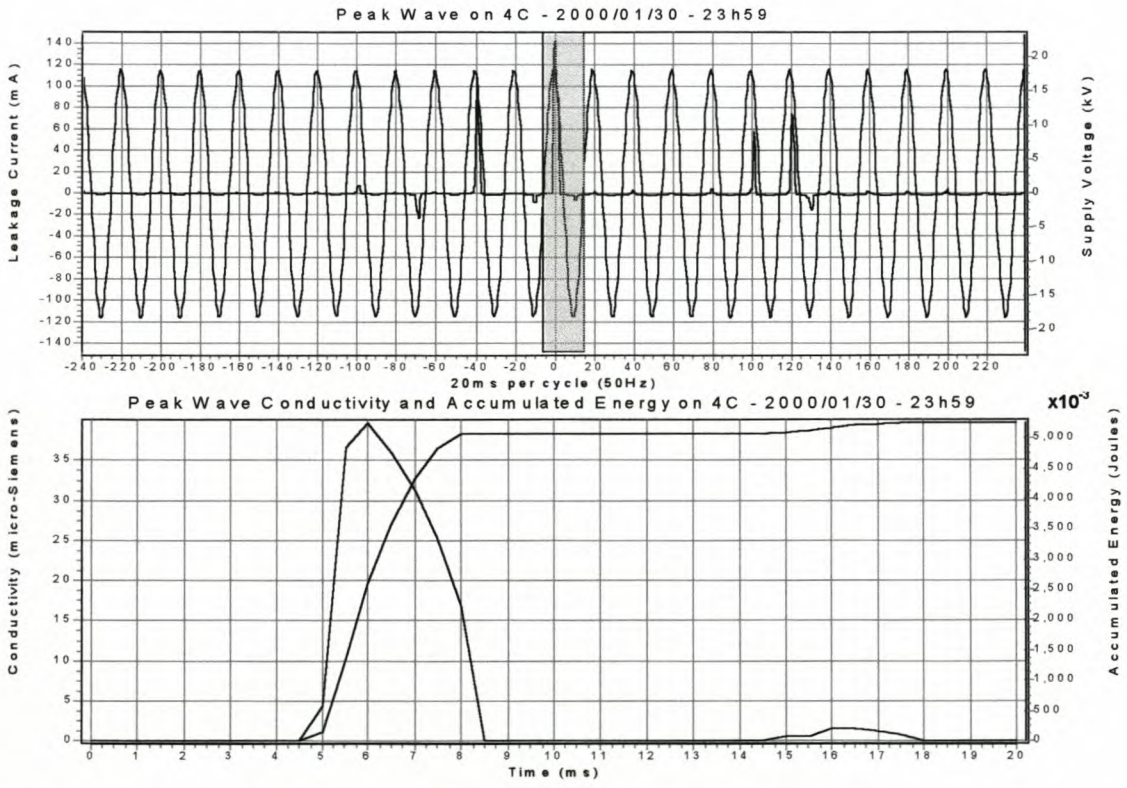

Figure 6. 19 Maximum daily peak leakage current and voltage waveform measured during the test period with associated conductivity and accumulated energy for the selected shaded area (20 ms cycle) for insulator 4C.

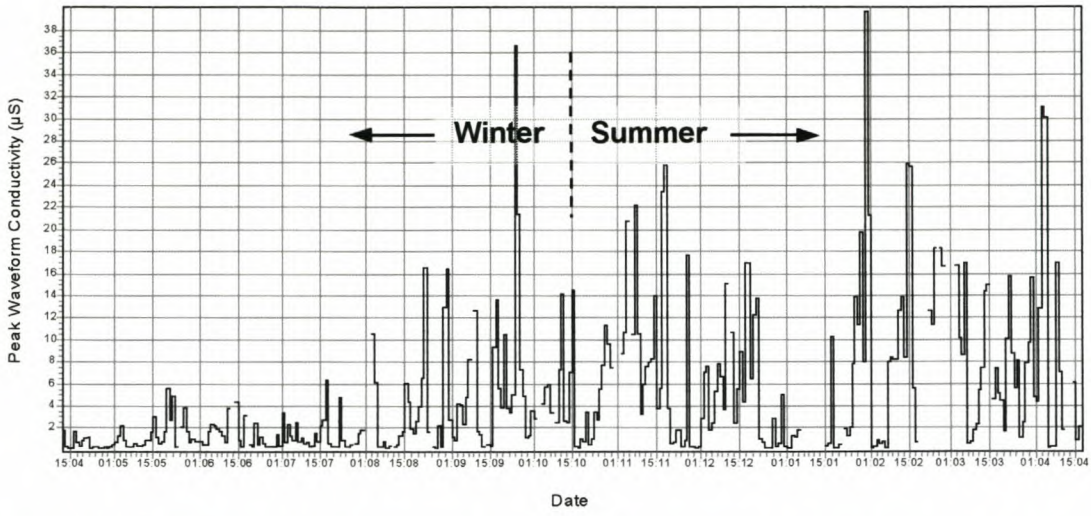

Figure 6. 20 Daily peak waveform conductivity measurements on insulator 4C for both winter and summer test programme cycles.

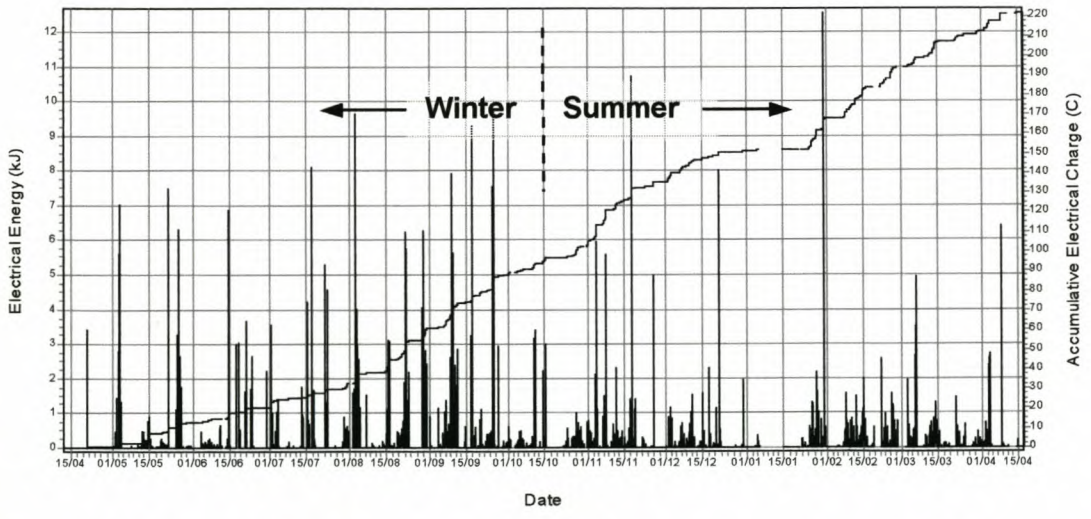

Figure 6. 21 Electrical energy and accumulative charge measurements on insulator 4C for both winter and summer test programme cycles.

6.1.5 Leakage current measurements on cyclo aliphatic insulator 5A

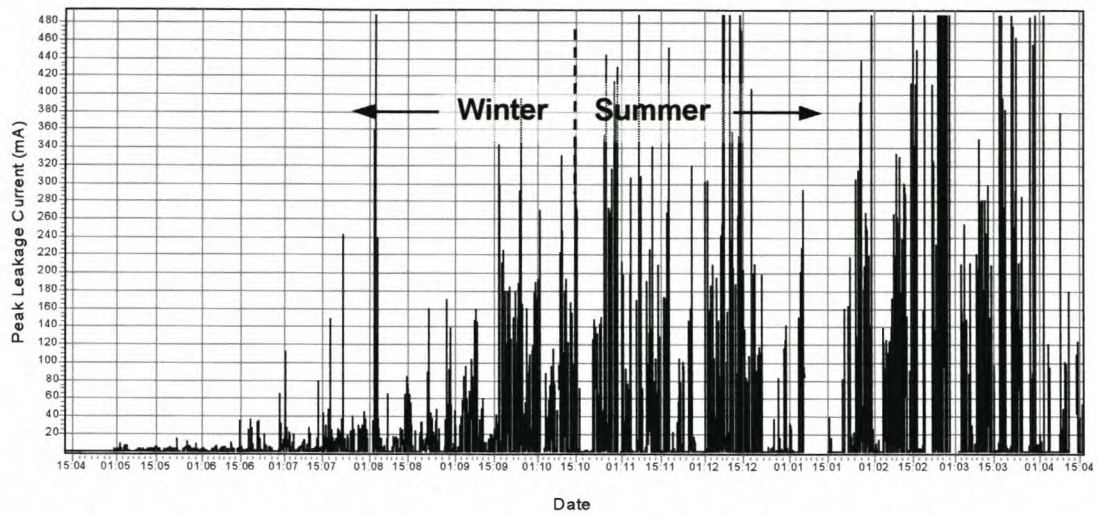

Figure 6. 22 Peak leakage current measurements on insulator 5A for both winter and summer test programme cycles.

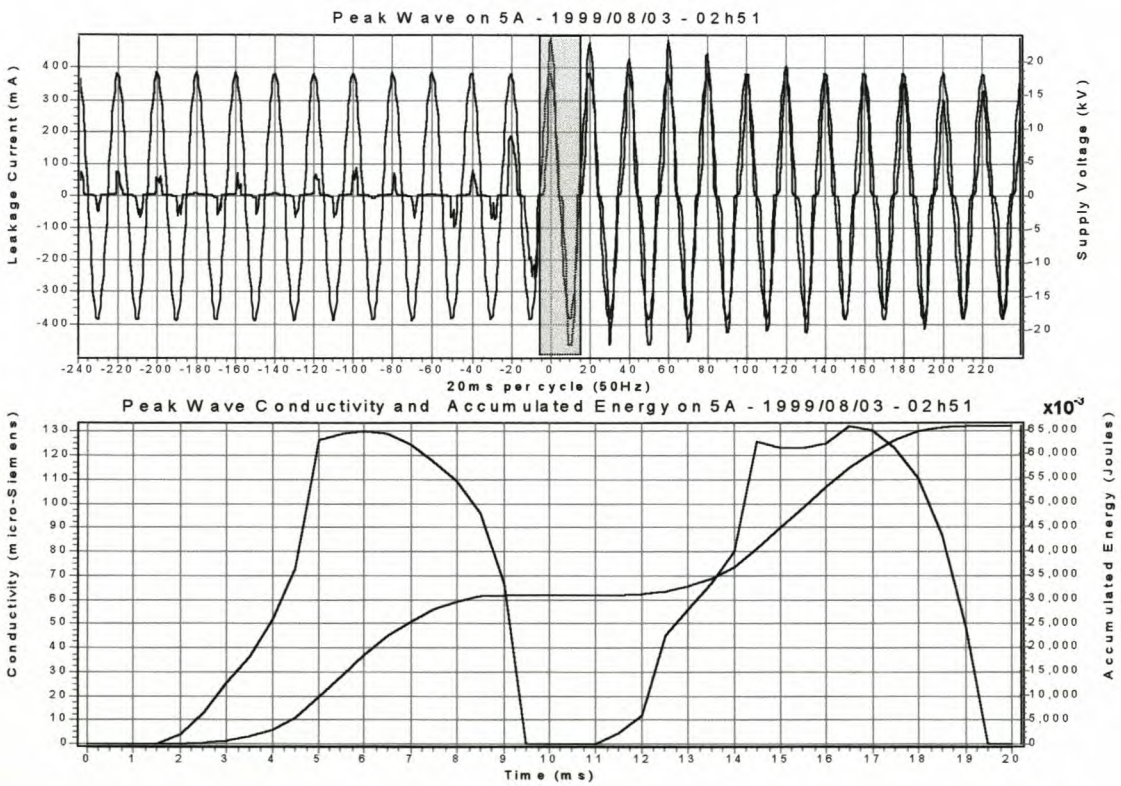

Figure 6. 23 Maximum daily peak leakage current and voltage waveform measured between 250 to 500 mA with associated conductivity and accumulated energy for the selected shaded area (20 ms cycle) is shown for insulator 5A.

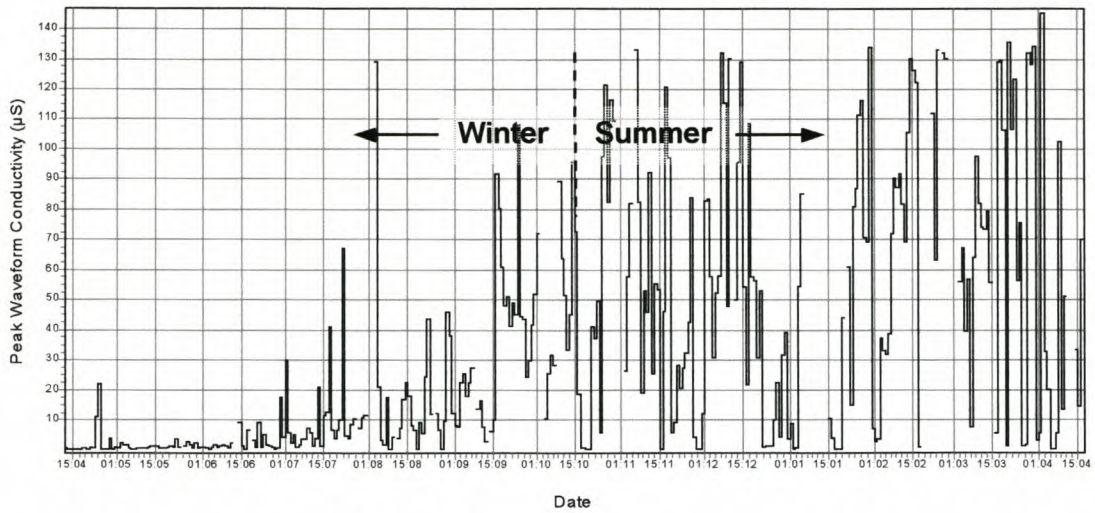

Figure 6. 24 Daily conductivity measurements, based on peak waveform, on insulator 5A for both winter and summer test programme cycles.

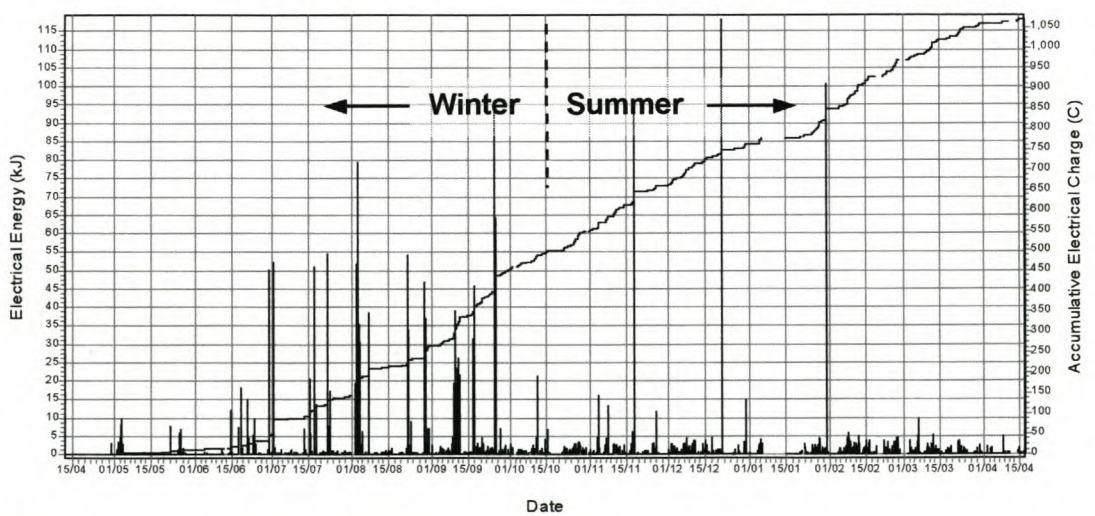

Figure 6. 25 Electrical energy and accumulative charge measurements on insulator 5A for both winter and summer test programme cycles.

6.1.6 Leakage current measurements on RG porcelain insulator 8R

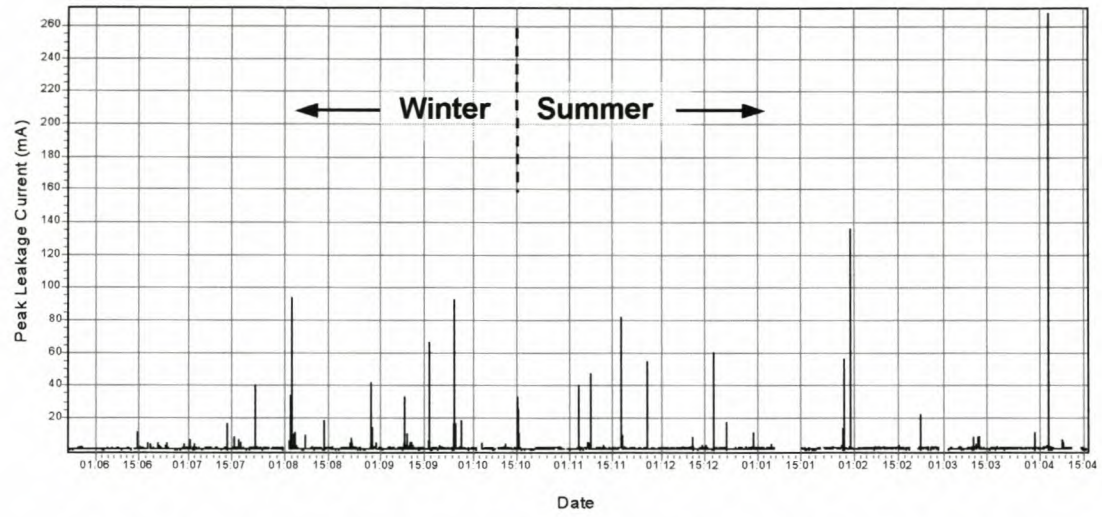

Figure 6. 26 Peak leakage current measurements on insulator 8R for both winter and summer test programme cycles.

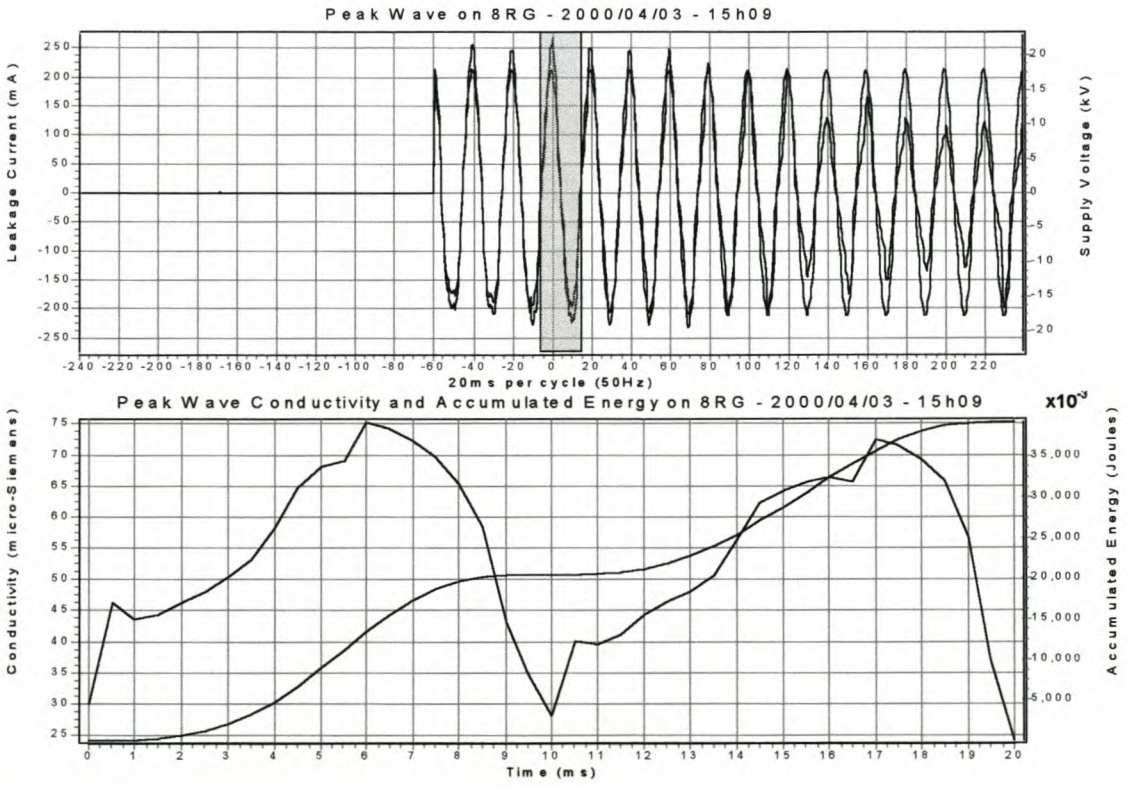

Figure 6. 27 Maximum daily peak leakage current and voltage waveform measured between 250 to 500 mA with associated conductivity and accumulated energy for the selected shaded area (20 ms cycle) is shown for insulator 8R.

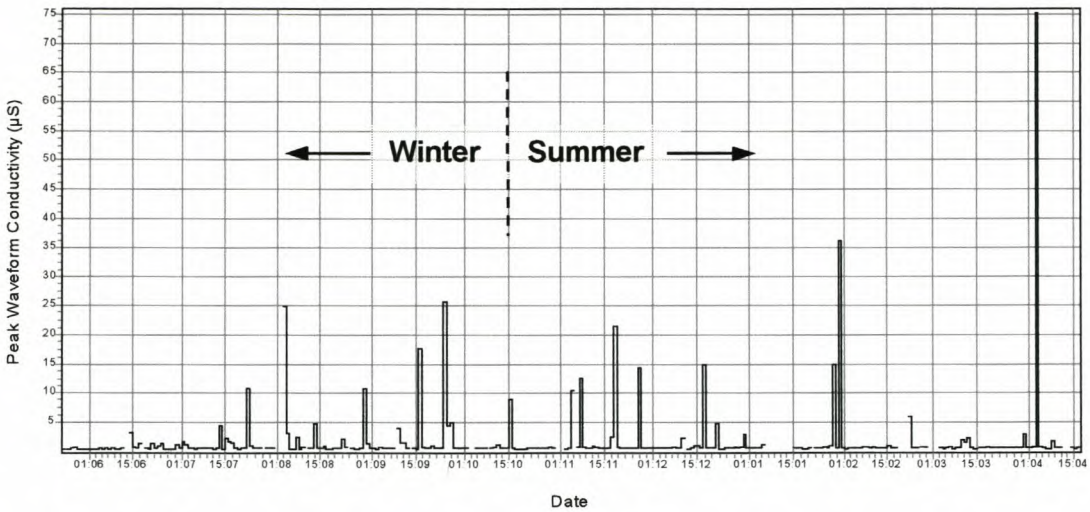

Figure 6. 28 Daily conductivity measurements, based on peak waveform, on insulator 8R for both winter and summer test programme cycles.

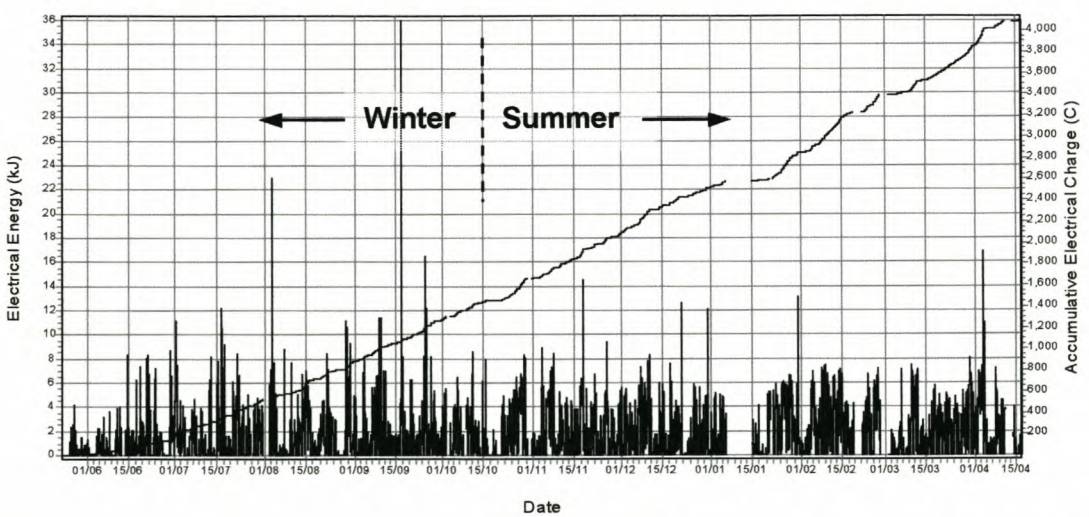

Figure 6. 29 Electrical energy and accumulative charge measurements on insulator 8R for both winter and summer test programme cycles.

6.2 ONE WEEK'S FOCUSED INSULATOR LEAKAGE CURRENT, ENVIRONMENTAL AND CLIMATIC CONDITION MEASUREMENTS

Due to the large volume of data recorded during the full test period it was decided to report only on a focused one-week section (although all the data was analysed). Week 24 (20/9/99 to 26/9/99) was chosen to focus on. It was almost midway through the test programme, the pollution build-up was very heavy, and it had also rained on some of the days so natural wetting and washing had taken place. Thus, week 24 was considered to be a fairly good representation of the events that occurred during the test programme.

The leakage current (only for insulator 3P), environmental and climatic measurements for week 24 are given below. The influence of the climatic and environmental parameters monitored on the leakage current measured for insulator 3P was investigated and is discussed.

The relative performances of the other test insulators 1S, 2E, 4C and 5A are compared at the end of this section. The resistive, glazed porcelain insulator (8R) is included in the leakage current comparison.

Leakage current measurements during week 24 on insulator 3P

The 10-minute leakage current measurements (peak leakage current, electrical energy, accumulated electrical charge) and daily peak waveform conductivity recorded in week 24 on insulator 3P is shown in Figure 6. 30 below.

Note: During day 5 (1999/09/24) a visual inspection was made on the test insulators, thus the voltage supply was de-energised between 08h20 and 13h50 and hence no leakage current measurements were recorded during this time.

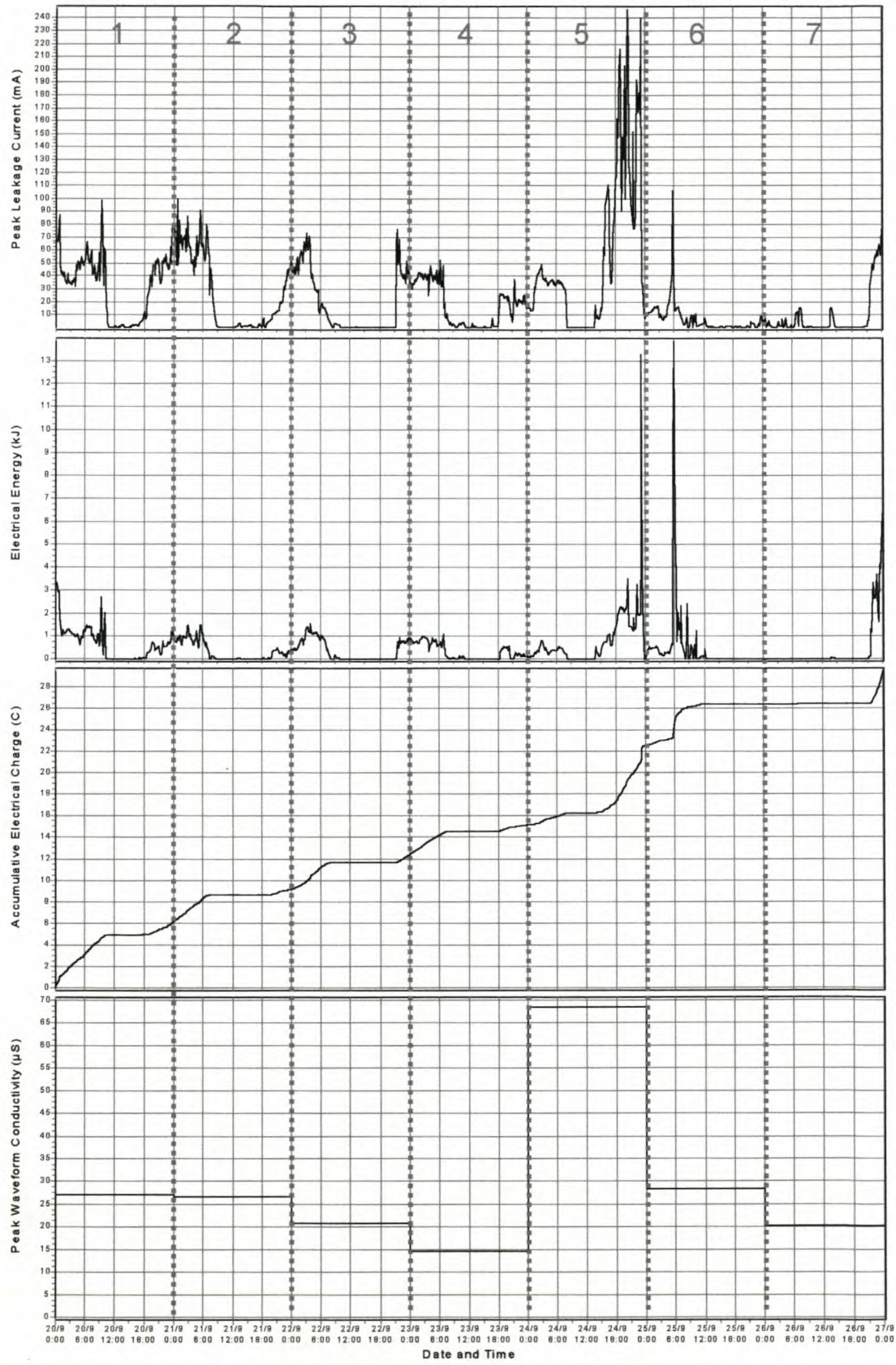

Figure 6. 30 Leakage current measurements on insulator 3P for week 24.

Environmental conditions measured on day 5 during week 24

- The six-weekly average DDG pollution measurements were exceptionally high (1336 μS/cm). The highest pollution emanated from the west (2178 μS/cm) and north (1707 μS/cm) and the lowest from the east (567 μS/cm). Note that the sea is situated on the western side of KIPTS and the land on the eastern side.
- The six-weekly ESDD pollution on a porcelain longrod was measured as heavy (0.16 mg/cm^2).
- The six-weekly NSDD pollution on a porcelain longrod was measured as very light (0.044 mg/cm^2).
- The LESDD on an energised SR insulator was very heavy (0.38 mg/cm^2). It was also very heavy on the EPDM insulator (0.37 mg/cm^2).

Climatic conditions measured during week 24

The daily weather for week 24 is summarised in Table 6. 1 below.

Table 6. 1 Table of daily weather summary for week 24.

Week	Date	Daily weather parameters												
		Rainfall	Relative Humidity (%)			Temperature (°C)			Wind speed (m/s) and Direction				UV-B (μW/cm^2)	
		(mm)	Ave	Max	Min	Ave	Max	Min	Ave	Max		Dominant	Ave	Max
24	1999/09/20	0.0	90	100	77	16.4	17.6	9.7	4.6	7.1	SW	SW	67	338
	1999/09/21	0.0	87	100	68	14.7	18.9	8.4	4.1	7.3	SW	SSE	76	317
	1999/09/22	0.0	89	100	64	14.9	21.6	7.1	3.5	6.4	SSW	SE	76	315
	1999/09/23	0.0	93	100	85	15.4	18.0	11.4	3.8	8.7	SSW	SW	79	329
	1999/09/24	2.0	90	100	79	16.5	18.9	13.0	6.8	12.1	NW	NW	63	353
	1999/09/25	5.7	87	100	71	14.2	17.0	7.4	6.8	12.4	W	SW	34	198
	1999/09/26	1.1	86	98	67	11.7	14.5	7.0	2.1	5.8	SSE	SSE	30	167

- It rained 2.0 mm on day 5, 5.7 mm on day 6 and 1.1 mm on day 7.
- The week was cool to moderate, with daily average humidity levels above 85%.
- The UV-B solar radiation had increased significantly since week 18, indicating the change in season from winter to summer.
- There was a strong north-westerly and westerly breeze on days 5 and 6.

The 10-minute climatic measurements (precipitation, relative humidity, UV-B solar radiation and ambient temperature) recorded in week 24 are plotted in Figure 6. 31 below.

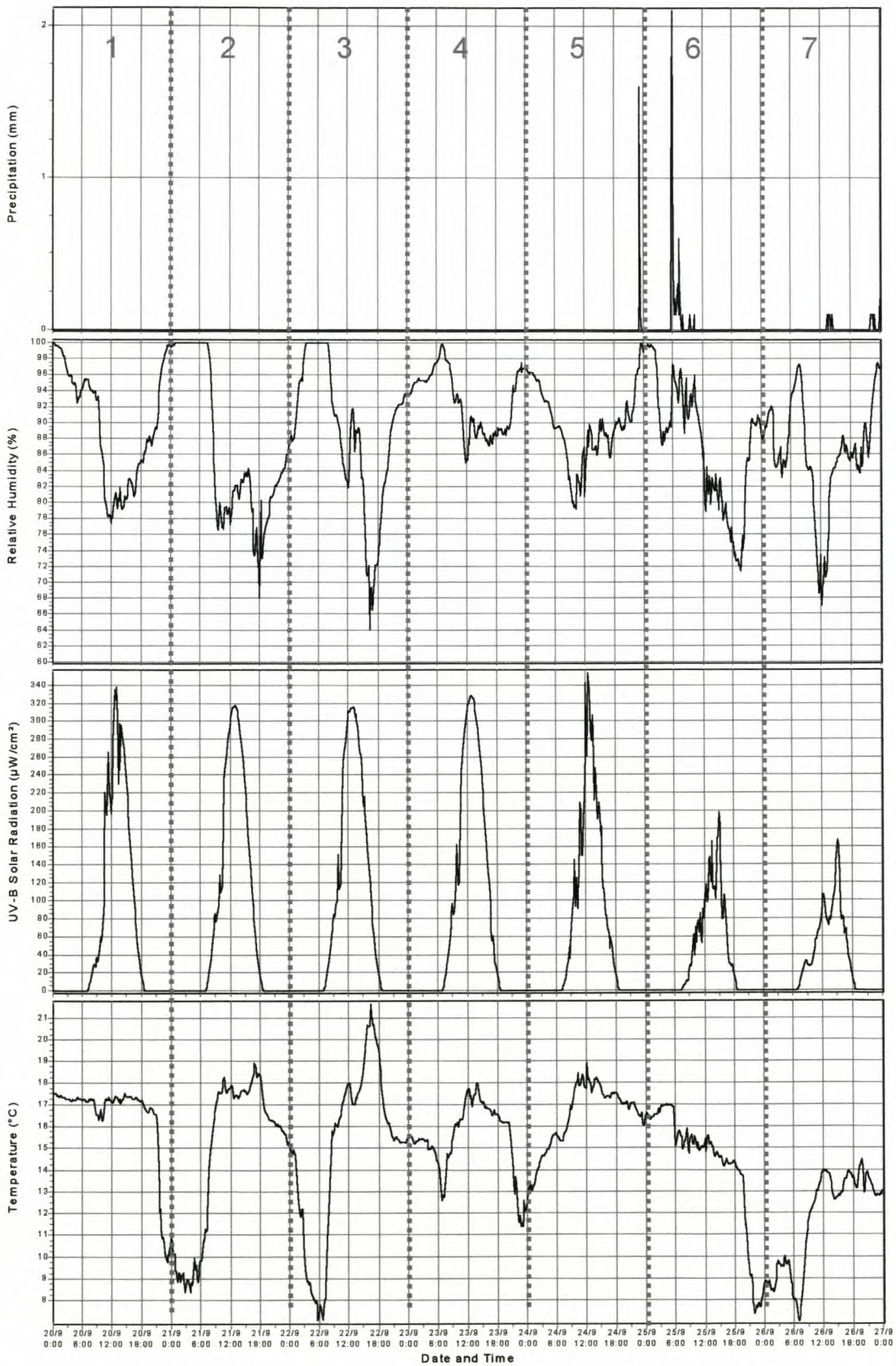

Figure 6. 31 Precipitation, relative humidity, UV-B solar radiation and ambient temperature measurements recorded during week 24.

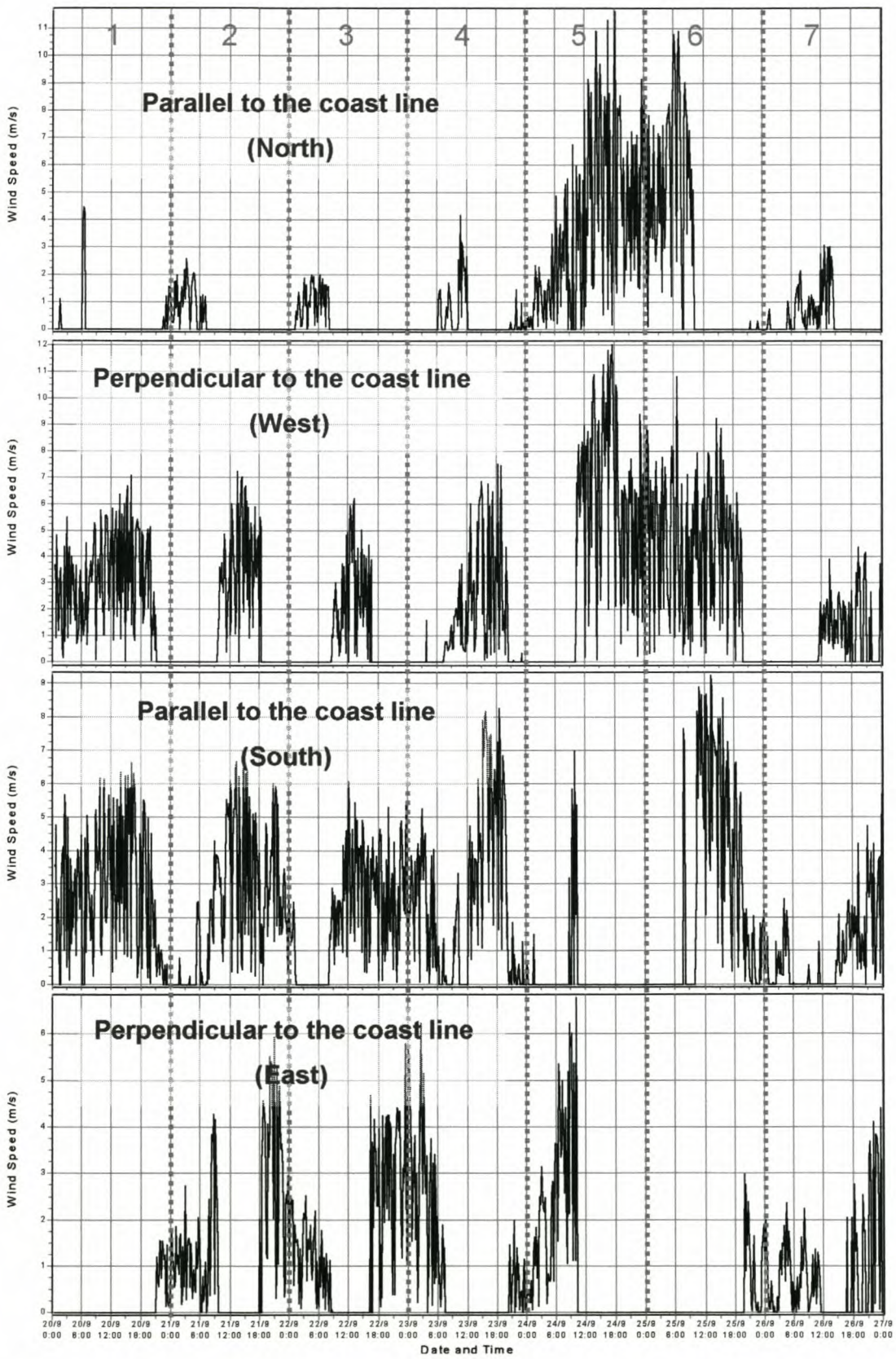

Figure 6. 32 Wind speed measurements recorded in week 24.

Discussion of the influence of the environmental and climatic parameters monitored on the leakage current measured for insulator 3P during week 24

The environmental, climatic and leakage current data given above for week 24 are discussed per day below focussing on pollution, wetting and washing events. It was decided to focus on the 10-minute peak leakage current (I_h) and the accumulated 10-minute energy values in relation to the climatic parameters.

To help with the analysis a daily cross correlation between the leakage current (I_h and energy) for insulator 3P and climatic parameters (temperature, humidity, UV-B, rainfall, and directional wind speed) was done for week 24 using the cross correlation statistical method as described in Appendix C7. Results are shown in Table 6. 2. The directional wind speed components used were calculated by using the statistical method described in Appendix C6. Note, positive values indicate a direct relationship and negative values an inverse relationship. Absolute values close to 100 show a very good correlation whereas a value close to 0 indicates virtually no correlation.

Table 6. 2: Cross correlation matrix of the leakage current for insulator 3P and climatic conditions monitored during week 24 in relation to one another.

		Cross correlation matrix (x100) for the leakage current and climatic conditions monitored in relation to one another								
		Temperature	Humidity	UV-B	Rainfall	Wind Speed	Wind Speed			
							340 (North)	70 (East)	160 (South)	250 (West)
1999/09/20	Ih	-38.2	84.4	-75.3	0.0	-60.8	23.8	24.3	-32.7	-44.3
	Energy	-3.1	78.7	-58.6	0.0	-26.0	17.9	-3.0	-13.4	-21.1
1999/09/21	Ih	-93.2	88.3	-58.3	0.0	-83.0	62.3	0.9	-63.6	-53.9
	Energy	-90.8	79.7	-53.1	0.0	-64.6	66.6	7.8	-52.4	-48.9
1999/09/22	Ih	-51.9	49.2	-52.9	0.0	-36.0	29.2	35.2	-39.7	-41.8
	Energy	-81.2	68.1	-55.1	0.0	-49.4	62.7	21.8	-53.3	-43.6
1999/09/23	Ih	-47.1	54.6	-68.8	0.0	-13.8	-24.5	68.8	-11.1	-44.9
	Energy	-28.5	48.3	-58.1	0.0	1.7	-21.3	77.4	0.8	-40.8
1999/09/24	Ih	5.2	35.3	-46.5	23.6	19.1	21.4	-30.8	-18.3	23.7
	Energy	4.7	34.2	-31.2	81.2	20.2	12.8	-24.0	-12.7	24.8
1999/09/25	Ih	32.8	40.3	-29.3	48.4	27.4	45.6	-13.4	-36.0	25.5
	Energy	16.0	27.7	-17.0	93.1	32.8	42.9	-10.0	-21.0	19.4
1999/09/26	Ih	12.6	44.1	-24.3	47.1	56.1	-9.6	36.3	48.4	-3.9
	Energy	17.6	38.3	-21.9	50.3	53.4	-16.4	32.0	48.3	1.8

- During the first 4 days of week 24, the dominant winds were mainly from the south-west and south-east. These winds do not normally blow saline pollution onto the insulators. However, the insulators were probably already contaminated before the start of the week. The highest leakage current activity was associated with periods when the north winds blew, which brought moisture onto the insulator surface and,

together with the high humidity levels at night, produced peak leakage currents of up to 80 mA on the porcelain test insulator 3P. This is in line with the classic insulator pre-deposit pollution and wetting process. Without any rain during these 4 days the pollution process was not disturbed by any major washing effect. However, seepage of pollution could have occurred during the periods of high humidity as a daily reduction in peak wave conductivity is noted on test insulator 3P.

- During day 5 a dominant north-westerly wind was blowing from the sea resulting in the depositing of saline pollution and moisture onto the insulator surface. The speed of this wind was very high, up to 6.8 m/s average and up to 12 m/s maximum was measured. Towards the end of day 5 the relative humidity increased, and when it reached approximately 90% the leakage current rapidly increased to about 200 mA. With a further increase of humidity a current of 250 mA was observed. At the end of the day it started to rain lightly, which increased the amount of water on the surface, which probably helped dissolve the surface pollution, and a current pulse of 230 mA was observed. It seemed as if the rain and very high humidity at the end of day 5 led to intensive washing of the porcelain insulator 3P. Therefore, a leakage current level of only 20 mA was observed in the beginning of day 6 (lower than the early morning values of previous days).
- More saline pollution was blown from the sea at the beginning of day 6 (the same winds were dominating). As most of the 'old' salt had already been washed off the leakage current was initially only in the order of 20 mA. Then when, around 06.00, a stronger north-westerly wind seemed to blow in more saline pollution and rain, increasing the humidity levels and producing more critical wetting, a high current pulse of 110 mA was observed. Then the rain naturally washed the test insulator 3P and the leakage current reduced again. Because the rain intensity was higher during day 6 than during day 5, and because part of the saline pollution had already been washed off at the end of day 5, the insulator was almost washed clean. Later during day 6 the wind changed direction to mostly south and south-west, the humidity reduced and the currents went down to levels below 10 mA.
- Even when the humidity went up once more during the beginning of day 7, the levels of currents were still below 10 mA as the insulator was still relatively clean. However, the winds were dominant from the land (south-south-east) during the afternoon, depositing industrial pollution on the test insulators, which resulted in an increase in leakage current levels at the end of day 7.

Wetting due to high (over 90%) relative humidity and light rain (max 1.5 – 2 mm/10 min.) is a good combination to produce large peaks of leakage currents (in our case up to 250 mA). However, especially for porcelain insulators, the rain combined with very high humidity produces strong natural washing, which removes most of the saline pollution deposition after the short pollution event. For porcelain insulators relative humidity and wind speed have a large effect on I_h values. Rainfall has the largest effect on energy.

Comparison of the daily performances of the test insulators in relation to one another during week 24

In the previous sections the leakage current performance of the porcelain test insulator 3P was discussed in relation to the environmental and climatic conditions monitored. In this section the daily relative performances of the other test insulators 1S, 2E, 4C, 5A and 8R are compared in relation to the porcelain insulator 3P.

The daily peak wave conductivity measurements shown in Figure 6. 33 below are used as an indicator of the maximum interaction of the insulator material surface with the deposited pollution and wetting. The process can be complex, as any one or combination of the three (material, pollution, wetting) could play a role in the final conductivity value. However, the test insulators are all exposed to the exact same environment and climate and as the designs and especially profiles are the same it is assumed the differences measured are mainly due to the material properties. The porcelain test insulator 3P is treated as the reference insulator.

From the table in Figure 6. 33 it can be seen that test insulator 5A always had the highest daily peak wave conductivity. Test insulator 8R always had the lowest daily peak wave conductivity and on average an order class lower when compared to insulator 5A. Test insulator 4C followed the performance of insulator 8R, with higher daily peak wave conductivity values, however always lower than the other test insulators. The peak waveform conductivity performance of test insulators 1S, 2E and 3P varied from day to day. However, when comparing these three test insulators, on average the test insulator 1S showed the lowest peak waveform conductivity value and 2E the highest.

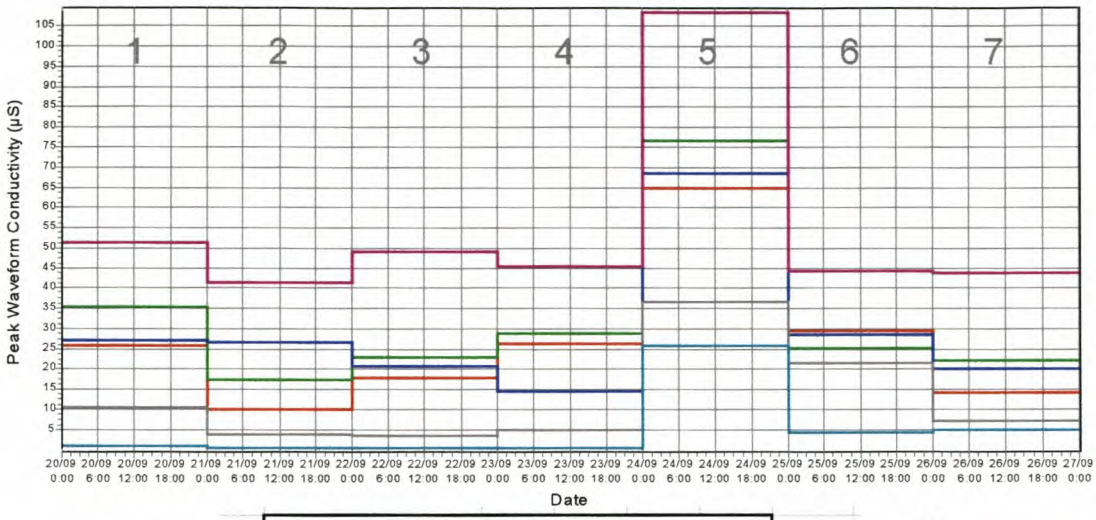

	Daily Peak Wave Conductivity							
	1	2	3	4	5	6	7	Average
1S	25.7	10.0	17.8	26.2	64.9	29.4	14.3	**26.9**
2E	35.4	17.4	23.1	28.9	76.7	25.2	22.0	**32.7**
3P	27.2	26.6	20.8	14.6	68.6	28.5	20.2	**29.5**
4C	10.5	3.8	3.8	5.5	36.2	21.4	7.3	**12.6**
5A	51.3	41.6	49.1	45.4	108.5	44.5	44.6	**55.0**
8R	1.0	0.3	0.3	0.3	24.8	4.2	5.0	**5.1**

Figure 6. 33 Daily peak waveform conductivity measurements on insulators 1S, 2E, 3P, 4C, 5A and 8R for week 24.

The test insulators' critical flashover voltage levels were calculated using equations (1.13) and (1.16). The results are plotted (see Figure 6. 34) below using the statistical technique as described in Appendix C4. The 90% withstand probability (also known as the 10% flashover probability, U_{10}) and the lowest critical flashover voltage is also shown for the test insulators.

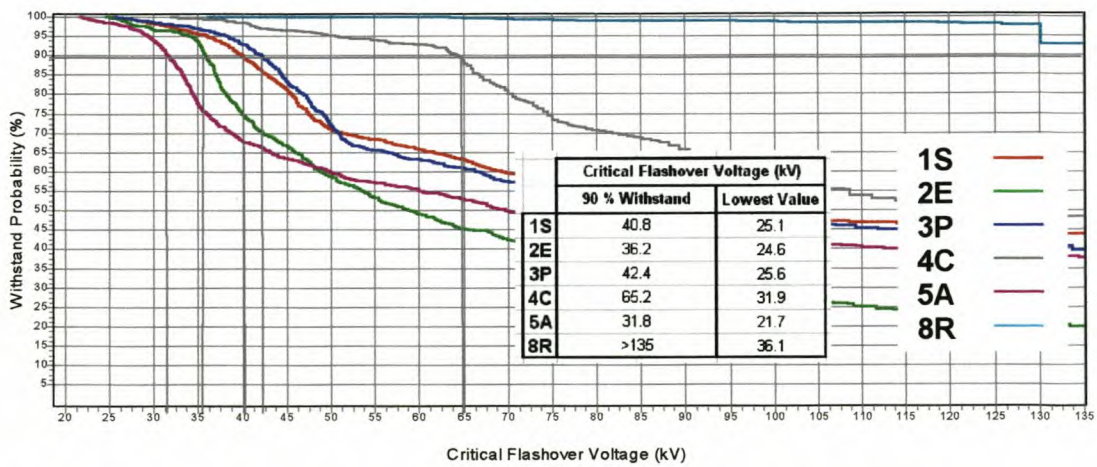

	Critical Flashover Voltage (kV)	
	90 % Withstand	Lowest Value
1S	40.8	25.1
2E	36.2	24.6
3P	42.4	25.6
4C	65.2	31.9
5A	31.8	21.7
8R	>135	36.1

Figure 6. 34 Probability of critical flashover voltage calculation results on insulators 1S, 2E, 3P, 4C, 5A and 8R for week 24.

The 90% withstand calculated critical flashover voltage for test insulator 8R is determined as >135 kV, which is larger than the external air flashover voltage. The lowest critical flashover voltage calculated for insulator 8R was 36.1 kV, which is well above the maximum supply voltage of 20 kV (phase-to-ground, peak). Insulator 8R had the lowest risk of flashover of all the test insulators during week 24.

Insulator 4C showed the next best performance with a 90% withstand voltage of 65.2 kV and a lowest critical flashover voltage of 31.9 kV.

Test insulator 5A had the worst 90% withstand voltage of 31.8 kV and the lowest critical flashover voltage of 21.7 kV, which is just above the maximum supply voltage. Insulator 5A had the highest risk of flashover of all the test insulators during week 24.

Test insulators 1S, 2E and 3P had similar 90% withstand and lowest critical flashover voltages. However, test insulator 2E was slightly lower (worse) than the other two.

The accumulated electrical charge flowing over the insulator surface is used as an indicator of the continuous interaction of the insulator material surface with the deposited pollution and wetting. For the same reasons as explained before (same environment and climate and same designs and profiles) it is assumed that the differences in accumulated electrical charge measured are mainly due to the material properties. Porcelain test insulator 3P is treated as the stable reference insulator.

The accumulative electrical charge measurements on insulator 1S, 2E, 3P, 4C, 5A and 8R for week 24 are shown in Figure 6. 35 below. The daily increase in accumulated electrical charge is also given, in the associated table.

It should be noted that test insulator 8R has a resistive/semiconductive-glazed surface, which results in a 50 Hz leakage current and permanent electrical charge dissipation. Higher values of accumulated electrical charge are thus expected on insulator 8R. However, when a parallel electrolytic pollution layer is present on the insulator surface an increase in the accumulated electrical charge should be seen.

As expected test insulator 8R had the highest daily (except on day 6) and overall accumulated electrical charge measured. However, on day 6 (1999/09/25) insulator 5A had the highest daily-accumulated electrical charge value.

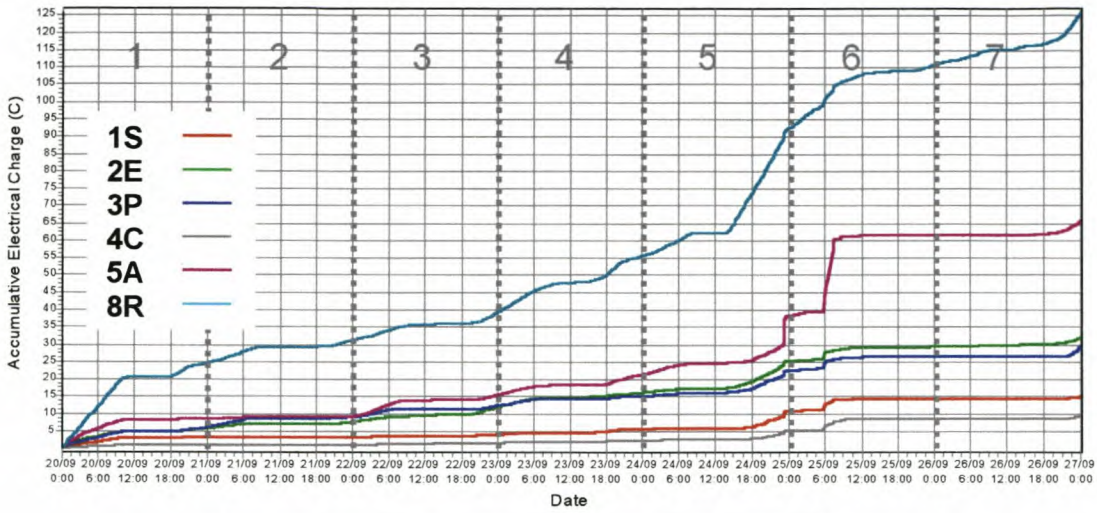

	Daily increase in Accumulative Charge							
	1	2	3	4	5	6	7	Total
1S	3.4	0.1	0.6	1.6	5.2	3.5	0.8	**15.3**
2E	6.1	1.9	4.4	3.0	10.1	4.2	2.7	**32.3**
3P	6.4	3.0	3.3	3.8	6.3	3.9	3.0	**29.6**
4C	1.2	0.0	0.7	0.6	2.9	3.3	0.9	**9.5**
5A	8.7	0.8	6.4	5.8	16.8	23.3	4.4	**66.2**
8R	24.5	7.2	8.1	16.3	36.9	18.3	15.0	**126.2**

Figure 6. 35 Accumulative electrical charge measurements on insulator 1S, 2E, 3P, 4C, 5A and 8R for week 24.

In relation to the porcelain reference test insulator 3P, the silicone rubber based test insulators 1S and 4C showed a lower daily and total accumulated electrical charge values.

The EPDM test insulator 2E showed a slightly higher total accumulated electrical charge value than the reference porcelain insulator 3P. However, on some days (days 1, 2, 4, and 7), its daily-accumulated electrical charge value was lower than the porcelain reference insulator 3P.

The cyclo aliphatic test insulator 5A showed a higher total accumulated electrical charge value when compared to the other test insulators 1S, 2E, 3P, and 4C. However, on day 2 (1999/09/21) the daily-accumulated electrical charge value was lower than 2E and 3P.

6.3 CORRELATION BETWEEN LEAKAGE CURRENT AND CLIMATIC PARAMETERS MEASURED

Due to the volume of leakage current and climatic data collected over the test period of one year, it was difficult to relate the various parameters by visual comparison of the graphically displayed data. It could only be done for smaller selections (see section 6.2 for a one week comparison). It was then decided to focus on the 10-minute peak leakage current (I_h) and the accumulated 10-minute energy values in relation to the climatic parameters. As discussed in section 6.1, using a combination of the peak and the energy values is considered to be the best way to describe the leakage-current waveform.

Cross correlation between the leakage current (I_h and energy) and climatic parameters (temperature, humidity, UV-B solar radiation, rainfall, and directional wind speed) was done using the cross correlation statistical method as described in Appendix C7. Results are shown in Table 6. 3. The directional wind speed components used were calculated by using the statistical method described in Appendix C6. Note, positive values indicate a direct relationship and negative values an inverse relationship. Absolute values close to 100 show a very good correlation whereas a value close to 0 indicates virtually no correlation.

The following were observed from the correlation results (Table 6. 3):

- Relative humidity and solar radiation have a greater influence on the I_h value than on the energy, for all the insulators except 8R.
- Rainfall has a greater influence on the energy than on the I_h value, for all the insulators except 8R.
- Wind speed has a greater influence on the energy than on the I_h value, for all the insulators. The speed of the northerly wind has an influence throughout the year and that of the westerly only in winter.
- Rainfall has the greatest influence of all the climatic parameters monitored.

Why is the resistive glazed porcelain insulator 8R different from the others?

Table 6. 3: Cross correlation matrix of the leakage current and climatic conditions monitored in relation to one another.

			Cross correlation matrix (x100) for the leakage current and climatic conditions monitored in relation to one another								
			Temperature	Humidity	UV-B	Rainfall	Wind Speed	Wind Speed			
								340 (North)	70 (East)	160 (South)	250 (West)
Winter	1S	Ih	-6.3	17.3	-17.5	3.1	6.8	2.5	-0.4	2.9	4.6
		Energy	-2.5	10.1	-8.2	48.5	26.2	17.4	-4.8	2.8	21.2
	2E	Ih	-12.1	23.8	-21.7	1.1	3.5	0.4	0.3	2.2	1.9
		Energy	-5.0	12.9	-10.3	43.0	23.2	14.8	-4.5	3.2	18.4
	3P	Ih	-7.6	17.2	-17.3	4.6	7.9	4.6	1.0	1.3	4.6
		Energy	-4.6	13.3	-10.1	41.6	22.0	13.4	-2.4	3.2	16.9
	4C	Ih	-3.5	15.3	-9.6	9.4	10.9	4.4	-5.3	4.4	11.2
		Energy	-2.4	9.4	-6.0	53.6	20.5	13.4	-4.8	3.5	16.2
	5A	Ih	-11.1	12.1	-15.7	3.6	8.6	3.3	2.3	4.1	3.9
		Energy	-4.3	6.6	-5.9	44.1	24.0	17.0	-3.3	1.8	17.9
	8R	Ih	-7.4	13.9	-8.5	34.5	15.1	11.2	-3.3	2.3	11.5
		Energy	-12.7	30.5	-21.1	27.6	32.4	21.1	0.2	6.7	22.0
Summer	1S	Ih	-21.3	35.8	-30.0	2.7	-6.6	6.8	2.5	-7.9	-7.0
		Energy	-14.2	28.1	-18.7	31.8	8.0	16.8	-2.1	-2.4	7.1
	2E	Ih	-27.9	45.7	-35.7	3.4	-14.6	12.2	-1.8	-15.6	-9.3
		Energy	-21.2	38.0	-27.0	24.3	0.0	16.7	-2.7	-7.6	1.9
	3P	Ih	-24.0	35.6	-33.4	2.9	-12.3	5.0	2.6	-10.3	-11.4
		Energy	-19.8	34.5	-30.2	22.5	3.9	12.1	5.4	-2.5	-2.4
	4C	Ih	-23.2	38.2	-28.8	9.3	-7.7	11.0	-1.1	-10.0	-5.2
		Energy	-12.9	23.4	-15.7	48.4	3.9	6.0	-2.9	-5.0	4.9
	5A	Ih	-20.8	34.1	-31.9	3.1	-9.5	2.4	3.7	-7.4	-10.4
		Energy	-9.4	17.9	-13.5	68.5	4.2	14.7	0.7	-3.9	1.4
	8R	Ih	-6.6	10.7	-6.3	26.4	2.3	11.5	-1.2	-3.0	1.5
		Energy	-21.4	40.2	-32.0	11.3	10.7	10.5	7.2	2.3	1.0
Full Year	1S	Ih	-4.3	21.4	-20.1	0.6	0.9	-0.8	2.8	0.9	-2.4
		Energy	-4.6	16.1	-11.3	41.9	18.8	15.1	-3.0	1.2	14.7
	2E	Ih	-10.0	29.6	-25.0	0.1	-4.5	0.9	0.2	-4.4	-4.2
		Energy	-7.1	21.4	-16.0	34.7	13.7	12.4	-2.8	-0.4	10.6
	3P	Ih	-3.0	18.7	-20.8	0.1	-2.5	-3.0	4.0	0.1	-5.8
		Energy	-3.8	18.5	-17.4	29.3	14.5	7.5	3.3	3.9	6.7
	4C	Ih	-3.6	21.6	-17.2	4.4	1.5	0.9	-0.5	0.2	0.7
		Energy	-4.7	14.6	-10.0	46.3	13.0	12.1	-3.5	-0.2	10.5
	5A	Ih	-3.9	18.2	-20.6	0.5	-0.5	-3.2	4.8	1.9	-5.1
		Energy	-4.8	10.5	-8.5	45.2	15.6	14.9	-1.8	-0.5	10.9
	8R	Ih	-4.6	10.3	-5.7	22.2	6.3	8.5	-1.6	-0.9	4.5
		Energy	-7.7	31.0	-22.5	17.0	20.8	10.3	5.8	8.0	10.0

6.4 COMPARATIVE ANALYSIS OF THE INSULATOR LEAKAGE CURRENT MEASUREMENTS

In this section the leakage current results measured and reported in section 6.1 are used to compare the relative performances of the energised test insulators 1S, 2E, 3P, 4C, 5A and 8R.

When inspecting the leakage current results measured, differences in performance between the various test insulators can be seen in the graphically displayed data. Statistical methods were used to emphasize these differences and results are reported below. The leakage current data, continuously sampled at 2 kHz, were rendered into 10-minute intervals, which were then used for analysis. The one-year test cycle was divided into a winter (medium pollution) and a summer (heavy pollution) test period.

6.4.1 Time-of-day trends of the average peak leakage currents

Differences in performance can be seen when comparing the peak leakage current plots shown in sections 6.1.1 to 6.1.6. However, when plotted on one graph (for the purpose of comparison), the volume of data makes the graph incomprehensible. The use of Scatter plots comparing the peak leakage current performance was tried, with no success. When zooming into a period of one day, or even one week, the information becomes more comprehensible. However, comparing the performance of the test insulators per day, per 10-minute interval, was found to be impractical. A daily peak leakage current pattern was noted (see Figure 6. 30) and the idea of using 10-minute average time-of-day plots (as discussed in Appendix C3) emerged.

The 10-minute average time-of-day plots for winter, summer and the full year are shown in Figure 6. 36. The time-of-day plots for the winter, summer and full year were compared during the early morning, midday and late evening. The 10-minute average time-of-day peak leakage current values are tabulated for comparison in Table 6. 4, for these times of day (early morning, midday, and late evening), and per season (winter, summer and full year).

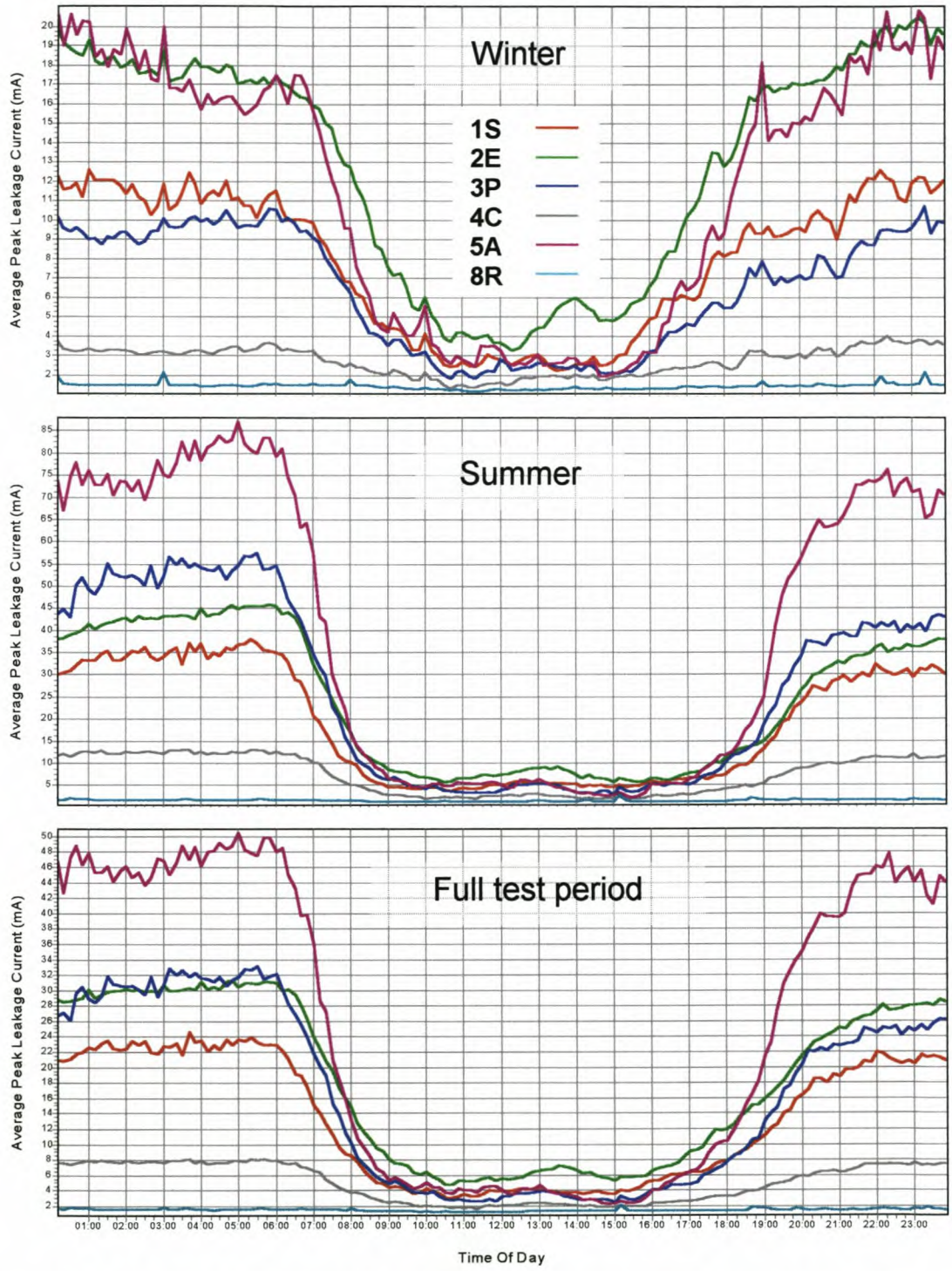

Figure 6. 36 Time-of-day trends of the 10-minute average peak leakage current measurements on insulators 1S, 2E, 3P, 4C, 5A and 8R for the winter, summer and the full test period.

Table 6. 4 Table showing the 10-minute average time-of-day peak leakage current measurements at 4h00, 12h00 and 22h00, for winter, summer and the full year. The average column value is those 3 values averaged.

		Morning (4h00)	Midday (12h00)	Evening (22h00)	Average
Winter	1S	10.9	2.8	12.1	**8.6**
	2E	18.0	3.7	19.1	**13.6**
	3P	9.9	2.8	8.8	**7.2**
	4C	3.3	1.6	3.7	**2.9**
	5A	15.8	3.3	19.9	**13.0**
	8R	1.5	1.3	1.5	**1.4**
Summer	1S	36.8	5.1	32.4	**24.7**
	2E	44.8	7.6	36.1	**29.5**
	3P	54.2	3.9	40.9	**33.0**
	4C	12.6	2.6	11.4	**8.9**
	5A	78.0	4.7	73.6	**52.1**
	8R	1.7	1.3	1.6	**1.5**
Full year	1S	23.8	3.9	22.2	**16.7**
	2E	31.4	5.6	27.6	**21.5**
	3P	32.0	3.3	24.8	**20.1**
	4C	7.9	2.1	7.5	**5.9**
	5A	46.9	4.0	46.7	**32.5**
	8R	1.6	1.3	1.5	**1.5**

The ranking of the energised test insulators based on the calculated 10-minute average time-of-day peak leakage current values in Table 6. 4 are given below from low to high as:

Winter : (Low) 8R, 4C, 3P, 1S, 5A and 2E (High)

Summer : (Low) 8R, 4C, 1S, 2E, 3P and 5A (High)

Full Year : (Low) 8R, 4C, 1S, 3P, 2E and 5A (High)

Looking at the full year's data, lower currents were observed on the RG and SR test insulators 8R, 4C and 1S.

6.4.2 Peak leakage current bin counts between set values, first occurrence and maximum value

The daily peak leakage current bin count plots between set values are shown in Appendix F and the bin count values are summarised in Table 6. 5(a). The day and time of first occurrence and of the maximum in the range were obtained from the leakage current waveforms given in Appendix F and are shown in Table 6. 5(b). The magnitude of the maximum peak leakage current in each range is also shown.

Table 6. 5: Tables of (a) peak leakage current bin counts between set values and, (b) first occurrence and maximum value.

(a)

		Peak Leakage Current Bin Counts														
		1 - 5 mA			5 - 20 mA			20 - 100 mA			100 - 250 mA			250 - 500 mA		
		Pos	Neg	Total	Pos	Neg	Total	Pos	Neg	Total	Pos	Neg	Total	Pos	Neg	Total
Winter	1S	3938	3301	7239	4392	4193	8585	2588	2625	5213	78	79	157	0	0	0
	2E	3336	3292	6628	7394	7506	14900	4575	4614	9189	87	95	182	2	3	5
	3P	3518	3625	7143	3845	3900	7745	2232	2275	4507	36	38	74	0	0	0
	4C	4799	5352	10151	2774	2883	5657	376	382	758	3	4	7	0	0	0
	5A	4807	4112	8919	3401	3213	6614	2625	2641	5266	568	559	1127	41	45	86
	8R	15461	5760	21221	50	47	97	8	7	15	0	0	0	0	0	0
Summer	1S	2335	2038	4373	3097	3179	6276	4999	5018	10017	850	879	1729	18	22	40
	2E	2936	2710	5646	4096	4116	8212	6907	6855	13762	1110	1149	2259	7	9	16
	3P	2106	2243	4349	2304	2330	4634	5418	5598	11016	1528	1415	2943	155	130	285
	4C	2726	2906	5632	3571	3513	7084	3013	3064	6077	13	13	26	0	0	0
	5A	1701	1458	3159	1644	1562	3206	3726	3710	7436	2686	2596	5282	689	732	1421
	8R	20473	11765	32238	74	58	132	20	24	44	1	1	2	1	0	1
Full Year	1S	6273	5339	11612	7489	7372	14861	7587	7643	15230	928	958	1886	18	22	40
	2E	6272	6002	12274	11490	11622	23112	11482	11469	22951	1197	1244	2441	9	12	21
	3P	5624	5868	11492	6149	6230	12379	7650	7873	15523	1564	1453	3017	155	130	285
	4C	7525	8258	15783	6345	6396	12741	3389	3446	6835	16	17	33	0	0	0
	5A	6508	5570	12078	5045	4775	9820	6351	6351	12702	3254	3155	6409	730	777	1507
	8R	35934	17525	53459	124	105	229	28	31	59	1	1	2	1	0	1

(b)

	First Peak Leakage Current pulses between set values, and Maximum Leakage Current pulse													
	1 - 5 mA		5 - 20 mA		20 - 100 mA		100 - 250 mA		250 - 500 mA		Maximum		
	Day	Time	Day	Time	Day	Time	Day	Time	Day	Time	mA	Day	Time
1S	7	18/04 04:30	9	20/04 22:00	10	21/04 00:50	114	03/08 03:00	198	26/10 02:30	288	243	10/12 01:50
2E	4	15/04 11:20	7	18/04 07:20	10	21/04 01:30	114	03/08 03:00	166	24/09 20:20	340	294	30/01 18:30
3P	8	19/04 03:40	10	21/04 02:30	21	02/05 04:40	114	03/08 03:00	198	26/10 22:10	> 498	319	24/02 05:30
4C	10	21/04 02:30	22	03/05 14:20	97	17/07 19:30	166	24/09 20:30	---	---	143	294	30/01 18:30
5A	19	30/04 02:40	21	02/05 05:50	64	14/06 13:40	81	01/07 06:40	114	03/08 03:00	> 489	114	03/08 03:00
8R	44 **	25/05 20:50	64	14/06 13:40	102	22/07 08:00	294	30/01 18:40	358	03/04 15:10	268 *	358	03/04 15:10

** Energised on day 42

* Due to wet swtich on

The ranking of the energised test insulators, based on the higher bin count values (100 – 250 mA) and (250 – 500 mA) in Table 6. 5(a), are given below from low to high as:

Winter : (Low) 8R, 4C, 3P, 1S, 2E and 5A (High)

Summer : (Low) 8R, 4C, 1S, 2E, 3P and 5A (High)

Full Year : (Low) 8R, 4C, 1S, 2E, 3P and 5A (High)

Looking at the full year's data, lower bin count values were observed on the RG and SR test insulators 8R, 4C and 1S. However, it should be noted that during the summer, when high levels of pollution were present, test insulator 1S had higher bin count values (250 – 500 mA) than that measured on insulator 2E. During the winter, when lower levels of pollution were present and more natural washing took place due to rain, test insulator 3P had lower bin count values than that measured on test insulators 1S and 2E.

Pollution events were identified using the summary of the peak leakage data given in Table 6. 5(b). The peak leakage currents measured during the days identified were determined using the peak leakage current plots shown in sections 6.1.1 to 6.1.6 and are shown as a percentage of the peak permissible current level (given by equation 1.3 and defined in section 1.3) in Table 6. 6 below.

Table 6. 6: Table of peak leakage current, also shown as percentage of the peak permissible current level (I_{perm} = 682 mA), during pollution events.

	Peak leakage current during pollution events					
	3/8/1999	**24/9/1999**	**10/12/1999**	**30/1/2000**	**24/2/2000**	**Average**
1S	189	236	288	245	231	**238**
2E	250	277	204	340	293	**273**
3P	119	247	470	378	>498	**>342**
4C	39	131	52	143	68	**87**
5A	>489	395	>489	>489	>489	**>470**
8R	95	92	8	135	2	**66**
	Note: Leakage current sensor can only measure less than 500 mA peak					
	Peak leakage current as a persentage of I_{perm} during pollution events					
	3/8/1999	**24/9/1999**	**10/12/1999**	**30/1/2000**	**24/2/2000**	**Average**
1S	27.7	34.6	42.2	35.9	33.9	**35**
2E	36.7	40.6	29.9	49.9	43.0	**40**
3P	17.5	36.2	68.9	55.4	>73.0	**>50**
4C	5.7	19.2	7.6	21.0	10.0	**13**
5A	>71.7	57.9	>71.7	>71.7	>71.7	**>69**
8R	13.9	13.5	1.2	19.8	0.3	**10**

The ranking of the energised test insulators, based on the peak leakage current as a percentage of the peak permissible current level in Table 6. 6, are given below from low to high as:

(Low) 8R, 4C, 1S, 2E, 3P and 5A (High)

During the pollution events monitored, test insulators 8R and 4C had the lowest percentage values (percentage of the peak permissible current level). Insulators 1S and 2E had similar percentages, with the latter on average 5% higher. Insulator 3P had a high percentage during 24 February 2000. However, during the other days insulator 3P had similar percentages than insulators 1S and 2E. Insulator 5A had the highest overall and daily percentages.

Note: The leakage current sensor could only measure currents below 500 mA, which is <70% of the permissible peak leakage current value. Thus, higher levels of leakage current could have been present on insulators 3P and 5A during the pollution events. No Mace fuses were blown on insulators 3P and 5A, thus it can be assumed that the leakage currents should have been below the 750 mA level (rating of the fuse).

6.4.3 Probability of daily peak leakage current waveform conductivity

The probability (of exceeding certain abscissa values, using the statistical technique as described in Appendix C4) of the daily peak leakage current waveform conductivity measurements on test insulators 1S, 2E, 3P, 4C, 5A and 8R for the winter, summer and full test period are given below. The 50% probability and the maximum conductivity values are summarised in Table 6. 7.

Note: As explained in section 6.2, the peak wave conductivity is used as an indicator of the interaction of the insulator material surface with the deposited pollution and wetting. The process can be complex, as any one or combination of the three (material, pollution, wetting) could play a role in the final conductivity value. However, the test insulators are all exposed to the exact same environment and climate and as the designs and especially profiles are the same, it is assumed the differences measured are mainly due to the material properties. The porcelain test insulator 3P is treated as the reference insulator.

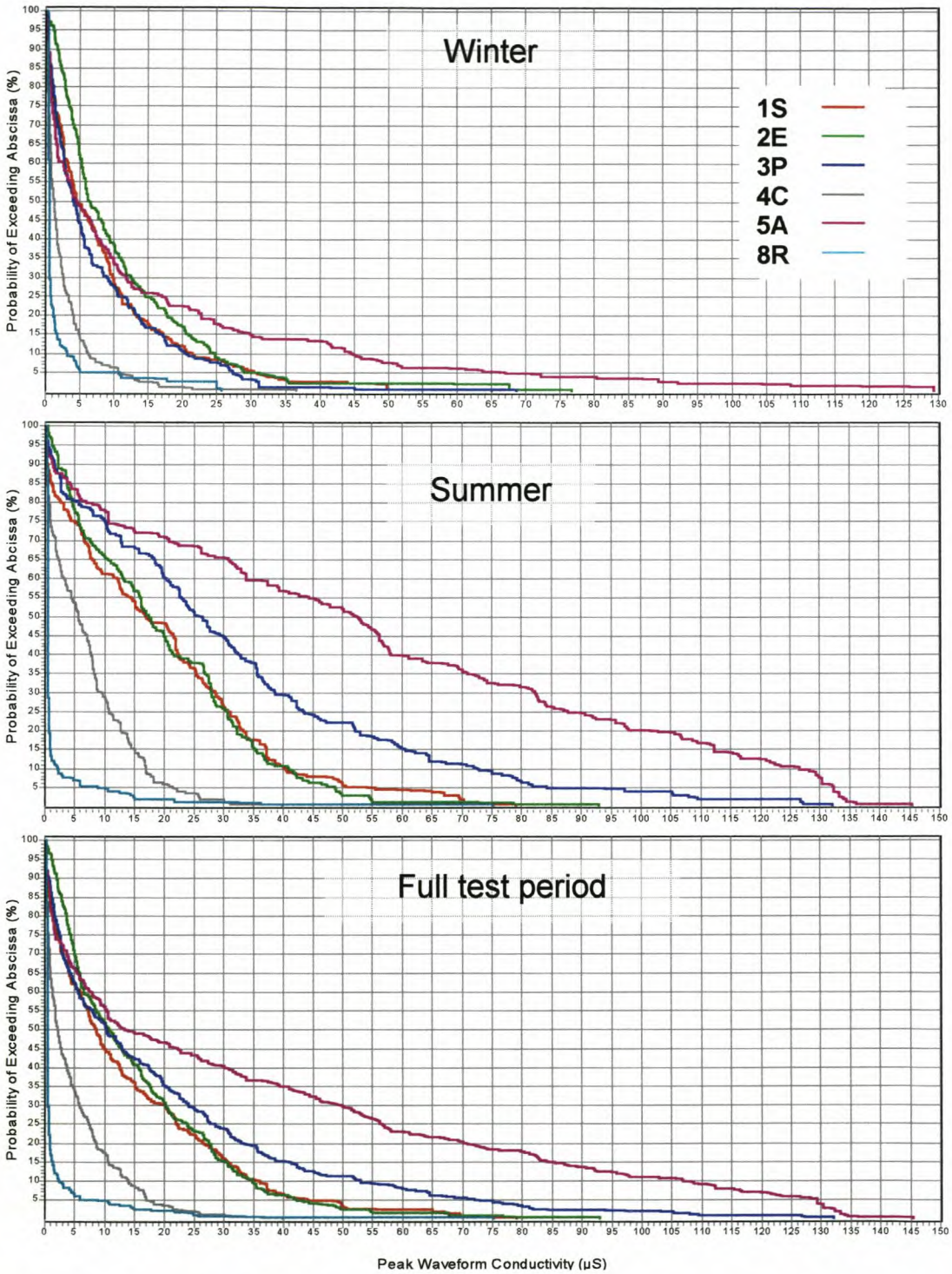

Figure 6. 37 Probability of the daily peak leakage current waveform conductivity measurements on insulators 1S, 2E, 3P, 4C, 5A and 8R for the winter, summer and full test period.

Table 6. 7: Daily peak leakage current waveform conductivity 50% probability and maximum values.

	Daily Peak Waveform Conductivity (μS)				
	50 % Value			Maximum Value	
	Winter	Summer	Full Year	Winter	Summer
1S	4.5	17.0	8.5	64.9	78.9
2E	6.3	17.4	10.6	76.7	92.9
3P	4.1	26.5	10.3	68.6	> 132.1
4C	1.2	5.6	2.2	36.6	39.7
5A	4.5	52.6	13.6	> 129.2	> 145.3
8R	0.5	0.5	0.5	25.7	75.2

The ranking of the energised test insulators, based on the full year's 50% values, are given below from low to high as:

Winter : (Low) 8R, 4C, 3P, 1S, 5A and 2E (High)

Summer : (Low) 8R, 4C, 1S, 2E, 3P and 5A (High)

Full Year : (Low) 8R, 4C, 1S, 3P, 2E and 5A (High)

Looking at the results, test insulators 8R and 4C had the lowest 50% and maximum values, followed by insulator 1S. Test insulators 2E and 3P had similar full year 50% values, the later (3P) lower in the winter and higher in the summer. Insulator 5A had the highest values of all the insulators tested.

6.4.4 Critical flashover voltage calculations

The test insulators' critical flashover voltage levels were calculated using equations (1.13) and (1.16). The results are plotted (see Figure 6. 38) below using the statistical technique as described in Appendix C4. The 90% withstand probability value (also known as the 10% flashover probability, U_{10}) and the lowest critical flashover voltages are also shown in Table 6. 8 for the test insulators.

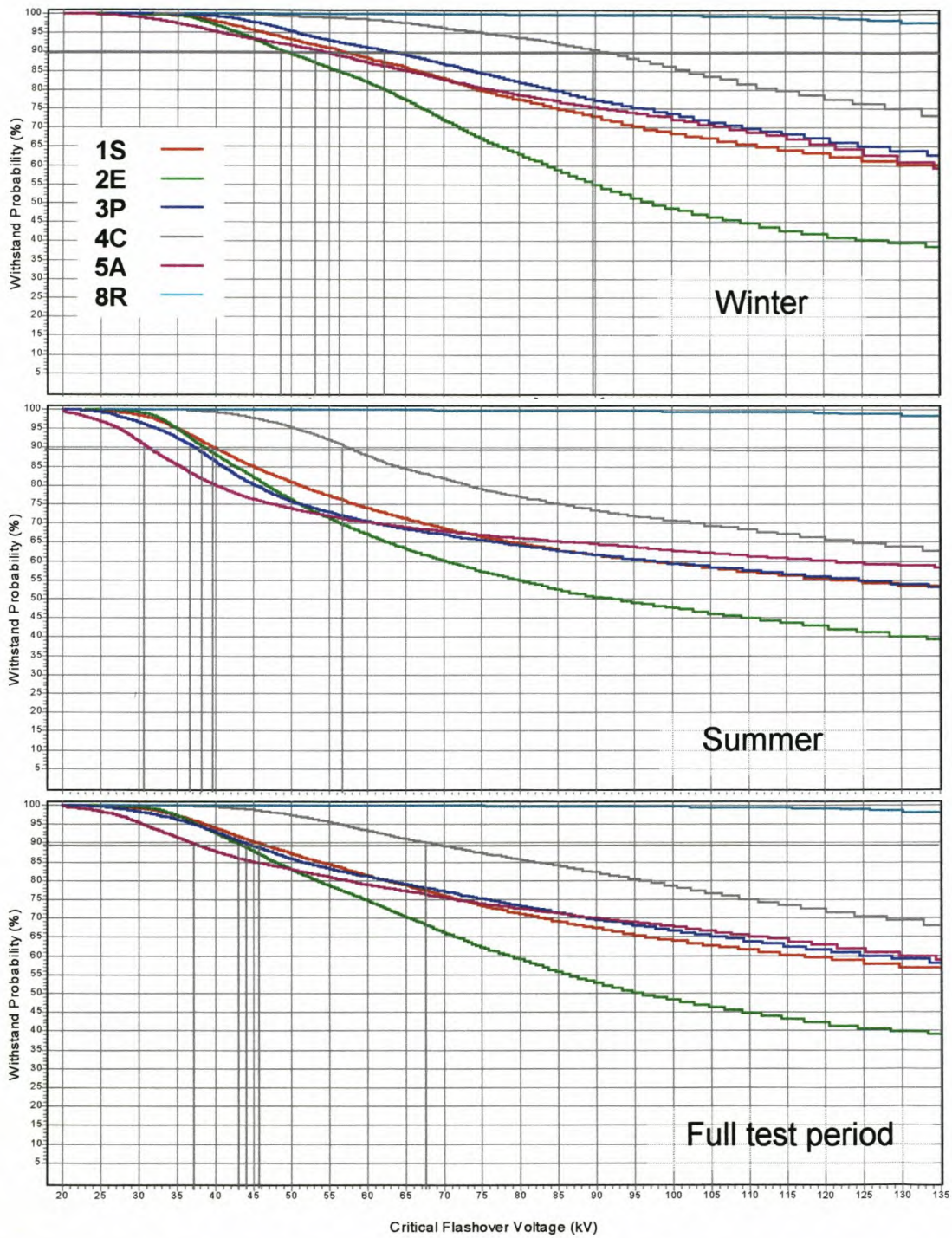

Figure 6. 38 Probability of critical flashover voltage calculation results on insulators 1S, 2E, 3P, 4C, 5A and 8R for the full test period.

Table 6. 8: Critical flashover voltage 90% probability and lowest values.

	Critical Flashover Voltage (kV)				
	90 % Withstand			Lowest Value Obtained	
	Winter	Summer	Full Year	Winter	Summer
1S	57.0	39.8	45.7	25.2	23.5
2E	49.3	38.5	42.9	24.6	22.9
3P	63.3	37.3	43.9	25.6	< 20.0
4C	91.6	57.4	68.4	32.0	31.0
5A	54.5	31.2	36.9	< 20.2	< 20.2
8R	> 135	> 135	> 135	35.9	24.9

The ranking of the energised test insulators, based on the full year's 90% withstand and lowest values obtained (as reported in Table 6. 8), are given below from high to low as:

(High) 8R, 4C, 1S, 3P, 2E and 5A (Low)

Looking at the full year's data, test insulator 8R followed by insulator 4C had the highest 90% withstand voltage. Test insulators 1S, 2E and 3P had similar values. Insulator 5A had the lowest 90% withstand voltage. Insulators 5A and 3P had the lowest critical flashover voltage.

6.4.5 Accumulative electrical charge

The accumulative electrical charge measurements on test insulators 1S, 2E, 3P, 4C, 5A and 8R for week 24 are shown in Figure 6. 39 below. The accumulated electrical charge is also given, in the associated table.

Note: As explained in section 6.2, the accumulated electrical charge flowing over the insulator surface is used as an indicator of the continuous interaction of the insulator material surface with the deposited pollution and wetting. For the same reasons as explained before (same environment and climate and same designs and profiles) it is assumed that the differences in accumulated electrical charge measured are mainly due to the material properties. Porcelain test insulator 3P is treated as the stable reference insulator. It should be noted that test insulator 8R has a resistive/semiconductive-glazed surface, which results in a 50 Hz leakage current and permanent electrical charge

dissipation. Higher values of accumulated electrical charge are thus expected on insulator 8R.

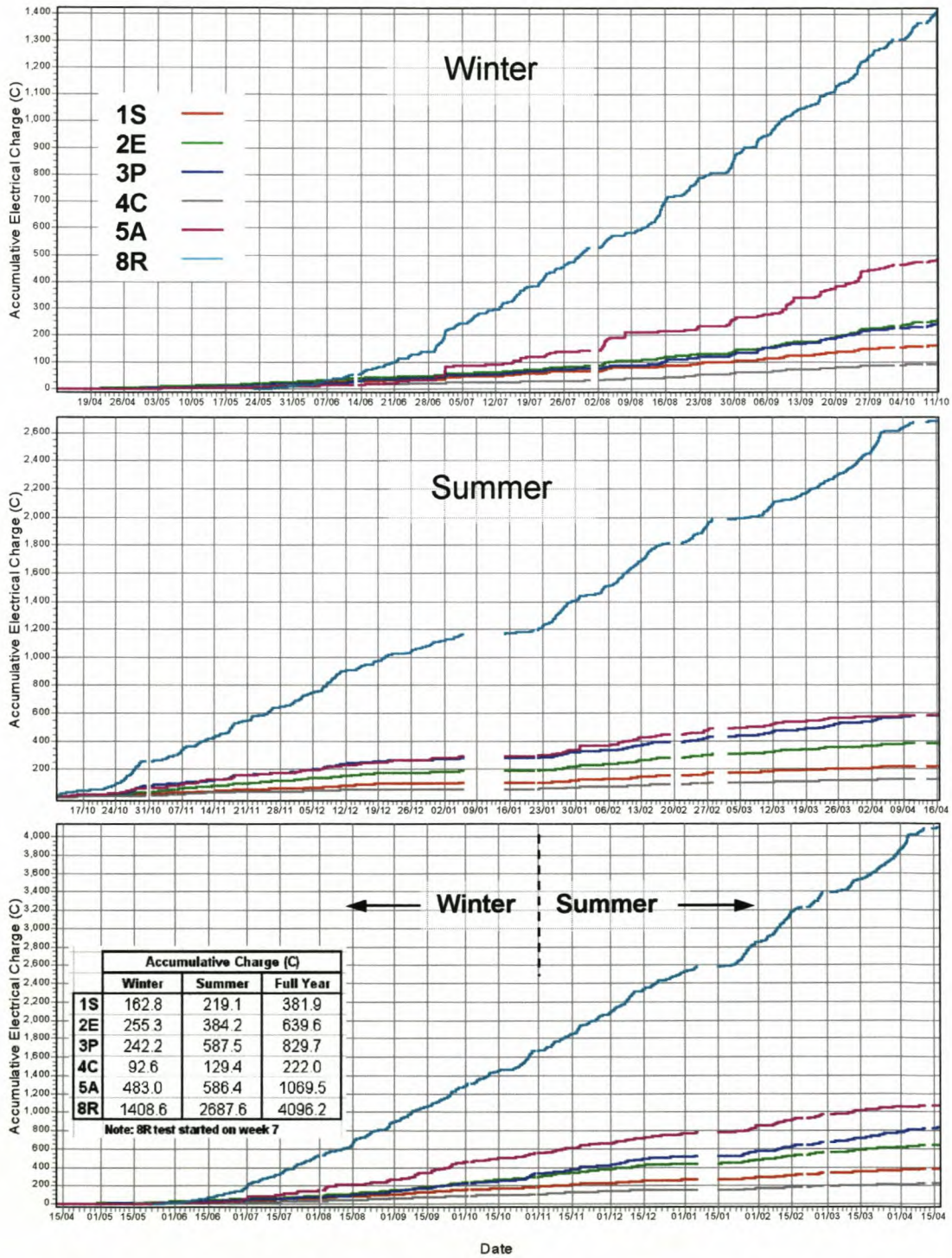

Figure 6. 39 Accumulative electrical charge measurements on insulators 1S, 2E, 3P, 4C, 5A and 8R for the winter, summer and full test period.

The ranking of the energised test insulators, based on the accumulated electrical charge measured (shown in Figure 6. 39), are given below from low to high as:

Winter :	(Low) 4C, 1S, 3P, 2E, 5A and 8R (High)
Summer :	(Low) 4C, 1S, 2E, 3P, 5A and 8R (High)
Full Year :	(Low) 4C, 1S, 2E, 3P, 5A and 8R (High)

As expected, test insulator 8R had the highest accumulated electrical charge measured. In relation to the porcelain reference test insulator 3P, the silicone rubber based test insulators 1S and 4C showed lower accumulated electrical charge values. Test insulator 2E had similar accumulated charge values to the reference insulator 3P. However, at times the values measured on 2E were higher when compared to 3P. Test insulator 5A had the highest accumulated charge value when compared to that measured on insulators 1S, 2E, 3P and 4C.

6.5 CONCLUDING REMARKS ON THE INSULATOR LEAKAGE CURRENT MEASUREMENTS

The peak (I_h) and energy values of the leakage current were identified as the two main parameters needed to describe the leakage current activity on the test insulators.

The test insulator's daily peak leakage current waveform surface conductivity value was found to be the main parameter to use as an indicator of the maximum interaction of the insulator material surface with the deposited pollution and wetting.

The accumulated electrical charge (or energy) flowing over the insulator surface was found to be the main parameter to use as an indicator of the continuous interaction of the insulator material surface with the deposited pollution and wetting.

Pre-deposit and 'rapid' saline pollution events were identified and the effects of wind, natural washing and wetting were also discussed.

The correlation between leakage current and climatic conditions showed that in general the relative humidity and solar radiation had a large effect on I_h values. Further, it was

found that rainfall had the largest effect on energy. However, the RG test insulator 8R showed the opposite performance.

The relative performances (best to worst) of the energised test insulators (1S, 2E, 3P, 4C, 5A and 8R) were investigated and a summary is given in Table 6. 9 below.

Table 6. 9: Table summarising the relative performances (best to worst) of the energised test insulators.

	Performance	Average peak leakage current time of day	I_h/I_{perm} during high pollution events	Peak leakage curent bin counts	Daily peak wave conductivity	Critical flashover voltage	Accumulated charge
Winter	Best	8R	N/A	8R	8R	8R	4C
		4C		4C	4C	4C	1S
		3P		3P	3P	3P	3P
		1S		1S	1S	1S	2E
		5A		2E	5A	5A	5A
	Worst	2E		5A	2E	2E	8R
Summer	Best	8R	N/A	8R	8R	8R	4C
		4C		4C	4C	4C	1S
		1S		1S	1S	1S	2E
		2E		2E	2E	2E	3P
		3P		3P	3P	3P	5A
	Worst	5A		5A	5A	5A	8R
Full year	Best	8R	8R	8R	8R	8R	4C
		4C	4C	4C	4C	4C	1S
		1S	1S	1S	1S	1S	2E
		3P	2E	2E	3P	3P	3P
		2E	3P	3P	2E	2E	5A
	Worst	5A	5A	5A	5A	5A	8R

From the results shown in Table 6. 9 the RG test insulator 8R had the best overall leakage current performance of all the insulators tested. The RTV SR coated porcelain insulator 4C was the next best performer followed by the HTV SR test insulator 1S. The EPDM test insulator 2E and the reference porcelain insulator 3P showed similar performance. The Cycloaliphatic epoxy resin test insulator 5A was the worst performer.

Note: The results reported in this chapter are relevant to these specific test insulators and caution must be applied when using this information for field application. For example, test insulators 3P, 4C, 5A and 8R cannot be used directly in the field, due to mechanical constraints of the shank. The author will not be held responsible for the misinterpretation or abuse of this information.

7 DISCUSSION OF SPECIFIC ASPECTS EMANATING FROM THE RESEARCH PROGRAMME

"The task is, not so much to see what no one has yet seen; but to think what nobody has yet thought, about that which everybody sees." - ***Erwin Schrödinger***

During the research programme observations were made (as reported in the previous chapters) which led to the development of new models, ideas and hypotheses. In this chapter some of these are discussed.

Based on these observations it is possible to propose a model to explain the discharge activity on the test insulators.

Also it was noted that although all the test insulators became hydrophilic in a short time and were exposed to the same environmental and climatic conditions, the leakage current levels differed widely for the various test insulators. A hypothesis is proposed to explain this phenomenon.

Further, by analysing the environmental, climatic and leakage current data, it was possible to develop a multiple regression model so as to determine the leakage current from the climatic and environmental data.

7.1 MODEL OF ELECTRICAL DISCHARGE ACTIVITY ON THE TEST INSULATORS

In Chapter 5 the results are shown for one year's visual (surface condition and electrical discharge activity) observations on the test insulators. It was found that the types of electrical discharge activity were similar on all of the test insulators monitored.

The various discharge activities observed in order of first occurrence were: water drop corona (WDC), spot corona or discharges (SCD), dry-band corona (DBC), and finally dry-band discharges (DBD).

Different electrical discharge activities were dominant on the test insulators during the following three main stages:

1. New (clean) insulator with light pollution starting - WDC
2. Polluted insulator with local dry band starting - WDC and SCD
3. Polluted insulator with dominant local dry band - DBC and DBD

A model showing the stages of development of the electrical discharge activity as observed on the test insulators is presented in Figure 7. 1 below.

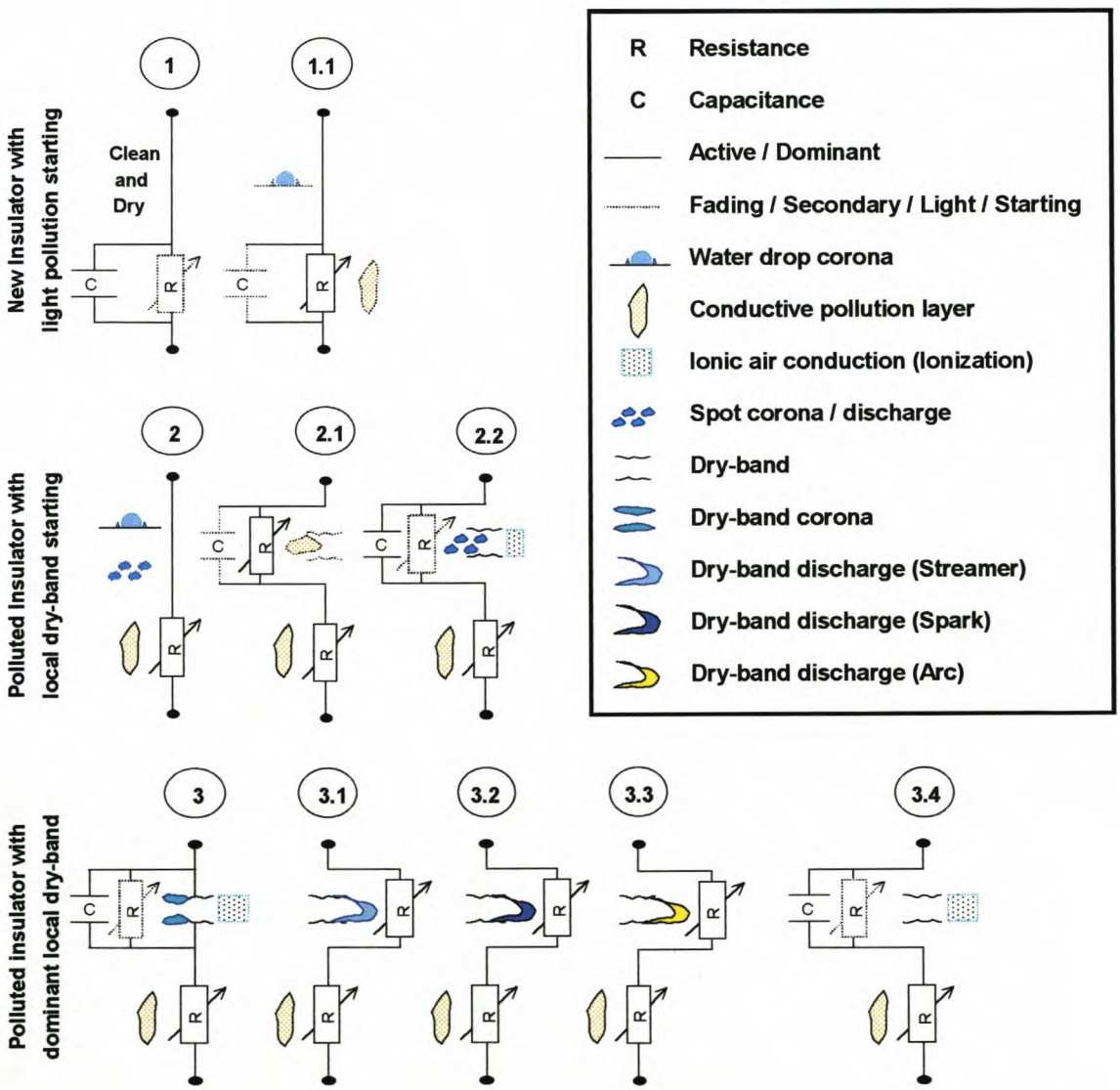

Figure 7. 1 Model of the electrical discharge activity observed on the test insulators.

The electrical discharge activity observed on the test insulators during the three stages modelled above (in Figure 7. 1) can be described as follows:

1. **New (clean) insulator with light pollution starting.** The clean and dry test insulators were assumed to be mainly capacitive as the levels of leakage current had a capacitive phase shift and were in the order of μA. The electrical field strength was assumed highest at the live side, close to the end fitting (see electric field simulation in section 5.2.3). No corona discharges were observed under this condition. However, when lightly polluted and wetted (as modelled in (1.1) of Figure 7. 1) the test insulator became more resistive and the leakage currents increased to an order of mA. The leakage current was too low for dry zones to form due to joule heating. The voltage was then divided resistively over the actual length of the test insulator and the field strength was highest at the shed tips, where the radius of curvature was the smallest (see electric field simulation in section 5.2.3). WDC was seen mainly in the region of the shed tips. However, this was found to be present mainly during the first few weeks of the test program.

2. **Polluted insulator with local dry band starting.** As the pollution increased and critical wetting took place the levels of leakage current increased, to the order of 10's of mA. The insulator was dominantly resistive. WDC was present mainly in the region of the shed tips and spot corona (also inter-water-drop discharges) was observed. Joule heating initiated the formation of a dry zone leading to a localised dry band (as modelled in (2.1) of Figure 7. 1). As this area dried out further SCD were seen. The dry band area was assumed more capacitive, and ionic by-products from the SCD were forming in the dry-band area (as modelled in (2.2) of Figure 7. 1). SCD were observed throughout the test programme, however mainly in the areas where dry bands were present or newly forming.

3. **Polluted insulator with dominant local dry band.** As the dry-band area fully dried out DBC was observed on the edges (and ionic by-products were still being generated), developing into DBD. In diagrams (3.1) to (3.3) of Figure 7. 1 the three types of DBD observed (streamer, spark and arc) are modelled. These were found to be dependent on the resistance of the conductive pollution layer and ultimately the level of the leakage current. Beyond a certain stage, when the dry band has sufficiently widened, no discharge activity was seen in the dry-band area. It is assumed that ionic by-products were still present in the gap (this is modelled in (3.4) of Figure 7. 1). Once a dominant dry band has formed the sequence described in 3 repeats itself. DBC and DBD were found to be the most dominant form of electrical discharge activity on all the test insulators.

The electrical discharge activity model proposed above was found relevant to all the test insulators monitored irrespective of material (excluding the RG test insulator, 8R).

7.2 HYPOTHESIS ON THE DIFFERENCE IN LEAKAGE CURRENT PERFORMANCE OF THE TEST INSULATORS

All the test insulators are identical except for material composition. The insulator pollution observations and measurements described in section 4.1 showed that the pollution deposits on all the different test insulators were similar. During the visual inspection of the test insulators it was also found that within the first few weeks all the insulators were hydrophilic (HC 6 – 7, i.e. wetted out totally on the surface, see section 4.2.1).

However, the surface conductivity measurements with the IPMA (see section 4.1.2) were found to be different for all the test insulators monitored. The ranking (see section 4.3) of the test insulators based on IPMA surface conductivity measurements were as follows "*The test performance decreased in the following order: 4C (best performer), 1S, 2E, 3P (reference) and 5A (worst performer).*"

The leakage current measurements over the one-year test period (as reported in Chapter 6) also show (see section 6.5) that there is a clear difference in the performance of the various material types tested "*...the RG test insulator 8R had the best overall leakage current performance of all the insulators tested. The RTV SR coated porcelain insulator 4C was the next best performer followed by the HTV SR test insulator 1S. The EPDM test insulator 2E and the reference porcelain insulator 3P showed similar performance. The Cycloaliphatic epoxy resin test insulator 5A was the worst performer.*"

The question therefore is asked: why is there a difference in the leakage currents measured on the test insulators?

In this section a hypothesis, based on the model previously presented in a publication "Proposed model to explain the difference in leakage current performance of EPDM and SR insulators at a severe marine site" by the author and Holtzhausen [64], is further explored. It was decided to focus on the results obtained on test insulators 1S and 4C (hydrophobic silicone polymer), 2E and 5A (hygroscopic polymer), using insulator 3P (hydrophilic stable material) as a reference.

The conclusions from this publication [64] is as follows "*It appears that, from a leakage current and a flashover perspective, silicone rubber insulators are superior to EPDM insulators, even if the SR insulators are completely hydrophilic and appear to be more polluted. This property of silicone insulators can be explained by their higher surface resistance, caused by the migration of the silicone oils from the bulk of the insulator into the pollution layer. Similar findings have been reported by other researchers [65,69].*"

It is suggested in this publication [64] that the insulator surface resistance could change due to the interaction of the insulator material with the pollution layer. This could help explain why the leakage current measured on the SR insulator was found to be at least tree times lower than that measured on the EPDM, even though both were hydrophilic. Further, the retention of pollution by the SR insulator is also demonstrated and the EPDM insulator showed signs of crazing (surface cracks) filled with pollution.

Visual observations made (on SR and EPDM test insulators) during and after this test programme on similar insulators (after 1 year, 2 years and 4 years energisation at KIPTS) can be seen in Figure 7. 2 and Figure 7. 3 below.

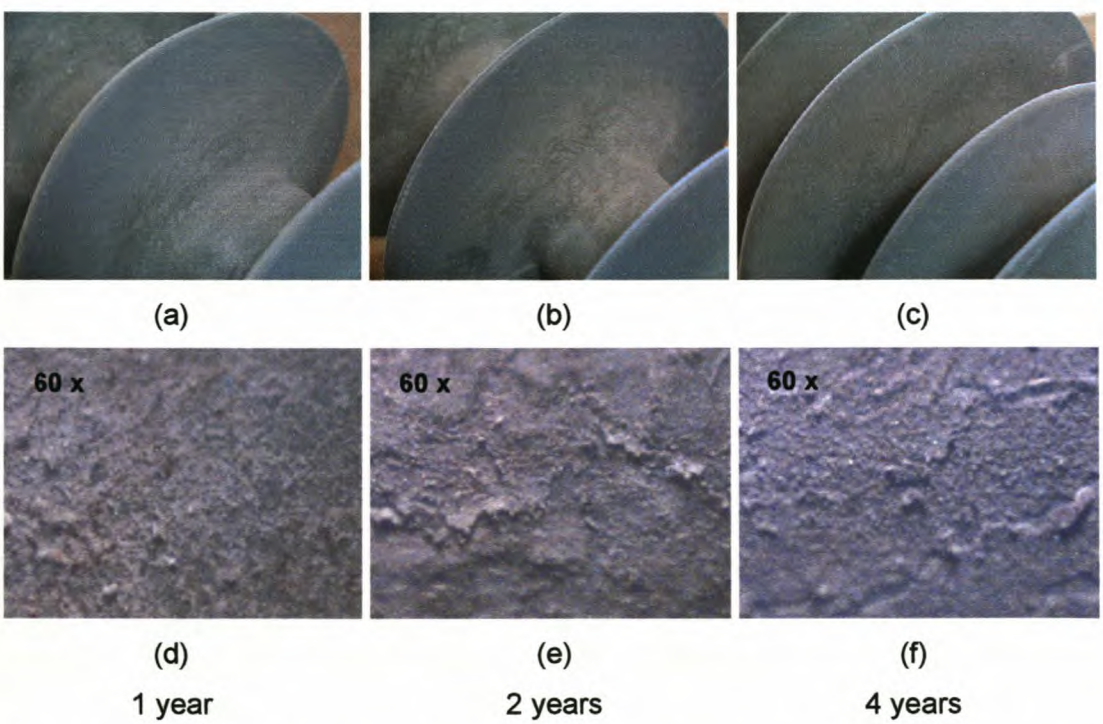

Figure 7. 2 Photos showing surface condition on SR test insulators 1S after one year, 6S after two years and a similar insulator after 4 years.

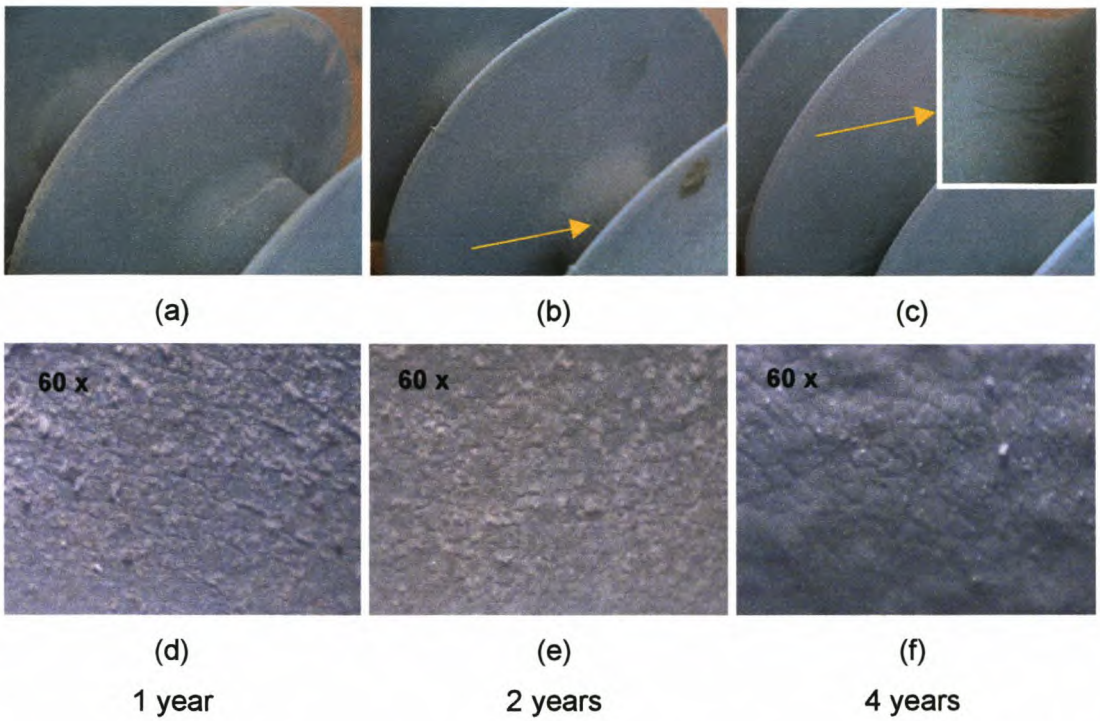

Figure 7. 3 Photos showing surface condition on EPDM test insulators 2E after one year, 7E after two years and a similar insulator after 4 years. The arrows indicate erosion in the material.

When comparing the SR (Figure 7. 2) and EPDM (Figure 7. 3) photos, a higher visible pollution build-up was found on the SR test insulators. The SR insulator material stayed stable with no signs of degradation. However, the pollution on the SR insulator surface started to flake off. The EPDM test insulator showed signs of crazing and finally erosion.

Analysis of the IPMA surface conductivity results (see section 4.1.2) led to the statement in section 4.3 "*The results suggest that there is an interaction between the insulator material surface and the pollution layer, which alters the resistivity (ρ) and the surface area (A_{pol}) available for leakage current flow.*" It was also reported "*Hydrophobicity transfer was also confirmed on the SR test insulators. It was more prominent on the RTV SR coating.*"

Based on the above the following hypothesis (as shown in Figure 7.4) is suggested to explain the difference in the leakage currents measured on the test insulators 1S and 4C (hydrophobic silicone polymer) and 2E and 5A (hygroscopic polymer) when compared to the reference porcelain insulator 3P (hydrophilic stable material).

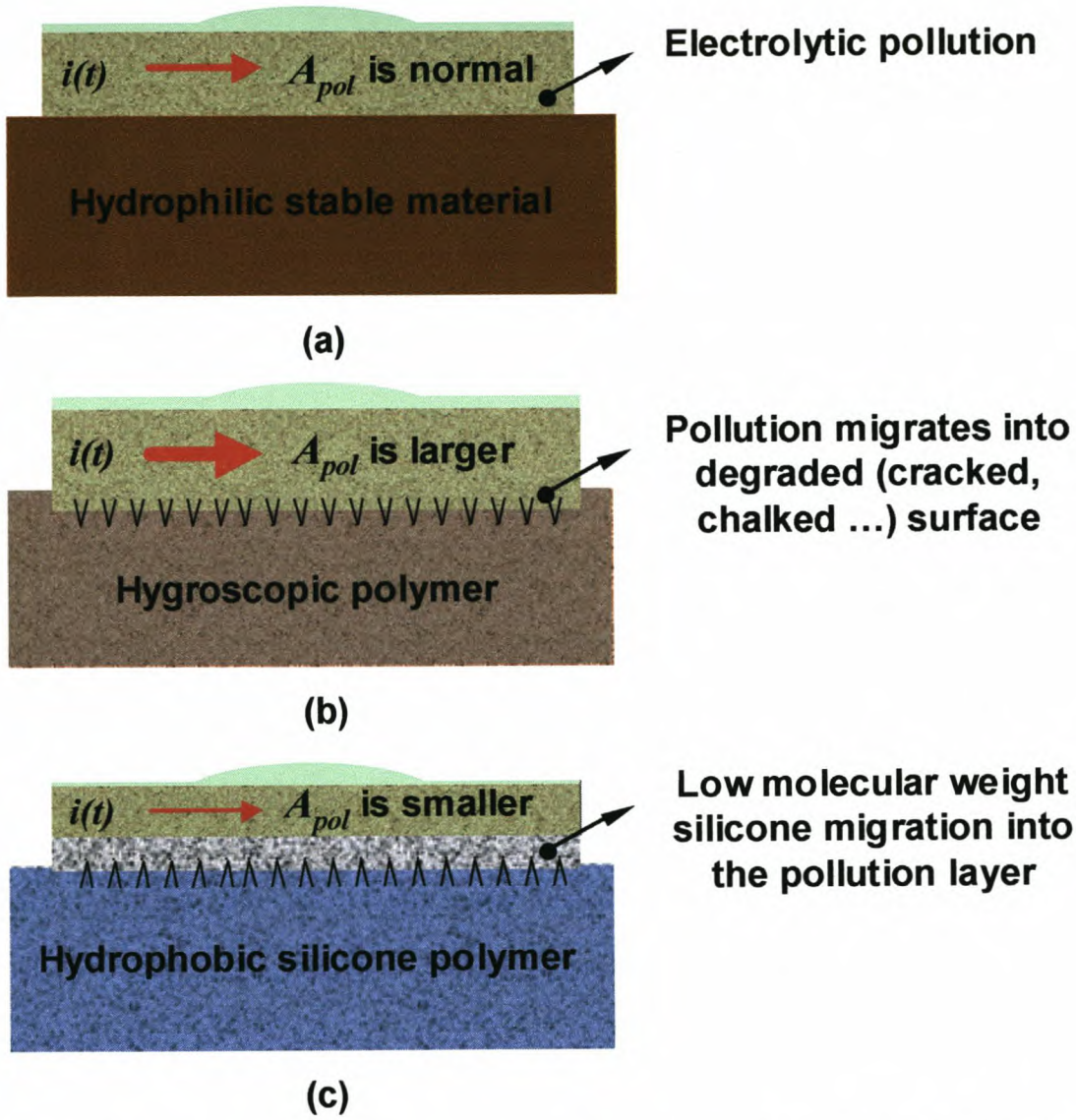

Figure 7.4 Schematic diagram representing an electrolytic pollution layer with leakage current *i(t)* on a hydrophilic, stable material (porcelain) (a), a hygroscopic polymer (b), and a hydrophobic silicone polymer (c).

1. **Hydrophilic stable material, 3P, Figure 7.4 (a):** The stable porcelain hydrophilic material of test insulator 3P does not interact with the electrolytic pollution layer. The area (A_{pol}) available for leakage current flow and the resistivity (ρ) is thus a resultant of the pollution and wetting only. This is used as a reference condition.

2. **Hygroscopic polymer, 2E and 5A, Figure 7.4 (b):** The visual surface condition is hydrophilic and looks similar to the reference porcelain. However, the leakage current was found to be higher at times than the reference porcelain. It is hypothesised that this is due to the surface of the material becoming hygroscopic which then absorbs the electrolytic pollution resulting in a larger surface area (A_{pol}) available for current flow. This results in a decrease in insulator surface resistance (R_{ins}) when compared to the reference porcelain, and hence an increase in leakage current levels.

3. **Hydrophobic silicone polymer, 1S and 4C, Figure 7.4 (c):** The visual surface condition is hydrophilic and looks similar to the reference porcelain. However, the leakage current was found to be lower than the reference porcelain. It is hypothesised that this is due to the migration of the low molecular weight silicones into the pollution layer resulting in the resistivity (ρ) becoming higher and hence a smaller surface area (A_{pol}) being available for current flow. This results in an increase in insulator surface resistance (R_{ins}) when compared to the reference porcelain, and hence a decrease in leakage current levels.

Test insulators 1S and 4C are treated as hydrophobic silicone polymer materials and the hypothesis as described above is relevant to both. However, the RTV SR coated porcelain test insulator 4C showed a better leakage current performance than the HTV SR insulator 1S. The difference is assumed to be mainly due to the low molecular weight silicone migrating faster into the pollution layer for the RTV SR than the HTV SR [56].

Note: The thermal properties of the material, which could have an effect on the wetting of the pollution layer, are not included in the above hypothesis, although they have been explored in section 4.2.2.

Test insulators 2E and 5A are treated as hygroscopic polymer materials and the hypothesis as described above is relevant to both. However, the cycloaliphatic insulator 5A showed higher leakage current levels than the EPDM test insulator 2E. It is assumed that this is due to the severe material degradation (chalking, tracking and erosion) found on the cycloaliphatic test insulator 5A, which increased the surface area (A_{pol}) available for leakage current flow far more than that found on the EPDM insulator 2E.

A further question asked is: why is the leakage current performance of the RG test insulator 8R so much better than the other insulators?

Similar results were found by NGK Insulators (Ltd) in Japan and the publication "Practical application of semiconducting glazed insulators" [66] explains the process why there is a difference in leakage current performance. In short it can be explained as follows:

On a normally glazed porcelain insulator, leakage currents flowing in the electrolytic pollution layer may result in the formation of dry bands due to localised joule heating. In these dry-band areas, electrical discharge activity such as sparking and/or arcing may occur across the dry band, as shown in Figure 7.5 (a).

On a resistive glazed porcelain insulator, the wetting of the pollution layer is restricted by the heating energy from the parallel current flowing in the resistive glazed surface beneath. This has the effect of lowering the levels of leakage current flowing in the electrolytic layer. When dry bands start to form the leakage current is diverted through the resistive glaze (as shown in Figure 7.5 (b)) resulting in a low volt drop across the dry band, which then suppresses the formation of electrical discharge activity.

This explains why there is such a big difference in leakage current performance of the RG test insulator in relation to the others.

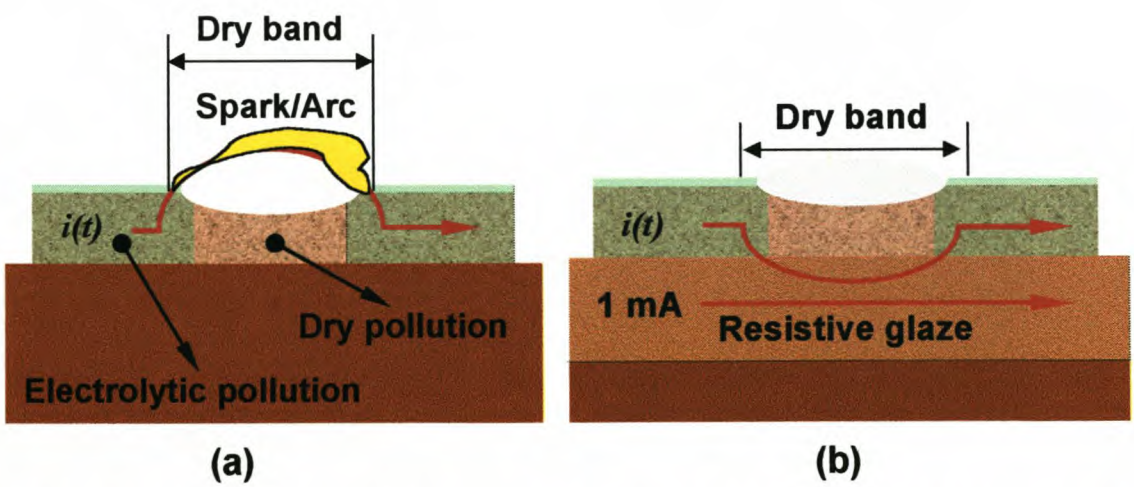

Figure 7.5 Schematic diagram representing an electrolytic pollution layer and dry band with leakage current on a normally glazed (a) and resistive glazed (b) porcelain insulator surface.

7.3 DETERMINING INSULATOR LEAKAGE CURRENT FROM ENVIRONMENTAL AND CLIMATIC CONDITIONS MONITORED AT KIPTS

In section 6.2 it has been shown that there is a correlation between the insulator leakage current and the climatic conditions monitored. The question which comes to mind, is whether the insulator leakage current can possibly be determined from the environmental and climatic conditions monitored? In this section, regression techniques are used to try and resolve this question.

The ESDD pollution measured on a non-energised porcelain longrod insulator identical to the test insulator 3P, during day 5 (1999/09/24) of week 24, was 0.16 mg/cm^2, which is rated as heavy. This can be related [31] to a layer conductivity of approximately 16 μS. The daily peak waveform conductivity measured on test insulator 3P the day before the ESDD measurement was 14.6 μS. These two values are very close and both fall within the pollution classification level of heavy, as indicated in Table 3.3 in chapter 3. Thus, the daily peak waveform conductivity measurement (as shown in section 6.1) can be used as an indication of the daily environmental (pollution) condition in week 24 and is treated as an independent variable (variable from day to day, though constant per day).

The 10-minute climatic parameters measured (humidity, rainfall, UV-B solar radiation, temperature, and directional wind speed) are used as independent variables along with the daily peak wave conductivity (representing the environmental pollution level), which together determine the dependent variables, namely the leakage current levels (peak value and electrical energy), using the linear and non-linear regression techniques as described in Appendix C8. The regression constants calculated for insulator 3P for week 24, using these techniques, are given in Table 7. 1 below. The coefficient of determination R^2, representing the "strength" or "magnitude" of the relationship, is also given (0 = poor, and 1 = excellent).

Table 7. 1: Table of regression constants for insulator 3P during week 24.

				Regresion constants for Insulator 3P during week 24						
				Day 1	Day 2	Day 3	Day 4	Day 5	Day 6	Day 7
Peak Leakage Currents (mA)	Linear	Peak Wave Conductivity		-5.3687	2.7589	-3.5473	-3.8565	-16.9444	-0.6770	-5.5097
		Humidity		2.1372	0.4395	1.0625	0.6773	6.7472	0.1944	1.0815
		Rainfall		0.0000	0.0000	0.0000	0.0000	44.0840	19.7066	215.2014
		UV-B		-0.0483	-0.0344	-0.0596	-0.0628	-0.4858	-0.0566	-0.0190
		Temperature		-0.3659	-5.2923	-0.0818	0.8741	39.9862	0.0889	1.5307
		Wind Speed	340 (North)	1.9039	-1.3559	-0.3569	-1.1987	-1.9185	1.0847	3.2788
			70 (East)	-1.1394	-1.7960	3.5354	4.7091	-6.7201	2.3379	2.4291
			160 (South)	-0.5705	-0.8234	-0.6435	-0.0385	-3.0782	0.5799	3.7223
			250 (West)	-0.8539	-0.7528	0.4982	-0.7025	-1.2550	1.3241	0.4955
		R^2		0.7405	0.8831	0.4354	0.6707	0.6394	0.4652	0.5569
	Non-linear	Peak Wave Conductivity		-12.8959	-15.2443	-8.4246	-17.2159	-2.2508	-7.8694	-9.7389
		Humidity		10.2194	11.0832	5.8381	9.2214	3.0656	5.4443	6.4279
		Rainfall		0.0000	0.0000	0.0000	0.0000	-0.4866	1.2544	15.4550
		UV-B		-0.2162	-0.4570	-0.3447	-0.5062	-0.6155	-0.2251	-0.1159
		Temperature		0.1976	1.6492	0.9267	3.1165	-0.6129	1.4080	0.6433
		Wind Speed	340 (North)	-0.1591	-0.1001	0.4367	0.2385	0.6227	0.0707	1.1177
			70 (East)	-0.2261	-0.1863	0.1516	0.0727	0.3393	0.1684	0.2775
			160 (South)	-0.0484	0.0157	-0.3218	-0.0009	0.2251	0.1436	0.6141
			250 (West)	-0.0685	0.1833	0.0935	0.0667	0.8076	0.1409	0.1983
		R^2		0.8503	0.9494	0.6743	0.9207	0.7053	0.7642	0.5585
Electrical Energy (kJ)	Linear	Peak Wave Conductivity		-0.3845	0.1243	0.0876	-0.2468	-0.2710	-0.0078	-0.3172
		Humidity		0.1051	-0.0111	-0.0018	0.0297	0.1114	0.0053	0.0570
		Rainfall		0.0000	0.0000	0.0000	0.0000	7.2237	6.3741	15.6581
		UV-B		0.0010	-0.0005	-0.0006	-0.0012	-0.0064	-0.0018	-0.0019
		Temperature		0.0818	-0.1535	-0.0997	0.0727	0.6017	-0.0482	0.1341
		Wind Speed	340 (North)	0.0724	0.0775	0.0766	-0.0071	-0.0212	0.1062	-0.0158
			70 (East)	0.0039	0.0367	0.0714	0.1292	-0.0736	0.1153	0.0914
			160 (South)	0.0466	0.0549	0.0388	0.0110	-0.0224	0.0631	0.1460
			250 (West)	0.0535	0.0538	0.0468	-0.0119	-0.0193	0.0747	-0.0173
		R^2		0.7220	0.8696	0.7201	0.7152	0.8899	0.8915	0.5262
	Non-linear	Peak Wave Conductivity		-6.8192	0.5658	0.0416	-6.0040	-2.8493	-1.2079	-4.2917
		Humidity		4.7954	0.1697	0.3382	2.8802	1.3526	0.8056	2.2811
		Rainfall		0.0000	0.0000	0.0000	0.0000	1.6927	2.3311	5.3255
		UV-B		0.0002	-0.0425	-0.0483	-0.0794	-0.1691	-0.0337	-0.0672
		Temperature		0.5165	-0.9104	-0.5071	1.3231	2.2456	0.1988	1.2462
		Wind Speed	340 (North)	0.0915	0.0997	0.1112	0.0711	0.1150	0.0772	0.0892
			70 (East)	-0.0347	0.0333	0.0669	0.1183	0.0427	0.0266	-0.0124
			160 (South)	0.0495	0.0907	0.0136	0.0538	0.1471	0.0448	0.0251
			250 (West)	0.0608	0.0954	0.0741	0.0125	0.1809	0.0456	-0.0785
		R^2		0.8330	0.9029	0.7584	0.8647	0.7897	0.8092	0.5237

Using the daily-calculated (linear and non-linear) regression coefficients in Table 7. 1 the 10-minute peak leakage currents expected on test insulator 3P are determined and then plotted, in relation to the actually measured peak leakage currents, in Figure 7. 6 below.

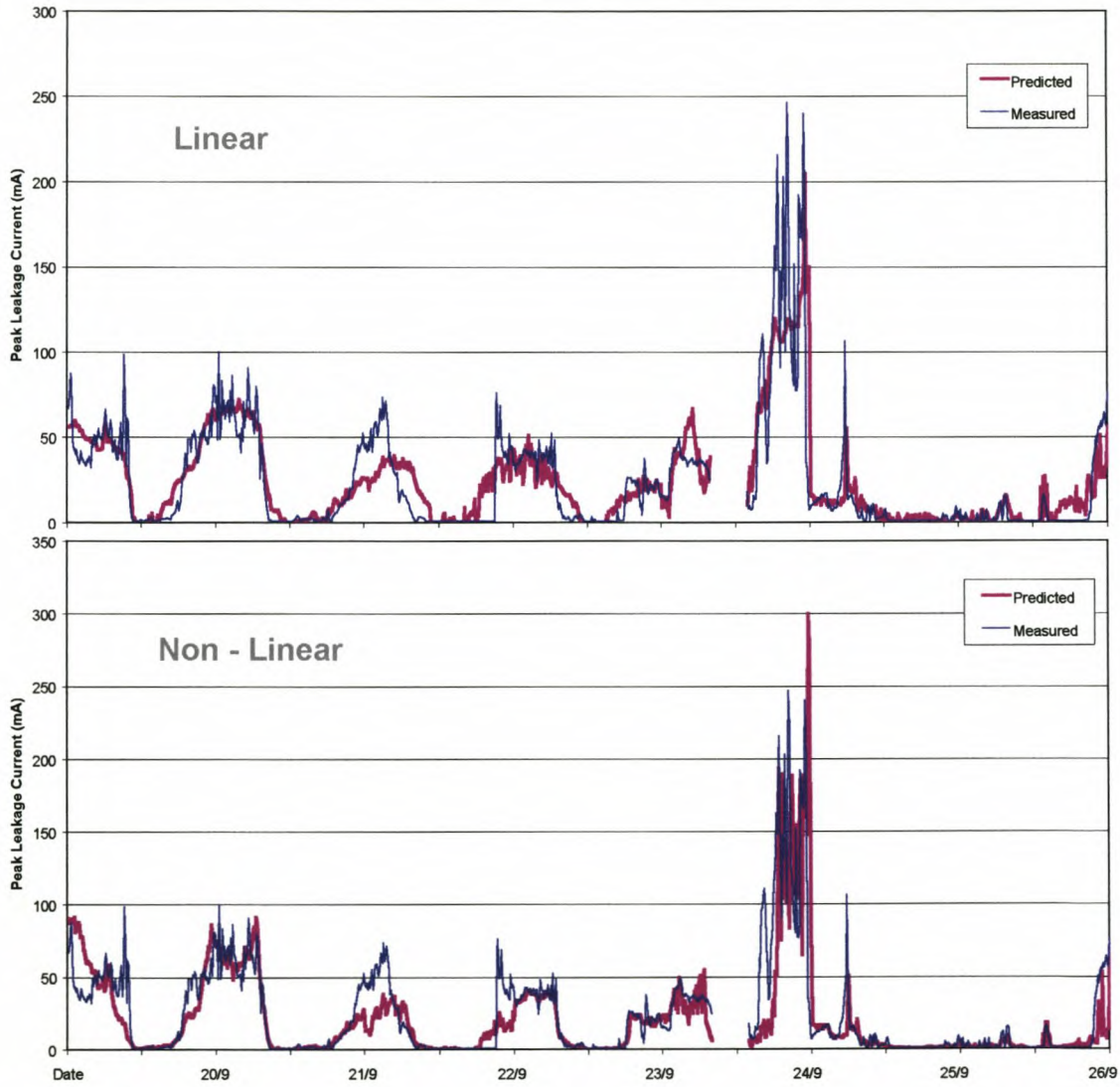

Figure 7. 6 Actually measured peak leakage current values versus calculated (predicted) values, using linear and non-linear regression results, and measured climatic and peak wave conductivity values for week 24.

Using the daily-calculated (linear and non-linear) regression coefficients in Table 7. 1 the 10-minute accumulated electrical energy values expected on test insulator 3P is determined and then plotted in relation to the actually measured electrical energy values in Figure 7. 7 below.

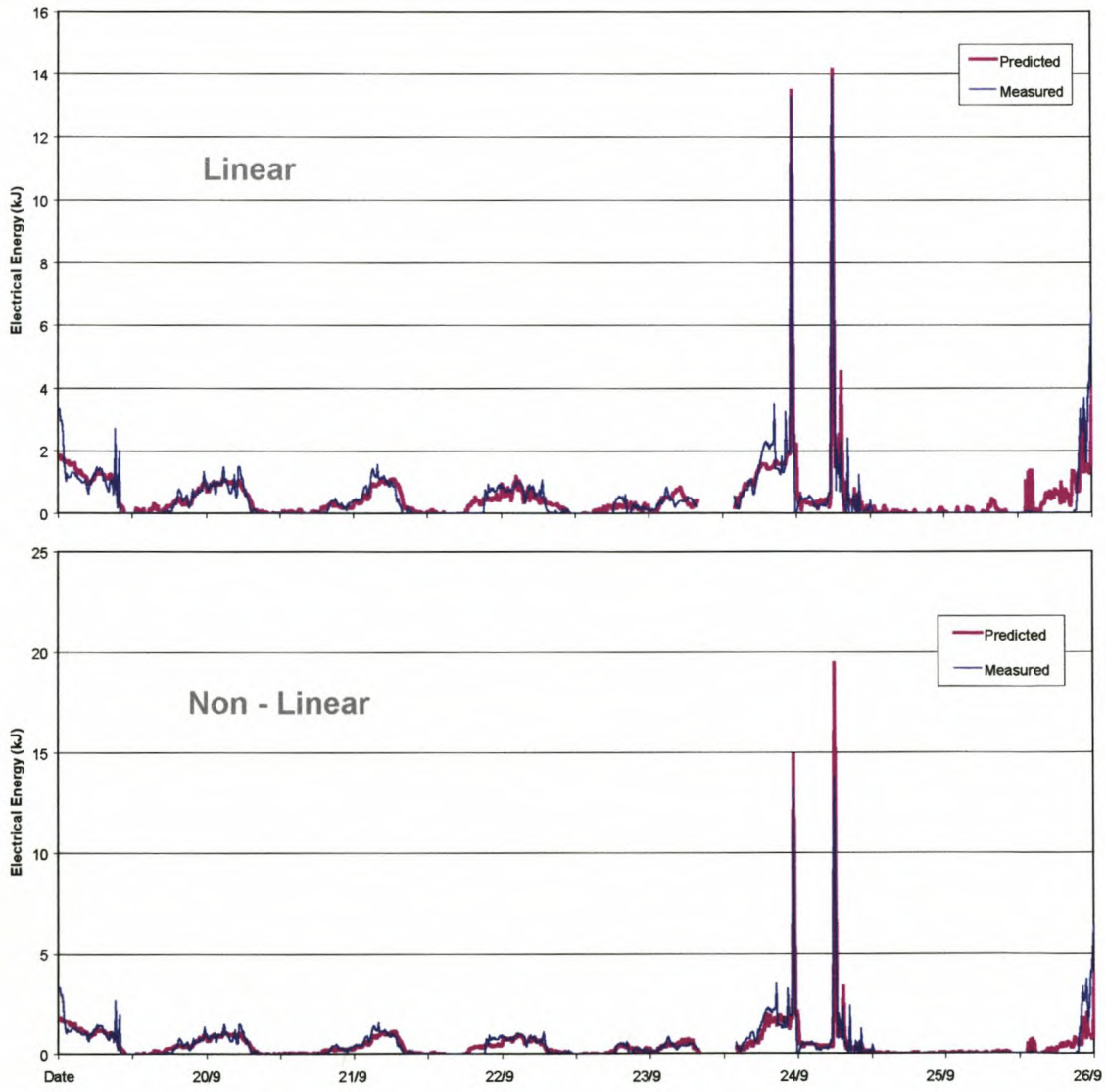

Figure 7. 7 Actually measured electrical energy values versus calculated (predicted) values, using linear and non-linear regression results, and measured climatic and peak wave conductivity values for week 24.

From the above it can be seen that it is possible to fairly accurately determine the insulator leakage current from the environmental and climatic conditions monitored.

7.4 CONCLUDING REMARKS

The dry band areas on the test insulators were found to be electrically the most active, thus this area should be further investigated from an ageing perspective.

It was further found that hydrophobicity measurement of the polluted insulator surface couldn't be used by itself as an indication of the condition of the test insulator. The insulator surface conductivity was found to be the best overall indicator of the interaction of the insulator with the climatic and environmental conditions.

The multiple regression techniques used to determine the leakage current on the test insulators from the climatic and environmental conditions monitored at KIPTS has proved to be very successful. The ideas should be explored further, for instance by using neural networks.

8 CONCLUSIONS AND RECOMMENDATIONS

"The world little knows how many of the thoughts and theories which have passed through the mind of the scientific investigator have been crushed in silence and secrecy by his own severe criticism and adverse examination; that in the most successful instances not a tenth of the suggestions, the hopes, the wishes, the preliminary conclusions have been realised." - ***Michael Faraday***

The main objective of this research programme was to compare the relative performance of new insulators over a one-year period, while observing the leakage current, climatic, environmental and surface conditions, and electrical discharge activity of the main types of insulating materials used for high-voltage insulators in South Africa when subjected to a severely polluted coastal environment as encountered along the local West Coast.

The scope of work was to:

- Establish a test programme and procedure
- Establish a test facility
- Establish instrumentation
- Collect data and make observations over a one-year period
- Analyse data, investigate trends, draw correlations and draw up a relative ranking.

It was envisaged that the knowledge gained could be used in the selection of suitable high-voltage insulator materials for use in severe coastal environments, both nationally and internationally.

The outputs of the above scope of work were achieved and are reported in Chapters 2 to 7. Concluding remarks are also given at the end of each chapter.

The action research methodology approach followed proved to work exceptionally well for this type of research programme.

There were some important findings and achievements that emanated from the research programme. Some of these are highlighted below:

1. Novel instrumentation was developed for this research programme, including instruments such as the CoroCAM corona detection cameras (also the world-first day-time corona observation camera), the IH48 and OLCA leakage current and climatic logger systems, and the IPMA and IPMR site severity monitoring systems.

2. Of all the leakage current parameters monitored, the peak (I_h) and energy values of the leakage current were identified as the two main parameters needed to describe the leakage current activity on the test insulators. The test insulators' daily peak leakage current waveform surface conductivity value was found to be the main parameter to use as an indicator of the maximum interaction of the insulator material surface with the deposited pollution and wetting. Further, the accumulated electrical charge (or energy) flowing over the insulator surface was found to be the main parameter to use as an indicator of the continuous interaction of the insulator material surface with the deposited pollution and wetting.

3. A correlation was found between the climatic, environmental and leakage current measurements made during the research programme. Further investigation led to the use of multiple regression techniques to successfully determine the leakage current from the climatic and environmental parameters monitored.

4. Water drop corona was found to be present on all the test insulators. Contrary to current belief that it will be present mainly at the live side, and close to the end fitting, as suggested in the work of Phillips [61], it was found to be towards the shed tips and anywhere from the live to the dead end. Further, dry-band corona and discharges were found to be the most dominant form of electrical discharge activity on all the insulators. Electrical field simulations, which included the electrolytic pollution layer, confirmed the high electrical stresses present in the areas where electrical discharge activity was observed.

5. By eliminating the non-material design variables (e.g. creepage distance, connecting length, inter-shed spacing, profile, etc.) the material properties and relative performance under natural ageing and pollution conditions could be compared. This revealed some of the advantages and disadvantages of the materials tested during the

research programme, i.e. the surprisingly good performance of the RTV SR coated porcelain test insulator 4C and that of the reference porcelain insulator 3P. Further, the expected good performance of RG porcelain insulators was confirmed by the excellent leakage current performance results obtained from test insulator 8R.

6. The relative ranking results showed that the RG test insulator 8R had the best overall leakage current performance of all the insulators tested. The RTV SR coated porcelain insulator 4C was the next best performer followed by the HTV SR test insulator 1S. The EPDM test insulator 2E and the reference porcelain insulator 3P showed similar performance. The Cycloaliphatic epoxy resin test insulator 5A was the worst performer.

7. Guidelines were given to Eskom Distribution for the selection of insulation materials for use in polluted environments in South Africa, using the information and experience gained in this research programme.

8. A natural ageing and pollution test procedure [67] was developed for use at KIPTS based on the information and knowledge gained from this research programme. The KIPTS test procedure is now a formal Eskom national standard, and is part of the Eskom Distribution insulator products specifications, and it is gaining international acceptance.

9. A model and hypothesis are proposed to describe the electrical discharge activity that takes place on the test insulators and explain the difference in leakage current performance of the various materials.

10. Various publications (see publications list in Appendix), Eskom research reports, and Master's degree theses, emanated from this research programme.

Note: The results reported in this dissertation are relevant to the specific test insulators and caution must be applied when using this information for practical application in the field. For example, test insulators 3P, 4C, 5A and 8R cannot be used directly in the field, due to mechanical constraints of the shank. The author will not be held responsible for the misinterpretation or abuse of any information given in this dissertation.

The following recommendations are given for further investigation and research:

1. The effects of solar radiation on the levels of leakage current present on insulators (together with the thermal properties of various materials) should be further investigated.

2. Material ageing modes (especially in the dry-band regions) must be further investigated (by using in-depth material studies).

3. The hypothesis on the difference in leakage current performance of the test insulators, using the interaction of the insulator material surface with the electrolytic pollution layer (as discussed in section 7.2), should be further investigated.

4. Hydrophobicity as an indicator of the insulator surface condition should be re-evaluated, especially on hydrophilic pollution surfaces on normally hydrophobic SR material insulators.

5. The multiple regression techniques used to determine the leakage current from the climatic and environmental parameters monitored showed promising results. However, other techniques should also be further investigated, for example methods using neural networks.

The project was rewarding on a personal level. It started with Mother Nature, a flat piece of earth, and the expectation of a severe marine pollution environment. Backed by an excellent financial support system from Eskom Research, manufacturer interaction, electronic and software development companies, and the interaction with students and peers, the author had the opportunity to explore the research topic to the level reported in this dissertation. It is envisaged that further analysis of the large volume of data and information generated in the research programme will lead to many future interesting findings and publications.

REFERENCES

[1] IEC Publication 60815, "Guide for the selection of insulators in respect of polluted conditions", 1986.

[2] RG Houlgate, DA Swift, "Composite rod insulators for AC power lines: Electrical performance of various designs at a coastal station", IEEE Transactions on Power Delivery, Vol. 5, No. 4, October 1990.

[3] WL Vosloo, JP Holtzhausen, AHA Roediger, "Leakage current performance of naturally aged non-ceramic insulators under a severe marine environment", IEEE, Africon '96, Stellenbosch, South Africa, September 1996.

[4] WL Vosloo, "Koeberg insulator pollution test station (KIPTS): Final report for 1996", Eskom internal report, TRR/E/96/EL223, December 1996.

[5] RE Macey, "Eliminating substation flashover ", Energize, March/April 1999.

[6] RE Macey, "The performance of high voltage, outdoor insulation in polluted environments", Master of Science Thesis, University of Cape Town, South Africa, April 1981.

[7] RE Macey, "The performance of High Voltage, outdoor insulation in contaminated environments", Transactions of the SAIEE, Vol. 78, April 1981.

[8] H Weihe, JP Reynders, RE Macey, "Field Experience and Testing of new Insulator Types in South Africa", CIGRE-session, Paris 1980.

[9] JP Holtzhausen, JM Smith, OCT Potgieter, "The on site leakage current performance of insulators of various designs and materials as a function of weather data", ISH, Dresden, August 1991.

[10] JP Holtzhausen, "Leakage current monitoring on synthetic insulators at a severe coastal site", Transactions of the SAIEE, September 1994.

[11] FF Bologna, WL Vosloo, JP Holtzhausen, "Comparing the performance of non-ceramic insulators in industrially and marine polluted areas", CIGRE, 2nd South African Regional Conference: Electric Power Systems in Sub-equatorial Africa, Durban, South Africa, May 1994.

[12] CN Ravera, AC Britten, J Oliver, DA Swift, "Service experience with polymeric insulators in Eskom, South Africa", IEE conference on transmission and HV DC, London, May 1996.

[13] WL Vosloo, JP Holtzhausen, "Insulator pollution performance test station: Design and operation", South African Universities Power Engineering Conference (SAUPEC94), Cape Town, South Africa, January 1994.

[14] WL Vosloo, "Koeberg insulator pollution test station (KIPTS): Final report for 1998", Eskom internal report, TRR/E/98/EL125, December 1998.

[15] WL Vosloo, JP Holtzhausen, "The Design Principles of On-Line Insulator Test Stations to be used on Power Distribution and Transmission Networks" AFRICON96, Stellenbosch, South Africa, 1996.

[16] I Gutman, R Hartings, WL Vosloo, "Field testing of composite insulators at Natal test stations in South Africa", ISH 99, London, UK, August 1999.

[17] WL Vosloo, FF Bologna, "High Voltage Insulators: The Backbone of Transmission and Distribution networks", TRI Research Conference, Johannesburg, South Africa, October 1998.

[18] CIGRE Taskforce 33-04-01, "Polluted Insulators: A Review of Current Knowledge", June 1999.

[19] CIGRE Working Group 33-04, "The measurement of site pollution severity and its application to insulator dimensioning for a.c. systems", Electra No. 64, 1979.

[20] JP Holtzhausen, "A critical evaluation of AC pollution flashover models for HV insulators having hydrophilic surfaces", PhD Thesis, University of Stellenbosch, South Africa, 1977.

[21] RG Houlgate, "Natural testing of composite insulators at Dungeness insulator testing station", Non-ceramic outdoor insulation international workshop, SEE, Paris, France, April 1993.

[22] MP Verma, "Highest leakage current impulse as criterion for the performance of polluted insulators", CIGRE 33-73 (WG 04) (6) IWD.

[23] JP Holtzhausen, LP du Toit, "Insulator pollution: interrelationship of highest leakage current, specific creepage distance and salinity in a salt fog test", Transactions of the SAIEE, August 1987.

[24] R Wilkins, "Flashover voltage of high voltage insulators with uniform surface pollution films", Procedures of the IEE, Vol. 116, No. 3, pp. 457- 465, 1969.

[25] JD Cobine, "Gaseous Conductors: Theory and Engineering Applications", Dover Publications Inc., 1941.

[26] B Dick, "Approaching an action research thesis: an overview", 1997, Internet site http://www.scu.edu.au/schools/gcm/ar/arp/phd.html.

[27] L van Wyk, WL Vosloo, JP Holtzhausen, "Environmental profile for Koeberg Insulator Pollution Test Station (KIPTS)", South African Universities Power Engineering Conference (SAUPEC), South Africa, January 1998.

[28] WL Vosloo, "Koeberg insulator pollution test station (KIPTS): Final report for 1997", Eskom internal report, TRR/E/97/EL189, December 1997.

[29] CIGRE Taskforce 33.04.03, "Round Robin Pollution Monitor Study Test Protocol", 33-93 (TF 04-03) 5 WD, July 1993.

[30] WL Vosloo, "Non-ceramic insulator material sampling procedure", Eskom internal report, TRR/E/96/EL099, December 1996.

[31] IEC 60507, "Artificial pollution tests on high-voltage insulators to be used on a.c. systems", 1991.

[32] WL Vosloo, "Insulator Leakage Current Recorder", CIGRE 33-95 (WG 04), Mabula, South Africa, May 1995.

[33] WL Vosloo, GR Stolper, P Baker, "Daylight corona discharge observation and recording system", 10th International Symposium on High Voltage Engineering (ISH), Montreal, Canada, September 1997.

[34] OCT Potgieter, "Development and Evaluation of an Insulator Pollution Monitoring Apparatus", MSc Thesis, University of Stellenbosch, South Africa, October 1991.

[35] A Bertrazzi, G Perego, G Sampaoli, Y Vachiratarapadorn, V Eamsa-as, "A Device for the automatic measurement of surface conductivity of insulators", 6th International Symposium on High Voltage Engineering (ISH), New Orleans, USA, Aug/Sept 1989.

[36] P Davel, "Development of an Insulator Pollution Monitoring, Including an Analysis of the Effects of Environmental Variables on the Test Results", MSc Thesis, University of Stellenbosch, South Africa, December 1994.

[37] L van Wyk, "Insulator pollution monitoring: Evaluation of various methods of severity measurements at a coastal site", MSc Thesis, University of Stellenbosch, South Africa, December 1996.

[38] P Davel, WL Vosloo, JP Holtzhausen, "Low voltage measurement of the pollution on High Voltage insulators", UPEC, Galway, Ireland, September 1994.

[39] L van Wyk, JP Holtzhausen, WL Vosloo, "Relation between surface conductivity, leakage current and humidity of ceramic insulators", UPEC, Iraklio, Crete, September 1996.

[40] L Van Wyk, JP Holtzhausen, WL Vosloo, "Surface Conductance as an Indication of Leakage Current, obtained for a Marine Test Site", 10th International Symposium on High Voltage Engineering, Montreal, Canada, September 1997.

[41] WH Scwardt, LD Borrill, WL Vosloo, JP Holtzhausen, "Determination of a calibration procedure for an insulator pollution monitoring relay", South African Universities Power Engineering Conference (SAUPEC-2001), Cape Town, January 2001.

[42] CIGRE Working Group 33.04, Study Committee 33, "A critical comparison of artificial pollution test methods for HV Insulators", Electra No. 64, 1979.

[43] IEEE Working Group on Insulator Contamination, Lightning and Insulator Subcommittee, T&D Committee, "Application Guide for Insulator in a Contaminated Environment", IEEE Trans. on PA&S, Sep/Oct 1979.

[44] G Riquel, E Spangenberg, P Mirabel, JY Saison, "Wetting Process of Pollution Layer on High Voltage Glass Insulators", 9th International Symposium on High Voltage Engineering (ISH), Graz, Austria, August 1995.

[45] Dr AH Roediger, Roediger agencies, Institute for Polymer Science, University of Stellenbosch, South Africa (personal communications).

[46] South African Weather Bureau publication, "The Weather and Climate of the extreme south-western Cape", 1996.

[47] Gieck, "A collection of Technical Formulae", Gieck Verlag, Germany, 1996.

[48] F Potgieter, Cape Weather Wise, Koeberg Nuclear Power Station weather software (personal communications).

[49] Y Mizuno, H Nakamura, K Naito, "Dynamic simulation of risk of flashover of contaminated ceramic insulators", IEEE Transactions on Power Delivery, Vol. 12, No. 3, July 1997.

[50] RS Gorur, EA Cherney, JT Burnham, "Outdoor Insulators", Ravi S Gorur, Inc, Phoenix, Arizona, USA, 1999.

[51] PD Tyson, RA Preston-Whyte, "The Weather and Climate of Southern Africa", Oxford, 1998.

[52] H Bin Ahmad, A Salam, SB Buntat, TB Tamsir, "Mathematical model for prediction of salt contamination on Power System insulators in Malaysia", 12th CEPSI, Pattaya, Thailand, 2-6 November 1998.

[53] CIGRE Taskforce 33.13.03, "Round Robin Pollution Monitor Study", August 2000.

[54] G Besztercey, GG Karady, DL Ruff, "A novel method to measure the contamination level of insulators – spot contamination measurement", IEEE International symposium on electrical insulation, Arlington VA, USA, June 1998.

[55] J Kindersberger, M Kuhl, "Effect on hydrophobicity on insulator performance", 6th International Symposium on High Voltage Engineering, New Orleans, USA, 1989.

[56] EA Cherney, RS Gorur, "RTV silicone rubber coatings for outdoor insulators", IEEE Transactions on Dielectrics and Electrical Insulation, Vol. 6, No. 5, October 1999.

[57] N Yoshimura, S Kumagai, S Nishimura, "Electrical and environmental aging of silicone rubber used in outdoor insulation", IEEE Transactions on Dielectrics and Electrical Insulation, Vol. 6, No. 5, October 1999.

[58] STRI guide "Hydrophobicity classification guide" 92/1,1992.

[59] STRI guide "Guide for Visual Identification of Deterioration & Damage on Suspension Composite Insulators" Guide 5, 98/1.

[60] IEC 61109, "Composite insulators for AC overhead lines with a nominal voltage greater than 1000 V - Definitions, test methods and acceptance criteria", 1992.

[61] AJ Phillips, DJ Childs, HM Schneider, "Water Drop Corona effects on full-scale 500 kV non-ceramic insulators", IEEE Transactions on Power Delivery, Vol. 14, No. 1, January 1999.

[62] JL Rasolonjanahary, L Krähenbühl; A Nicolas, "Computation of electric fields and potential on polluted insulators using a boundary element method", IEEE Transactions on magnetics, Vol. 28, No. 2, March 1992.

[63] MARM Fernando, "Performance of non-ceramic insulators in tropical environments", PhD Thesis, Chalmers University of Technology, Sweden, 1999.

[64] WL Vosloo, JP Holtzhausen, "A proposed model explaining the difference between the leakage current performance of silicone and EPDM rubber insulators at KIPTS", CIGRE, 3rd South African Regional Conference, May 1998.

[65] De la O, RS Gorur, JT Burnham, "Electrical performance of non-ceramic insulators in artificial contamination tests, role of resting time", IEEE Transactions on Dielectrics and Electrical |Insulation, Vol. 3, No. 6, December 1996.

[66] K Morits, R Matsweka, S Matsui, Y Suzuki, Y Nakashima, "Practical application of semiconducting glazed insulators", International Conference on Electrical Engineering, Beijing, China, August 1996.

[67] WL Vosloo, R Swinny, JP Holtzhausen, "Koeberg insulator pollution test station (KIPTS) - an in-house insulator product ageing test standard", CIGRE 4th Southern Africa regional conference, Cape Town, October 2001.

[68] C Chatfield, "Statistics for technology", Penguin Books, 1970.

[69] JP Reynders, IR Jandrell, SM Reynders, "Review of ageing and recovery of silicone rubber insulation for outdoor use", IEEE Transactions on Dielectrics and Electrical |Insulation, Vol. 6, No. 5, October 1999.

REFERENCES

[1] IEC Publication 60815, "Guide for the selection of insulators in respect of polluted conditions", 1986.

[2] RG Houlgate, DA Swift, "Composite rod insulators for AC power lines: Electrical performance of various designs at a coastal station", IEEE Transactions on Power Delivery, Vol. 5, No. 4, October 1990.

[3] WL Vosloo, JP Holtzhausen, AHA Roediger, "Leakage current performance of naturally aged non-ceramic insulators under a severe marine environment", IEEE, Africon '96, Stellenbosch, South Africa, September 1996.

[4] WL Vosloo, "Koeberg insulator pollution test station (KIPTS): Final report for 1996", Eskom internal report, TRR/E/96/EL223, December 1996.

[5] RE Macey, "Eliminating substation flashover ", Energize, March/April 1999.

[6] RE Macey, "The performance of high voltage, outdoor insulation in polluted environments", Master of Science Thesis, University of Cape Town, South Africa, April 1981.

[7] RE Macey, "The performance of High Voltage, outdoor insulation in contaminated environments", Transactions of the SAIEE, Vol. 78, April 1981.

[8] H Weihe, JP Reynders, RE Macey, "Field Experience and Testing of new Insulator Types in South Africa", CIGRE-session, Paris 1980.

[9] JP Holtzhausen, JM Smith, OCT Potgieter, "The on site leakage current performance of insulators of various designs and materials as a function of weather data", ISH, Dresden, August 1991.

[10] JP Holtzhausen, "Leakage current monitoring on synthetic insulators at a severe coastal site", Transactions of the SAIEE, September 1994.

[11] FF Bologna, WL Vosloo, JP Holtzhausen, "Comparing the performance of non-ceramic insulators in industrially and marine polluted areas", CIGRE, 2nd South African Regional Conference: Electric Power Systems in Sub-equatorial Africa, Durban, South Africa, May 1994.

[12] CN Ravera, AC Britten, J Oliver, DA Swift, "Service experience with polymeric insulators in Eskom, South Africa", IEE conference on transmission and HV DC, London, May 1996.

[13] WL Vosloo, JP Holtzhausen, "Insulator pollution performance test station: Design and operation", South African Universities Power Engineering Conference (SAUPEC94), Cape Town, South Africa, January 1994.

[14] WL Vosloo, "Koeberg insulator pollution test station (KIPTS): Final report for 1998", Eskom internal report, TRR/E/98/EL125, December 1998.

[15] WL Vosloo, JP Holtzhausen, "The Design Principles of On-Line Insulator Test Stations to be used on Power Distribution and Transmission Networks" AFRICON96, Stellenbosch, South Africa, 1996.

[16] I Gutman, R Hartings, WL Vosloo, "Field testing of composite insulators at Natal test stations in South Africa", ISH 99, London, UK, August 1999.

[17] WL Vosloo, FF Bologna, "High Voltage Insulators: The Backbone of Transmission and Distribution networks", TRI Research Conference, Johannesburg, South Africa, October 1998.

[18] CIGRE Taskforce 33-04-01, "Polluted Insulators: A Review of Current Knowledge", June 1999.

[19] CIGRE Working Group 33-04, "The measurement of site pollution severity and its application to insulator dimensioning for a.c. systems", Electra No. 64, 1979.

[20] JP Holtzhausen, "A critical evaluation of AC pollution flashover models for HV insulators having hydrophilic surfaces", PhD Thesis, University of Stellenbosch, South Africa, 1977.

[21] RG Houlgate, "Natural testing of composite insulators at Dungeness insulator testing station", Non-ceramic outdoor insulation international workshop, SEE, Paris, France, April 1993.

[22] MP Verma, "Highest leakage current impulse as criterion for the performance of polluted insulators", CIGRE 33-73 (WG 04) (6) IWD.

[23] JP Holtzhausen, LP du Toit, "Insulator pollution: interrelationship of highest leakage current, specific creepage distance and salinity in a salt fog test", Transactions of the SAIEE, August 1987.

[24] R Wilkins, "Flashover voltage of high voltage insulators with uniform surface pollution films", Procedures of the IEE, Vol. 116, No. 3, pp. 457- 465, 1969.

[25] JD Cobine, "Gaseous Conductors: Theory and Engineering Applications", Dover Publications Inc., 1941.

[26] B Dick, "Approaching an action research thesis: an overview", 1997, Internet site http://www.scu.edu.au/schools/gcm/ar/arp/phd.html.

[27] L van Wyk, WL Vosloo, JP Holtzhausen, "Environmental profile for Koeberg Insulator Pollution Test Station (KIPTS)", South African Universities Power Engineering Conference (SAUPEC), South Africa, January 1998.

[28] WL Vosloo, "Koeberg insulator pollution test station (KIPTS): Final report for 1997", Eskom internal report, TRR/E/97/EL189, December 1997.

[29] CIGRE Taskforce 33.04.03, "Round Robin Pollution Monitor Study Test Protocol", 33-93 (TF 04-03) 5 WD, July 1993.

[30] WL Vosloo, "Non-ceramic insulator material sampling procedure", Eskom internal report, TRR/E/96/EL099, December 1996.

[31] IEC 60507, "Artificial pollution tests on high-voltage insulators to be used on a.c. systems", 1991.

[32] WL Vosloo, "Insulator Leakage Current Recorder", CIGRE 33-95 (WG 04), Mabula, South Africa, May 1995.

[33] WL Vosloo, GR Stolper, P Baker, "Daylight corona discharge observation and recording system", 10th International Symposium on High Voltage Engineering (ISH), Montreal, Canada, September 1997.

[34] OCT Potgieter, "Development and Evaluation of an Insulator Pollution Monitoring Apparatus", MSc Thesis, University of Stellenbosch, South Africa, October 1991.

[35] A Bertrazzi, G Perego, G Sampaoli, Y Vachiratarapadorn, V Eamsa-as, "A Device for the automatic measurement of surface conductivity of insulators", 6th International Symposium on High Voltage Engineering (ISH), New Orleans, USA, Aug/Sept 1989.

[36] P Davel, "Development of an Insulator Pollution Monitoring, Including an Analysis of the Effects of Environmental Variables on the Test Results", MSc Thesis, University of Stellenbosch, South Africa, December 1994.

[37] L van Wyk, "Insulator pollution monitoring: Evaluation of various methods of severity measurements at a coastal site", MSc Thesis, University of Stellenbosch, South Africa, December 1996.

[38] P Davel, WL Vosloo, JP Holtzhausen, "Low voltage measurement of the pollution on High Voltage insulators", UPEC, Galway, Ireland, September 1994.

[39] L van Wyk, JP Holtzhausen, WL Vosloo, "Relation between surface conductivity, leakage current and humidity of ceramic insulators", UPEC, Iraklio, Crete, September 1996.

[40] L Van Wyk, JP Holtzhausen, WL Vosloo, "Surface Conductance as an Indication of Leakage Current, obtained for a Marine Test Site", 10th International Symposium on High Voltage Engineering, Montreal, Canada, September 1997.

[41] WH Scwardt, LD Borrill, WL Vosloo, JP Holtzhausen, "Determination of a calibration procedure for an insulator pollution monitoring relay", South African Universities Power Engineering Conference (SAUPEC-2001), Cape Town, January 2001.

[42] CIGRE Working Group 33.04, Study Committee 33, "A critical comparison of artificial pollution test methods for HV Insulators", Electra No. 64, 1979.

[43] IEEE Working Group on Insulator Contamination, Lightning and Insulator Subcommittee, T&D Committee, "Application Guide for Insulator in a Contaminated Environment", IEEE Trans. on PA&S, Sep/Oct 1979.

[44] G Riquel, E Spangenberg, P Mirabel, JY Saison, "Wetting Process of Pollution Layer on High Voltage Glass Insulators", 9th International Symposium on High Voltage Engineering (ISH), Graz, Austria, August 1995.

[45] Dr AH Roediger, Roediger agencies, Institute for Polymer Science, University of Stellenbosch, South Africa (personal communications).

[46] South African Weather Bureau publication, "The Weather and Climate of the extreme south-western Cape", 1996.

[47] Gieck, "A collection of Technical Formulae", Gieck Verlag, Germany, 1996.

[48] F Potgieter, Cape Weather Wise, Koeberg Nuclear Power Station weather software (personal communications).

[49] Y Mizuno, H Nakamura, K Naito, "Dynamic simulation of risk of flashover of contaminated ceramic insulators", IEEE Transactions on Power Delivery, Vol. 12, No. 3, July 1997.

[50] RS Gorur, EA Cherney, JT Burnham, "Outdoor Insulators", Ravi S Gorur, Inc, Phoenix, Arizona, USA, 1999.

[51] PD Tyson, RA Preston-Whyte, "The Weather and Climate of Southern Africa", Oxford, 1998.

[52] H Bin Ahmad, A Salam, SB Buntat, TB Tamsir, "Mathematical model for prediction of salt contamination on Power System insulators in Malaysia", 12th CEPSI, Pattaya, Thailand, 2-6 November 1998.

[53] CIGRE Taskforce 33.13.03, "Round Robin Pollution Monitor Study", August 2000.

[54] G Besztercey, GG Karady, DL Ruff, "A novel method to measure the contamination level of insulators – spot contamination measurement", IEEE International symposium on electrical insulation, Arlington VA, USA, June 1998.

[55] J Kindersberger, M Kuhl, "Effect on hydrophobicity on insulator performance", 6th International Symposium on High Voltage Engineering, New Orleans, USA, 1989.

[56] EA Cherney, RS Gorur, "RTV silicone rubber coatings for outdoor insulators", IEEE Transactions on Dielectrics and Electrical Insulation, Vol. 6, No. 5, October 1999.

[57] N Yoshimura, S Kumagai, S Nishimura, "Electrical and environmental aging of silicone rubber used in outdoor insulation", IEEE Transactions on Dielectrics and Electrical Insulation, Vol. 6, No. 5, October 1999.

[58] STRI guide "Hydrophobicity classification guide" 92/1,1992.

[59] STRI guide "Guide for Visual Identification of Deterioration & Damage on Suspension Composite Insulators" Guide 5, 98/1.

[60] IEC 61109, "Composite insulators for AC overhead lines with a nominal voltage greater than 1000 V - Definitions, test methods and acceptance criteria", 1992.

[61] AJ Phillips, DJ Childs, HM Schneider, "Water Drop Corona effects on full-scale 500 kV non-ceramic insulators", IEEE Transactions on Power Delivery, Vol. 14, No. 1, January 1999.

[62] JL Rasolonjanahary, L Krähenbühl; A Nicolas, "Computation of electric fields and potential on polluted insulators using a boundary element method", IEEE Transactions on magnetics, Vol. 28, No. 2, March 1992.

[63] MARM Fernando, "Performance of non-ceramic insulators in tropical environments", PhD Thesis, Chalmers University of Technology, Sweden, 1999.

[64] WL Vosloo, JP Holtzhausen, "A proposed model explaining the difference between the leakage current performance of silicone and EPDM rubber insulators at KIPTS", CIGRE, 3rd South African Regional Conference, May 1998.

[65] De la O, RS Gorur, JT Burnham, "Electrical performance of non-ceramic insulators in artificial contamination tests, role of resting time", IEEE Transactions on Dielectrics and Electrical |Insulation, Vol. 3, No. 6, December 1996.

[66] K Morits, R Matsweka, S Matsui, Y Suzuki, Y Nakashima, "Practical application of semiconducting glazed insulators", International Conference on Electrical Engineering, Beijing, China, August 1996.

[67] WL Vosloo, R Swinny, JP Holtzhausen, "Koeberg insulator pollution test station (KIPTS) - an in-house insulator product ageing test standard", CIGRE 4th Southern Africa regional conference, Cape Town, October 2001.

[68] C Chatfield, "Statistics for technology", Penguin Books, 1970.

[69] JP Reynders, IR Jandrell, SM Reynders, "Review of ageing and recovery of silicone rubber insulation for outdoor use", IEEE Transactions on Dielectrics and Electrical |Insulation, Vol. 6, No. 5, October 1999.

APPENDIX A: LIST OF VARIABLES

Variable	Description
Δ_t	Time increment in ms
A	10 (Arc constant)
a	0.53 (Constant)
α	Wind Direction
A_{ins}	Area of washed or sampled insulator (cm^2)
A_{pol}	Cross sectional area of the electrolytic pollution layer at position *l* in m^2
b_i	Regression coefficients (i = 1,2, ...N)
b_o	Intercept coefficient
C_{db}	Capacitance of the dry band in pF
D	Days DDG installed
$D(l)$	Diameter of insulator at position *l* along the insulator creepage path in mm
F	Sampling frequency in Hz
G_{ins}	Conductance of the insulator in µS
$G_{ins}(t)$	Conductance of the insulator at time t in µS
$G_{pol}(l_{db})$	Conductance of the electrolytic pollution layer considering the dry band in µS
h_{pol}	Thickness of the uniform electrolytic pollution layer in mm
$i(n)$	n^{th} value of the leakage current *i* at time t in ampere
$i(t)$	Leakage current in mA
I_h	Peak value of the leakage current in mA
I_{perm}	Highest permissible peak value of the leakage current
k_1	7.6 (Holtzhausen)
k_2	0.35 (Holtzhausen)

Variable	Description
k_t	Temperature constant
L	Total insulator creepage distance in mm
l_{arc}	Length of the arc in mm
l_{db}	Length of the dry band in mm
L_{Trfr}	Winding inductance in mH
M_1	Weight of dry clean filter paper in mg
M_2	Weight of dry contaminated filter paper in mg
N	Number of samples
$Q_{ins(pos)}$	Positive electrical charge in Coulomb
R_c	Critical insulator resistance in MΩ, which is the critical value R_{ins}
Rh	Relative humidity
R_{ins}	Resistance of the insulator in MΩ
R_{pol}	Surface layer resistance of the insulator electrolytic pollution layer without an arc in MΩ,
$R_{pol(l_{db})}$	Resistance of the insulator electrolytic pollution layer with a dry band in MΩ
R_{Trfr}	Winding resistance in ohm
T_a	Atmospheric temperature in °C
T	Time interval in ms
T_{Dew}	Dew point temperature in °C
t_s	Solution temperature in °C
U_{max}	Maximum rms system voltage phase to phase in kV
$v_{(n)}$	n^{th} value of the supply voltage v at time t in volts
$v_{(t)}$	Supply voltage in kV

Variable	Description
$V_{\perp,Left}$	Wind speed perpendicular to coast line from left (West)
$V_{\perp,Right}$	Wind speed perpendicular to coast line from right (East)
V_c	Critical insulator flashover voltage in kV
V_d	Volume distilled water used (cm^3)
$v_{db}(t)$	Voltage across the dry band in kV
V_{Ih}	Peak value of the supply voltage in kV when the leakage current is at peak
$V_{ll,Bottom}$	Wind speed parallel to coast line from bottom (South)
$V_{ll,Top}$	Wind speed parallel to coast line from top (North)
V_p	Peak value of the supply voltage in kV
$v_{pol}(t)$	Voltage across the electrolytic pollution layer in kV
V_w	Wind speed in m/s
W_{ins}	Energy loss over the insulator in joules
x,y	Variables
X_i	Independent variables (i = 1,2, ...N)
Y	Dependent variable
σ	Volume conductivity of insulator electrolytic pollution layer in µS/mm
σ_{20}	Volume conductivity corrected to 20 °C
σ_d	Measured volume conductivity of distilled water in µS/cm
σ_{ins}	Conductivity of insulator in µS
σ_s	Surface conductivity of insulator electrolytic pollution layer in µS
σ_t	Measured volume conductivity in µS/cm
β	Direction of coastline to top bottom axes (20°)

APPENDIX B: TIME LINE

Time line (Week, Day and Date) for the Winter (12/04/1999 to 10/10/1999) and Summer (11/10/1999 to 16/04/2000) test periods

Week	Day	Date	Week	Day	Date	Week	Day	Date	Week	Day	Date	Week	Day	Date	Week	Day	Date	Week	Day	Date	Week	Day	Date
	1	12-04-99		43	24-05-99		85	05-07-99		127	16-08-99		169	27-09-99		211	08-11-99		253	20-12-99		295	31-01-00		337	13-03-00
	2	13-04-99		44	25-05-99		86	06-07-99		128	17-08-99		170	28-09-99		212	09-11-99		254	21-12-99		296	01-02-00		338	14-03-00
	3	14-04-99		45	26-05-99		87	07-07-99		129	18-08-99		171	29-09-99		213	10-11-99		255	22-12-99		297	02-02-00		339	15-03-00
1	4	15-04-99	7	46	27-05-99	13	88	08-07-99	19	130	19-08-99	25	172	30-09-99	31	214	11-11-99	37	256	23-12-99	43	298	03-02-00	49	340	16-03-00
	5	**16-04-99**		47	28-05-99		89	09-07-99		131	20-08-99		173	01-10-99		215	12-11-99		257	24-12-99		299	04-02-00		341	17-03-00
	6	17-04-99		48	29-05-99		90	10-07-99		132	21-08-99		174	02-10-99		216	13-11-99		258	25-12-99		300	05-02-00		342	18-03-00
	7	18-04-99		49	30-05-99		91	11-07-99		133	22-08-99		175	03-10-99		217	14-11-99		259	26-12-99		301	06-02-00		343	19-03-00
	8	19-04-99		50	31-05-99		92	12-07-99		134	23-08-99		176	04-10-99		218	15-11-99		260	27-12-99		302	07-02-00		344	20-03-00
	9	20-04-99		51	01-06-99		93	13-07-99		135	24-08-99		177	05-10-99		219	16-11-99		261	28-12-99		303	08-02-00		345	21-03-00
	10	21-04-99		52	02-06-99		94	14-07-99		136	25-08-99		178	06-10-99		220	17-11-99		262	29-12-99		304	09-02-00		346	22-03-00
2	11	22-04-99	8	53	03-06-99	14	95	15-07-99	20	137	26-08-99	26	179	07-10-99	32	221	18-11-99	38	263	30-12-99	44	305	10-02-00	50	347	23-03-00
	12	**23-04-99**		54	04-06-99		96	16-07-99		138	27-08-99		180	08-10-99		222	19-11-99		264	31-12-99		306	11-02-00		348	24-03-00
	13	24-04-99		55	05-06-99		97	17-07-99		139	28-08-99		181	09-10-99		223	20-11-99		265	01-01-00		307	12-02-00		349	25-03-00
	14	25-04-99		56	06-06-99		98	18-07-99		140	29-08-99		182	10-10-99		224	21-11-99		266	02-01-00		308	13-02-00		350	26-03-00
	15	26-04-99		57	07-06-99		99	19-07-99		141	30-08-99		183	11-10-99		225	22-11-99		267	03-01-00		309	14-02-00		351	27-03-00
	16	27-04-99		58	08-06-99		100	20-07-99		142	31-08-99		184	12-10-99		226	23-11-99		268	04-01-00		310	15-02-00		352	28-03-00
	17	28-04-99		59	09-06-99		101	21-07-99		143	01-09-99		185	13-10-99		227	24-11-99		269	05-01-00		311	16-02-00		353	29-03-00
3	18	29-04-99	9	60	10-06-99	15	102	22-07-99	21	144	02-09-99	27	186	14-10-99	33	228	25-11-99	39	270	06-01-00	45	312	17-02-00	51	354	30-03-00
	19	**30-04-99**		61	11-06-99		103	23-07-99		145	03-09-99		187	15-10-99		229	26-11-99		271	07-01-00		313	18-02-00		355	31-03-00
	20	01-05-99		62	12-06-99		104	24-07-99		146	04-09-99		188	16-10-99		230	27-11-99		272	08-01-00		314	19-02-00		356	01-04-00
	21	02-05-99		63	13-06-99		105	25-07-99		147	05-09-99		189	17-10-99		231	28-11-99		273	09-01-00		315	20-02-00		357	02-04-00
	22	03-05-99		64	14-06-99		106	26-07-99		148	06-09-99		190	18-10-99		232	29-11-99		274	10-01-00		316	21-02-00		358	03-04-00
	23	04-05-99		65	15-06-99		107	27-07-99		149	07-09-99		191	19-10-99		233	30-11-99		275	11-01-00		317	22-02-00		359	04-04-00
	24	05-05-99		66	16-06-99		108	28-07-99		150	08-09-99		192	20-10-99		234	01-12-99		276	12-01-00		318	23-02-00		360	05-04-00
4	25	06-05-99	10	67	17-06-99	16	109	29-07-99	22	151	09-09-99	28	193	21-10-99	34	235	02-12-99	40	277	13-01-00	46	319	24-02-00	52	361	06-04-00
	26	**07-05-99**		68	18-06-99		110	30-07-99		152	10-09-99		194	22-10-99		236	03-12-99		278	14-01-00		320	25-02-00		362	07-04-00
	27	08-05-99		69	19-06-99		111	31-07-99		153	11-09-99		195	23-10-99		237	04-12-99		279	15-01-00		321	26-02-00		363	08-04-00
	28	09-05-99		70	20-06-99		112	01-08-99		154	12-09-99		196	24-10-99		238	05-12-99		280	16-01-00		322	27-02-00		364	09-04-00
	29	10-05-99		71	21-06-99		113	02-08-99		155	13-09-99		197	25-10-99		239	06-12-99		281	17-01-00		323	28-02-00		365	10-04-00
	30	11-05-99		72	22-06-99		114	03-08-99		156	14-09-99		198	26-10-99		240	07-12-99		282	18-01-00		324	29-02-00		366	11-04-00
	31	12-05-99		73	23-06-99		115	04-08-99		157	15-09-99		199	27-10-99		241	08-12-99		283	19-01-00		325	01-03-00		367	12-04-00
5	32	13-05-99	11	74	24-06-99	17	116	05-08-99	23	158	16-09-99	29	200	28-10-99	35	242	09-12-99	41	284	20-01-00	47	326	02-03-00	53	368	13-04-00
	33	**14-05-99**		75	25-06-99		117	06-08-99		159	17-09-99		201	29-10-99		243	10-12-99		285	21-01-00		327	03-03-00		**369**	**14-04-00**
	34	15-05-99		76	26-06-99		118	07-08-99		160	18-09-99		202	30-10-99		244	11-12-99		286	22-01-00		328	04-03-00		370	15-04-00
	35	16-05-99		77	27-06-99		119	08-08-99		161	19-09-99		203	31-10-99		245	12-12-99		287	23-01-00		329	05-03-00		371	16-04-00
	36	17-05-99		78	28-06-99		120	09-08-99		162	20-09-99		204	01-11-99		246	13-12-99		288	24-01-00		330	06-03-00			
	37	18-05-99		79	29-06-99		121	10-08-99		163	21-09-99		205	02-11-99		247	14-12-99		289	25-01-00		331	07-03-00			
	38	19-05-99		80	30-06-99		122	11-08-99		164	22-09-99		206	03-11-99		248	15-12-99		290	26-01-00		332	08-03-00			
6	39	20-05-99	12	81	01-07-99	18	123	12-08-99	24	165	23-09-99	30	207	04-11-99	36	249	16-12-99	42	291	27-01-00	48	333	09-03-00			
	40	**21-05-99**		**82**	**02-07-99**		**124**	**13-08-99**		**166**	**24-09-99**		**208**	**05-11-99**		**250**	**17-12-99**		**292**	**28-01-00**		**334**	**10-03-00**			
	41	22-05-99		83	03-07-99		125	14-08-99		167	25-09-99		209	06-11-99		251	18-12-99		293	29-01-00		335	11-03-00			
	42	23-05-99		84	04-07-99		126	15-08-99		168	26-09-99		210	07-11-99		252	19-12-99		294	30-01-00		336	12-03-00			

Note: Winter weeks are indicated in **blue**, and summer in **red**. The weeks when daily electrical discharge activity were made are shaded in grey and Friday visual inspection dates shown in **bold**.

APPENDIX C: STATISTICAL METHODS

A brief description of the statistical methods used in this dissertation is given below.

C 1 ABSOLUTE AND RESULTING VALUE PLOTS

Absolute: The maximum of the mathematical absolute of the positive and negative data is presented as a positive value per measuring interval.

Resulting: The resulting value is the summation of the absolute positive and negative data per measuring interval.

C 2 ACCUMULATIVE VALUE WITH TIME PLOTS

The accumulative value plots show the growth of the summated data per measuring interval with time.

C 3 TIME OF DAY TRENDS (MAXIMUM, MINIMUM AND MEAN)

The time of day trend plots show the maximum, minimum, and mean (average) value, in relation to time of day, in steps of the measuring interval, of the relevant data (e.g. leakage current) over a selected period.

C 4 PROBABILITY OF EXCEEDING ABSCISSA PLOTS

The data values are presented on the x-axes, sorted in ascending order (small to large). The corresponding probability is plotted in percentage on the y-axes, in steps of 100 divided by the number of data values. The resulting values on the curve are interpreted as the percentage probability of exceeding the corresponding x-axes value. There is virtually a 100% probability of exceeding the minimum data value, and virtually a 0% probability of exceeding the maximum.

C 5 POLAR PLOTS

Polar plots (in the form of a scatter plot) are used here to present the selected data in relation to the wind direction at the time.

C 6 WIND SPEED PARALLEL AND PERPENDICULAR TO THE COASTLINE

The wind speed parallel and perpendicular to the coastline is shown in Figure C. 1 and defined in equations C1 to C4 below.

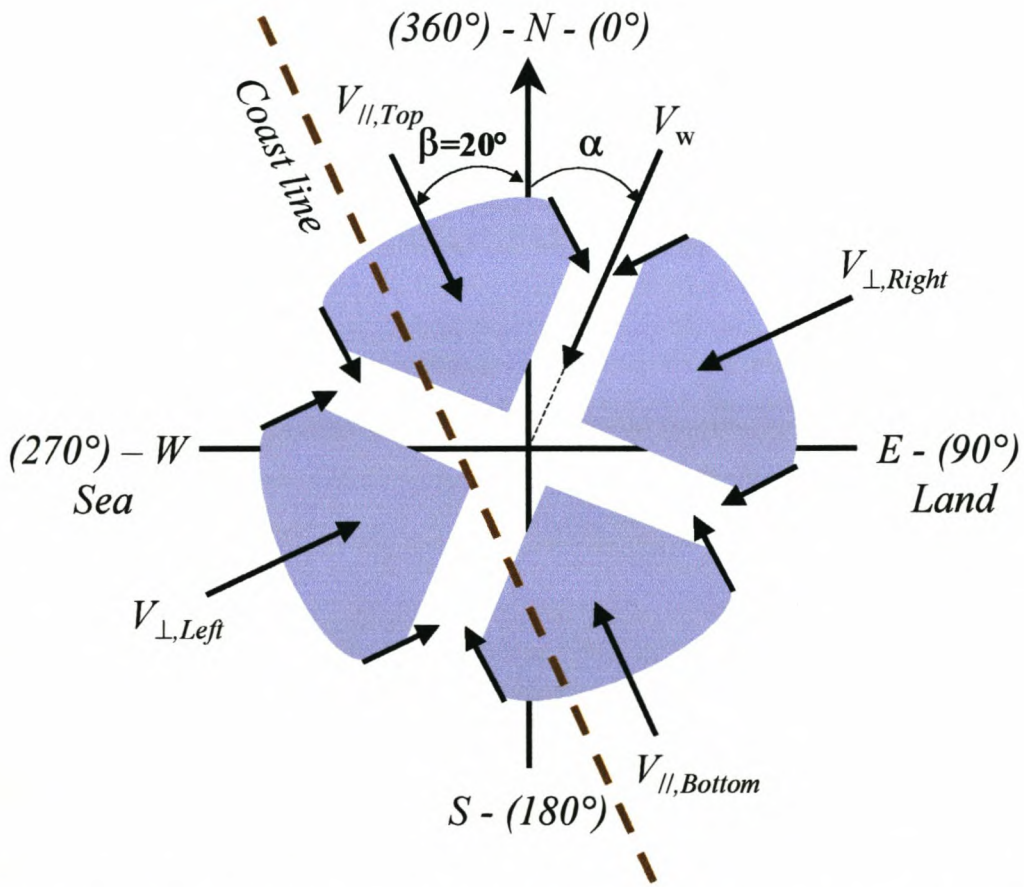

Figure C. 1 Diagram showing sea and land winds and also winds parallel to the coastline.

$$V_{//,Top} = V_w \cdot \left|\cos(\beta - \alpha)\right| \quad where \quad (270 - \beta) \le \alpha \le (90 - \beta) \tag{C1}$$

$$V_{//,Bottom} = V_w \cdot \left|\cos(\beta - \alpha)\right| \quad where \quad (360 - \beta) \le \alpha \le (180 - \beta) \tag{C2}$$

$$V_{\perp,Left} = V_w \cdot |\sin(\beta - \alpha)| \quad where \quad (270 - \beta) \leq \alpha \leq (90 - \beta) \tag{C3}$$

$$V_{\perp,Right} = V_w \cdot |\sin(\beta - \alpha)| \quad where \quad (360 - \beta) \leq \alpha \leq (180 - \beta) \tag{C4}$$

where

$V_{//,Top}$ = wind speed parallel to coastline from top (North)

$V_{//,Bottom}$ = wind speed parallel to coastline from bottom (South)

$V_{\perp,Rignt}$ = wind speed perpendicular to coastline from right (East)

$V_{\perp,Left}$ = wind speed perpendicular to coastline from right (West)

V_w = wind speed in m/s

β = direction of coastline to top bottom axes (20°)

α = wind direction

C 7 CROSS CORRELATION MATRICES

Correlation is a measure of the relation between two variables. Correlation coefficients can range from –1 to 1. The value of -1 represents a perfect negative correlation while a value of 1 represents a perfect positive correlation. A value of 0 represents a lack of correlation.

The correlation coefficient (*r*) is given as [68]:

$$r = \frac{\sum_{i=1}^{N}[(x_i - \bar{x}) \cdot (y_i - \bar{y})]}{\sqrt{\sum_{i=1}^{N}(x_i - \bar{x})^2 \cdot \sum_{i=1}^{N}(y_i - \bar{y})^2}} \tag{C5}$$

where

x,y = variables

N = number of samples

and

$$\bar{x} = \frac{\sum_{i=1}^{N} x_i}{N} \text{ and } \bar{y} = \frac{\sum_{i=1}^{N} y_i}{N}$$

If the correlation coefficient is squared, then the resulting value (the coefficient of determination) will represent the "strength" or "magnitude" of the relationship.

The coefficient of determination (0 – poor, and 1 – excellent) is given as [68]:

$$R^2 = r \cdot r \tag{C6}$$

where

r = correlation coefficient

C 8 LINEAR REGRESSION

The general purpose of a linear regression is to learn more about the relationship between several independent (predictor) variables and a dependent (criterion) variable. The main use would be for prediction of the dependant variable value using regression constants determined from historic values and the values of measured independent variables.

C 8.1 LINEAR

The linear model structure used for the regression technique is given as [68]:

$$Y = b_0 + b_1 X_1 + b_2 X_2 + \ldots + b_N X_N \tag{C7}$$

where

Y = dependent variable

X_i = independent variables (i = 1,2, ... N)

b_0 = intercept coefficient

b_i = regression coefficients (i = 1,2, ... N)

The linear regression function of Microsoft Excel (Office 2000) is used to calculate the regression and intercept coefficients.

C 8.2 NON-LINEAR TO LINEAR CONVERSION

The relationship can be non-linear and given as [68]:

$$y = k \cdot x_1^{b_1} \cdot x_2^{b_2} \cdot \ldots \cdot x_N^{b_N} \qquad \text{(C8)}$$

Taking the natural log on both sides to convert the equation to a linear format, then

$$\ln(y) = \ln(k) + b_1 \cdot \ln(x_1) + b_2 \cdot \ln(x_2) + \ldots + b_N \cdot \ln(x_N) \qquad \text{(C9)}$$

let

$$Y = \ln(y),\ X_i = \ln(x_i) \text{ and } b_0 = \ln(k)$$

then

$$Y = b_0 + b_1 X_1 + b_2 X_2 + \ldots + b_N X_N \qquad \text{(C10)}$$

which has exactly the same format as the linear equation C7 above

where

Y	=	dependent variable
X_i	=	predictor variables (i = 1,2, ... N)
b_0	=	intercept coefficient
b_i	=	regression coefficients (i = 1,2, ... N)

The multiple linear regression function of Microsoft Excel (Office 2000) is used to calculate the regression and intercept coefficients.

APPENDIX D: INSULATOR SURFACE CONDITION INSPECTIONS

Note that all surface condition inspections were done on the Friday of the week.

Surface condition inspection of week 1

HTV SR insulator 1S: Energised – No signs of deterioration were found. **Non-energised –** No signs of deterioration were found.

EPDM insulator 2E: Energised – Light signs of patchy discolouration were found. Light corrosion run off from the dead end-fitting was noted on the shed top (also on the non-energised). **Non-energised –** No signs of deterioration were found.

Porcelain insulator 3P: Energised – No signs of material deterioration were found. However, light corrosion run off from the dead end-fitting was noted on the shed top (also on the non-energised). **Non-energised –** No signs of material deterioration were found.

RTV SR coated porcelain insulator 4C: Energised – No signs of material deterioration were found. Light corrosion run off from the dead end-fitting was noted on the shed top (also on the non-energised). **Non-energised –** No signs of material deterioration were found.

Cycloaliphatic insulator 5A: Energised – No signs of deterioration were found. **Non-energised –** No signs of deterioration were found.

Surface condition inspection of week 2

HTV SR insulator 1S: Energised – The first signs of possible dry band activity were observed, showing light discolouration. **Non-energised –** No signs of deterioration were found.

EPDM insulator 2E: Energised – Light patchy discolouration was still found. Light corrosion run off from the dead end-fitting was still noted on the shed top (also on the non-energised). **Non-energised –** No signs of deterioration were found.

Porcelain insulator 3P: Energised – No signs of material deterioration were found. However, light corrosion run off from the dead end-fitting was still noted on the shed top (also on the non-energised). **Non-energised** – No signs of material deterioration were found.

RTV SR coated porcelain insulator 4C: Energised – Light patchy discolouration (pink in colour) on the bottom of all sheds was found. Light corrosion run off from the dead end-fitting was still noted on the shed top (also on the non-energised). **Non-energised** – No signs of material deterioration were found.

Cycloaliphatic insulator 5A: Energised – The first signs of slight blackening in the mould line were observed (see Figure D.1, which also shows the initially good hydrophobic properties of the insulator). **Non-energised** – No signs of deterioration were found.

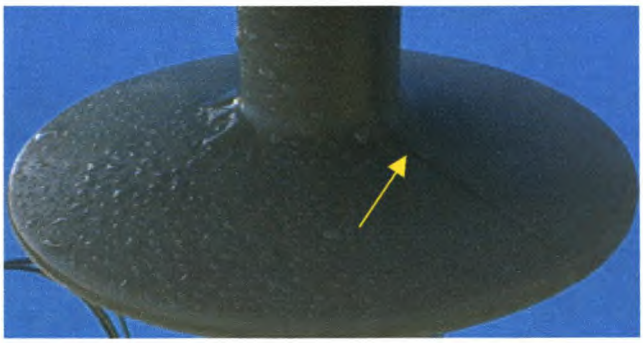

Figure D.1 Photo of slight blackening in mould line on insulator 5A observed in week 2.

Surface condition inspection on the Friday of week 3

HTV SR insulator 1S: Energised – Clear signs of dry band activity were observed, with associated light discolouration. **Non-energised** – No signs of deterioration was found.

EPDM insulator 2E: Energised – The first signs of possible dry band activity were observed, showing light discolouration. Light patchy discolouration was still found. Light corrosion run off from the dead end-fitting was still noted on the shed top (also on the non-energised) and progressed to the shed tip. **Non-energised** – No signs of deterioration were found.

Porcelain insulator 3P: Energised – No signs of material deterioration were found. However, light corrosion run off from the dead end-fitting was still noted on the shed top (also on the non-energised). **Non-energised** – No signs of material deterioration were found.

RTV SR coated porcelain insulator 4C: Energised – The first signs of possible dry band activity were observed, showing light discolouration (pink in colour). Light patchy discolouration was still found. Light corrosion run off from the dead end-fitting was still noted on the shed top (also on the non-energised). **Non-energised** – No signs of material deterioration were found.

Cycloaliphatic insulator 5A: Energised – Slight blackening in the mould line was still observed. **Non-energised** – No signs of deterioration were found.

Surface condition inspection of week 4

HTV SR insulator 1S: Energised – Clear signs of dry band activity were still observed, with associated light discolouration. The first signs of end-fitting corrosion affecting the polymeric material moulded over it were observed on the dead end (see Figure D.2). **Non-energised** - No signs of deterioration were found.

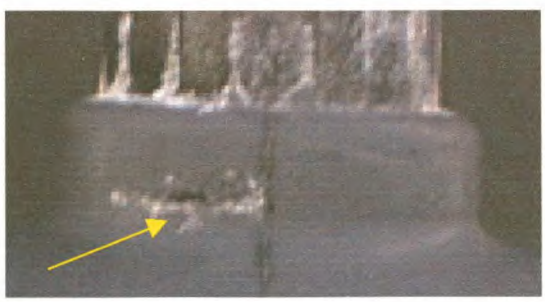

Figure D.2 Photo of end-fitting corrosion (dead end) affecting the polymer material on insulator 1S observed in week 4.

EPDM insulator 2E: Energised – Signs of possible dry band activity were still observed, showing light discolouration. Light patchy discolouration was still found. Light corrosion run off from the dead end-fitting was still noted (also on the non-energised). **Non-energised** – No signs of deterioration were found.

Porcelain insulator 3P: Energised – No signs of material deterioration were found. However, light corrosion run off from the dead end-fitting was still noted on the shed top (also on the non-energised). **Non-energised** – No signs of material deterioration were found.

RTV SR coated porcelain insulator 4C: Energised – Clear signs of dry band activity were observed, showing light discolouration (see Figure D.3). Light patchy discolouration was still found. Light corrosion run off from the dead end-fitting was still noted on the shed top (also on the non-energised). **Non-energised** – No signs of material deterioration were found.

Figure D.3 Photo of dry band activity on insulator 4C observed in week 4.

Cycloaliphatic insulator 5A: Energised – Blackening in the mould line was still observed. **Non-energised** – No signs of deterioration were found.

Surface condition inspection of week 5

HTV SR insulator 1S: Energised – Clear signs of dry band activity were still observed, with associated light discolouration. More prominent signs of end-fitting corrosion affecting the polymeric material moulded over it were observed on the dead end. **Non-energised** – No signs of deterioration were found.

EPDM insulator 2E: Energised – Signs of dry band activity were still observed, showing light discolouration. Light patchy discolouration was still found. Light corrosion run off from the dead end-fitting was still noted (also on the non-energised). **Non-energised** – No signs of deterioration were found.

Porcelain insulator 3P: Energised – No signs of material deterioration were found. However, the first signs of dry band activity were noted, in the form of a white residue. Light corrosion run off from the dead end-fitting was still noted on the shed top (also on the non-energised). **Non-energised** – No signs of material deterioration were found.

RTV SR coated porcelain insulator 4C: Energised – Clear signs of dry band activity were still observed, showing medium discolouration. Patchy discolouration was still found. Light corrosion run off from the dead end-fitting was still noted on the shed top (also on the non-energised). **Non-energised** – No signs of material deterioration were found.

Cycloaliphatic insulator 5A: Energised – Blackening in the mould line was still observed and the first signs of white discolouration adjacent to the mould line were noted. The first signs of possible dry band activity were observed, showing light discolouration. **Non-energised** – No signs of deterioration were found.

Surface condition inspection of week 6

HTV SR insulator 1S: Energised – Clear signs of dry band activity were still observed, now with more prominent, medium, discolouration. Clear signs of end-fitting corrosion affecting the polymeric material moulded over it were still observed on the dead end. **Non-energised** - No signs of deterioration were found.

EPDM insulator 2E: Energised – Signs of dry band activity were still observed, showing light discolouration. Light patchy discolouration was still found. Light corrosion run off from the dead end-fitting was still noted (also on the non-energised). The first signs of end-fitting corrosion affecting the polymeric material moulded over it were observed on the dead end. **Non-energised** – No signs of deterioration were found.

Porcelain insulator 3P: Energised – No signs of material deterioration were found. Signs of dry band activity were still noted, in the form of a white residue. Light corrosion run off from the dead end-fitting was still noted on the shed top (also on the non-energised). **Non-energised** – No signs of material deterioration were found.

RTV SR coated porcelain insulator 4C: Energised – Clear signs of dry band activity were still observed, showing medium discolouration. Patchy discolouration was still found. Light corrosion run off from the dead end-fitting was still noted on the shed top (also on the non-energised). **Non-energised –** No signs of material deterioration were found.

Cycloaliphatic insulator 5A: Energised – Blackening in the mould line and white discolouration adjacent to the mould line (see Figure D.4, which also shows the worsening hydrophobic properties of the insulator) was still observed. Dry band activity was still observed, showing light black discolouration. **Non-energised –** No signs of deterioration were found.

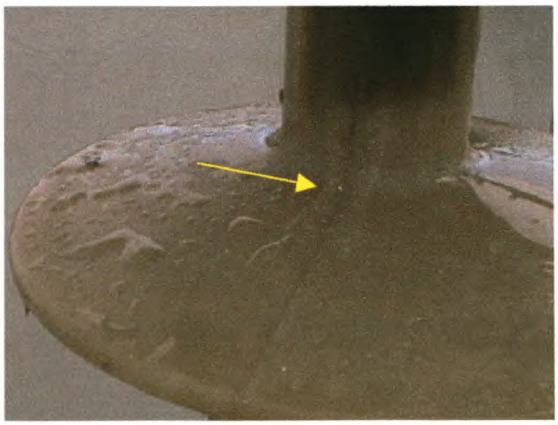

Figure D.4 Photo showing black and white discolouration at mould line on insulator 5A observed in week 6.

Surface condition inspection of week 12

HTV SR insulator 1S: Energised – Clear signs of dry band activity were still observed, with associated medium discolouration. Clear signs of end-fitting corrosion affecting the polymeric material moulded over it were still observed on the dead end and started to show for the first time on the live end. **Non-energised** - No signs of deterioration were found.

EPDM insulator 2E: Energised – Signs of dry band activity were still observed, showing light discolouration. Light patchy discolouration was still found. Light corrosion run off from the dead end-fitting was still noted (also on the non-energised). Signs of end-fitting

corrosion affecting the polymeric material moulded over it were still observed on the dead end and started to show for the first time on the live end. **Non-energised** – No signs of deterioration were found.

Porcelain insulator 3P: Energised – No signs of material deterioration were found. Signs of dry band activity were still noted, in the form of a white residue. Light corrosion run off from the dead end-fitting was still noted on the shed top (also on the non-energised). **Non-energised** – No signs of material deterioration were found.

RTV SR coated porcelain insulator 4C: Energised – Clear signs of dry band activity were still observed, showing medium discolouration (the colour is starting to change from pink to white). Patchy discolouration was still found. Light signs of crazing (possibly in the pollution layer) were observed for the first time. Light corrosion run off from the dead end-fitting was still noted on the shed top (also on the non-energised). **Non-energised** – No signs of material deterioration were found.

Cycloaliphatic insulator 5A: Energised – Blackening in the mould line and white discolouration adjacent to the mould line was still observed. Dry band activity was still observed, showing light discolouration. The first signs of crazing were observed. **Non-energised** – No signs of deterioration were found.

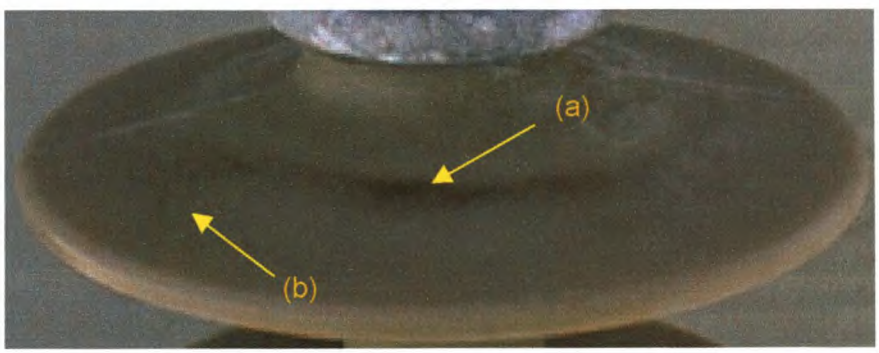

Figure D.5 Photo showing (a) signs of dry band activity with associated discolouration and (b) light crazing on insulator 5A observed in week 12.

Surface condition inspection of week 18

HTV SR insulator 1S: Energised - Medium discolouration in the regions of the dry bands was still observed. Light corrosion run off from the dead end-fitting was noted on the shed top for the first time (also on the non-energised). End-fitting corrosion protruding through the polymeric material moulded over it was observed for the first time on both the dead and live ends. **Non-energised** - Signs of end-fitting corrosion affecting the polymeric material moulded over it were observed for the first time on both ends. However, no further signs of deterioration were found.

EPDM insulator 2E: Energised – Signs of dry band activity were still observed, showing light discolouration. Light patchy discolouration was still found. Light corrosion run off from the dead end-fitting was still noted (also on the non-energised). Clear signs of end-fitting corrosion affecting the polymeric material moulded over it were still observed on both ends and started to protrude on the dead end. **Non-energised** – Signs of end-fitting corrosion affecting the polymeric material moulded over it were observed for the first time on both ends. However, no further signs of deterioration were found.

Porcelain insulator 3P: Energised – No signs of material deterioration were found. Signs of dry band activity were still noted, in the form of a white residue. Light corrosion run off from the dead end-fitting was still noted on the shed top (also on the non-energised). **Non-energised** – No signs of material deterioration were found.

RTV SR coated porcelain insulator 4C: Energised – Clear signs of dry band activity were still observed, showing medium discolouration. Patchy discolouration was still found. Light signs of crazing (possibly in the pollution layer) were still observed. Light signs of tracking were observed for the first time (on the shank just below the dead end-fitting). Light corrosion run off from the dead end-fitting was still noted on the shed top (also on the non-energised). **Non-energised** – No signs of material deterioration were found. However, the coating over spray started to peel on the corroded end fittings (also on the energised).

Cycloaliphatic insulator 5A: Energised – Blackening in the mould line and white discolouration adjacent to the mould line was still observed. Dry band activity was still observed, showing light discolouration. Light signs of crazing were still observed. The insulator had a bad smell (similar to baby nappies). **Non-energised** – No signs of deterioration were found.

Surface condition inspection of week 24

HTV SR insulator 1S: Energised - Medium discolouration in the regions of the dry bands was still observed. Light corrosion run off from the dead end-fitting was still noted (also on the non-energised). End-fitting corrosion protruding through the polymeric material moulded over it was still observed on both ends. Light signs of crazing in the pollution layer were observed for the first time. **Non-energised** - Signs of end-fitting corrosion affecting the polymeric material moulded over it were still observed on both ends. However, no further signs of deterioration were found.

EPDM insulator 2E: Energised – Signs of dry band activity were still observed, showing light discolouration. The patchy discolouration has increased to medium. Light corrosion run off from the dead end-fitting was still noted (also on the non-energised). End-fitting corrosion protruding through the polymeric material moulded over it was still observed on both ends. Light signs of crazing in the pollution layer were observed for the first time. **Non-energised** – Signs of end-fitting corrosion affecting the polymeric material moulded over it were still observed on both ends. However, no further signs of deterioration were found.

Porcelain insulator 3P: Energised – No signs of material deterioration were found. Signs of dry band activity were still noted, in the form of a white residue. Light corrosion run off from the dead end-fitting was still noted on the shed top (also on the non-energised). **Non-energised** – No signs of material deterioration were found.

RTV SR coated porcelain insulator 4C: Energised – Clear signs of dry band activity were still observed, showing heavy discolouration. Patchy discolouration was still found. Medium signs of crazing (possibly in the pollution layer) were now observed. Light tracking (possibly in the pollution layer) was still observed (see Figure D.6). Light corrosion run off from the dead end-fitting was still noted on the shed top (also on the non-energised). **Non-energised** – No signs of material deterioration were found. The coating over spray was still peeling from the corroded end fittings (also on the energised).

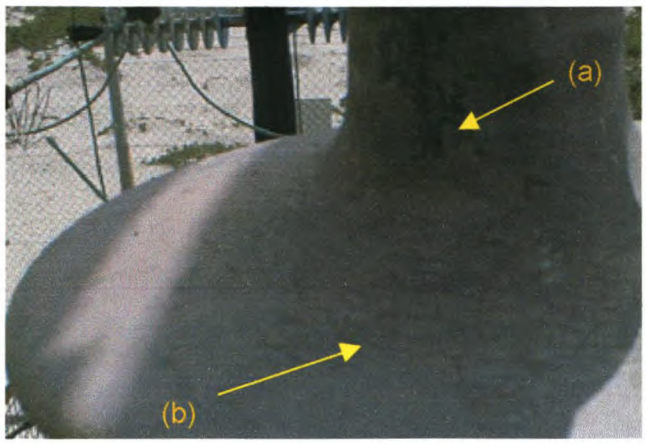

Figure D.6 Photo showing light tracking (a) and medium crazing (b) on insulator 4C observed in week 24.

Cycloaliphatic insulator 5A: Energised – Blackening in the mould line and white discolouration adjacent to the mould line was still observed and has worsened by widening (especially towards the shed tips). Dry band activity was still observed, now showing medium discolouration. Light signs of crazing were still observed. The first signs of light tracking were observed on the shank at the mould line. The insulator still had a bad smell (similar to baby nappies). Light corrosion was observed on the end fittings (also on the non-energised). **Non-energised –** The first signs of slight whitening in the mould line were observed (see Figure D.7). However, no further signs of deterioration were found.

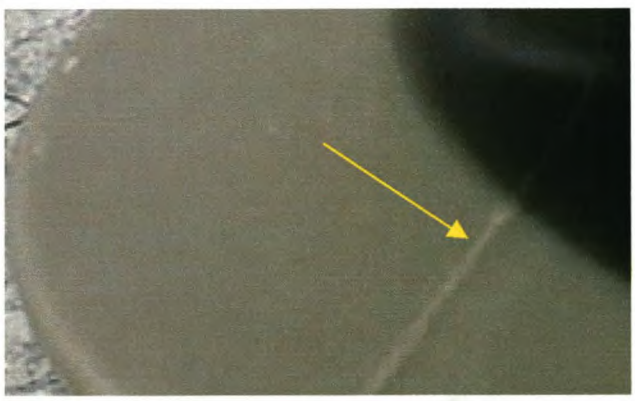

Figure D.7 Photo showing light discolouration in the mould line on non-energised insulator 5A observed in week 24.

Surface condition inspection of week 30

HTV SR insulator 1S: Energised - Medium discolouration in the regions of the dry bands was still observed. Light corrosion run off from the dead end-fitting was still noted (also on the non-energised). End-fitting corrosion protruding through the polymeric material moulded over it was still observed on both ends. On the live end-fitting material interface the first signs of tracking were observed developing from a corrosion protrusion (see Figure D.8). Light signs of crazing in the pollution layer were still observed. **Non-energised** - End-fitting corrosion affecting the polymeric material moulded over it was still observed on both ends. However, no further signs of deterioration were found.

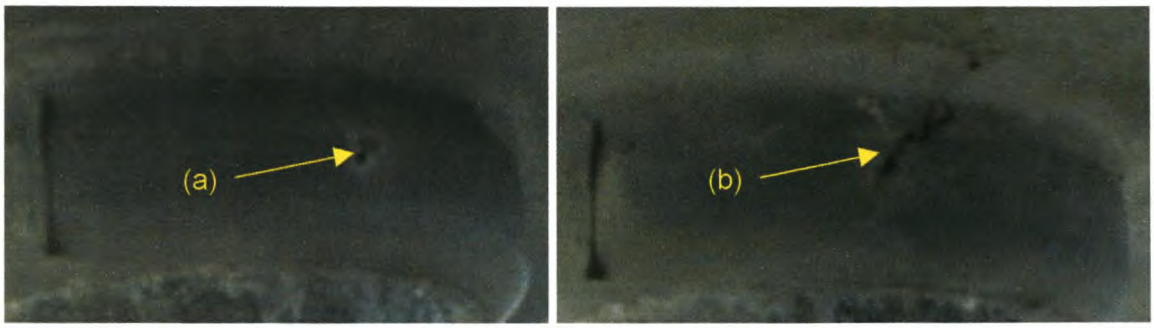

Figure D.8 Photo of end-fitting corrosion (live end) protruding through the polymer material (a) seen during week 24, leading to signs of tracking (b) seen during week 30, on insulator 1S.

EPDM insulator 2E: Energised – Signs of dry band activity were still observed, showing light discolouration. Medium patchy discolouration was found (see Figure D.9). Light corrosion run off from the dead end-fitting was still noted (also on the non-energised). End-fitting corrosion protruding through the polymeric material moulded over it was still observed on both ends. Light signs of crazing in the pollution layer were still observed. **Non-energised** – Signs of end-fitting corrosion affecting the polymeric material moulded over it were still observed on both ends. However, no further signs of deterioration were found.

Figure D.9 Photo showing medium patchy discolouration and light crazing in the pollution layer on insulator 2E seen in week 30.

Porcelain insulator 3P: Energised – No signs of material deterioration were found. Signs of dry band activity were still noted, in the form of a white residue. However, there were signs of crazing in the pollution layer (see Figure D.10). Light corrosion run off from the dead end-fitting was still noted on the shed top (also on the non-energised). **Non-energised –** No signs of material deterioration were found.

Figure D.10 Photo showing white residue and light crazing in the pollution layer on insulator 3P seen in week 30.

RTV SR coated porcelain insulator 4C: Energised – Clear signs of dry band activity were still observed, showing heavy discolouration. Patchy discolouration was still found. Medium signs of crazing (possibly in the pollution layer) were still observed. Medium tracking (possibly in the pollution layer) was now observed. Light corrosion run off from the dead end-fitting was still noted on the shed top (also on the non-energised). **Non-**

energised – No signs of material deterioration were found. The coating over spray was still peeling from the corroded end fittings (also on the energised).

Cycloaliphatic insulator 5A: Energised – Blackening in the mould line and white discolouration adjacent to the mould line was still observed. Dry band activity was still observed, now showing heavy discolouration. Light crazing was still observed. Light tracking was still observed on the shank at the mould line. Light chalking was seen for the first time (see Figure D.11) The insulator still had a bad smell (similar to baby nappies). Light corrosion was still observed on the end fittings showing run off onto the shed for the first time (also on the non-energised). **Non-energised** – Light whitening in the mould line was still observed. However, no further signs of deterioration were found.

Figure D.11 Photo showing chalking on insulator 5A seen in week 30.

Surface condition inspection of week 36

HTV SR insulator 1S: Energised - Medium discolouration in the regions of the dry bands was still observed. Light corrosion run off from the dead end-fitting was still noted (also on the non-energised). End-fitting corrosion protruding through the polymeric material moulded over it was still observed on both ends. On the live end-fitting material interface tracking was still observed. Light signs of crazing in the pollution layer were still observed. **Non-energised** - End-fitting corrosion affecting the polymeric material moulded over it was still observed on both ends. However, no further signs of deterioration were found.

EPDM insulator 2E: Energised – Dry band activity was still observed, showing light discolouration. Medium patchy discolouration was still found. Light corrosion run off from the dead end-fitting was still noted (also on the non-energised). End-fitting corrosion protruding through the polymeric material moulded over it was still observed on both ends. Light signs of crazing in the pollution layer were still observed. **Non-energised** – End-fitting corrosion affecting the polymeric material moulded over it was still observed on both ends. However, no further signs of deterioration were found.

Porcelain insulator 3P: Energised – No signs of material deterioration were found. Signs of dry band activity were still noted, in the form of a white residue. Light corrosion run off from the dead end-fitting was still noted on the shed top (also on the non-energised). **Non-energised** – No signs of material deterioration were found.

RTV SR coated porcelain insulator 4C: Energised – Clear signs of dry band activity were still observed, showing heavy discolouration. Patchy discolouration was still found. Medium signs of crazing (possibly in the pollution layer) were still observed. Medium tracking (possibly in the pollution layer) was still observed. The first signs of light erosion were observed, where tracking was previously present. Light corrosion run off from the dead end-fitting was still noted on the shed top (also on the non-energised). **Non-energised** – No signs of material deterioration were found. The coating over spray was still peeling from the corroded end fittings (also on the energised).

Cycloaliphatic insulator 5A: Energised – Blackening in the mould line and white discolouration adjacent to the mould line was still observed. Dry band activity was still observed, still showing heavy discolouration. Light crazing was still observed. Medium tracking was now observed on the shank at the mould line. Light erosion was seen for the first time in the same area were tracking was seen previously (see Figure D.12). Light chalking was still seen. The insulator still had a bad smell (similar to baby nappies). Light corrosion was still observed on the end fittings showing run off onto the shed (also on the non-energised). **Non-energised** – Light whitening in the mould line was still observed. However, no further signs of deterioration were found.

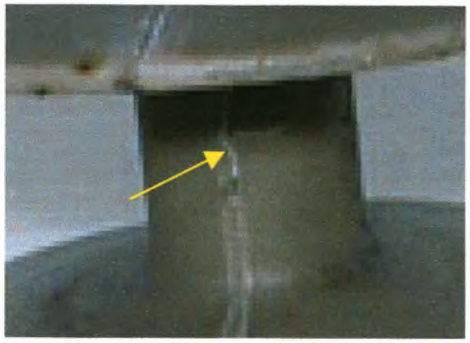

Figure D.12 Photo showing light erosion on insulator 5A seen in week 36.

Surface condition inspection of week 42

HTV SR insulator 1S: Energised - Medium discolouration in the regions of the dry bands was still observed. Light corrosion run off from the dead end-fitting was still noted (also on the non-energised). End-fitting corrosion protruding through the polymeric material moulded over it was still observed on both ends. On the live end-fitting material interface tracking was still observed. The crazing in the pollution layer increased to medium. **Non-energised** - End-fitting corrosion affecting the polymeric material moulded over it was still observed on both ends. However, no further signs of deterioration were found.

EPDM insulator 2E: Energised – Dry band activity was still observed, showing light discolouration. Medium patchy discolouration was still found. Light corrosion run off from the dead end-fitting was still noted (also on the non-energised). End-fitting corrosion protruding through the polymeric material moulded over it was still observed on both ends. Light signs of crazing in the pollution layer were still observed. **Non-energised** – End-fitting corrosion affecting the polymeric material moulded over it was still observed on both ends. However, no further signs of deterioration were found.

Porcelain insulator 3P: Energised – No signs of material deterioration were found. Signs of dry band activity were still noted, in the form of a white residue (see Figure D.13). Light corrosion run off from the dead end-fitting was still noted on the shed top (also on the non-energised). **Non-energised** – No signs of material deterioration were found.

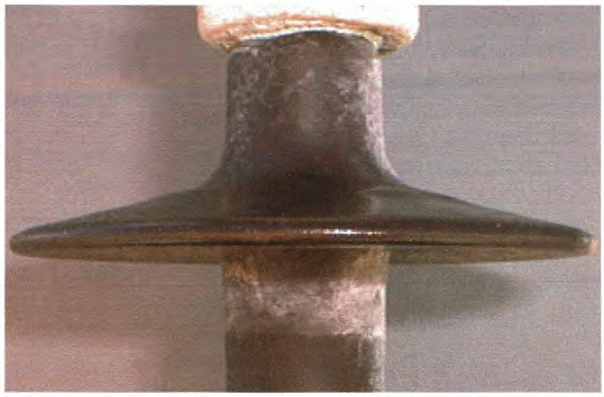

Figure D.13 Photo showing signs of dry band activity and white residue on insulator 3P seen in week 42.

RTV SR coated porcelain insulator 4C: Energised – Clear signs of dry band activity were still observed, showing heavy discolouration. Patchy discolouration was still found. Medium signs of crazing (possibly in the pollution layer) were still observed. Heavy tracking (possibly in the pollution layer) was now observed. Light erosion was still observed, where tracking was previously present. Light corrosion run off from the dead end-fitting was still noted on the shed top (also on the non-energised). **Non-energised** – No signs of material deterioration were found. The coating over spray was still peeling from the corroded end fittings (also on the energised).

Cycloaliphatic insulator 5A: Energised – Blackening in the mould line and white discolouration adjacent to the mould line was still observed. Dry band activity was still observed, still showing heavy discolouration. Medium crazing was now observed, starting to change colour from black to white. Medium tracking was still observed on the shank at the mould line. Light erosion was still seen in the same area were tracking was seen previously. Medium chalking was now seen (see Figure D.14). The insulator still had a bad smell (similar to baby nappies). Light corrosion was still observed on the end fittings showing run off onto the shed (also on the non-energised). **Non-energised** – Light whitening in the mould line was still observed. However, no further signs of deterioration were found.

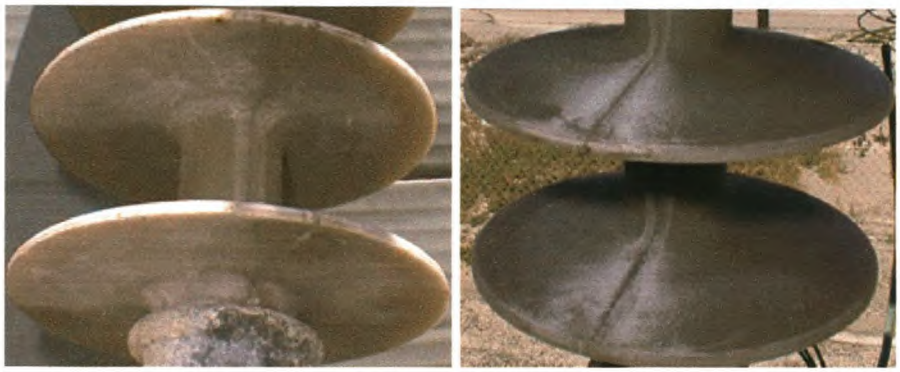

(a) (b)

Figure D.14 Photos showing (a) discolouration on the bottom of sheds and (b) chalking on insulator 5A seen in week 42.

Surface condition inspection of week 48

HTV SR insulator 1S: Energised - Medium discolouration in the regions of the dry bands was still observed. Light corrosion run off from the dead end-fitting was still noted (also on the non-energised). End-fitting corrosion protruding through the polymeric material moulded over it was still observed on both ends. On the live end-fitting material interface signs of erosion were observed where tracking was previously seen. Medium crazing in the pollution layer was still observed. **Non-energised** - End-fitting corrosion affecting the polymeric material moulded over it was still observed on both ends. However, no further signs of deterioration were found.

EPDM insulator 2E: Energised – Dry band activity was still observed, with the discolouration increasing to medium. Medium patchy discolouration was still found. Light corrosion run off from the dead end-fitting was still noted (also on the non-energised). End-fitting corrosion protruding through the polymeric material moulded over it was still observed on both ends. Light signs of crazing in the pollution layer were still observed. Light tracking (possibly only in the pollution layer) was observed (see Figure D.15). **Non-energised** – End-fitting corrosion affecting the polymeric material moulded over it was still observed on both ends. However, no further signs of deterioration were found.

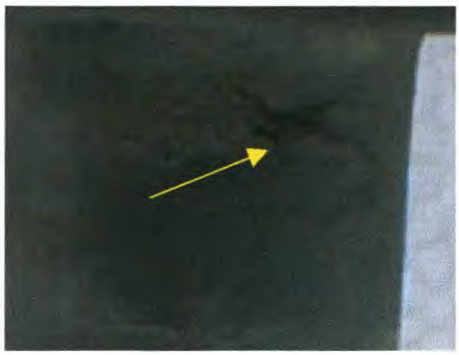

Figure D.15 Photo showing light tracking (possibly only in the pollution layer) on insulator 2E seen in week 48.

Porcelain insulator 3P: Energised – No signs of material deterioration were found. Signs of dry band activity were still noted, in the form of a white residue. Light corrosion run off from the dead end-fitting was still noted on the shed top (also on the non-energised). **Non-energised –** No signs of material deterioration were found.

RTV SR coated porcelain insulator 4C: Energised – Clear signs of dry band activity were still observed, showing heavy discolouration. Patchy discolouration was still found. Heavy signs of crazing (possibly in the pollution layer) were now observed. Heavy tracking (possibly in the pollution layer) was still observed. Light erosion was still observed, where tracking was previously present. Light corrosion run off from the dead end-fitting was still noted on the shed top (also on the non-energised). **Non-energised –** No signs of material deterioration were found. The coating over spray was still peeling from the corroded end fittings (also on the energised).

Cycloaliphatic insulator 5A: Energised – Blackening in the mould line and white discolouration adjacent to the mould line was still observed. Dry band activity was still observed, now showing very heavy discolouration. Medium crazing (white) was still observed. Medium tracking was still observed on the shank at the mould line. Light erosion was still seen in the same area were tracking was seen previously. Medium chalking was still seen. The insulator still had a bad smell (similar to baby nappies). Light corrosion was still observed on the end fittings showing run off onto the shed (also on the non-energised). **Non-energised –** Light whitening in the mould line was still observed. However, no further signs of deterioration were found.

Surface condition inspection of week 53

HTV SR insulator 1S: Energised - Medium discolouration in the regions of the dry bands was still observed. Light corrosion run off from the dead end-fitting was still noted (also on the non-energised). End-fitting corrosion protruding through the polymeric material moulded over it was still observed on both ends. On the live end-fitting material interface erosion was still observed. Medium crazing in the pollution layer was still observed. **Non-energised** - End-fitting corrosion affecting the polymeric material moulded over it was still observed on both ends. However, no further signs of deterioration were found.

EPDM insulator 2E: Energised – Dry band activity was still observed, showing medium discolouration. Medium patchy discolouration was still found. Light corrosion run off from the dead end-fitting was still noted (also on the non-energised). End-fitting corrosion protruding through the polymeric material moulded over it was still observed on both ends. Light signs of crazing in the pollution layer were still observed. The light tracking observed in week 48 was not visible anymore, however very light erosion was now seen in its place. **Non-energised –** End-fitting corrosion affecting the polymeric material moulded over it was still observed on both ends. Signs of light discolouration were observed on the northern side on the shed tops for the first time (see Figure D.16). However, no further signs of deterioration were found.

Figure D.16 Photo showing light discolouration on non-energised insulator 2E seen in week 53.

Porcelain insulator 3P: Energised – No signs of material deterioration were found. Signs of dry band activity were still noted, in the form of a white residue. Light signs of

tracking in the pollution layer were also observed. Light corrosion run off from the dead end-fitting was still noted on the shed top (also on the non-energised). **Non-energised –** No signs of material deterioration were found.

RTV SR coated porcelain insulator 4C: Energised – Clear signs of dry band activity were still observed, showing heavy discolouration. Patchy discolouration was still found. Heavy signs of crazing (possibly in the pollution layer) were still observed. Heavy tracking (possibly in the pollution layer) was still observed. Light erosion was still observed, where tracking was previously present. Light corrosion run off from the dead end-fitting was still noted on the shed top (also on the non-energised). **Non-energised –** No signs of material deterioration were found. The coating over spray was still peeling from the corroded end fittings (also on the energised).

Cycloaliphatic insulator 5A: Energised – Blackening in the mould line and white discolouration adjacent to the mould line was still observed. Dry band activity was still observed, still showing very heavy discolouration. Heavy crazing (white) was now observed. Heavy tracking was now observed on the shank at the mould line. Medium erosion was now seen in the same area were tracking was seen previously. Medium chalking was still seen. The insulator still had a bad smell (similar to baby nappies). Light corrosion was still observed on the end fittings showing run off onto the shed (also on the non-energised). **Non-energised –** Light whitening in the mould line was still observed. However, no further signs of deterioration were found.

APPENDIX E: ELECTRICAL DISCHARGE ACTIVITY OBSERVATIONS

Details of the electrical discharge observations, as summarised in Tables 5.2 and 5.3 along with the climatic and environmental conditions, are discussed below.

Electrical discharge activity observations during week 1

HTV SR insulator 1S: WDC (Water drop corona) was seen for the first time on day 2, and on days 3, 5 and 6. The WDC was located on the bottom of the sheds near the middle of the insulator and none on the live end. SCD (Spot corona/discharges) were seen for the first time on day 7.

EPDM insulator 2E: WDC was seen for the first time on day 2, and on days 4, 5 and 6. The WDC was located on the bottom of the sheds near the middle of the insulator. SCD were seen for the first time on day 3 and then again on day 7. DBC (Dry band corona) and DBD (Dry band discharges) were observed on day 7 for the first time, with an associated leakage current measurement of 1 mA.

Porcelain insulator 3P: WDC was seen for the first time on day 7, located on the bottom of the sheds on the earth side.

RTV SR-coated porcelain insulator 4C: No electrical discharge activity or leakage currents were observed.

Cycloaliphatic insulator 5A: No electrical discharge activity or leakage currents were observed.

Climatic and environmental conditions: Day 1 of the week was hot, with relatively low humidity levels. The rest of the week was cooler with higher humidity levels. It rained on days 4 and 7. There was a fresh north-westerly breeze on day 2. The ESDD (Equivalent salt deposit density) pollution deposit for the week on a porcelain long rod was measured as light (0.03 mg/cm^2). The LESDD (localised equivalent salt deposit density) on an energised SR insulator was extremely low (0.009 mg/cm^2), however on the EPDM insulator it was found to be medium (0.07 mg/cm^2).

Hydrophobicity: Insulators 1S, 4C and 5A were hydrophobic (class 2). 3P and 2E were hydrophilic (class 6 and 7).

Electrical discharge activity observations during week 2

HTV SR insulator 1S: WDC was only seen on day 1. SCD were seen on days 1 to 4. DBC and DBD were observed on day 2 for the first time, with an associated leakage current measurement of 2 mA. DBC was further seen on days 5 to 7, and DBD on days 5 and 6 with associated leakage currents both measured as 8 mA.

EPDM insulator 2E: WDC was seen on days 2 and 6. SCD was seen on days 1 to 3 and then again on days 5 and 7. DBC was seen on days 2 and 4 to 6. DBD were observed on days 1, 2 and 4 to 6, with associated leakage current measurements of 1 to 12 mA.

Porcelain insulator 3P: WDC was only seen on day 3. SCD were seen for the first time on day 2 and then again on day 4. No further electrical discharge activity or leakage currents were observed.

RTV SR-coated porcelain insulator 4C: WDC was seen from day 2 onwards. SCD were seen from day 4 onwards. No further electrical discharge activity or leakage currents were observed.

Cycloaliphatic insulator 5A: WDC was seen for the first time on day 2, and on days 6 and 7. No further electrical discharge activity or leakage currents were observed.

Climatic and environmental conditions: The week was cool with high humidity levels. It rained on days 1, 3, 5 and 6. There was a strong north-westerly breeze on days 2 and 3. The ESDD pollution deposit for the week on a porcelain long rod was measured as medium (0.09 mg/cm^2). The LESDD on an energised SR insulator was heavy (0.21 mg/cm^2), and on the EPDM insulator it was also found to be heavy (0.14 mg/cm^2).

Hydrophobicity: Insulator 5A was still hydrophobic (class 3). The other insulators were all hydrophilic (classes 6 and 7).

Electrical discharge activity observations during week 3

HTV SR insulator 1S: WDC was only seen on day 2. SCD were seen only on day 7. DBC was seen on day 1. DBC and DBD were seen on days 2 to 6, with associated leakage current measurements of 2 to 12 mA.

EPDM insulator 2E: WDC was only seen on day 2. SCD were seen on days 1, 2 and 7. DBC was seen on day 3. DBC and DBD were seen on days 4 to 6, with associated leakage current measurements of 8 to 20 mA.

Porcelain insulator 3P: No WDC was seen. SCD were seen on days 4 to 7. DBC and DBD were observed on day 4 for the first time, with associated leakage current measurement of 3 mA.

RTV SR-coated porcelain insulator 4C: WDC was seen on days 1 to 4. SCD were seen on days 2 to 4. DBC was seen on day 5 for the first time, and again on days 6 and 7. DBD were seen on day 6 for the first time, with associated leakage current measurement of 1 mA.

Cycloaliphatic insulator 5A: WDC was seen on days 1 and 2. SCD were seen for the first time on day 5. DBC was seen on days 6 (for the first time) and 7. No further electrical discharge activity or leakage currents were observed.

Climatic and environmental conditions: The first two days of the week were warm to hot, with relatively low humidity levels. The rest of the week was cool with high humidity levels. It rained on days 5 and 7. There was a fresh south-south-westerly breeze on day 7. The ESDD pollution deposit for the week on a porcelain long rod was measured as medium (0.06 mg/cm^2). The LESDD on an energised SR insulator was very heavy (0.35 mg/cm^2), and on the EPDM insulator it was also found to be very heavy (0.24 mg/cm^2).

Hydrophobicity: Insulator 5A was still hydrophobic (class 3). The other insulators were still all hydrophilic (classes 6 and 7).

Electrical discharge activity observations during week 4

HTV SR insulator 1S: No WDC was seen. SCD were seen on days 1, 2, 4 and 5. DBC and DBD were seen on days 6 and 7, with associated leakage current measurements of 2 and 4 mA.

EPDM insulator 2E: No WDC was seen. SCD were seen on days 3 and 4. DBC and DBD were seen on days 1, 2 and 5 to 7, with associated leakage current measurements of 2 to 20 mA.

Porcelain insulator 3P: No WDC was seen. SCD were seen on days 5 to 7. DBC was seen on day 5. DBC and DBD were observed on day 6, with associated leakage current measurement of 1 mA.

RTV SR coated porcelain insulator 4C: WDC was seen on days 1 and 5. SCD were seen on days 2 to 7. No further electrical discharge activity or leakage currents were observed.

Cycloaliphatic insulator 5A: WDC was seen on days 1 to 3. SCD were seen on days 1, 2, 4 and 5. DBC was seen on days 6 and 7. DBD were seen for the first time on day 7, with associated leakage current measurement of 1 mA.

Climatic and environmental conditions: Day 4 of the week was warm, with relatively low humidity levels. The rest of the week was cool with high humidity levels. It rained on days 1 and 2. There was a strong north-westerly breeze on day 1. The wind shifted to a southern direction during the week. The ESDD pollution deposit for the week on a porcelain long rod was measured as verging on heavy (0.12 mg/cm^2). The LESDD on an energised SR insulator was medium (0.1 mg/cm^2), and on the EPDM insulator it was also found to be verging on heavy (0.12 mg/cm^2).

Hydrophobicity: Insulator 5A was losing hydrophobicity (class 4). Insulator 4C has regained some hydrophobicity (improved from class 6 to 4). The other insulators were still all hydrophilic (classes 6 and 7).

Electrical discharge activity observations during week 5

HTV SR insulator 1S: WDC was seen on days 5 and 6. SCD were seen only on day 7. DBC and DBD were seen on days 1 to 6, with associated leakage current measurements of 1 and 36 mA.

EPDM insulator 2E: WDC was only seen on day 5. SCD were seen on all days except day 5. DBC was seen on days 1 to 5. DBD were seen on days 1 to 3 and 5, with associated leakage current measurements of 3 to 24 mA.

Porcelain insulator 3P: WDC was seen on days 6 and 7. SCD were seen on days 1 and 5 to 7. DBC was seen on day 2. DBC and DBD were observed on days 5 and 6, with associated leakage current measurements of 5 and 12 mA.

RTV SR coated porcelain insulator 4C: WDC was seen on days 5 to 7. SCD were seen only on day 7. DBC and DBD were observed on all days except day 7, with associated leakage current measurements of 1 to 4 mA.

Cycloaliphatic insulator 5A: WDC was seen only on day 6. SCD were seen only on day 7. DBC was seen on all days except day 7. DBD were seen on days 2 to 5, with associated leakage current measurements of 2 to 4 mA.

Climatic and environmental conditions: The week was warm to hot, with relatively low humidity levels on day 7. No rain was recorded. There was a fresh south-easterly breeze on day 1 and a fresh south-south-easterly on day 6. The ESDD pollution deposit for the week on a porcelain long rod was measured as heavy (0.2 mg/cm^2). The LESDD on an energised SR insulator was very heavy (0.32 mg/cm^2), and on the EPDM insulator it was also found to be verging on heavy (0.19 mg/cm^2).

Hydrophobicity: Insulator 5A was still class 4. Insulator 1S had regained some hydrophobicity (improved from class 6 to 5). Insulator 4C has lost hydrophobicity again (from class 4 to 6). The other insulators were still all hydrophilic (classes 6 and 7).

Electrical discharge activity observations during week 6

HTV SR insulator 1S: WDC was seen on days 4 to 6. SCD were seen on days 1 to 3 and 7. DBC was seen on days 1 and 4 to 6. DBD were seen on days 1, 4 and 5, with associated leakage current measurements of 2 to 15 mA.

EPDM insulator 2E: WDC was seen on days 3 and 5. SCD were seen only on day 4. DBC was seen on all days. DBD were seen on all days except day 1, with associated leakage current measurements of 7 to 26 mA.

Porcelain insulator 3P: WDC was seen on days 1 to 4. SCD were seen on days 1,2 and 7. DBC was seen on days 2 to 6. DBD were observed on days 2, 3, 5 and 6, with associated leakage current measurements of 2 to 12 mA.

RTV SR-coated porcelain insulator 4C: WDC was seen only on day 1. SCD were seen only on day 7. DBC was seen on all days except day 7. DBD were observed on days 1 to 5, with associated leakage current measurements of 2 to 4 mA.

Cycloaliphatic insulator 5A: WDC was seen on days 1 and 7. No SCD were seen. DBC was seen on all days. DBD were seen on days 2, 3, 5 and 6, with associated leakage current measurements of 2 mA.

Climatic and environmental conditions: The first day was warm to hot, with relatively low humidity levels. The humidity levels were extremely high on day 3 and it rained on days 4 and 6. There was also a strong north-north-westerly breeze on day 6. The UV-B solar radiation on day 6 was exceptionally low, indicating heavy cloud cover. The ESDD pollution deposit for the week on a porcelain long rod was measured as light (0.06 mg/cm^2). The LESDD on an energised SR insulator was heavy (0.14 mg/cm^2), and on the EPDM insulator it was also found to be heavy (0.14 mg/cm^2).

Hydrophobicity: Insulator 5A had further lost hydrophobicity (from class 4 to 5). Insulator 1S had lost hydrophobicity again (from class 5 to 6). Insulator 4C regained hydrophobicity (from class 6 to 5). The other insulators were still all hydrophilic (classes 6 and 7).

Electrical discharge activity observations during week 12

HTV SR insulator 1S: WDC was seen only on day 2. SCD were seen on days 1, 2, 4 and 7. DBC and DBD were seen on days 3, 5 and 6, with associated leakage current measurements of 2 to 9 mA.

EPDM insulator 2E: No WDC was seen. SCD were seen on days 3, 6 and 7. DBC was seen on all days. DBD were seen on all days except day 7, with associated leakage current measurements of 7 to 18 mA.

Porcelain insulator 3P: WDC was seen only on day 2. SCD were seen on all days except day 6. DBC was only seen on day 6. DBD were observed on days 2, 3 and 5, with associated leakage current measurements of 3 to 6 mA.

RTV SR coated porcelain insulator 4C: No WDC was seen. SCD were seen on all days except day 6. DBC was only seen day 6. No further electrical discharge activity or leakage currents were observed.

Cycloaliphatic insulator 5A: WDC was only seen on day 4. SCD were seen on days 2 and 7. DBC was seen on days 1 and 3 to 6. DBD were seen on days 2 to 5, with associated leakage current measurements of 2 to 14 mA.

Climatic and environmental conditions: The first day was warm to hot, with relatively low humidity levels and a fresh south-westerly breeze. The rest of the week was cool with high humidity levels. It rained on days 2, 4, 6 and 7. The humidity levels were extremely high on day 6. There was also a fresh to strong north-north-westerly breeze on days 2 to 4. The ESDD pollution deposit for the 6 weeks on a porcelain long rod was measured as light (0.05 mg/cm^2). The LESDD on an energised SR insulator was light (0.05 mg/cm^2), and on the EPDM insulator it was also found to be medium (0.08 mg/cm^2).

Hydrophobicity: Insulator 5A had further lost hydrophobicity (from class 5 to 6). Insulator 4C had lost hydrophobicity (from class 5 to 6). The other insulators were still all hydrophilic (classes 6 and 7).

Electrical discharge activity observations during week 18

HTV SR insulator 1S: No WDC was seen. SCD were seen on days 2 and 3. DBC was on days 1 and 4 to 7. DBD were seen on days 1 and 5 to 7, with associated leakage current measurements of 4 to 50 mA.

EPDM insulator 2E: No WDC was seen. No SCD were seen. DBC and DBD were seen on all days, with associated leakage current measurements of 3 to 48 mA.

Porcelain insulator 3P: WDC was seen on days 3, 6 and 7. SCD were seen on all days except day 3. DBC was only seen only on day 3. DBD were observed on days 3 to 7, with associated leakage current measurements of 8 to 21 mA.

RTV SR-coated porcelain insulator 4C: WDC was seen on days 1 and 7. SCD were seen on all days. No DBC was seen. DBD were observed on days 3, 6 and 7, with associated leakage current measurements of 1 to 10 mA.

Cycloaliphatic insulator 5A: No WDC was seen. SCD were seen on days 2 to 5. DBC was seen on days 1, 2, 6 and 7. DBD were seen on days 1 and 4 to 7, with associated leakage current measurements of 7 to 24 mA.

Climatic and environmental conditions: The week was moderate, with average humidity levels. No rain was recorded. There was a fresh north-north westerly breeze on days 5 and 6. The ESDD pollution deposit for the 6 weeks on a porcelain long rod was measured as verging on very heavy (0.24 mg/cm^2). The LESDD on an energised SR insulator was exceptional (0.53 mg/cm^2), and on the EPDM insulator it was also found to be heavy (0.19 mg/cm^2).

Hydrophobicity: Insulator 4C regained hydrophobicity (from class 6 to 5). The other insulators were still all hydrophilic (classes 6 and 7).

Electrical discharge activity observations during week 24

HTV SR insulator 1S: WDC was only seen on day 3. SCD were seen on days 1 and 6. DBC was seen on days 2 to 5 and 7. DBD were seen on days 2, 3, 5 and 7, with associated leakage current measurements of 15 to 100 mA.

EPDM insulator 2E: WDC was only seen on day 6. SCD were only seen on day 1. DBC was seen on all days except day 1. DBD were seen on all days, with associated leakage current measurements of 7 to 140 mA.

Porcelain insulator 3P: No WDC was seen. SCD were seen on days 1 to 4 and 6. DBC was only seen on days 5 and 7. DBD were observed on all days except day 6, with associated leakage current measurements of 6 to 55 mA.

RTV SR-coated porcelain insulator 4C: WDC was only seen on day 1. SCD were seen on days 2, 6 and 7. DBC was seen on days 1, 3 to 5 and 7. DBD were observed on days 3 to 5 and 7, with associated leakage current measurements of 12 to 20 mA.

Cycloaliphatic insulator 5A: No WDC was seen. SCD were seen on days 1, 6 and 7. DBC was seen on days 2 to 5 and 7. DBD were seen on all days except day 6, with associated leakage current measurements of 2 to 120 mA.

Climatic and environmental conditions: The UV-B solar radiation showed a dramatic increase since week 18, indicating the change in season from winter to summer. The week was cool to moderate, with average humidity levels. It rained on days 5 to 7. There was a strong north-westerly and westerly breeze on days 5 and 6. The ESDD pollution deposit for the 6 weeks on a porcelain long rod was measured as heavy (0.16 mg/cm^2). The LESDD on an energised SR insulator was very heavy (0.38 mg/cm^2), and on the EPDM insulator it was also found to be very heavy (0.37 mg/cm^2).

Hydrophobicity: Insulator 4C lost hydrophobicity (from class 5 to 6). The other insulators were still all hydrophilic (classes 6 and 7).

Electrical discharge activity observations during week 30

HTV SR insulator 1S: WDC was seen on days 3 and 4. SCD were seen on all days except days 7. DBC and DBD were seen on days 1 to 3, 6 and 7, with associated leakage current measurements of 24 to 42 mA.

EPDM insulator 2E: No WDC was seen. SCD were only seen on day 4. DBC was seen on days 1 to 3, 5 and 7. DBD were seen on days 1 to 3 and 5 to 7, with associated leakage current measurements of 5 to 60 mA.

Porcelain insulator 3P: No WDC was seen. SCD were seen on all days except day 2. DBC was only seen on day 2. DBD were observed on days 3, 4, 6 and 7, with associated leakage current measurements of 2 to 48 mA.

RTV SR coated porcelain insulator 4C: No WDC was seen. SCD were seen on days 4 and 5. DBC and DBD were observed on days 1 to 3, 6 and 7, with associated leakage current measurements of 15 to 34 mA.

Cycloaliphatic insulator 5A: No WDC was seen. SCD were seen on days 4 to 6. DBC was seen on days 1 to 3 and 7. DBD were seen on days 1 to 3, 6 and 7, with associated leakage current measurements of 40 to 120 mA.

Climatic and environmental conditions: The week was moderate to warm, with average humidity levels. It rained on days 4 and 7. There was a fresh south to south-south-westerly breeze on days 2 to 4. The UV-B solar radiation increased further. The ESDD pollution deposit for the 6 weeks on a porcelain long rod was measured as very heavy (0.32 mg/cm^2). The LESDD on an energised SR insulator was verging on heavy (0.12 mg/cm^2), and on the EPDM insulator it was also found to be heavy (0.21 mg/cm^2).

Hydrophobicity: All insulators were still hydrophilic (classes 6 and 7).

Electrical discharge activity observations during week 36

HTV SR insulator 1S: No WDC was seen. SCD were seen on days 1, 2 and 4. DBC was seen on days 2, 3 and 5 to 7. DBD were seen on days 2, 5 and 6, with associated leakage current measurements of 18 to 46 mA.

EPDM insulator 2E: WDC was only seen on day 4. SCD were seen on days 1 and 7. DBC was seen on days 2 to 6. DBD were seen on all days except day 1, with associated leakage current measurements of 9 to 65 mA.

Porcelain insulator 3P: No WDC was seen. SCD were seen on all days except day 5. DBC was only seen on day 5. DBD were observed on days 2 and 5, with associated leakage current measurements of 25 to 42 mA.

RTV SR-coated porcelain insulator 4C: WDC was seen only on day 1. SCD were seen only on day 1. DBC was seen on all days except day 1. DBD were observed on days 2 and 5, with associated leakage current measurements of 5 to 24 mA.

Cycloaliphatic insulator 5A: No WDC was seen. SCD were seen on all days except day 7. DBC was seen on days 6 and 7. DBD were seen on days 2, 3 and 5 to 7, with associated leakage current measurements of 20 to 160 mA.

Climatic and environmental conditions: The week was warm to hot (day 1), with average humidity levels (except day 1, which was low). No rain was recorded. There was a fresh north-westerly breeze on day 7. The ESDD pollution deposit for the 6 weeks on a porcelain long rod was measured as verging on heavy (0.12 mg/cm^2). The LESDD on an energised SR insulator was heavy (0.18 mg/cm^2), and on the EPDM insulator it was also found to be heavy (0.14 mg/cm^2).

Hydrophobicity: All insulators were still hydrophilic (classes 6 and 7).

Electrical discharge activity observations during week 42

HTV SR insulator 1S: WDC was only seen on day 6. No SCD were seen. DBC and DBD were seen on all days with associated leakage current measurements of 15 to 75 mA.

EPDM insulator 2E: No WDC was seen. No SCD were seen. DBC and DBD were seen on all days, with associated leakage current measurements of 24 to 110 mA.

Porcelain insulator 3P: WDC was only seen on day 7. SCD were seen on all days. DBC was only seen on day 1. DBD were observed on all days except day 5, with associated leakage current measurements of 20 to 72 mA.

RTV SR coated porcelain insulator 4C: No WDC was seen. No SCD were seen. DBC was seen on all days. DBD were observed on all days except day 5, with associated leakage current measurements of 5 to 65 mA.

Cycloaliphatic insulator 5A: No WDC was seen. SCD were seen on days 1 and 3. DBC was seen on all days except day 3. DBD were seen on all days with associated leakage current measurements of 20 to 296 mA (on day 3 it was exceptionally high).

Climatic and environmental conditions: The week was moderate to warm (day 1), with average humidity levels. It rained on days 5 and 7. There was a strong north-westerly breeze on day 7. The ESDD pollution deposit for the 6 weeks on a porcelain long rod was measured as heavy (0.13 mg/cm^2). The LESDD on an energised SR insulator was heavy (0.22 mg/cm^2), and on the EPDM insulator it was also found to be verging on very heavy (0.24 mg/cm^2).

Hydrophobicity: All insulators were still hydrophilic (now class 7).

Electrical discharge activity observations during week 48

HTV SR insulator 1S: No WDC was seen. SCD were seen on days 1 to 4 and 7. DBC and DBD were seen on days 3 to 7, with associated leakage current measurements of 8 to 30 mA.

EPDM insulator 2E: WDC was only seen on day 7. SCD were seen on all days. DBC was seen on days 2 to 4, 6 and 7. DBD were seen on days 3 to 7, with associated leakage current measurements of 8 to 90 mA.

Porcelain insulator 3P: No WDC was seen. SCD were seen on all days except day 5. DBC was only seen on day 5. DBD were observed on days 3 to , with associated leakage current measurements of 20 to 80 mA.

RTV SR-coated porcelain insulator 4C: No WDC was seen. SCD were seen on days 2 to 4 and 7. DBC was seen on days 1, 3 and 5 to 7. DBD were observed on days 3 and 5 to 7, with associated leakage current measurements of 2 to 16 mA.

Cycloaliphatic insulator 5A: No WDC was seen. SCD were seen on days 1 to 3, 5 and 6. DBC was seen on days 3, 4 and 7. DBD were seen on days 3 to 7, with associated leakage current measurements of 10 to 96 mA.

Climatic and environmental conditions: The week was warm, with average humidity levels. However, the temperature dropped on days 6 and 7, and humidity levels were high. It rained lightly on day 7. There was a strong south-south-easterly breeze on day 1 and a fresh south to south-south-easterly breeze on days 3 and 4. The UV-B solar radiation levels started to decrease, indicating a change in season. The ESDD pollution deposit for the 6 weeks on a porcelain long rod was measured as very heavy (0.34 mg/cm^2). The LESDD on an energised SR insulator was exceptional (0.76 mg/cm^2), and on the EPDM insulator it was also found to be verging on very heavy (0.42 mg/cm^2).

Hydrophobicity: All insulators were still hydrophilic (class 7).

Electrical discharge activity observations during week 53

HTV SR insulator 1S: No WDC was seen. SCD were seen on all days except day 6. DBC and DBD were seen on days 1 to 3, with associated leakage current measurements of 14 to 30 mA.

EPDM insulator 2E: No WDC was seen. SCD were seen on days 1, 2, 4, 5 and 7. DBC was seen on days 1, 3, 5 and 7. DBD were seen on days 1 to 3 and 7, with associated leakage current measurements of 14 to 60 mA.

Porcelain insulator 3P: No WDC was seen. SCD were seen on all days except day 6. No DBC was seen. DBD were observed on days 1 to 3 and 7, with associated leakage current measurements of 28 to 50 mA.

RTV SR coated porcelain insulator 4C: No WDC was seen. SCD were seen on days 1, 2, 4 and 5. DBC and DBD were observed on days 3 and 7, with associated leakage current measurements of 20 and 6 mA.

Cycloaliphatic insulator 5A: No WDC was seen. SCD were seen on days 4 and 5. DBC was seen on days 1, 3 and 7. DBD were seen on days 1 to 4 and 7, with associated leakage current measurements of 24 to 130 mA.

Climatic and environmental conditions: No climatic data was recorded for days 2 to 4. However, the other days were warm, with relatively low humidity levels. No rain was recorded. There was a fresh southerly breeze on day 5. The ESDD pollution deposit for the 6 weeks, on a porcelain long rod, was measured as heavy (0.14 mg/cm^2). The LESDD on an energised SR insulator was heavy (0.22 mg/cm^2), and on the EPDM insulator it was also found to be exceptional (0.64 mg/cm^2).

Hydrophobicity: All insulators were still hydrophilic, however slight recovery was seen on 1S (class 5), 2E and 4C (class 6).

APPENDIX F: LEAKAGE CURRENT MEASUREMENTS

Leakage current measurements on HTV SR insulator 1S

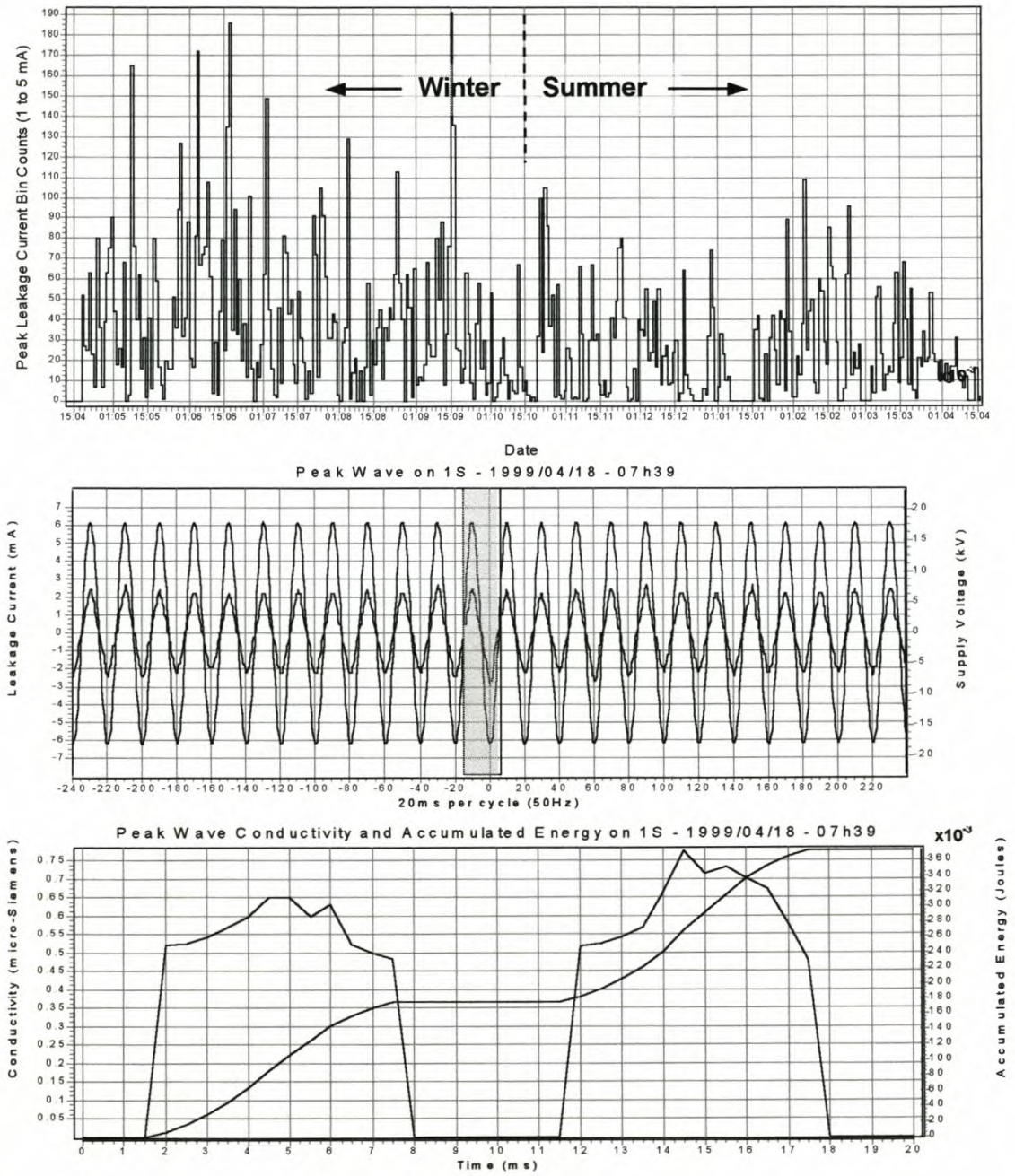

Figure F. 1 The daily bin counts for insulator **1S** are shown for the peak leakage current pulses in size range **1 to 5 mA**. The first peak leakage current and voltage waveform measured in this range, with associated conductivity and accumulated energy for the selected 20 ms cycle (shaded area), are also shown.

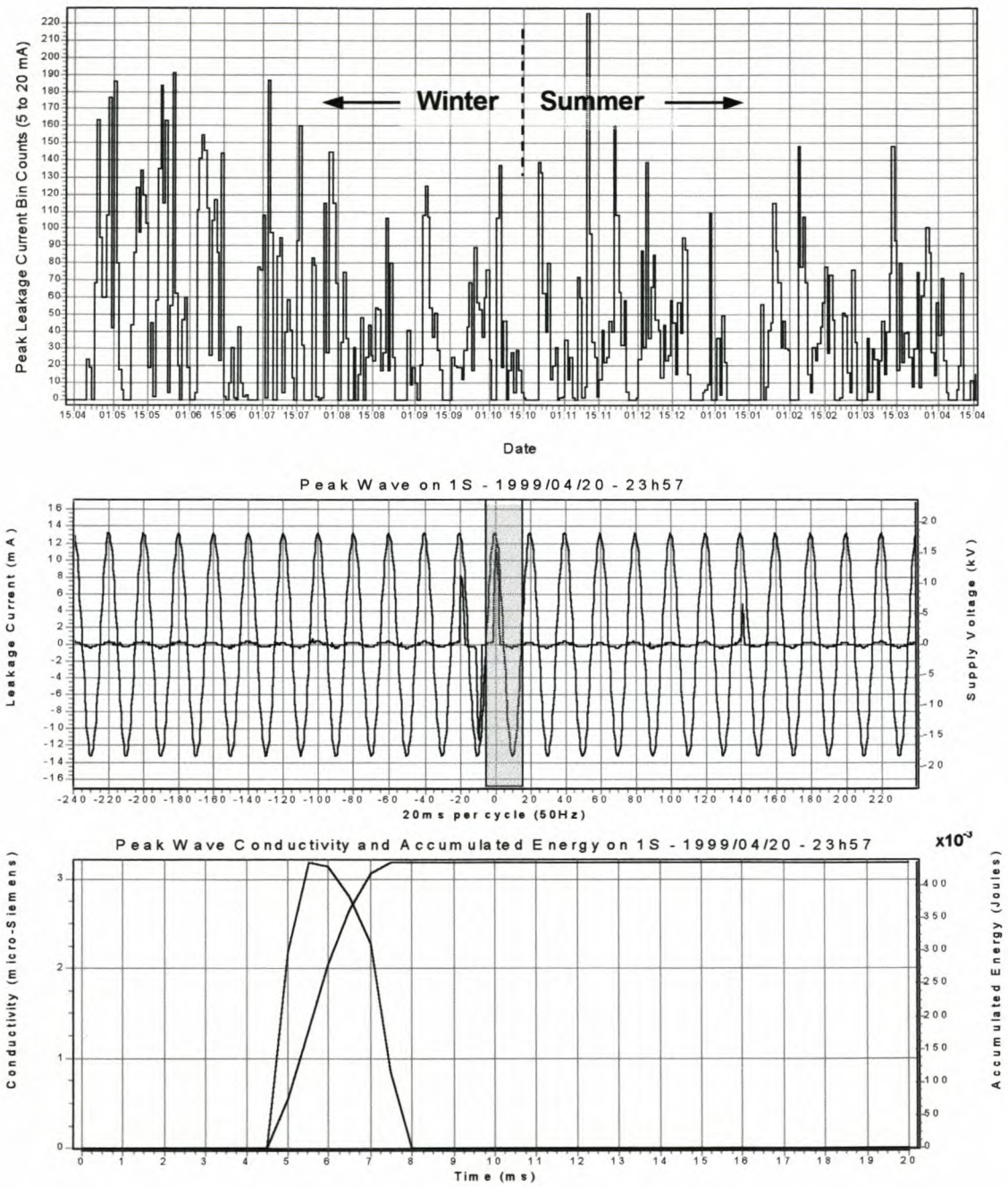

Figure F. 2 The daily bin counts for insulator **1S** are shown for the peak leakage current pulses in size range **5 to 20 mA**. The first peak leakage current and voltage waveform measured in this range, with associated conductivity and accumulated energy for the selected 20 ms cycle (shaded area), are also shown.

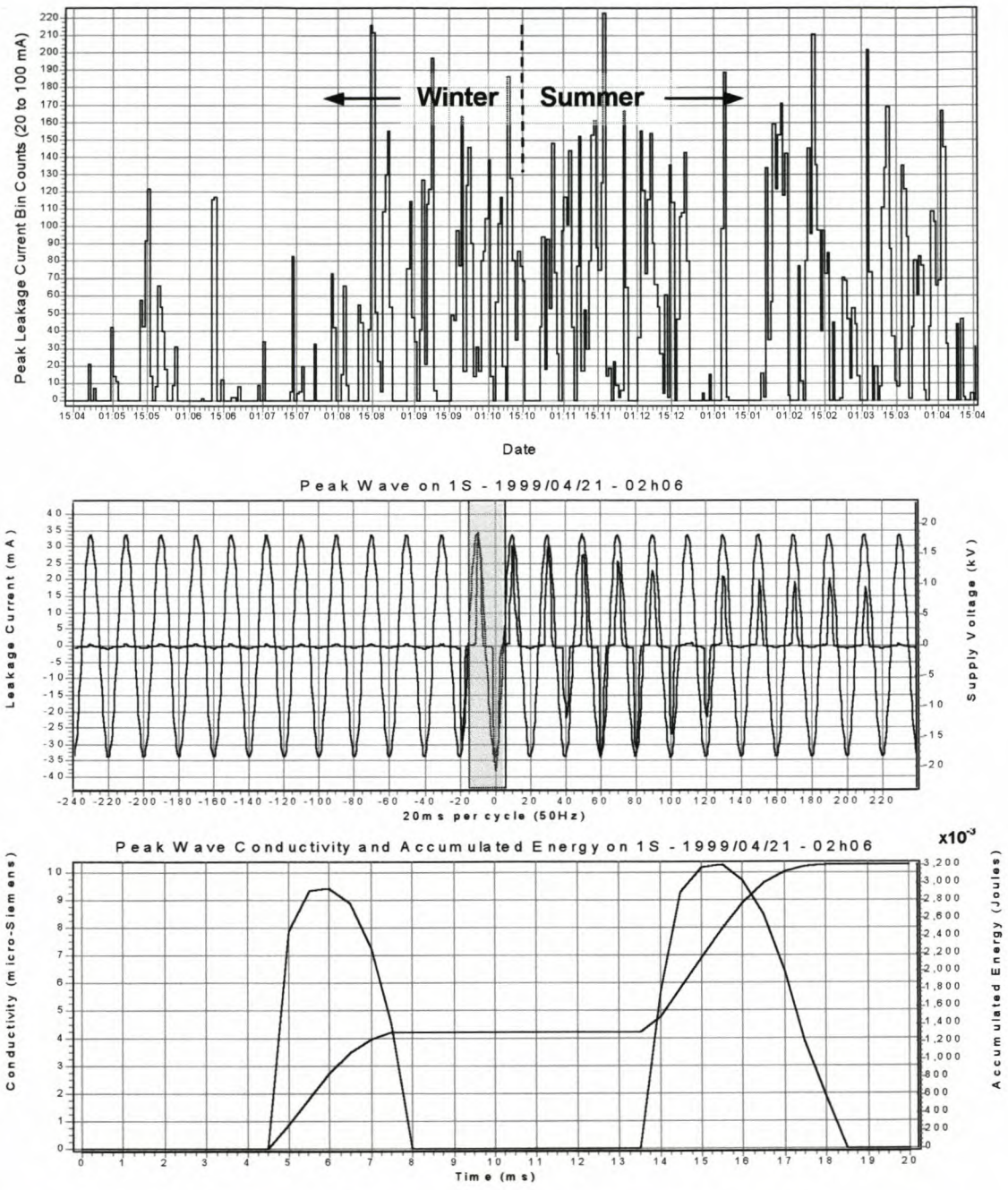

Figure F. 3 The daily bin counts for insulator **1S** are shown for the peak leakage current pulses in size range **20 to 100 mA**. The first peak leakage current and voltage waveform measured in this range, with associated conductivity and accumulated energy for the selected 20 ms cycle (shaded area), are also shown.

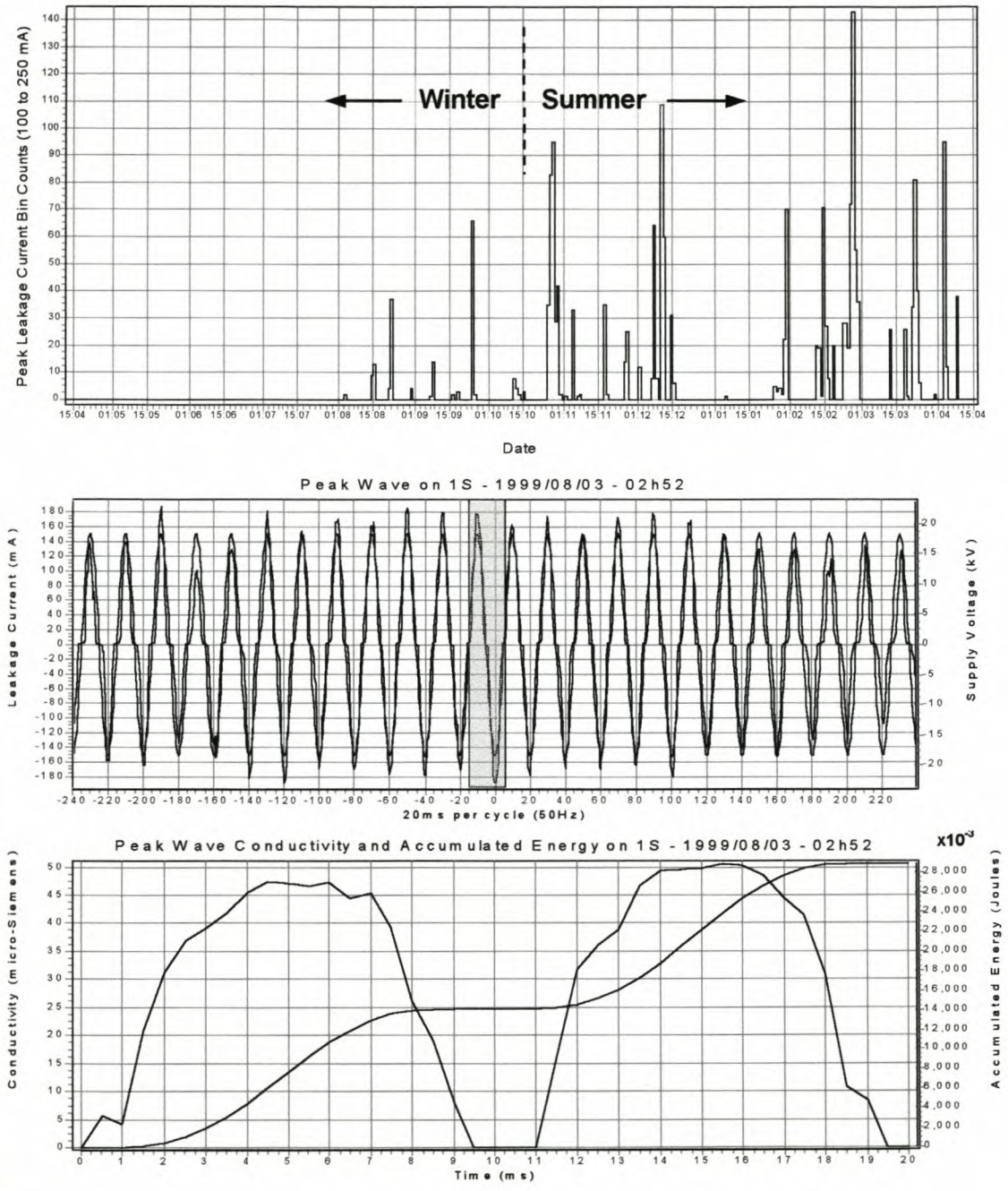

Figure F. 4 The daily bin counts for insulator **1S** are shown for the peak leakage current pulses in size range **100 to 250 mA**. The first peak leakage current and voltage waveform measured in this range, with associated conductivity and accumulated energy for the selected 20 ms cycle (shaded area), are also shown.

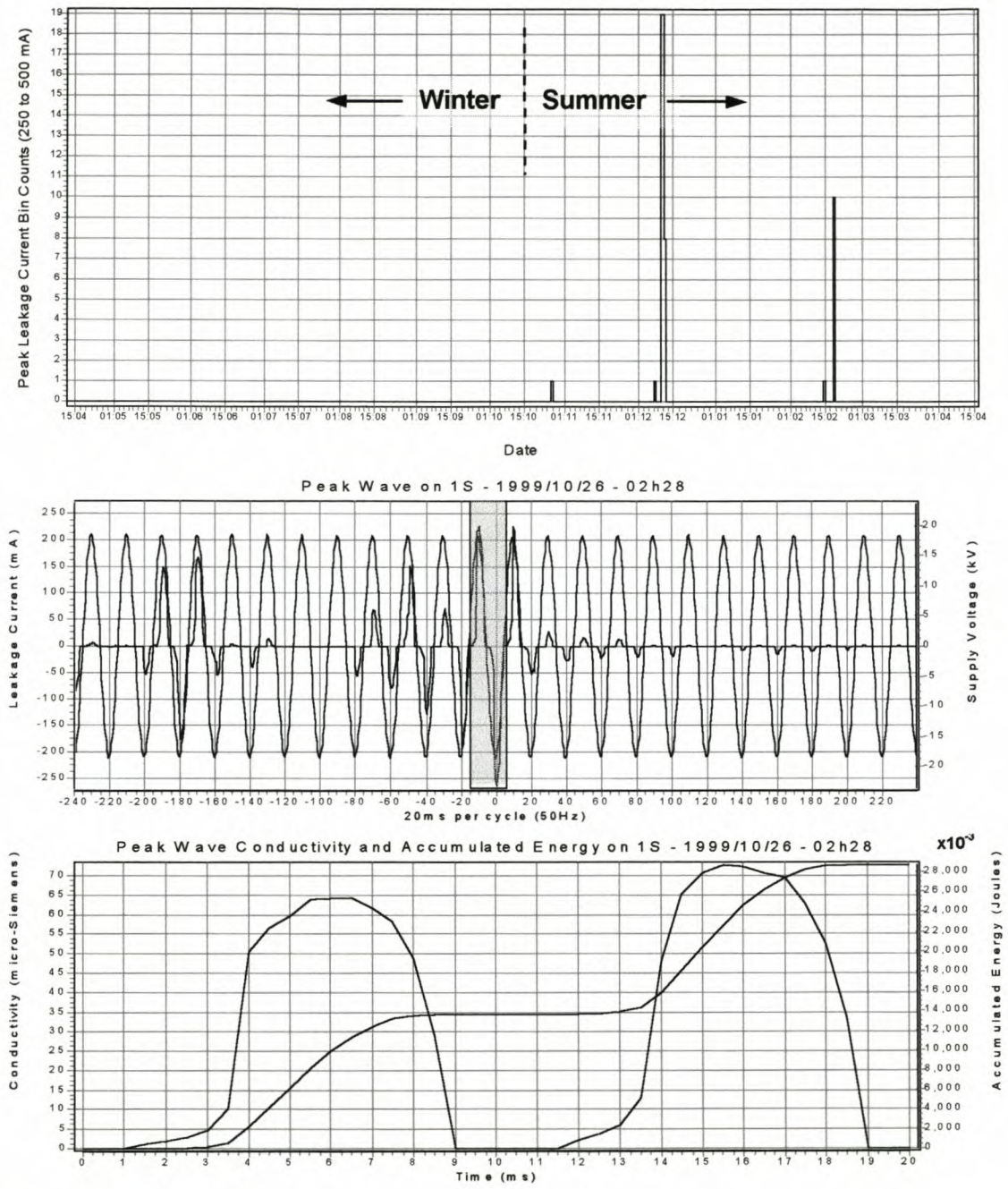

Figure F. 5 The daily bin counts for insulator **1S** are shown for the peak leakage current pulses in size range **250 to 500 mA**. The first peak leakage current and voltage waveform measured in this range, with associated conductivity and accumulated energy for the selected 20 ms cycle (shaded area), are also shown.

Leakage current measurements on EPDM insulator 2E

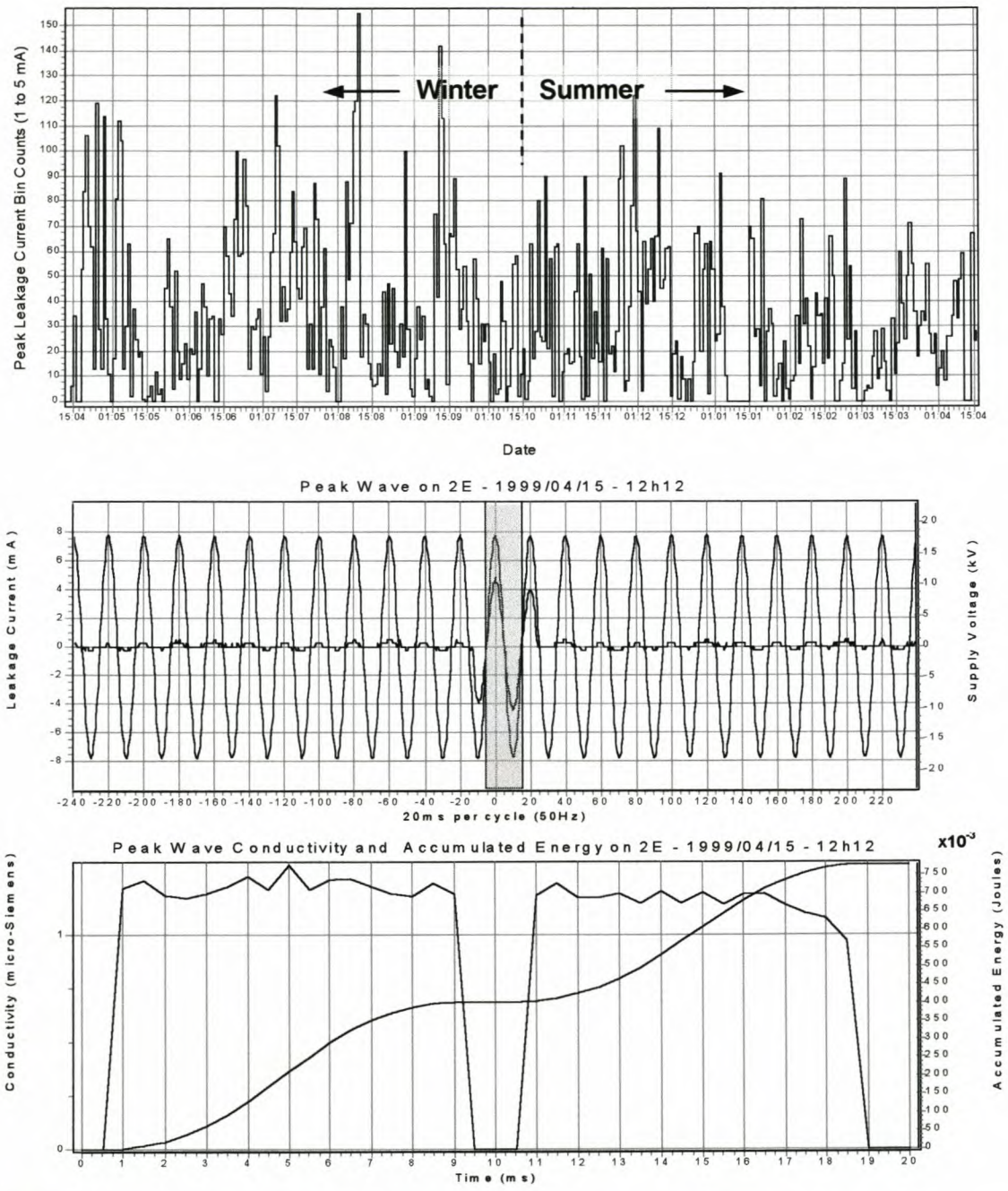

Figure F. 6 The daily bin counts for insulator **2E** are shown for the peak leakage current pulses in size range **1 to 5 mA**. The first peak leakage current and voltage waveform measured in this range, with associated conductivity and accumulated energy for the selected 20 ms cycle (shaded area), are also shown.

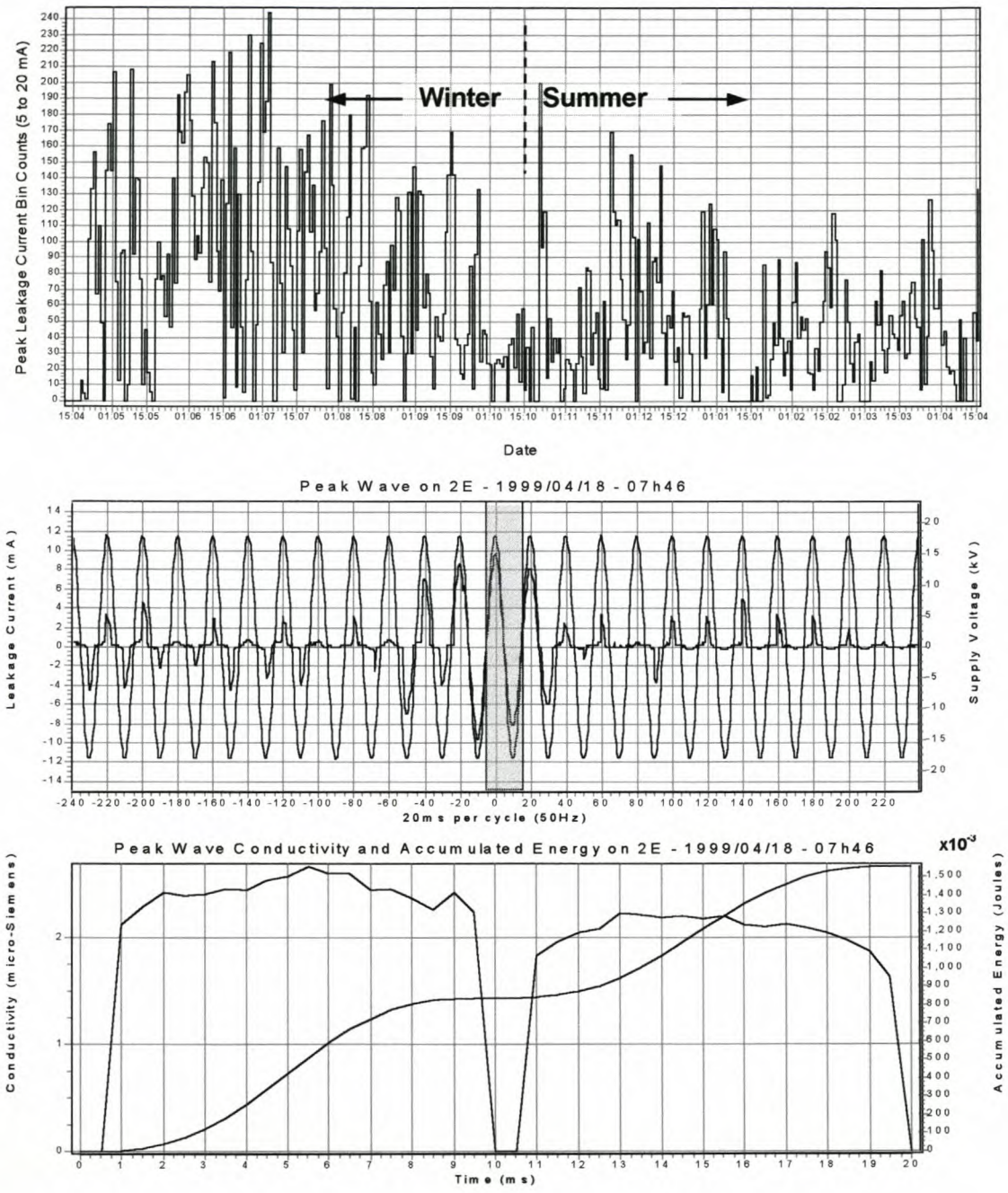

Figure F. 7 The daily bin counts for insulator **2E** are shown for the peak leakage current pulses in size range **5 to 20 mA**. The first peak leakage current and voltage waveform measured in this range, with associated conductivity and accumulated energy for the selected 20 ms cycle (shaded area), are also shown.

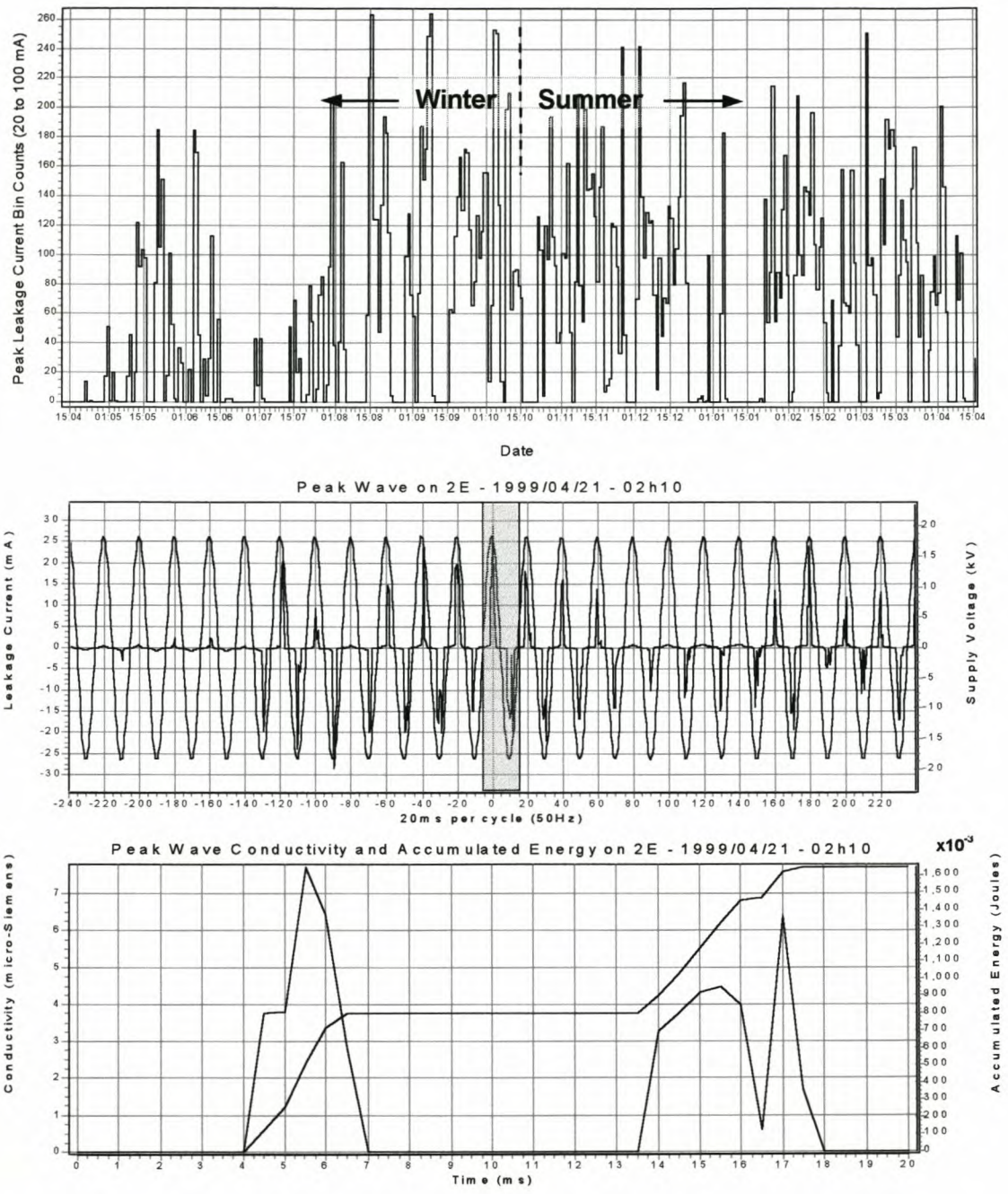

Figure F. 8 The daily bin counts for insulator **2E** are shown for the peak leakage current pulses in size range **20 to 100 mA**. The first peak leakage current and voltage waveform measured in this range, with associated conductivity and accumulated energy for the selected 20 ms cycle (shaded area), are also shown.

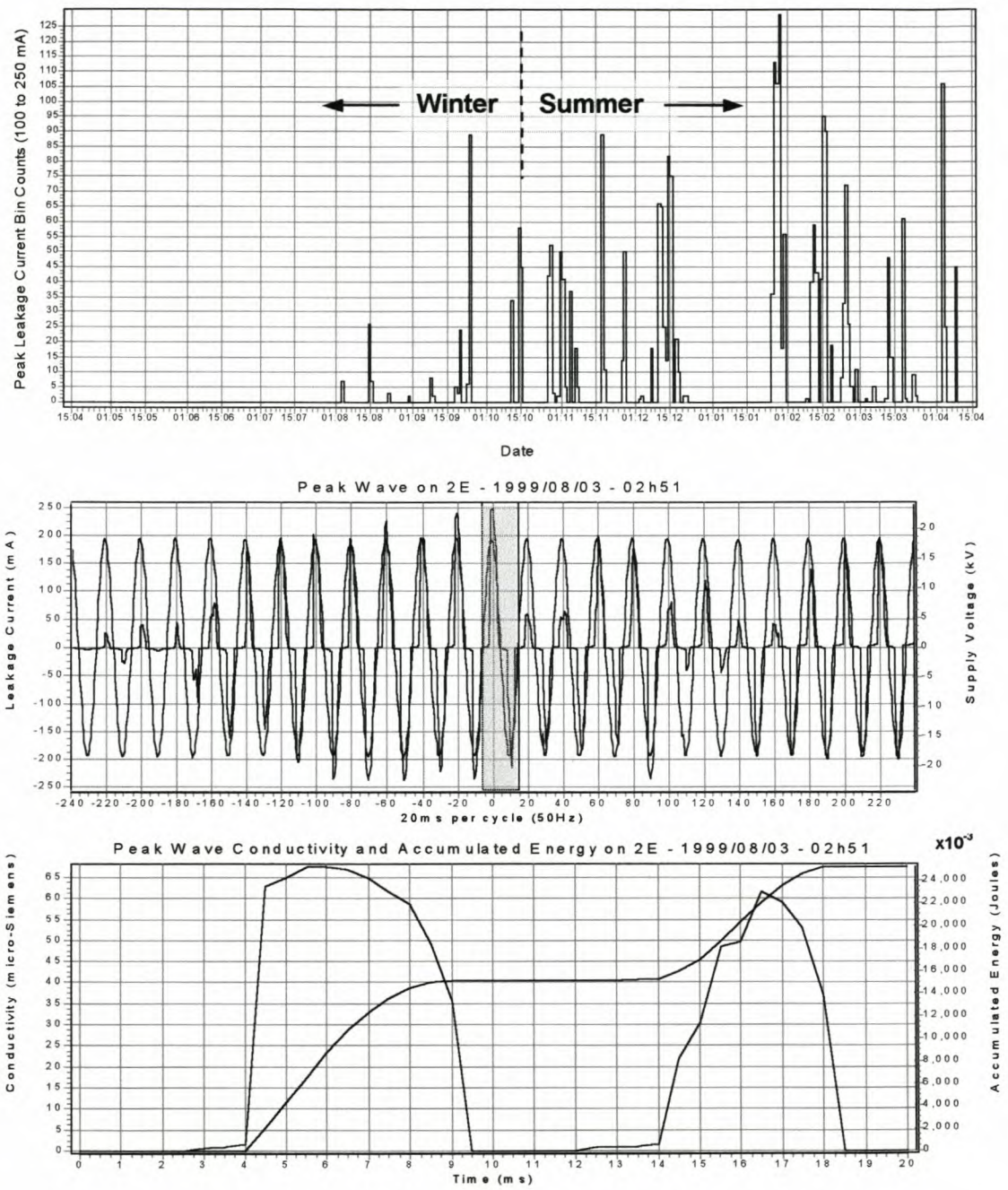

Figure F. 9 The daily bin counts for insulator **2E** are shown for the peak leakage current pulses in size range **100 to 250 mA**. The first peak leakage current and voltage waveform measured in this range, with associated conductivity and accumulated energy for the selected 20 ms cycle (shaded area), are also shown.

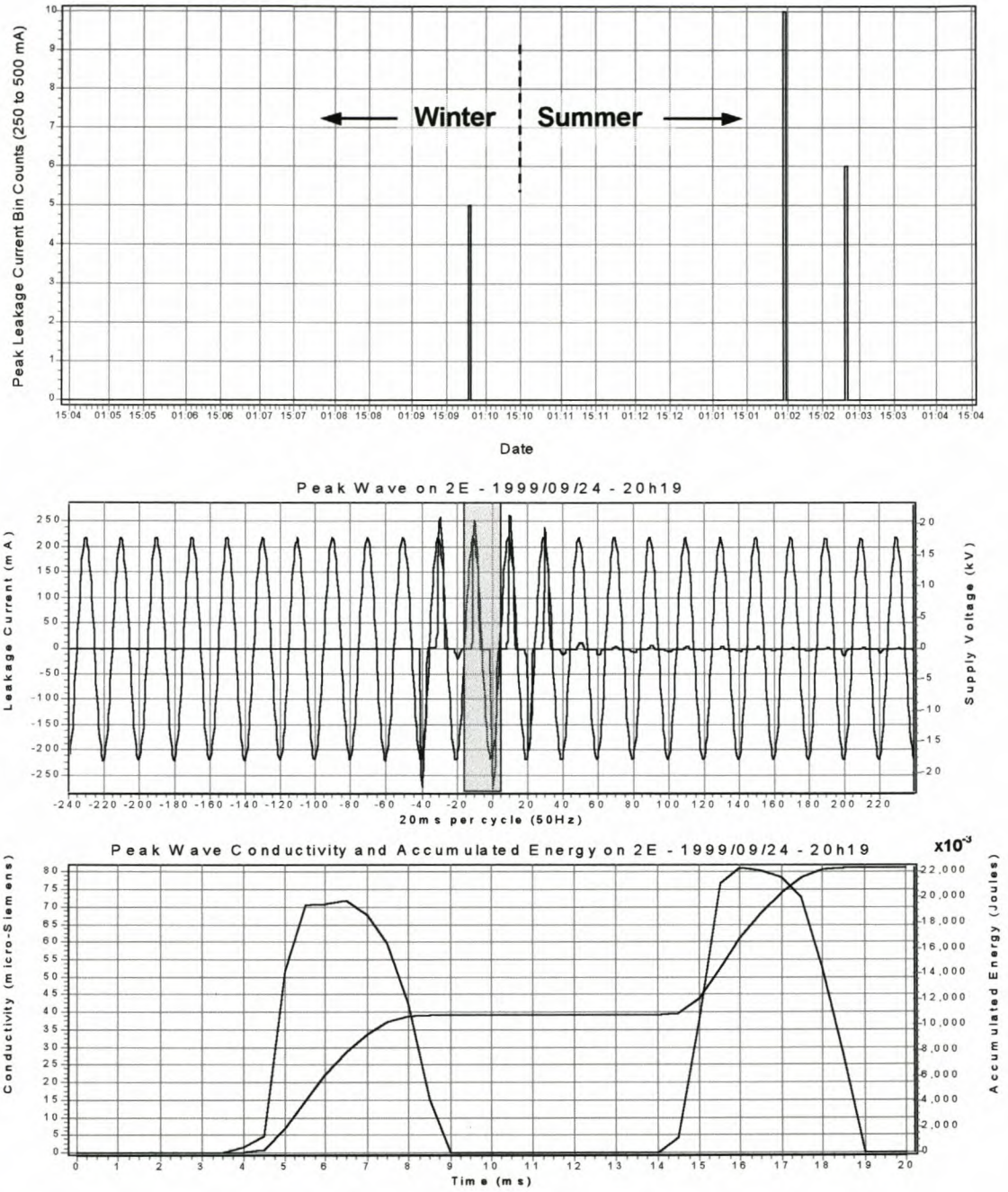

Figure F. 10 The daily bin counts for insulator **2E** are shown for the peak leakage current pulses in size range **250 to 500 mA**. The first peak leakage current and voltage waveform measured in this range, with associated conductivity and accumulated energy for the selected 20 ms cycle (shaded area), are also shown.

Leakage current measurements on porcelain insulator 3P

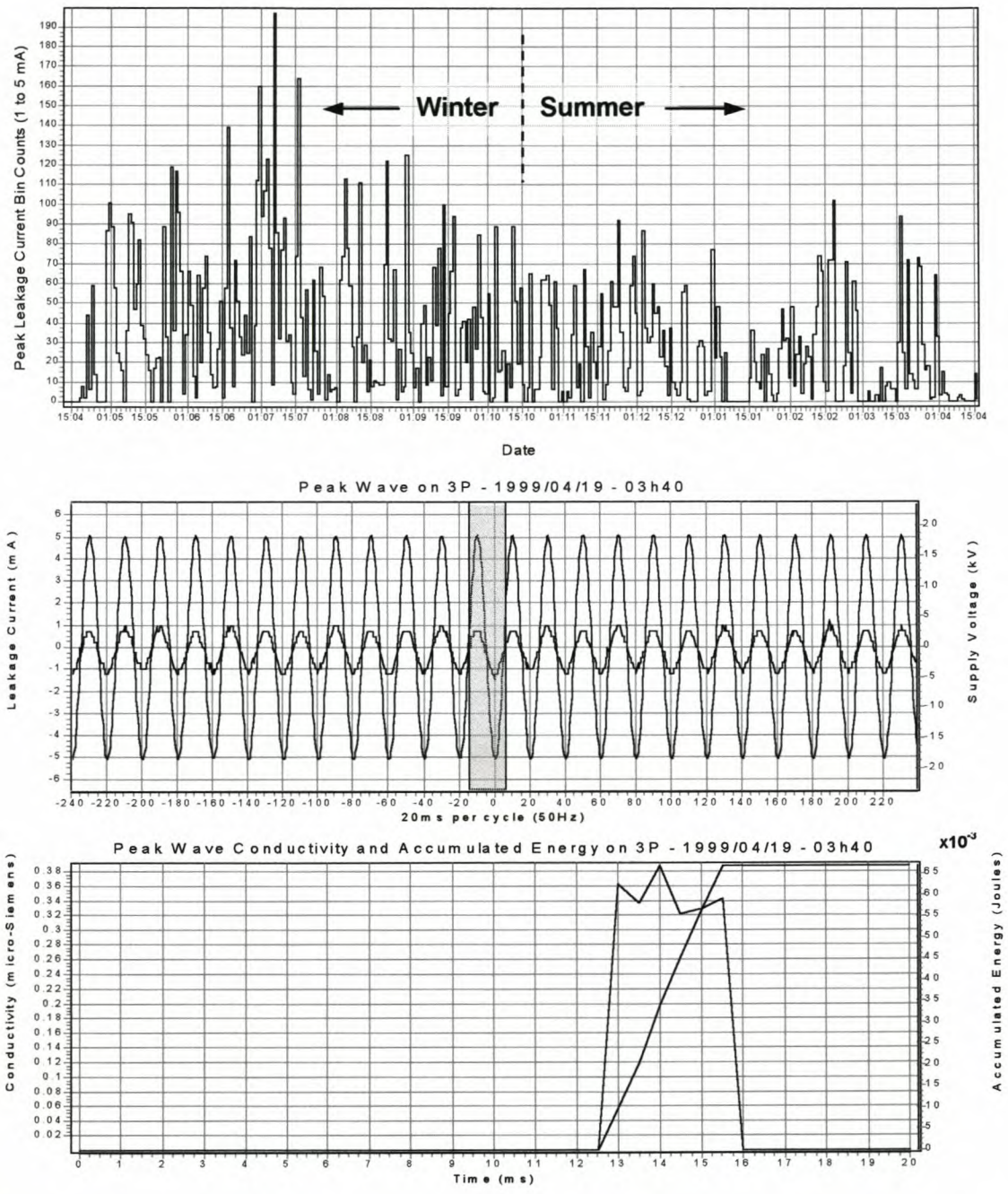

Figure F. 11 The daily bin counts for insulator **3P** are shown for the peak leakage current pulses in size range **1 to 5 mA**. The first peak leakage current and voltage waveform measured in this range, with associated conductivity and accumulated energy for the selected 20 ms cycle (shaded area), are also shown.

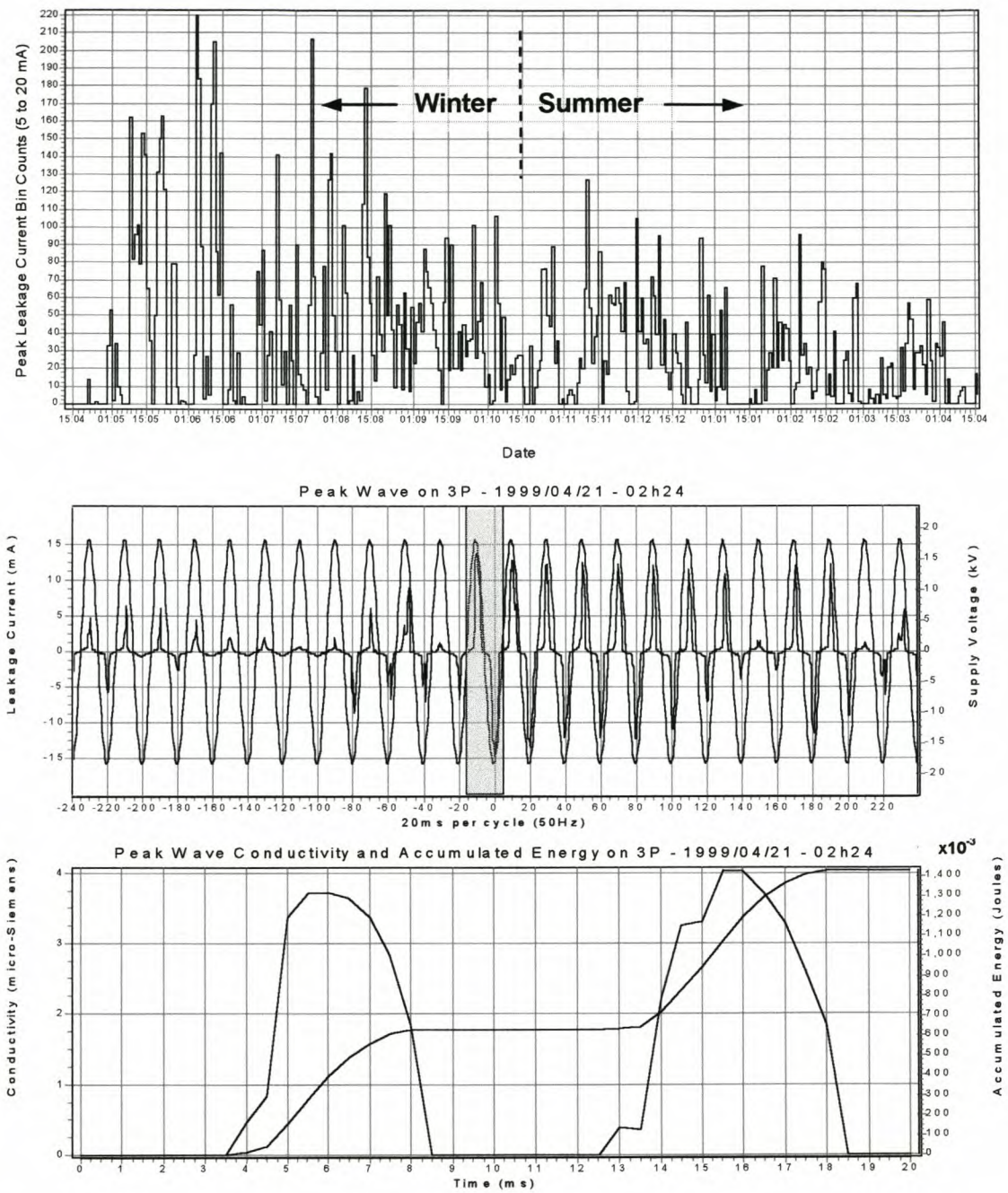

Figure F. 12 The daily bin counts for insulator **3P** are shown for the peak leakage current pulses in size range **5 to 20 mA**. The first peak leakage current and voltage waveform measured in this range, with associated conductivity and accumulated energy for the selected 20 ms cycle (shaded area), are also shown.

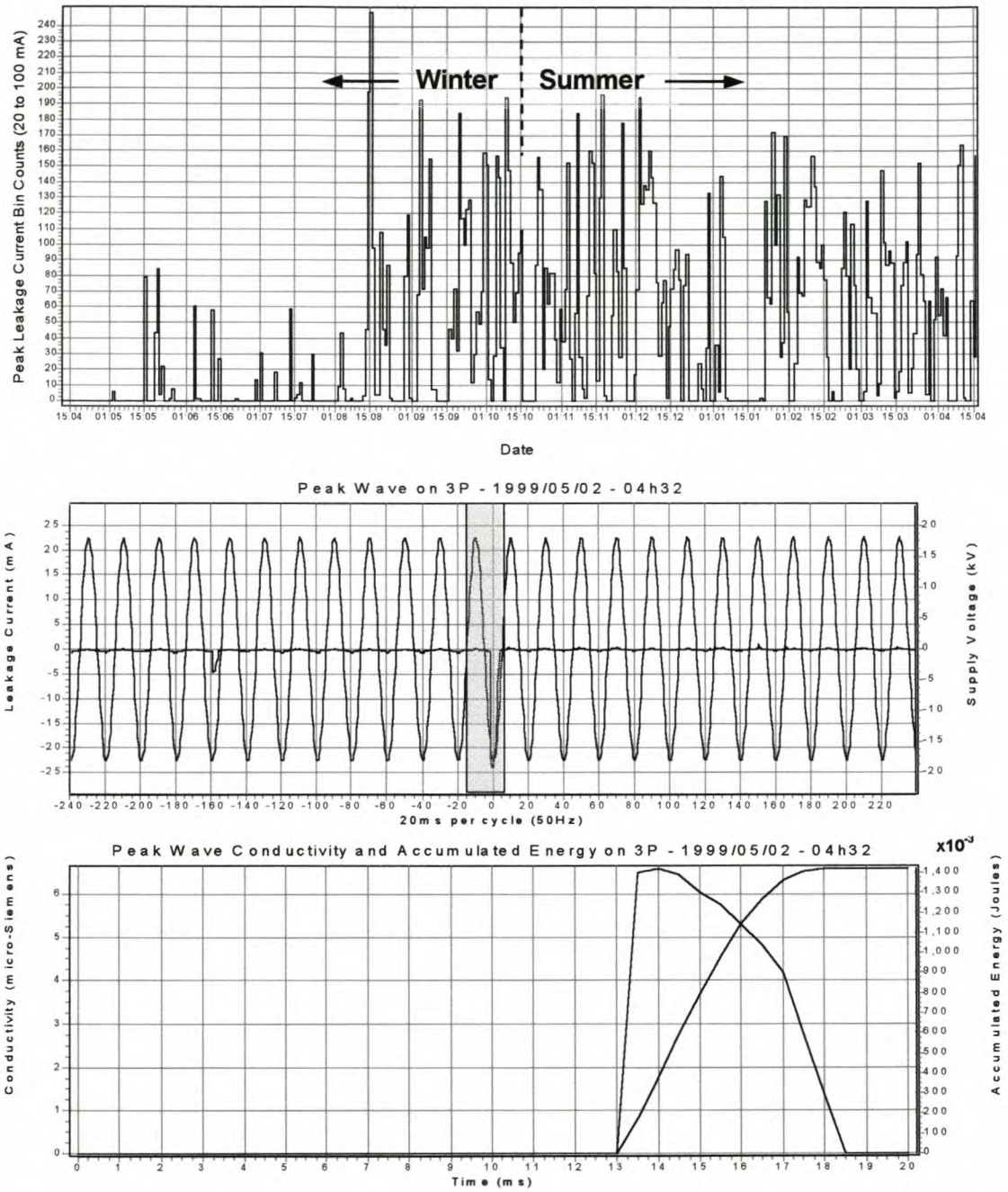

Figure F. 13 The daily bin counts for insulator **3P** are shown for the peak leakage current pulses in size range **20 to 100 mA**. The first peak leakage current and voltage waveform measured in this range, with associated conductivity and accumulated energy for the selected 20 ms cycle (shaded area), are also shown.

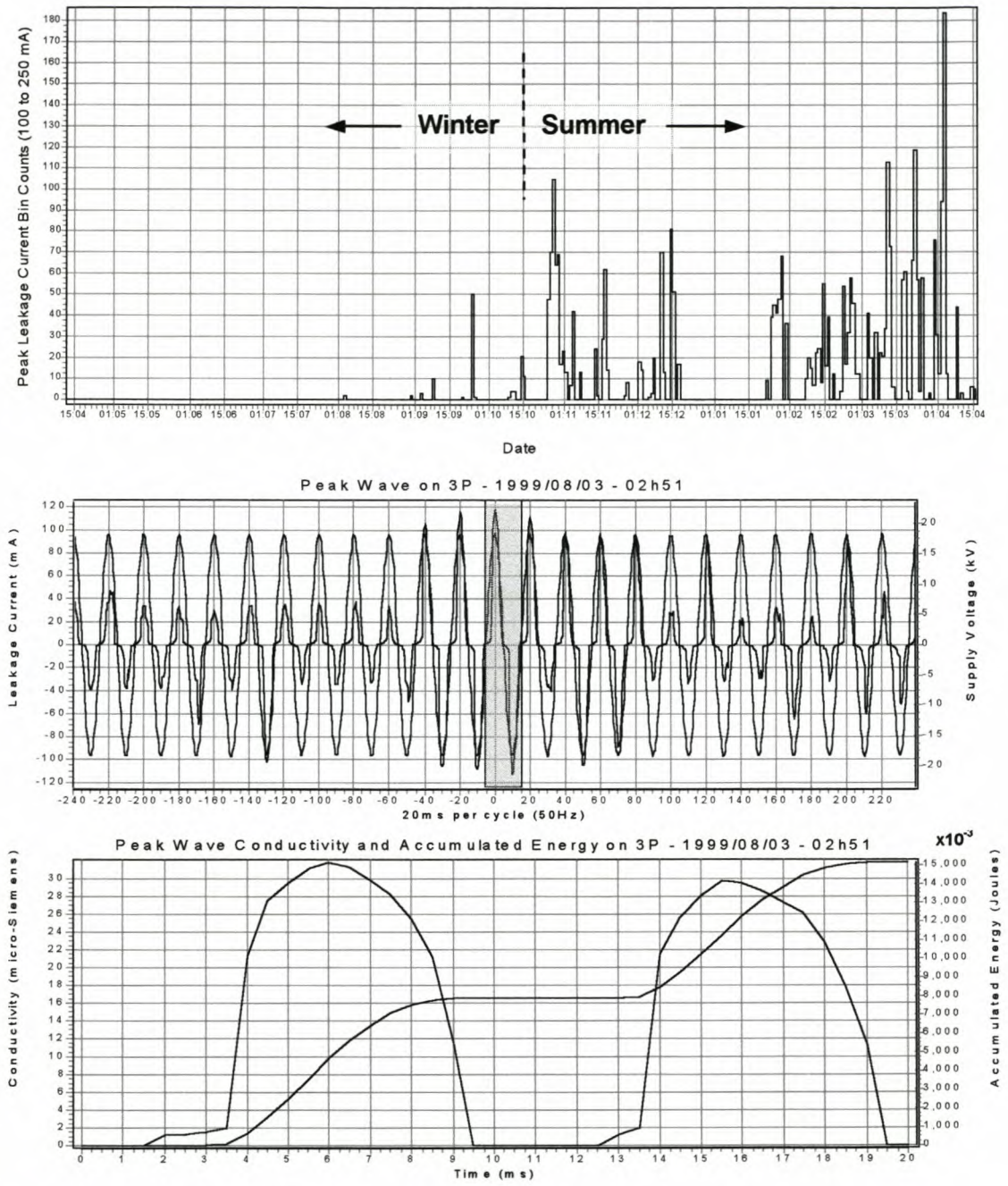

Figure F. 14 The daily bin counts for insulator **3P** are shown for the peak leakage current pulses in size range **100 to 250 mA**. The first peak leakage current and voltage waveform measured in this range, with associated conductivity and accumulated energy for the selected 20 ms cycle (shaded area), are also shown.

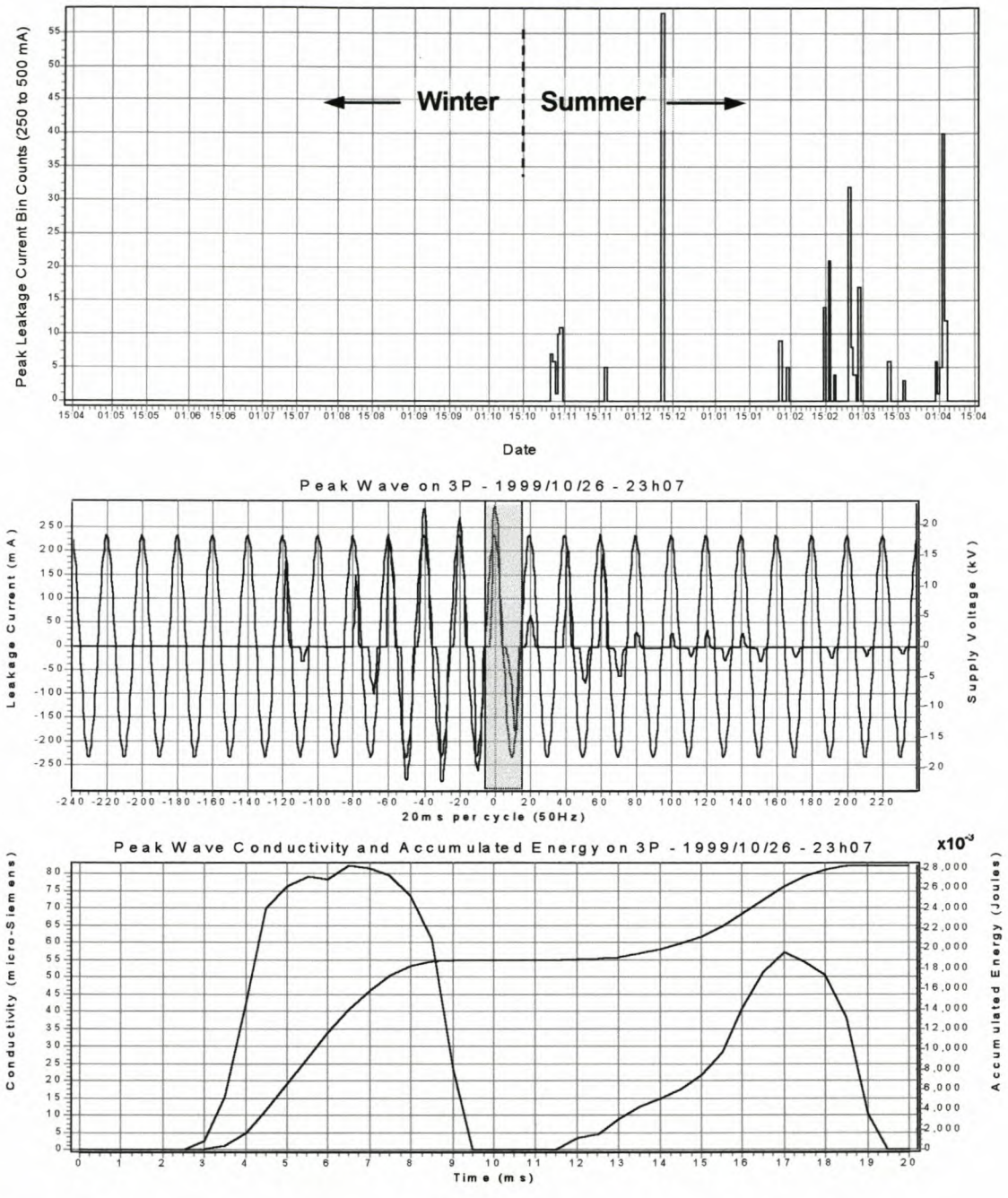

Figure F. 15 The daily bin counts for insulator **3P** are shown for the peak leakage current pulses in size range **250 to 500 mA**. The first peak leakage current and voltage waveform measured in this range, with associated conductivity and accumulated energy for the selected 20 ms cycle (shaded area), are also shown.

Leakage current measurements on RTV SR-coated porcelain insulator 4C

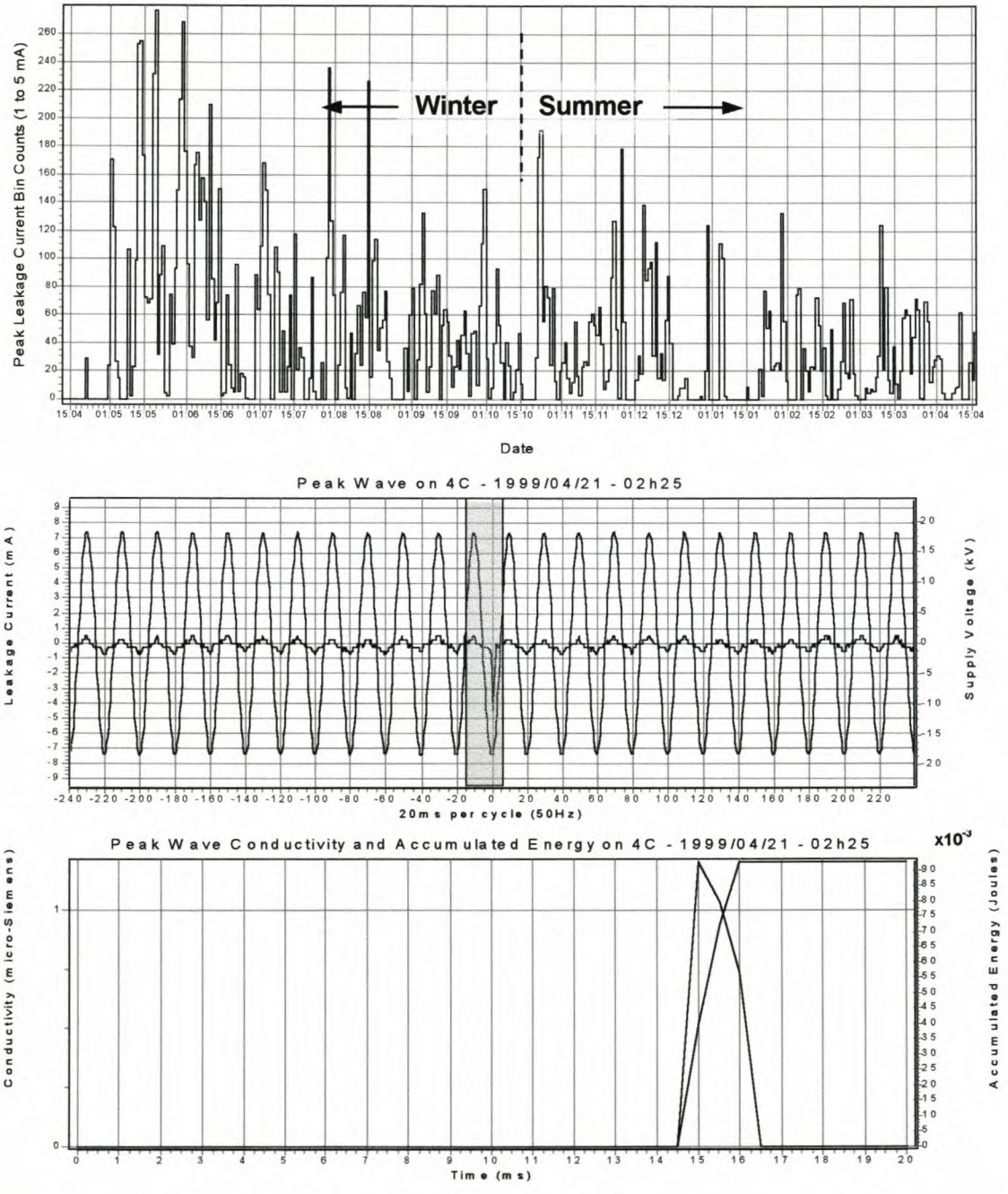

Figure F. 16 The daily bin counts for insulator **4C** are shown for the peak leakage current pulses in size range **1 to 5 mA**. The first peak leakage current and voltage waveform measured in this range, with associated conductivity and accumulated energy for the selected 20 ms cycle (shaded area), are also shown.

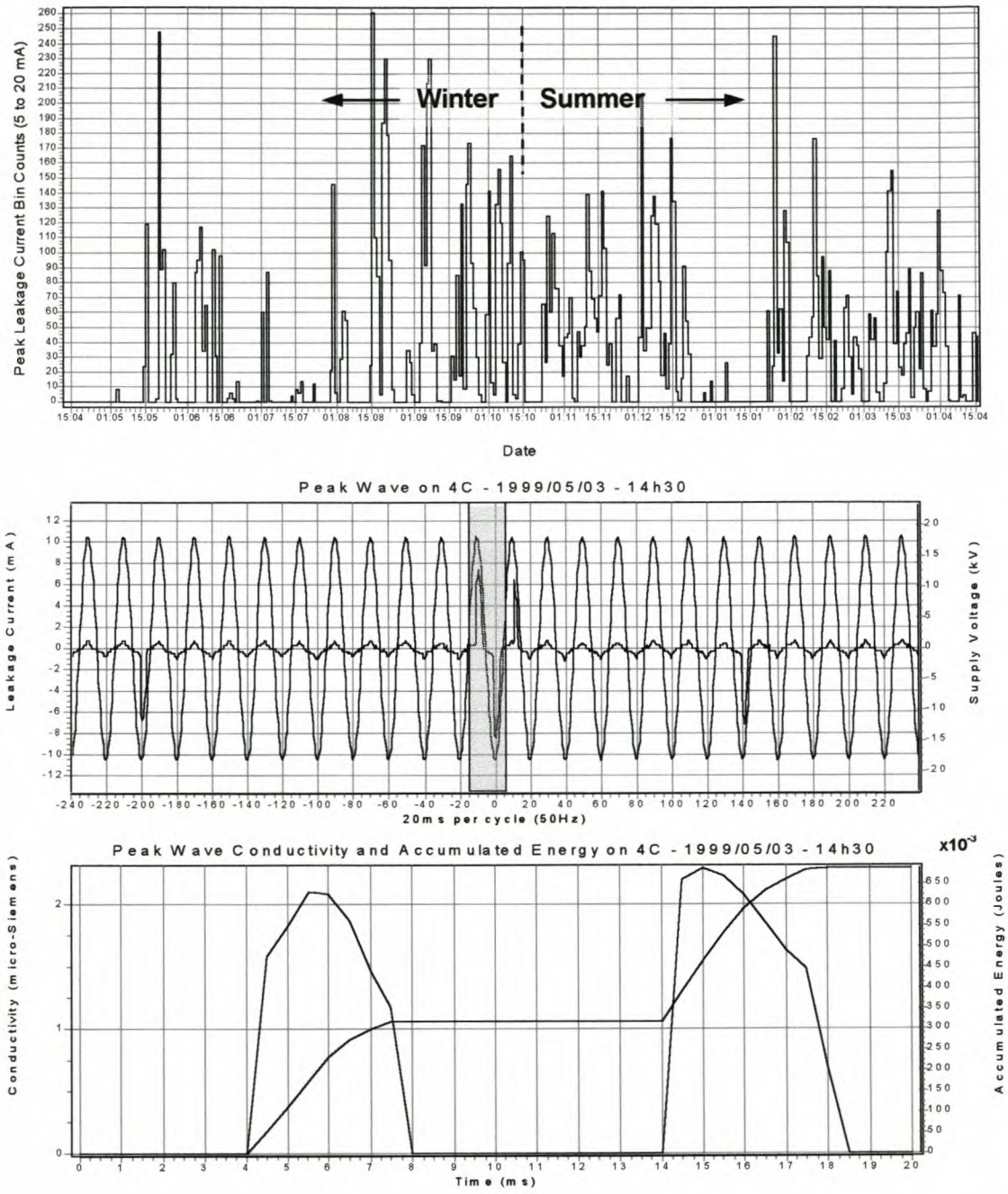

Figure F. 17 The daily bin counts for insulator **4C** are shown for the peak leakage current pulses in size range **5 to 20 mA**. The first peak leakage current and voltage waveform measured in this range, with associated conductivity and accumulated energy for the selected 20 ms cycle (shaded area), are also shown.

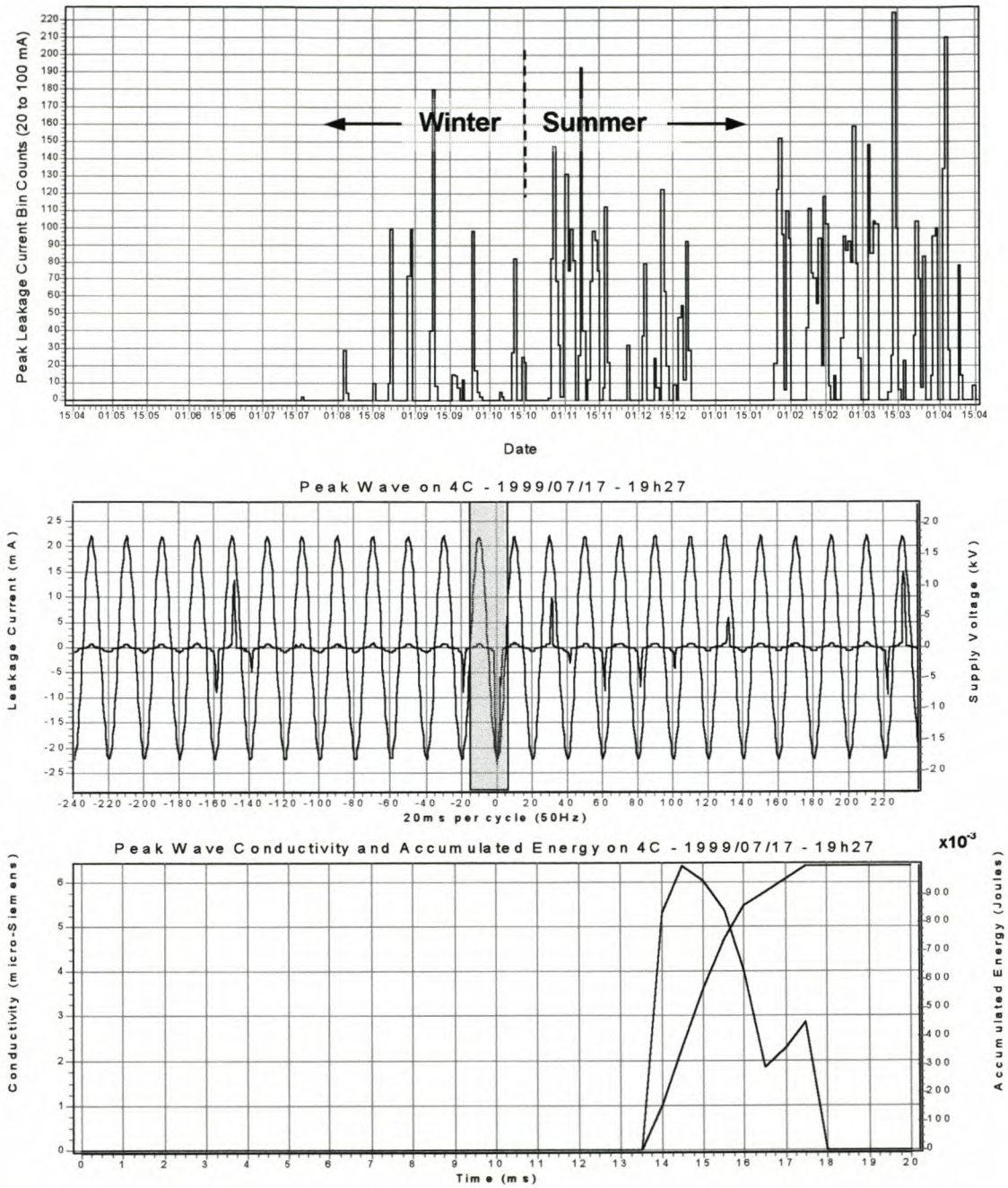

Figure F. 18 The daily bin counts for insulator **4C** are shown for the peak leakage current pulses in size range **20 to 100 mA**. The first peak leakage current and voltage waveform measured in this range, with associated conductivity and accumulated energy for the selected 20 ms cycle (shaded area), are also shown.

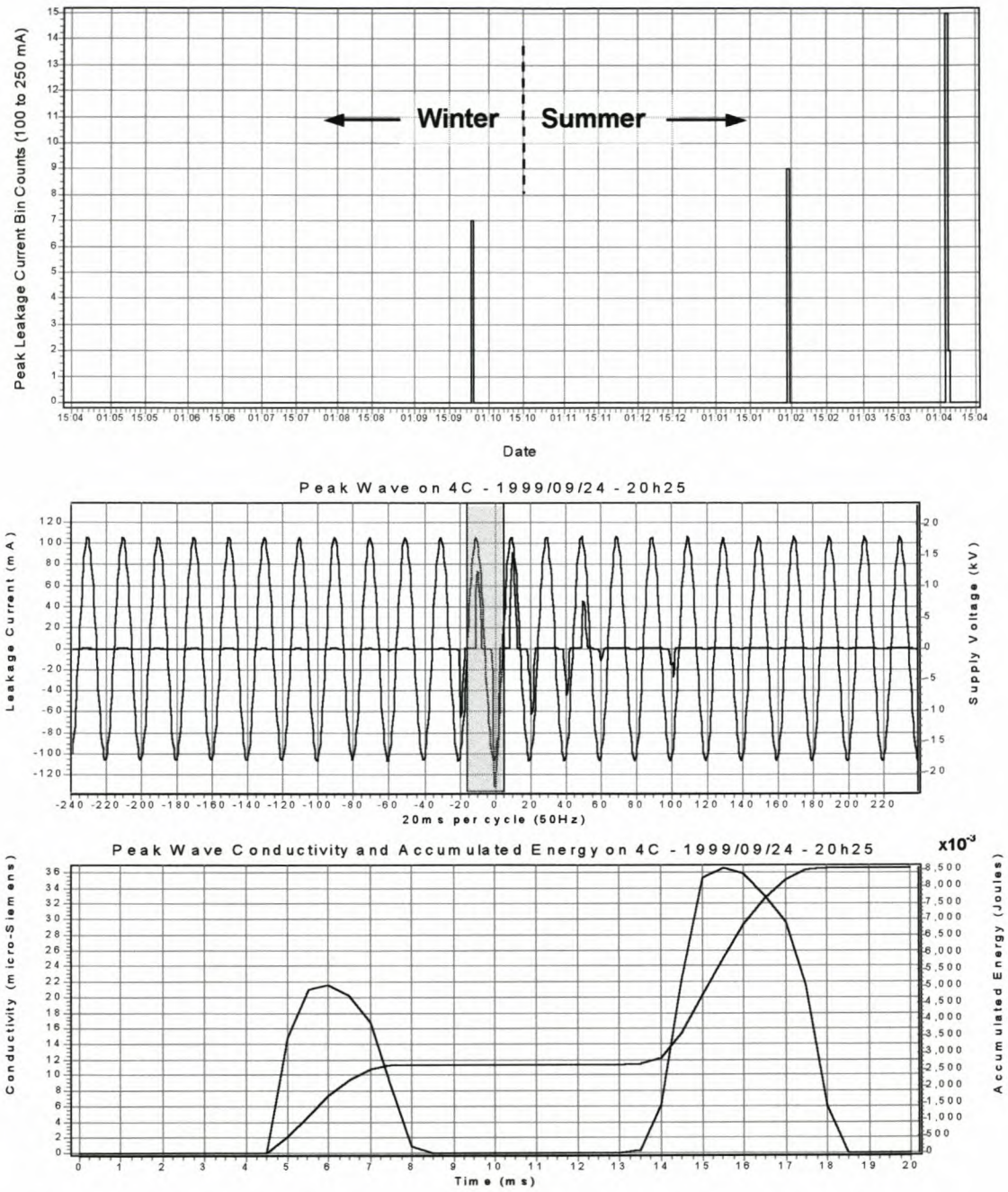

Figure F. 19 The daily bin counts for insulator **4C** are shown for the peak leakage current pulses in size range **100 to 250 mA**. The first peak leakage current and voltage waveform measured in this range, with associated conductivity and accumulated energy for the selected 20 ms cycle (shaded area), are also shown.

There were no daily bin counts for the size range **250 to 500 mA** for insulator **4C**.

Leakage current measurements on cyclo aliphatic insulator 5A

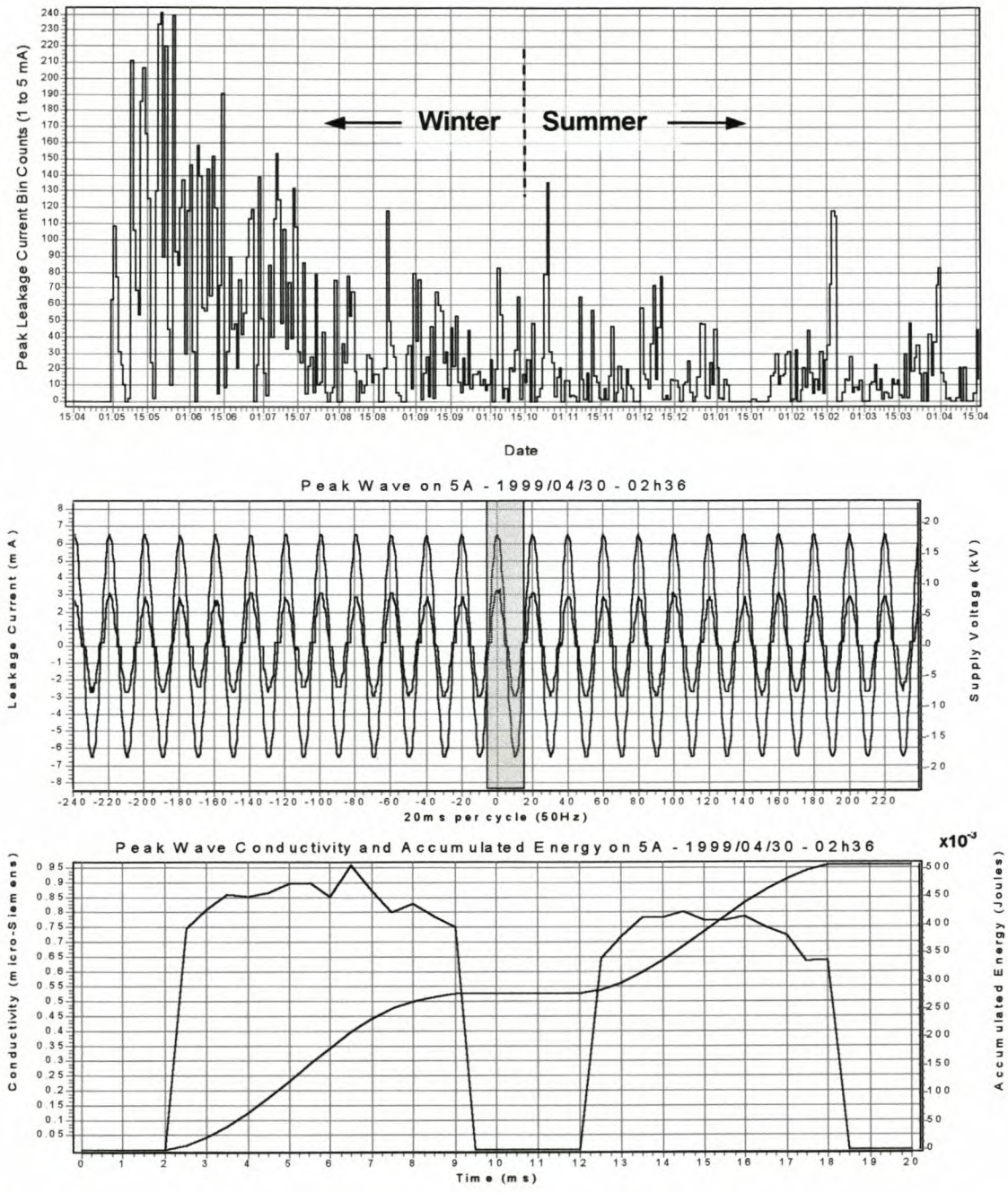

Figure F. 20 The daily bin counts for insulator **5A** are shown for the peak leakage current pulses in size range **1 to 5 mA**. The first peak leakage current and voltage waveform measured in this range, with associated conductivity and accumulated energy for the selected 20 ms cycle (shaded area), are also shown.

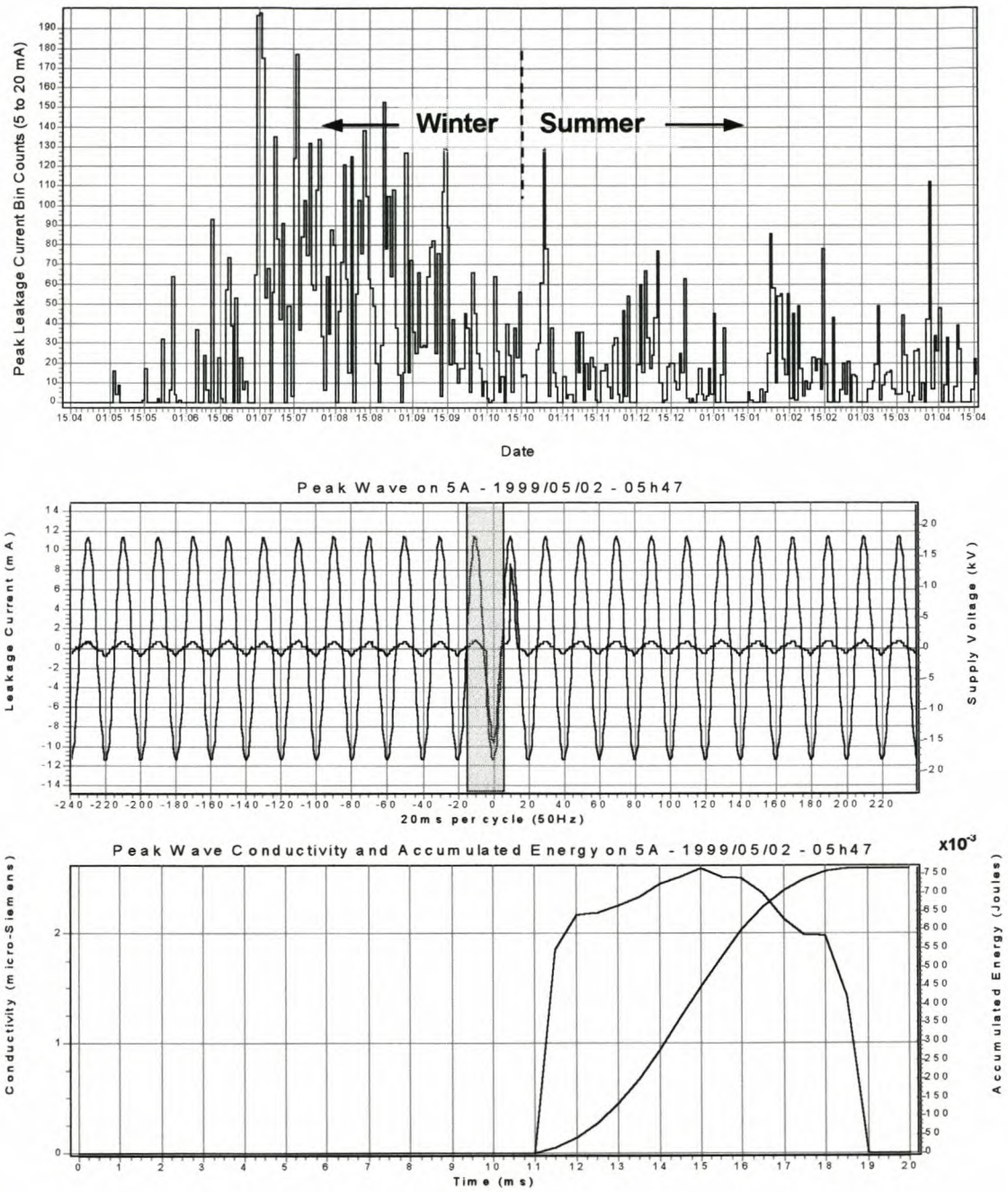

Figure F. 21 The daily bin counts for insulator **5A** are shown for the peak leakage current pulses in size range **5 to 20 mA**. The first peak leakage current and voltage waveform measured in this range, with associated conductivity and accumulated energy for the selected 20 ms cycle (shaded area), are also shown.

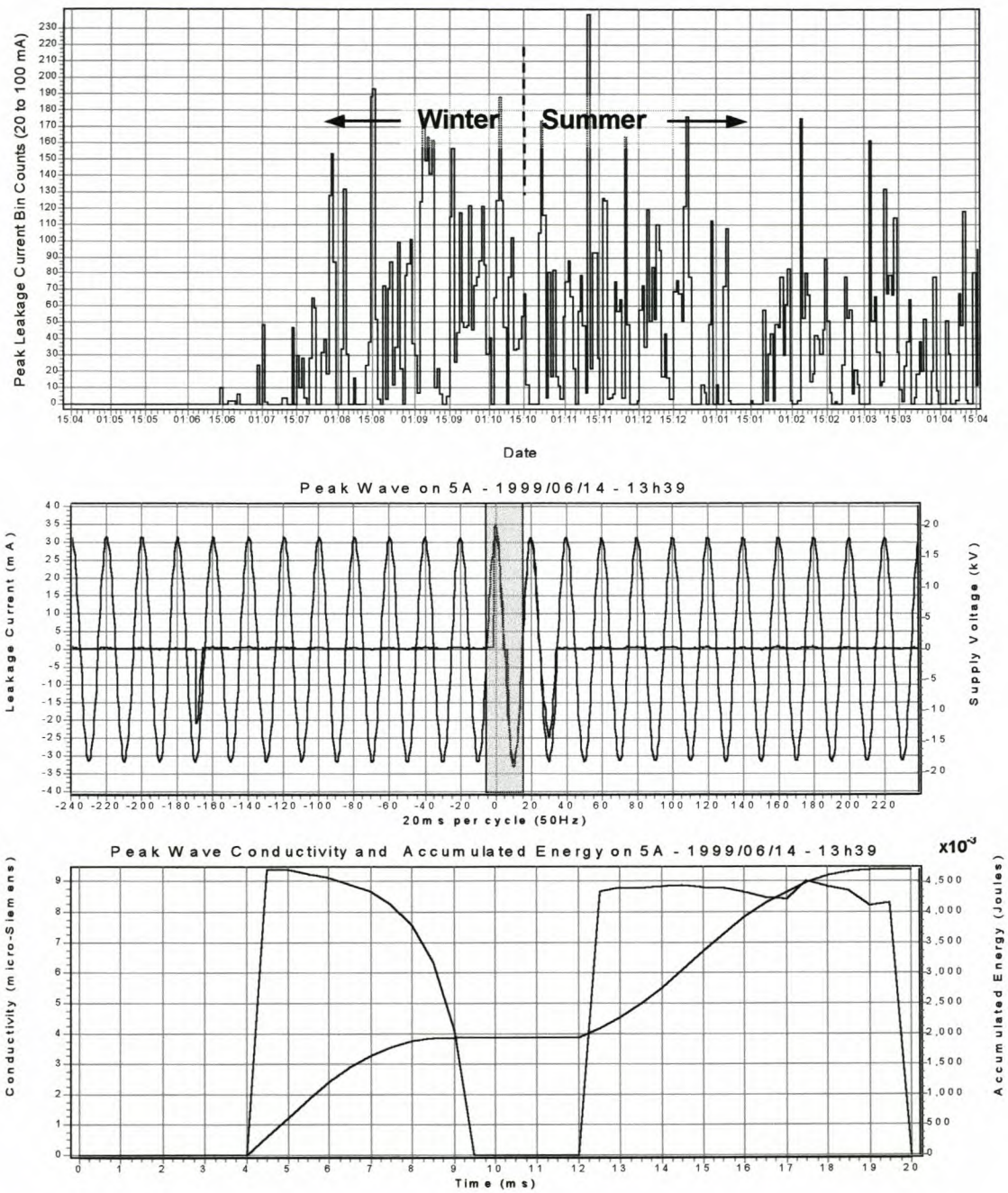

Figure F. 22 The daily bin counts for insulator **5A** are shown for the peak leakage current pulses in size range **20 to 100 mA**. The first peak leakage current and voltage waveform measured in this range, with associated conductivity and accumulated energy for the selected 20 ms cycle (shaded area), are also shown.

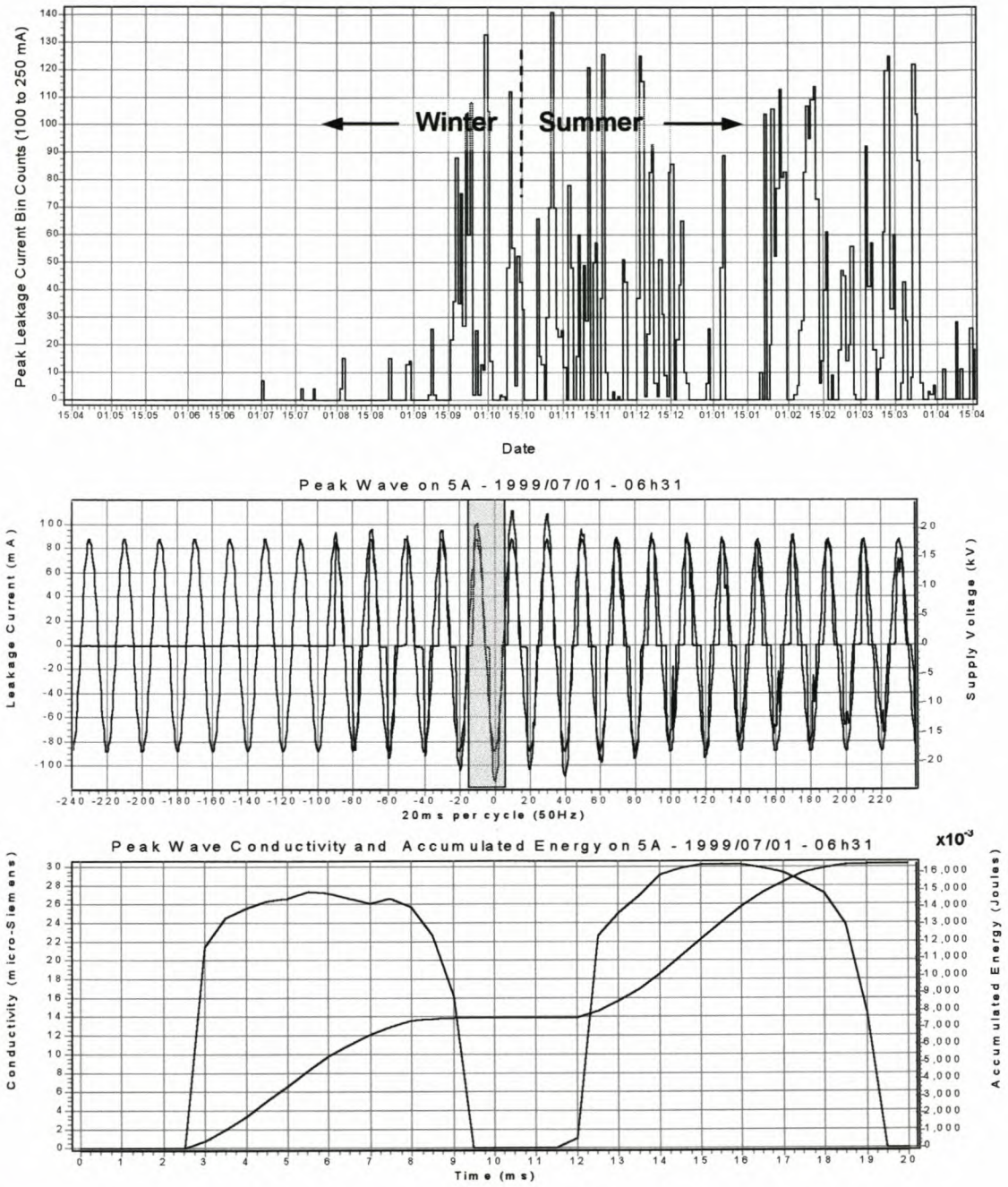

Figure F. 23 The daily bin counts for insulator **5A** are shown for the peak leakage current pulses in size range **100 to 250 mA**. The first peak leakage current and voltage waveform measured in this range, with associated conductivity and accumulated energy for the selected 20 ms cycle (shaded area), are also shown.

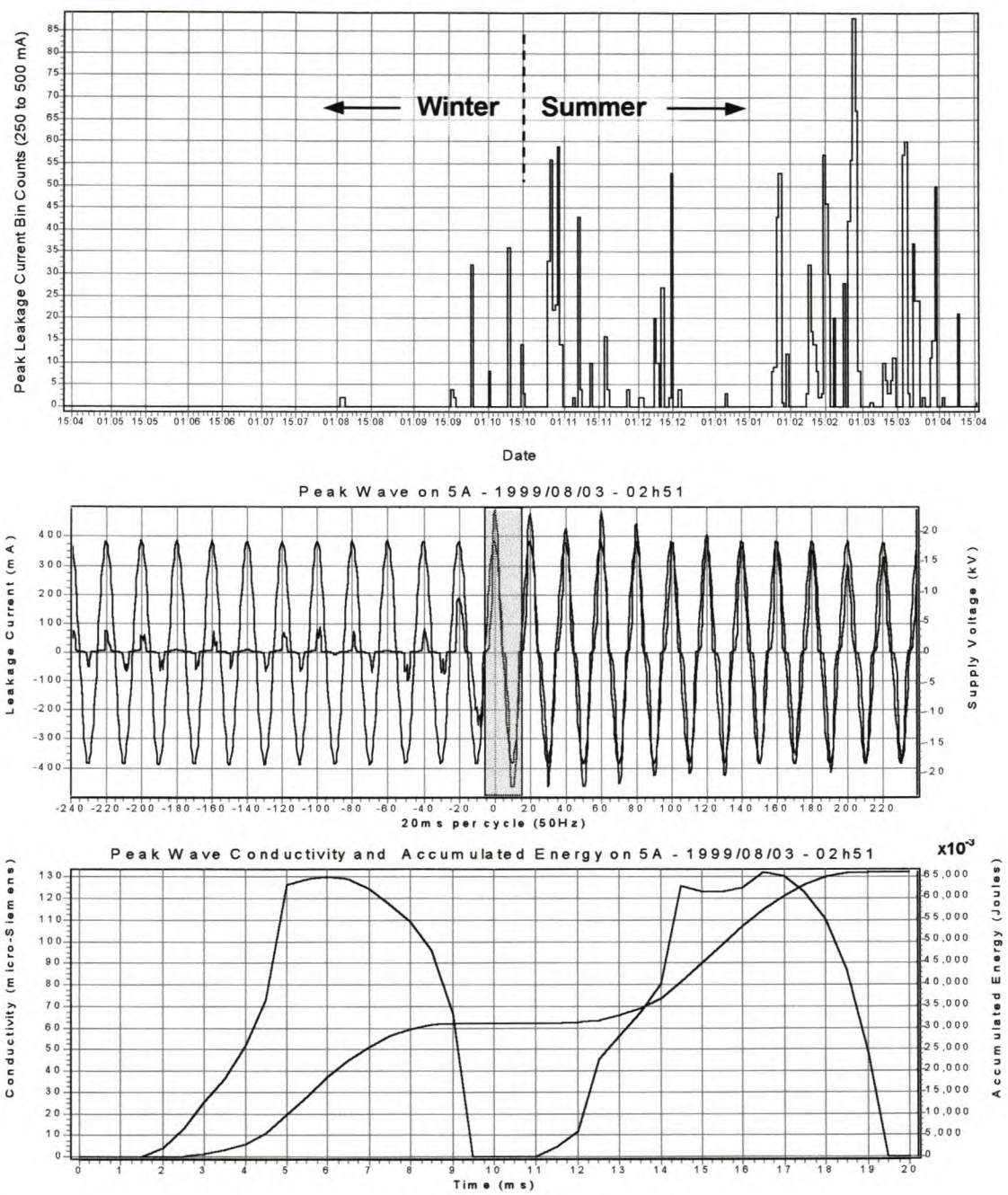

Figure F. 24 The daily bin counts for insulator **5A** are shown for the peak leakage current pulses in size range **250 to 500 mA**. The first peak leakage current and voltage waveform measured in this range, with associated conductivity and accumulated energy for the selected 20 ms cycle (shaded area), are also shown.

Leakage current measurements on RG porcelain insulator 8R

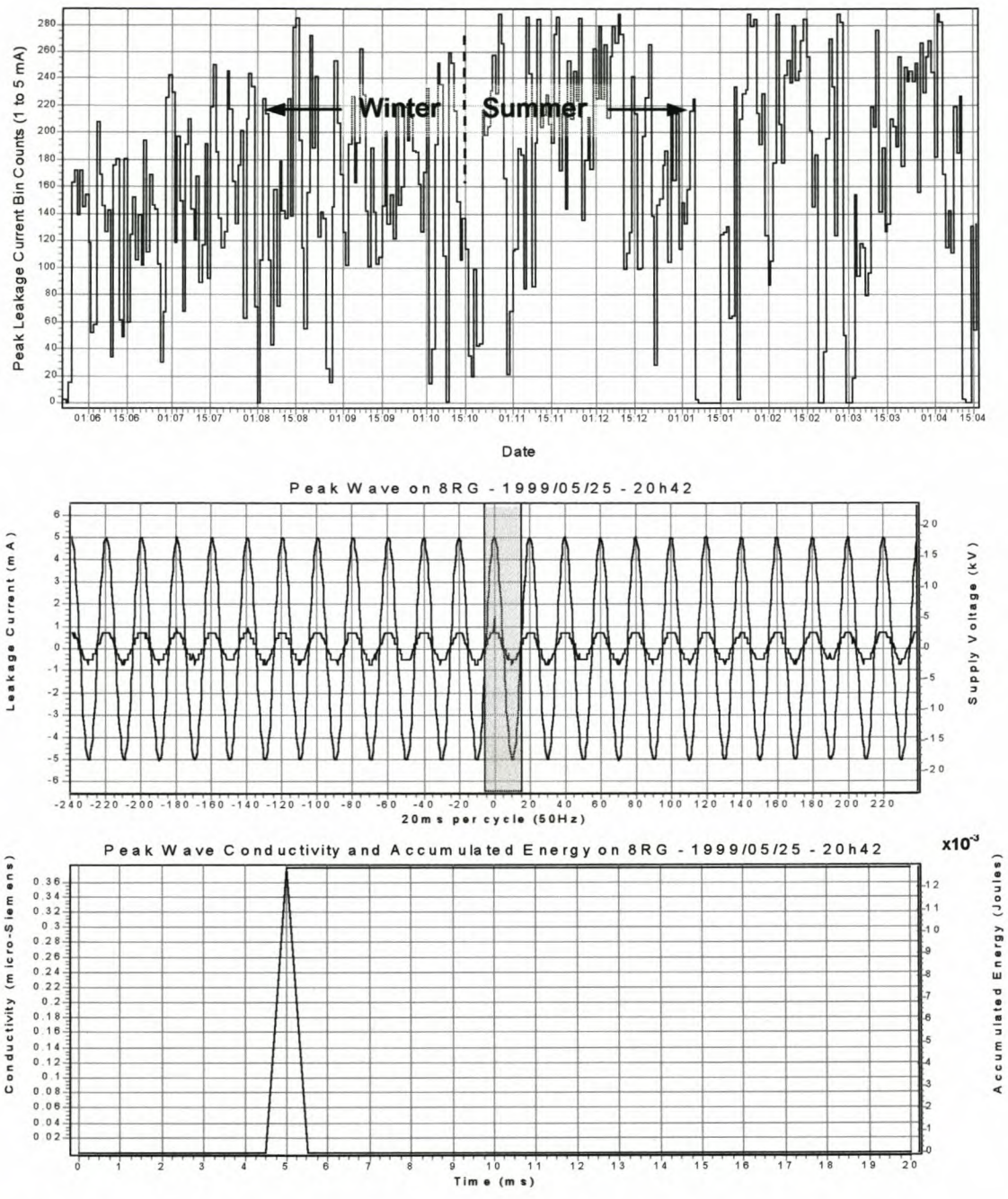

Figure F. 25 The daily bin counts for insulator **8R** are shown for the peak leakage current pulses in size range **1 to 5 mA**. The first peak leakage current and voltage waveform measured in this range, with associated conductivity and accumulated energy for the selected 20 ms cycle (shaded area), are also shown.

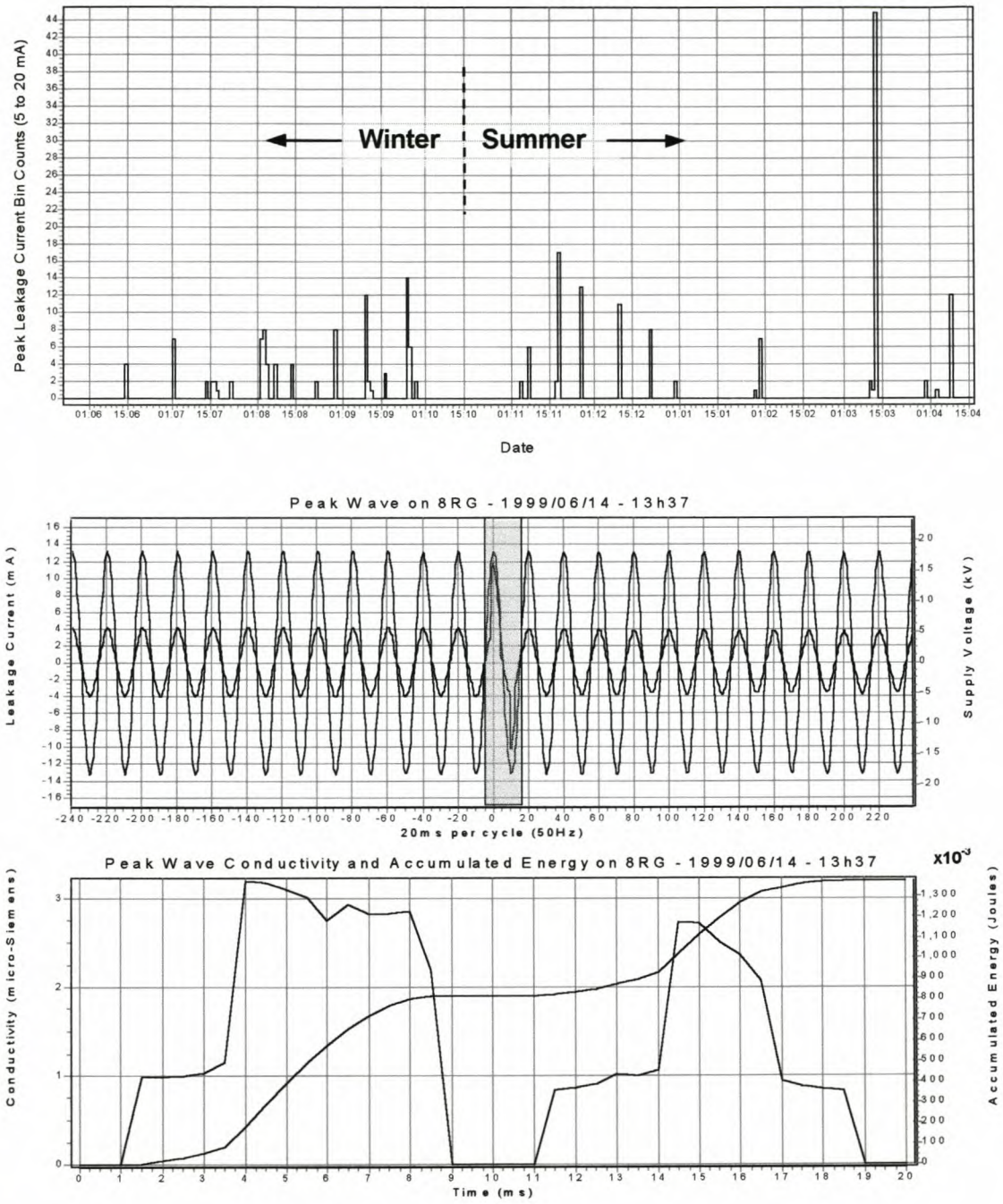

Figure F. 26 The daily bin counts for insulator **8R** are shown for the peak leakage current pulses in size range **5 to 20 mA**. The first peak leakage current and voltage waveform measured in this range, with associated conductivity and accumulated energy for the selected 20 ms cycle (shaded area), are also shown.

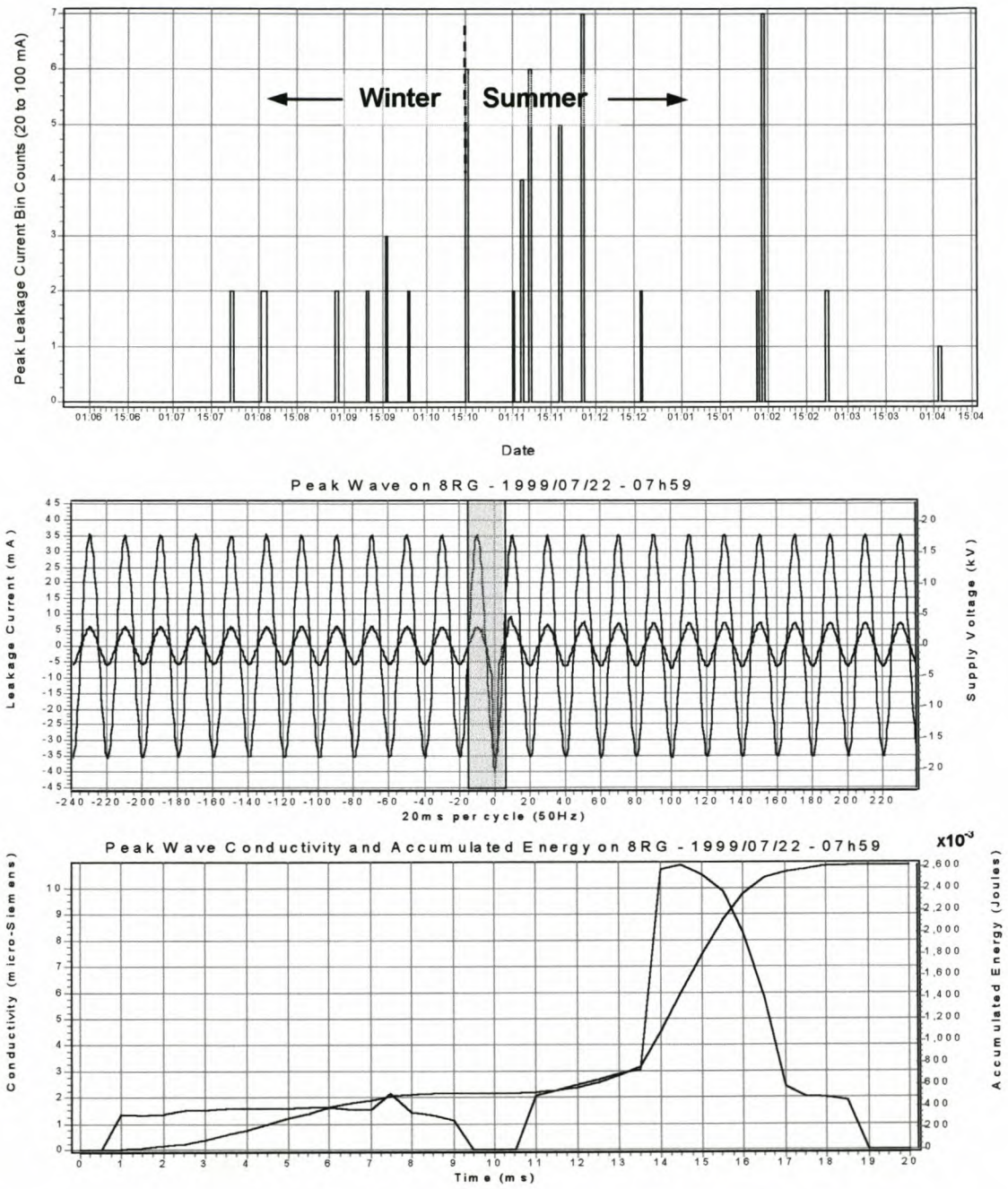

Figure F. 27 The daily bin counts for insulator **8R** are shown for the peak leakage current pulses in size range **20 to 100 mA**. The first peak leakage current and voltage waveform measured in this range, with associated conductivity and accumulated energy for the selected 20 ms cycle (shaded area), are also shown.

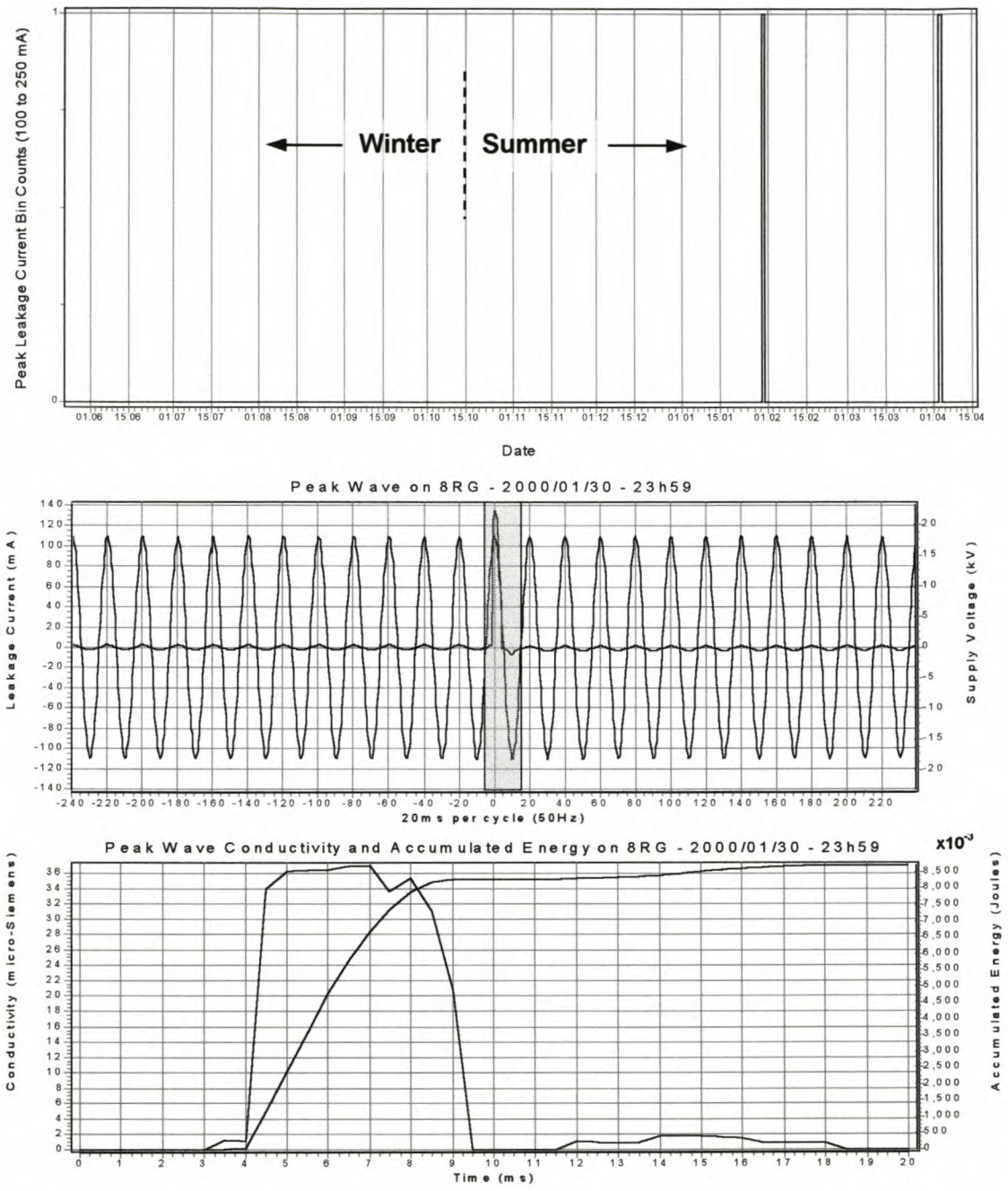

Figure F. 28 The daily bin counts for insulator **8R** are shown for the peak leakage current pulses in size range **100 to 250 mA**. The first peak leakage current and voltage waveform measured in this range, with associated conductivity and accumulated energy for the selected 20 ms cycle (shaded area), are also shown.

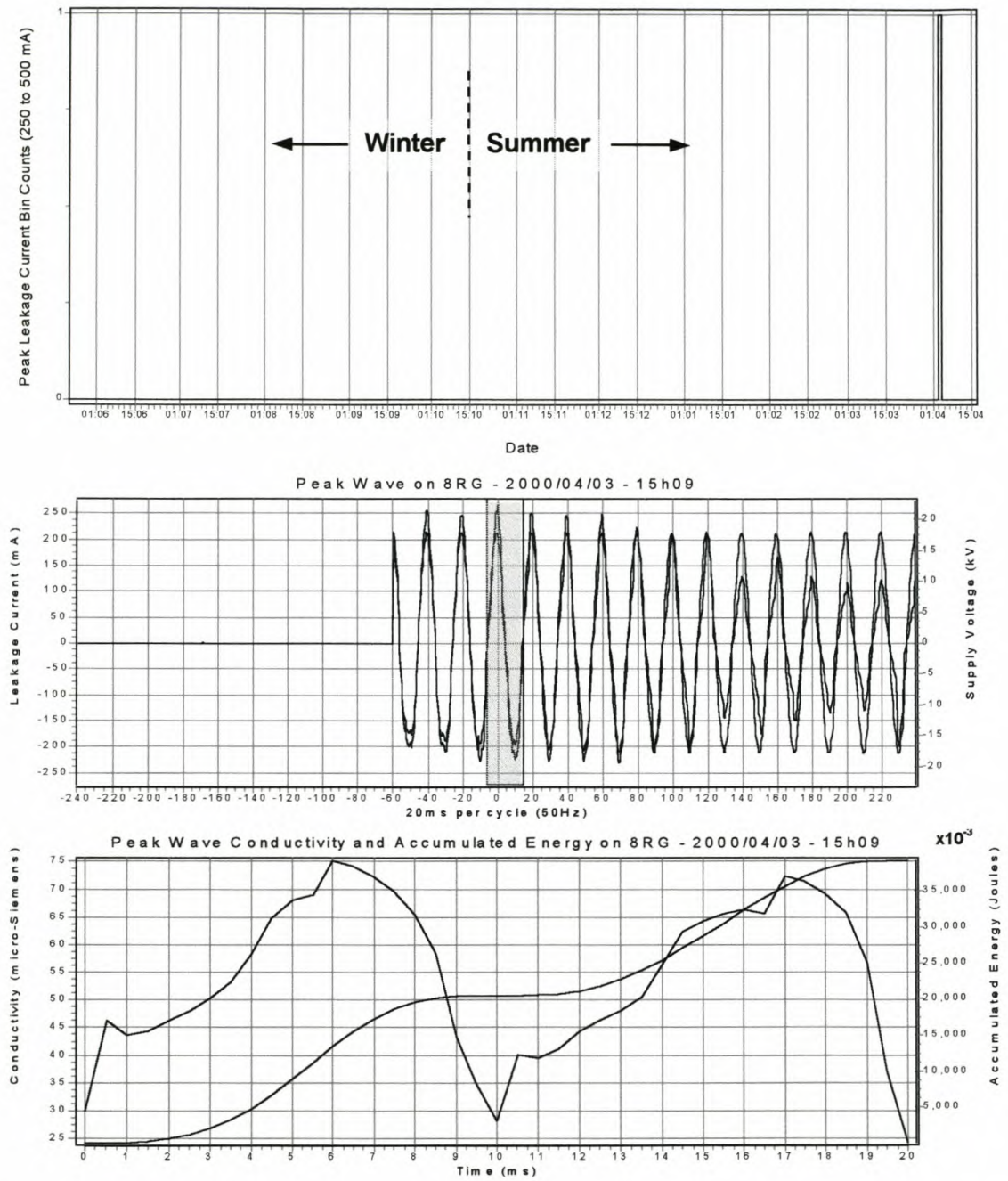

Figure F. 29 The daily bin counts for insulator **8R** are shown for the peak leakage current pulses in size range **250 to 500 mA**. The first peak leakage current and voltage waveform measured in this range, with associated conductivity and accumulated energy for the selected 20 ms cycle (shaded area), are also shown.